Hydrogen Sulfide (H_2S) as a Regulator of Myocardial Redox State and the Redox-Sensitive Regulation of Cystathionine γ-Lyase (CSE)



A Thesis Submitted for the Degree of Doctor of Philosophy

University of Oxford

Akansha Tarun

Balliol College

Radcliffe Department of Medicine

Division of Cardiovascular Medicine

John Radcliffe Hospital

Supervisors: Professor Charalambos Antoniades

Professor Barbara Casadei

Michaelmas 2017

Abstract

Hydrogen Sulfide (H_2S) as a Regulator of Myocardial Redox State and the Redox-Sensitive Regulation of Cystathionine γ-Lyase (CSE).

Akansha Tarun
Balliol College

A Thesis Submitted for the Degree of Doctor of Philosophy
University of Oxford

Michaelmas 2017

In advanced stages, cardiac disease causes millions of deaths each year. Superoxide anions ($O_2^{\cdot-}$) and their derivative peroxynitrite ($ONOO^-$) contribute to cardiac disease pathogenesis, yet strategies to reduces these reactive oxygen species through antioxidants in large scale clinical trials have largely been unsuccessful. Better understanding of pathways regulating enzymatic sources of $O_2^{\cdot-}$ like NADPH oxidases, uncoupled nitric oxide synthases (NOSs) and mitochondrial oxidases are required to regulate myocardial oxidative stress in patients with advanced stages of cardiac disease. Hydrogen sulfide (H_2S) is a gaseous signalling molecule generated by transsulfuration pathway enzymes cystathionine γ-lyase (CSE), cystathionine β-synthase (CBS), and 3-mercaptopyruvate sulfurtransferase (MST). H_2S regulates oxidative stress in animal models and shows promise for cardiovascular therapeutic strategy. This thesis investigates whether H_2S/CSE biology is related to human myocardial redox state in a cohort of individuals with advanced cardiac disease (Oxford Heart, Fat, Vessels Cohort; Ox-HVF). Individuals with varying levels of myocardial oxidative stress and function were extensively phenotyped for H_2S biology. Individuals with high myocardial oxidative stress from NADPH oxidases and NOSs were found to have high expression of myocardial CSE. To examine first the positive association with NADPH oxidase activity, CSE expression was examined after myocardial oxidative injury and CSE was found to be redox-sensitive. Furthermore, direct effects of two exogenous H_2S donors (NaHS and GYY4137) demonstrated a direct regulation of $O_2^{\cdot-}$ from NOSs in myocardium from individuals with advanced cardiac disease, further supporting H_2S's direct role in the regulation of NOS biology. Finally, identification of a SNP in CSE further demonstrated CSE's causal role in the regulation of $O_2^{\cdot-}$ generation from mitochondrial oxidases. Taken together, we demonstrate for the first time that H_2S and CSE biology are linked to human myocardial redox state and have a causal role in redox regulation in the human heart. These findings suggest H_2S/CSE biology are important endogenous regulators of myocardial redox state in humans and continued exploration of these pathways may develop novel therapeutic strategies against myocardial oxidative stress in cardiac disease.

Acknowledgements

First I would like to give a tremendous thank you to my Supervisor Prof. Charalambos Antoniades for his remarkable scientific advice and mentorship throughout my time in the laboratory and writing-up. Your enthusiasm for translational research, creativity, and high-level of productivity combined with attentive care of patients in clinic are inspiring. Thank you so much for your dedication to our work. I look forward to our many discussions ahead and our continued work together including original publications coming ahead.

I would also like to thank my second supervisor Prof. Barbara Casadei for her mentorship and thoughtful guidance. At our meetings, I always learned so much and am grateful for your curiosity, enthusiasm, and forward thinking. I am also grateful to my Balliol College Advisor, Prof. Robin Choudhury, who has helped me navigate research at Oxford for all four years. Thank you for your enthusiastic discussions and for being a role model in balancing the duties of interventional cardiology and academic medicine.

I would like to also thank the incredible team members of our laboratory for their teaching and support: Dr. Costas Psarros, Dr. Fabio Sanna, thank you so much for your insightful experimental and scientific advice and for your tremendous mentorship in this graduate journey. Dr. Ioannis Akoumianakis, Ms. Laura Herdman, Dr. Marios Margaritis, Dr. Alexis Antonopoulos, and Ms. Sheena Thomas, thank you for such warm guidance and mentorship from the very start and throughout the DPhil. Dr. Evangelos Oikonomou, Dr. Jennifer Mancio, and Dr. Nadia Akawi, thank you for your tremendous enthusiasm for research and knowledge.

I would like to also thank the Graduate Studies Team, and especially Prof. Martin Farrall and Prof. Deborah Gill, who have been rooting for my success. Thank you also to Prof. Paul Leeson, Prof. Stefan Neubauer, Prof. Keith Channon, Prof. Tom Melham, Prof. Manuela Zaccolo, Dr. Mark Crabtree, Dr. Svetlana Reilly, Mr. Phil Townsend, Mr. James Brown, Dr. Paul Robinson, and Dr. Ricardo Carnicer for their feedback at key DPhil milestones, meetings, and symposia.

I would like to thank all the incredible mentors and friends in our division. Thank you to Dr. Surawee Chuaiphichai, Dr. Jillian Simon, Dr. Naveed Akbar, Dr. Adam Lewandowski, Dr. Sam Dawkins, Dr. Alice Recalde, Dr. Cameron Turtle, and Dr. Drew Duglan who encouraged me in DPhil milestones and excitedly discussed research with me. Thank you to all the friends in the lab who kept me smiling and laughing: Mr. Mehroz Ehsan, Ms. Alexandra Mighiu, Ms. Laurienne Edgar, Ms. Maria Cristina Carena, Ms. Jade Bailey, Dr. Simona Mafrici, and Ms. Ritu Arya. Thank you also to Kailan Sierra-Davidson, Chris Kelly, Rahul Nath, Andrew Paverd, Natasha Ng, Soren Thomsen, Vassili Bazinas, and Helen Taylor for DPhil advice and making Oxford such a great community.

I am most grateful to my family: my younger brother, my older sister, and my parents. Thank you for supporting me in everything I do.

Memorandum

This project was conducted under the supervision and mentorship of Professor Charalambos Antoniades and Professor Barbara Casadei. The experiments were conducted with the guidance of postdoctoral fellows in our lab at the West Wing of the John Radcliffe Hospital and the Wellcome Trust Centre for Human Genetics at the University of Oxford. The experiments presented here and this DPhil thesis are entirely my own original work, except where collaborations are clearly stated. This work has not been submitted, in part or whole, for any other degree at this University or any other institution.

Collaborations

Chapter 4: I would like to thank Dr. Surawee Chuaiphichai from Professor Keith Channon's group and Dr. Fabio Sanna and Dr. Costas Psarros for their help in training and running biopterin and dihydroethidium measurements using High-Performance Liquid Chromatography.

Chapter 5: I would like to thank our group for genotyping the *CYBA* single nucleotide polymorphisms. I would also like to thank our collaborators Prof. Sander Verheule, Dr. Hussein M. Nasrallah, and Dr. Dragan Opacic at Maastricht University (The Netherlands), for their generation of the large animal model (one-week rapid atrial paced pigs) and for their gracious help in obtaining myocardial samples from these animals for processing.

Chapter 6: I would like to thank Dr. Costas Psarros for his help in growing four clonal populations of cells transfected with scrambled shRNA. I would like to thank Dr. Jillian Simon from Professor Barbara Casadei's group for her training and advice in power analysis.

Oxford Cohort of Heart, Vessels, and Fat (Ox-HVF): I would like to thank our clinical team in our laboratory including our collaborating cardiothoracic surgeons for making our projects possible with surgery, patient recruitment, sample collection, and measurements (DNA and RNA extraction and cohort-wide myocardial superoxide measurements). I would like to thank the patients who volunteered to take part in our studies, without whom this research would not be possible and for whom we hope this research will make a difference.

Funding Acknowledgements

This research would not have been possible without the generous support and funding of the Radcliffe Department of Medicine (RDM) Scholarship 2013-2017. I am also grateful for travel awards and additional funding from the Division of Cardiovascular Medicine (Prof. Hugh Watkins and Ms. Philippa Major), Balliol College (Dr. Nicola Trott, Dr. Stacey McGowen, College Advisor Prof. Robin Choudhury, and Academic Administrators), and our laboratory (Principal Investigator (PI): Prof. Antoniades).





Table of Contents

Abstract ... ii

List of Common Abbreviations ... ix

List of Tables ... x

List of Figures ... xi

Chapter 1 Introduction ... 1

1.1 Myocardial Redox State and Cardiac Disease ... 1

1.1.1 Role of Myocardial ROS in Physiological Redox Signalling ... 2

1.1.2 Role of Myocardial Oxidative Stress in Cardiac Disease ... 5

1.1.3 Enzymatic sources of $O_2^{\cdot-}$ in the human heart ... 7

1.1.4 Antioxidant Defence Mechanisms and Biomarkers of Oxidative Damage ... 17

1.1.5 Potential Therapeutic Targets in Cardiac Disease ... 18

1.1.6 The Unmet Need: To Target Myocardial Redox State using Novel Approaches ... 25

1.2 Hydrogen Sulfide (H_2S) as a Regulator of Redox Signalling ... 27

1.2.1 H_2S as a Physiological Molecule in Humans and the Cardiovascular System ... 29

1.2.2 Regulation of H_2S in the Heart: Endogenous, Enzymatic Sources ... 31

1.2.3 Non-Enzymatic Sources and Catabolic Processes of H_2S in the Heart ... 34

1.2.4 Modulating H_2S in the Heart via Pharmacological Donors ... 36

1.2.5 Detecting and Quantifying H_2S Levels in the Cardiovascular System ... 37

1.2.6 Direct Signalling Effects of H_2S: Posttranslational Modifications & Scavenging ... 39

1.2.7 Importance of H_2S in the Heart and Redox State ... 41

1.2.8 The Unmet Need: Role of H_2S as a Regulator of Myocardial Redox Signalling ... 46

1.3 Cystathionine γ-Lyase (CSE) and Redox State ... 46

1.3.1 CSE in Transsulfuration Pathway and 'Switching' Reactions ... 46

1.3.2 Transcriptional Regulation of CSE ... 49

1.3.3 Regulation of CSE Enzyme and CSE Enzyme Localization ... 50

1.3.4 Importance of CSE in the Heart and Redox State ... 51

1.3.5 Regulation of CSE Gene and Protein Expression ... 54

1.3.6 CSE Single Nucleotide Polymorphism and Homocysteinemia ... 54

1.4 Clinical Importance of H_2S and CSE Biology ... 57

1.4.1 Human Plasma H_2S/Sulfide levels in Cardiovascular Disease ... 57

1.4.2 H_2S-releasing drugs and Randomized Clinical Trials ... 60

1.4.3 Key Questions in the Field ... 61

1.5 Hypothesis and Aims ... 63

1.5.1 Hypothesis ... 63

1.5.2 Aims ... 64

Chapter 2 Experimental Design and Methods ... 66

2.1 Study Design ... 66

2.1.1 Clinical Study Design: The Oxford Heart-Vessels-Fat (Ox-HVF) Cohort ... 66

2.1.2 Technical Aims....68
2.2 Clinical Measurements....74
2.2.1 DNA Extraction and Genotyping....74
2.2.2 Human Myocardium Ex Vivo Models....77
2.3 Lucigenin- and Luminol-Enhanced Chemiluminescence....80
2.3.1 Sample Preparation and Measurements....81
2.3.2 Source-Specific Inhibitors and Data Analysis....83
2.4 Organic Chemistry Analytical Techniques....85
2.4.1 Dihydroethidium High-Performance Liquid Chromatography....85
2.4.2 Reversed-Phase High-Performance Liquid Chromatography for Biopterins....86
2.5 General Molecular Biology Techniques....90
2.5.1 Nucleic Acid Gel Electrophoresis....90
2.5.2 RNA Extraction, Reverse Transcription, and Quantitative-PCR....90
2.5.3 Western Blot and Antibodies....94
2.5.4 Pig Model of Oxidative Stress....97
2.5.5 General Buffers and Probes....99
2.6 Statistical Analysis....101
2.6.1 Ex Vivo, In Vitro, and In Vivo Studies....101
2.6.2 Clinical Correlations and Power Calculations....102
Chapter 3 Development of Methods and Models....103
3.1 Human Plasma H_2S by Methylene Blue Assay....103
3.1.1 Standards, Sample Preparation, and Measurements....103
3.1.2 Data Analysis....105
3.1.3 Validation for Human Plasma H_2S Measurements....105
3.2 Amperometric Sensor Set-Up for Real-Time H_2S Measurement....107
3.2.1 Set-up and Development of Real-time H_2S Monitoring....107
3.2.2 Measuring H_2S in Experimental Conditions....112
3.3 Model of Oxidative Stress in Cell Culture....113
3.3.1 H9C2 Rat Cell Line Proliferation and Differentiation....113
3.3.2 Development of acute model of oxidative stress in H9C2 cardiomyocytes....114
3.3.3 MTT Assay for Cell Viability....116
3.3.4 Characterization of oxidative stress in H9C2 cardiomyocytes....117
3.4 CSE Knockdown in Cell Culture via shRNA....120
3.4.1 Bacteria Transformation and Plasmid Amplification....120
3.4.2 Immunofluorescence and Staining Method....123
3.4.3 Stable Transfection of Cell Line by shRNA Transfection....125
3.4.4 Imaging of Transfected Cells Transfected Cells....126
3.4.5 Characterization of Stably Transfected Cells after Batch and Clonal Selection....131
Chapter 4 H_2S and Myocardial Redox State....135
4.1 Plasma H_2S/Sulfide, Demographics, & Myocardial Redox State....135
4.1.1 Plasma H_2S/Sulfide and Patient Demographics....136

4.1.2 Plasma H_2S/Sulfide and Myocardial Redox State 140
4.2 Kinetic Release Profiles of Fast- and Slow-Releasing H_2S Donors 140
4.2.1 H_2S Release from NaHS in Physiological Conditions 142
4.2.2 H_2S Release from GYY4137 in Physiological Conditions 142
4.2.3 Effects of Elevated H_2S on pH in organ bath studies 145
4.3 The Effects of H_2S from NaHS on Myocardial Redox State 146
4.3.1 The Effects of NaHS on $O_2^{\cdot-}$ and $ONOO^-$ in H9C2 Cardiomyocytes 146
4.3.2 NaHS improves NOS Coupling and reduces $ONOO^-$ in Human Myocardium 146
4.3.3 The Effects of NaHS on Human Myocardial $O_2^{\cdot-}$ from Various Sources 146
4.3.4 Mechanisms of NaHS's prevention of NOS Uncoupling in Human Myocardium 147
4.4 The Effects of H_2S from GYY4137 on Myocardial Redox State 151
4.4.1 The Effects of GYY4137 on $O_2^{\cdot-}$ and $ONOO^-$ in H9C2 Cardiomyocytes 151
4.4.2 GYY4137 increases uncoupling of NOSs in Human Myocardium 151
4.4.3 The Effects of GYY4137 on Human Myocardial $O_2^{\cdot-}$ from Various Sources 151
Chapter 5 Bidirectional Effects of CSE and Myocardial Oxidative Stress 154
5.1 CSE, CBS, and MST Gene Expression and Patient Demographics 154
5.1.1 Metabolic Profile and Hypertension 157
5.1.2 Cardiac Disease and Left Ventricular Function 159
5.1.3 Systemic Oxidative Stress and Inflammation 161
5.2 CSE, CBS, and MST Gene Expression and Myocardial Redox State 164
5.2.1 CSE and Myocardial Redox State 164
5.2.2 CBS and Myocardial Redox State 165
5.2.3 MST and Myocardial Redox State 169
5.3 Redox-Sensitivity of Myocardial CSE & CBS Gene Expression 170
5.3.1 Characterization of Acute Model of Oxidative Stress in H9C2 Cardiomyocytes 170
5.3.2 Acute Oxidative Stress Reduces CSE Gene Expression in vitro 170
5.3.3 Characterization of Myocardial Redox State of Rapid Atrial Paced Pigs 172
5.3.4 Acute Oxidative Stress Reduces CSE Gene Expression in vivo 174
5.4 Redox-Sensitivity of CSE, CBS, and MST Gene Expression (Chronic) 174
5.4.1 Characterization of the Additive CYBA ($p22^{phox}$) SNP Model 175
5.4.2 CYBA ($p22^{phox}$) SNPs and Myocardial CSE, CBS, and MST Expression 177
Chapter 6 Causal Role of CSE in Myocardial Redox State 179
6.1 CSE in Regulating Myocardial $O_2^{\cdot-}$ from NOSs and $ONOO^-$ 180
6.1.1 Characterization of CSE Knockdown Cells 180
6.1.2 Basal $O_2^{\cdot-}$ Generation, $O_2^{\cdot-}$ from NOSs, and $ONOO^-$ Levels 182
6.2 Human SNPs in CSE and CBS and Patient Demographics 183
6.2.1 CSE rs1021737G>T and Metabolic Profile, Cardiac Disease, & Systemic Stress 184
6.2.2 CBS rs2851391C>T and Metabolic Profile, Cardiac Disease, & Systemic Stress 187
6.2.3 CBS rs234709C>T and Metabolic Profile, Cardiac Disease, & Systemic Stress 190
6.3 Human SNP rs1021737G>T in CSE and Myocardial Redox State 193
6.3.1 $O_2^{\cdot-}$ from Mitochondrial Oxidases in the Heart 193

6.3.2 $O_2^{\cdot-}$ from NOSs and $ONOO^-$ in the Heart 195
6.3.3 Basal $O_2^{\cdot-}$ and $O_2^{\cdot-}$ from NADPH Oxidases in the Heart 195
6.3.4 Plasma H_2S/Sulfide Levels and Myocardial Gene Expression 195

Chapter 7 Discussion 200

7.1 H_2S/CSE Biology and Mitochondrial Oxidases 200

7.1.1 H_2S/Sulfide and Mitochondrial Redox State 201
7.1.2 CSE/CBS and Mitochondrial Redox State 201

7.2 H_2S/CSE Biology and NOSs 202

7.2.1 Direct Effects of H_2S on and NOS Coupling Status 202
7.2.2 Myocardial CSE and CBS Expression and NOS Coupling Status 205

7.3 Bidirectional Interaction of H_2S Biology and Oxidative Stress 205

7.3.1 CSE on Basal $O_2^{\cdot-}$ in an Unchallenged Model 205
7.3.2 Redox-Sensitivity of CSE 206

7.4 H_2S/CSE Biology, Cardiac Disease, and Clinical Risk Factors 207

7.4.1 Endogenous H_2S/Sulfide and Gender 207
7.4.2 Endogenous H_2S/Sulfide and Insulin Resistance 208
7.4.3 Myocardial CBS Expression Reduced in Hypercholesterolemia 209
7.4.4 Myocardial MST in Hypertension and Cardiac Function 210

7.5 Study Limitations 210

7.5.1 Measurements of H_2S 210
7.5.2 Power Analysis 211

7.6 Future Directions 214

7.6.1 Computational Analysis of SNPs and/or Site-Directed Mutagenesis 214
7.6.2 Nested Case-Control Studies 215
7.6.3 Limitations and Potential of the Field 217

7.7 Conclusion 218

Appendix 219

List of References 223

List of Common Abbreviations

B	Biopterin
BH_2	Dihydrobiopterin
BH_4	Tetrahydrobiopterin
BMI	Body mass index
BNP	B-Natriuretic peptide
CABG	Coronary artery bypass grafting
CBS	Cystathionine β-synthase
CRP	C-Reactive Protein
CSE	Cystathionine γ-lyase
CYBA	Cytochrome b-245 alpha chain
DHE	Dihydroethidium
DM	Diabetes mellitus
GFP	Green fluorescent protein
GSH	Glutathione
GYY4137	Morpholin-4-ium 4 methoxyphenyl(morpholino) phosphinodithioate
H_2S	Hydrogen sulfide
HCL	Hypercholesterolemia
Hcy	Homocysteine
HOMA-IR	Homeostatic model assessment of insulin resistance
HPLC	High-performance liquid chromatography
HTN	Hypertension
IR	Insulin resistance
LA	Left atrium
L-NAME	N^G-nitro-L-arginine methyl ester
LV	Left ventricle
LVEDD	Left ventricular end diastolic diameter
LVEDV	Left ventricular end diastolic volume
LVESD	Left ventricular end systolic diameter
LVESV	Left ventricular end systolic volume
MAF	Minor allele frequency
MDA	Malondialdehyde
MST	3-mercaptopyruvate sulfurtransferase
NaHS	Sodium hydrogen sulfide
NADPH	Nicotinamide adenine dinucleotide phosphate
NOS	Nitric oxide synthase
NOX	NADPH oxidase
O_2	Oxygen
$O_2^{\cdot-}$	Superoxide anions
$ONOO^-$	Peroxynitrite
PGK1	Phosphoglycerate kinase 1
RAA	Right atrial appendage
RAP	Rapid atrial pacing
ROS	Reactive oxygen species
SEM	Standard error of mean
shRNA	Short-hairpin RNA
SNP	Single nucleotide polymorphism
SOD	Superoxide dismutase
SP1	Specificity protein 1

List of Tables

Table 1.1 Biologically-Relevant Physical, Chemical, & Toxicological H_2S Properties .. 31
Table 1.2 Cystathionine γ-Lyase (CSE): Gene, Protein, Function 52
Table 1.3 H_2S and CSE Biology in the Human Cardiovascular System 61
Table 2.1 Genotyping Program by Applied Biosystems for PCR Conditions..... 74
Table 2.2 Mobile Phase Components for HPLC Column 87
Table 2.3 Reverse Transcription Program by Applied Biosystems..... 92
Table 2.4 Gene Expression Probes 93
Table 2.5 Primary and Secondary Antibodies for Western Blotting 97
Table 2.6 Pig Primers for Myocardial Gene Expression Quantification 98
Table 2.7 Krebs HEPES Buffer Components..... 99
Table 2.8 Tyrode's Buffer Components 99
Table 2.9 Krebs Henseleit Buffer Components..... 100
Table 2.10 Genotyping Probes..... 100
Table 3.1 Scrambled and CTH shRNA 29mer Construct Sequences..... 125
Table 4.1 Demographics Characteristics of Study Participants in Chapter 4 136
Table 5.1 Demographics Characteristics of Study Participants in Chapter 5 155
Table 5.2 Correlation Coefficients for CSE, CBS, and MST Gene Expression..... 169
Table 5.3 Number of Individuals with CYBA rs4673 and rs1049255 SNP..... 176
Table 6.1 Demographics Characteristics of Study Participants in Chapter 6 180
Table 6.2 Number of Individuals with CSE and CBS SNPs 183

List of Figures

Figure 1.1 ROS Signalling, Antioxidant Defence, and Myocardial Oxidative Stress 7
Figure 1.2 NADPH Oxidase Isoforms as a Source of $O_2^{\cdot -}$ in the Cardiovascular System ... 8
Figure 1.3 Mitochondrial Electron Transport Chain in Myocardial Oxidative Stress 11
Figure 1.4 Uncoupled Nitric Oxide Synthases in Myocardial Oxidative Stress 13
Figure 1.5 Proposed Therapeutic Strategies Targeting Myocardial Oxidative Stress 22
Figure 1.6 Meta-Analysis of Antioxidants in Cardiovascular Clinical Trials 24
Figure 1.7 Folates, Vitamin B_6, and Vitamin B_{12} Treatment and Cardiovascular Death .. 28
Figure 1.8 Enzymatic Reactions Important in the Generation of By-Product H_2S 47
Figure 1.9 Overview of Original DPhil Hypothesis 64
Figure 2.1 Clinical Study with the Oxford Heart-Vessels-Fat (Ox-HVF) Cohort 67
Figure 2.2 Study Design to Address Chapter 4 Aims 69
Figure 2.3 Study Design to Address Chapter 5 Aims 71
Figure 2.4 Study Design to Address Chapter 6 Aims 73
Figure 2.5 Genotyping using TaqMan® Probes 75
Figure 2.6 DNA Amplification Plot for Genotyping 76
Figure 2.7 Analysis of Genotyping in an Allelic Discrimination Plot 76
Figure 2.8 Human Myocardium (Right Atrial Appendage) 78
Figure 2.9 Experimental Design for Ex Vivo Studies and H_2S Donors 79
Figure 2.10 Lucigenin- and Luminol-Enhanced Chemiluminescence Setup 82
Figure 2.11 Lucigenin-Enhanced Chemiluminescence Trace (NADPH Oxidases) 83
Figure 2.12 DHE-HPLC Chromatogram from RAA 86
Figure 2.13 Electrochemical Chromatogram for Quantification of BH_4 88
Figure 2.14 Fluorescence Chromatogram for Quantification of BH_2 and B 89
Figure 2.15 Study Design for Quantifying CSE, CBS, and MST Gene Expression 93
Figure 2.16 Image Analysis for Western Blotting 96
Figure 2.17 Study Design for Genotyping CSE and CBS SNPs 100
Figure 3.1 Methylene Blue Reaction for Measuring H_2S/Sulfide 104
Figure 3.2. Methylene Blue Standard Stability & Comparison of Plasma and Serum 106
Figure 3.3. Experimental and Schematic Set-up of Amperometric H_2S Sensor 108
Figure 3.4 LabScribe Software: Trace of 40 µM NaHS 112
Figure 3.5 Development of Acute Oxidative Stress Model in H9C2 Cells 115

Figure 3.6 Viability of H9C2 Cells in Krebs HEPES Buffer with FBS 118
Figure 3.7 Cells Exposed to 1mM NADPH after placement in Fresh Krebs HEPES 119
Figure 3.8 Schematic for Measuring $O_2^{\cdot -}$ in H9C2 Cells after NADPH Incubation.....119
Figure 3.9 Schematic for the Generation of CSE Knockdown H9C2 Cells 120
Figure 3.10 Microscopy for Imaging Fluorescent Cells 124
Figure 3.11 Screenshot of ImageJ Analysis.....124
Figure 3.12 Immunofluorescence and Brightfield Images Post-Transfection 127
Figure 3.13 Puromycin Concentrations for H9C2 cells: 1-4 μg/mL, Day 0-2 128
Figure 3.14 Puromycin Concentrations for H9C2 cells: 0.1-0.75 μg/mL, Day 0-2 129
Figure 3.15 Puromycin Concentrations for H9C2 cells: 0.1-0.75μg/mL, Day 3-5 130
Figure 3.16 Immunofluorescence Images & Gene Expression Post-Batch Selection 134
Figure 4.1 Plasma H_2S/Sulfide and Patient Demographics 137
Figure 4.2 Plasma H_2S/Sulfide, Metabolic Profile, and Heart Failure 138
Figure 4.3 Plasma H_2S/Sulfide, Obesity, and Myocardial Function 139
Figure 4.4 Plasma H_2S/Sulfide and Myocardial Redox State.....141
Figure 4.5 H_2S Release from NaHS (Four Physiological Conditions) 142
Figure 4.6 H_2S Release from GYY4137 (Four Physiological Conditions) 143
Figure 4.7 H_2S Release from NaHS and GYY4137 in Krebs HEPES Buffer.....144
Figure 4.8 Effects of NaHS on pH in Physiological Conditions 145
Figure 4.9 Effects of NaHS on $O_2^{\cdot -}$ from NOSs and $ONOO^-$ in vitro and ex vivo 148
Figure 4.10 Effects of NaHS on NADPH oxidases and Mitochondrial Oxidases.....149
Figure 4.11 Effects of NaHS on Basal $O_2^{\cdot -}$ and Biopterins.....150
Figure 4.12 Effects of GYY4137 on $O_2^{\cdot -}$ from NOSs and $ONOO^-$ in vitro and ex vivo .152
Figure 4.13 Effects of GYY4137 on NADPH Oxidases and Mitochondrial Oxidases ...153
Figure 5.1 Myocardial CSE, CBS, and MST Gene Expression & Demographics 156
Figure 5.2 Myocardial CSE, CBS, and MST Gene Expression & Metabolic Profile 157
Figure 5.3 Myocardial CSE, CBS, and MST, Hypertension, & Hypercholesterolemia..159
Figure 5.4 Myocardial CSE, CBS, and MST Gene Expression and Heart Failure.....160
Figure 5.5 Myocardial CSE, CBS, and MST Expression and LV Function.....162
Figure 5.6 Myocardial CSE, CBS, and MST & Systemic Markers of Stress.....163
Figure 5.7 CSE Gene Expression and Myocardial Redox State.....166
Figure 5.8 CBS Gene Expression and Myocardial Redox State.....167
Figure 5.9 MST Gene Expression and Myocardial Redox State.....168

Figure 5.10 Model of Acute Oxidative Stress in H9C2 Cells.....171
Figure 5.11 CSE Gene Expression in In Vitro Model of Acute Oxidative Stress.....172
Figure 5.12 Redox State in Left Atria of Rapid Atrial Paced Pig Hearts.....173
Figure 5.13 CSE Gene Expression in In Vivo Model of Acute Oxidative Stress.....175
Figure 5.14 CYBA rs4673C and rs1049255G SNPs and Myocardial Redox State.....177
Figure 5.15 CYBA rs4673C and rs1049255G SNPs and CSE, CBS, & MST.....178
Figure 6.1 CSE Gene Expression and Protein Levels.....181
Figure 6.2 Redox State in CSE Knockdown Cells.....182
Figure 6.3 CSE SNP rs1021737, Patient Demographics, and Metabolic Profile.....185
Figure 6.4 CSE SNP rs1021737, LA Dimensions, and LV Function.....186
Figure 6.5 CSE SNP rs1021737 & Systemic Markers of Stress.....187
Figure 6.6 CBS SNP rs2851391, Patient Demographics, and Metabolic Profile.....188
Figure 6.7 CBS SNP rs2851391, LA Dimensions, and LV Function.....189
Figure 6.8 CBS SNP rs2851391 & Systemic Markers of Stress.....190
Figure 6.9 CBS SNP rs234709, Patient Demographics, and Metabolic Profile.....191
Figure 6.10 CBS SNP rs234709, LA Dimensions, and LV Function.....192
Figure 6.11 CBS SNP rs234709 & Systemic Markers of Stress.....193
Figure 6.12 CSE and CBS SNPs and Mitochondrial Redox State.....194
Figure 6.13 CSE and CBS SNPs and $O_2^{\cdot -}$ from NOSs and $ONOO^-$ Levels.....196
Figure 6.14 CSE and CBS SNPs, $O_2^{\cdot -}$ from NADPH oxidases, and Basal $O_2^{\cdot -}$.....197
Figure 6.15 CSE and CBS SNPs and Plasma H_2S/Sulfide.....198
Figure 6.16 CSE SNP and Myocardial Gene Expression.....198
Figure 6.17 CBS SNPs and Myocardial Gene Expression.....199
Figure 7.1 Overview of Bidirectional Interaction: H_2S, CSE & Redox State.....200
Figure 7.2 Power Calculations for CSE SNP rs1021737 and $O_2^{\cdot -}$ from NOSs.....213
Figure 7.3 Detailed Overview of Bidirectional Interaction in the Human Heart.....216

Chapter 1 Introduction

1.1 Myocardial Redox State and Cardiac Disease

The Global Burden of Cardiac Disease

Cardiac disease can be considered an umbrella term for many different forms of heart disease: heart failure, cardiomyopathies (e.g. hypertrophic cardiomyopathy), inflammation of the heart (myocarditis), heart valve disease, and cardiac arrhythmias (e.g. atrial fibrillation, bradycardia).[1] These diseases affect millions of individuals around the world, remaining a major health problem and a major cause of death globally each year.[2,3] In addition to an increasing global prevalence of many of these pathologies, the financial burden of cardiac disease is large: costs-of-illness in primary and secondary prevention (e.g. hospitalizations, procedures, treatments), out-of-pocket expenses in households, and healthcare expenditure remain high.[1,4]

Current tools to begin addressing these different forms of heart disease range from multidrug regimens (e.g. β-blockers, statins, diuretics, angiotensin converting enzyme inhibitors), surgeries (e.g. coronary artery bypass graft), to implantation of devices (e.g. implantable cardioverter defibrillator).[1] These specific tools, however, are limited by our understanding of the underlying mechanisms of cardiac disease like heart failure and arrhythmias. To develop further treatment options that are both cost-effective and targeted, and to prevent cardiac disease, we crucially need a better and more clear understanding of the pathophysiology and the mechanisms behind heart disease: how does it develop, how is it sustained, and what exacerbates it?

Human myocardial redox state, broadly described, is the balance of reactive oxygen species (ROS) in their oxidized and reduced forms in the heart; this state is regulated by the sources of ROS and antioxidant defence systems in the myocardium.[5] While physiological ROS signalling is crucial to the function of the heart, uncontrolled ROS

generation resulting in myocardial oxidative stress can contribute to disease pathogenesis. Therefore, a nuanced understanding of the mechanisms regulating myocardial redox state may lead to the discovery of new targets in cardiac disease pathogenesis and the development of novel therapeutic strategies in cardiovascular medicine.[6]

1.1.1 Role of Myocardial ROS in Physiological Redox Signalling

To coordinate and regulate critical physiological processes, the myocardium requires highly reactive signalling molecules known as ROS.[7] ROS include oxygen-based, reactive species like superoxide ($O_2^{\cdot-}$) and hydroxyl ($OH^{-}\cdot$) anions which are involved in reversible signalling processes.[7] Other ROS involved in signalling processes include peroxynitrite ($ONOO^-$), hydrogen peroxide (H_2O_2), and hypochlorite anion (OCl^-).[7,8] The short-lived nature of these various ROS allow them to communicate rapidly in signalling pathways.

$O_2^{\cdot-}$, a free radical formed from the one-electron reduction of molecular oxygen (O_2) resulting in an unpaired electron, has a half-life estimated to be 10^{-9} to 10^{-10} seconds in the absence of scavenging enzyme superoxide dismutase (SOD).[9] Impermeable to membranes, $O_2^{\cdot-}$ is rapidly converted to H_2O_2, a nonradical that can cross membranes with a half-life estimated to be 10^{-3} seconds in the absence of catalase.[8,9] The half-life of $O_2^{\cdot-}$ and H_2O_2 in the presence of SOD and catalase, respectively, is even shorter than described above.[9] As a result, these ROS can facilitate intercellular and intracellular communication quickly within and between various cell types of the myocardium which include atrial and ventricular cardiomyocytes, fibroblasts, endothelial cells, smooth muscle cells, pacemaker cells, and purkinje fibers.[10]

Indeed, ROS have been shown to play an important role in physiological signalling in the heart.[11] From contribution in regulating cardiac proliferation and differentiation, contractility, adaptive stress responses to hypoxia and ischemia,

senescence, to apoptosis, ROS affect and maintain important physiological processes.[7,12] For example, it has been shown that reducing ROS by silencing a ROS-generating Nox isoform (Nox4) led to reduced ability of mouse embryonic stem cells to generate cardiomyocytes.[12] Furthermore, reducing ROS by silencing Nox isoforms (Nox2 and 4) led to an increase in expression of cardiac precursor cells and a decrease in expression of genes for differentiation.[7,12] These studies provide a few of the many important examples demonstrating the importance of ROS in proliferation of cardiomyocytes, their differentiation, and physiological processes of the heart.

How is it that ROS affect these various processes? One of their main methods of action is via posttranslational modifications of proteins. ROS are known to modify important cysteine residues by a) oxidation of the residue's thiol group into sulfenic (SOH), sulfinic (SO_2^-), or sulfonic acid (SO_3^-), b) S-glutathionylation or the addition of a glutathione (GSH) group to a thiol group, or c) S-nitrosylation where nitric oxide (NO) chemically interacts with a thiol radical to form S-nitrosothiol (SNO).[11] Through these posttranslational modifications of active site cysteine thiols, ROS have been shown to regulate a) phosphatases like phosphatase and tensin homolog (PTEN) and protein tyrosine phosphatases (PTP), b) kinases like calcium/calmodulin-dependent protein kinase II (CaMKII) and protein kinase A (PKA), c) ion channels and transporters and structural proteins, and d) redox-sensitive transcription factors like nuclear factor-kappa B (NF-κB) and nuclear factor E2-related factor-2 (Nrf2).[11,12]

In addition to modification of cysteine residues, ROS are known to also modify methionine residues. Posttranslational modification of methionine residues (e.g. oxidizing methionine sulfur to methionine sulfoxide) has implications for the activation or deactivation of proteins.[11] For example, ROS-dependent oxidation of methionine on

CaMKII activates the kinase, which has a direct impact on downstream signalling processes in the heart.[11]

One important example of ROS's effects on physiological processes through these posttranslational modifications of both cysteine and methionine residues occurs in cardiac contractility where ROS modify the machinery that facilitates excitation-contraction coupling.[7] ROS can oxidize methionine residues on voltage-gated sodium channels ($Na_v1.5$) which depolarize the cell, leading to inactivation of $Na_v1.5$ and increased intracellular Na^+ ions.[7] ROS can activate not only CaMKII but also PKA and protein kinase C (PKC) to regulate the opening of L-type Ca^{2+} channels (LTCC), which are important to induce Ca^{2+} release from the Ca^{2+} stores in the sarcoplasmic reticulum and result in an increase in Ca^{2+} through LTCC.[7] ROS can also oxidize cysteine residues on ryanodine receptors which leads to increased Ca^{2+} and increased cardiac contractility.[7] Furthermore, it is believed that ROS may modify residues of the Na^+/Ca^{2+} exchanger (NCX) and Ca^{2+}-ATPase SERCA (which regulates Ca^{2+} reuptake by the sarcoplasmic reticulum after contraction) but the literature is conflicting and more research is needed to clarify ROS's exact role.[7] These studies taken together highlight the various and wide-ranging role ROS play (and roles being identified) in modifying critical processes like contractility.

More recently, it has also been shown that small bursts of ROS, or "oxidative burst," also have a homeostatic role in the heart. Low grade oxidative stress from the endoplasmic reticulum can lead to autophagy which can reduce cardiac hypertrophy.[7] ROS production through "oxidative burst" can also act as a defence against foreign pathogens; ROS production from macrophages can lower the threshold required of T lymphocytes to be activated by antigens at their antigen receptor, thereby making an immune response to environmental pathogens more effective.[13] Moreover, ROS have

additional physiological roles that are being explored. ROS can act as an O_2 sensor although the mechanisms are not clear.[13] ROS can also increase antioxidant responses: ROS-induced oxidation of cysteine residues on Kelch-like ECH-associated protein 1 (Keap1) is thought to inactivate it and frees its complexed redox-sensitive transcription factor Nrf2; Nrf2 nuclear localization increases transcription of antioxidant response element (ARE) genes.[11]

While myocardial ROS play a crucial role in regulatory processes that are critical for the proper functioning of the heart as these examples demonstrate, myocardial ROS can also contribute to cardiac disease. An increase in ROS locally or temporally (myocardial oxidative stress) can cause dysregulation of homeostatic processes.

1.1.2 Role of Myocardial Oxidative Stress in Cardiac Disease

Although ROS play a key role in physiological signalling in the heart, uncontrolled ROS production (myocardial oxidative stress) has been implicated in cardiac disease pathogenesis, from heart failure to arrhythmias to cardiomyopathies. Myocardial ROS, and particularly $O_2^{\cdot -}$, is derived from a variety of enzymatic sources (NADPH oxidases, mitochondrial oxidases, uncoupled nitric oxide synthases). The mechanisms by which $O_2^{\cdot -}$ or ROS affect myocardial structure include reacting with lipids leading to lipid peroxidation, reacting with DNA causing DNA damage, modifying redox-sensitive residues like that on ryanodine receptors (RyR) which regulate Ca^{2+} homeostasis, contributing to mitochondrial damage, and others.[12,14,15] Moreover, ROS can induce pro-fibrotic mechanisms and promote myocardial infiltration of inflammatory cells leading to fibrosis.[16] In apoptotic signalling, ROS may also lead to mitochondrial permeability transition pore (MPTP) opening, p53 transcription factor-activation, or apoptosis signalling kinase-1 (ASK-1) activation, ultimately leading to cell death.[12]

The activation of these molecular and cellular changes through ROS alters larger cardiac processes like cardiac structural and electrical remodelling and functional changes in contractility.[16] For example, CaMKII and PKA hyperphosphorylate RyR2, and RyR2 is modified directly by ROS, rendering RyR2 dysfunctional; this leads to diastolic Ca^{2+} leak from the sarcoplasmic reticulum which results in changes in Ca^{2+} that ultimately affects the development of arrhythmias.[12] Moreover, ROS may affect Na^{+} and K^{+} pumps contributing to Na^{+}/Ca^{2+} overload and ultimately arrhythmias.[12] ROS-induced SERCA2a oxidation also affects Ca^{2+} transients which influences contractile function as do changes in disulphide bridge formation in a segment of titin.[12] Furthermore, calcineurin, a serine/threonine phosphatase that is activated by a calmodulin-dependent mechanism and oxidative stress, dephosphorylates transcription factor nuclear factor of activated T cells (NFAT), allowing it to promote transcription of hypertrophy-promoting genes.[7] Thus, these ROS-induced and ROS-mediated changes lead to changes in function of the heart in terms of contractility, electrical stability, maladaptive remodelling, and hypertrophy.

Ultimately, although cardiac pathologies differ largely in terms of mechanism, at least one common thread has emerged: alterations in myocardial redox state and particularly myocardial oxidative stress are strongly implicated in cardiac disease.[12] In humans, myocardial redox state (basal $O_2^{\cdot -}$ and $ONOO^{-}$) are important predictors of post-operative atrial fibrillation and length of hospital stay – one example of many.[6] Thus, understanding how and what regulates myocardial oxidative stress will be crucial to finding appropriate therapeutic targets (Figure 1.1). Given that oxidative stress plays a causal and predictive role in cardiac disease, particularly local increased ROS production, how do we successfully target oxidative stress and maintain physiological ROS signalling? A better understanding of the regulation of ROS production and recycling will be important.

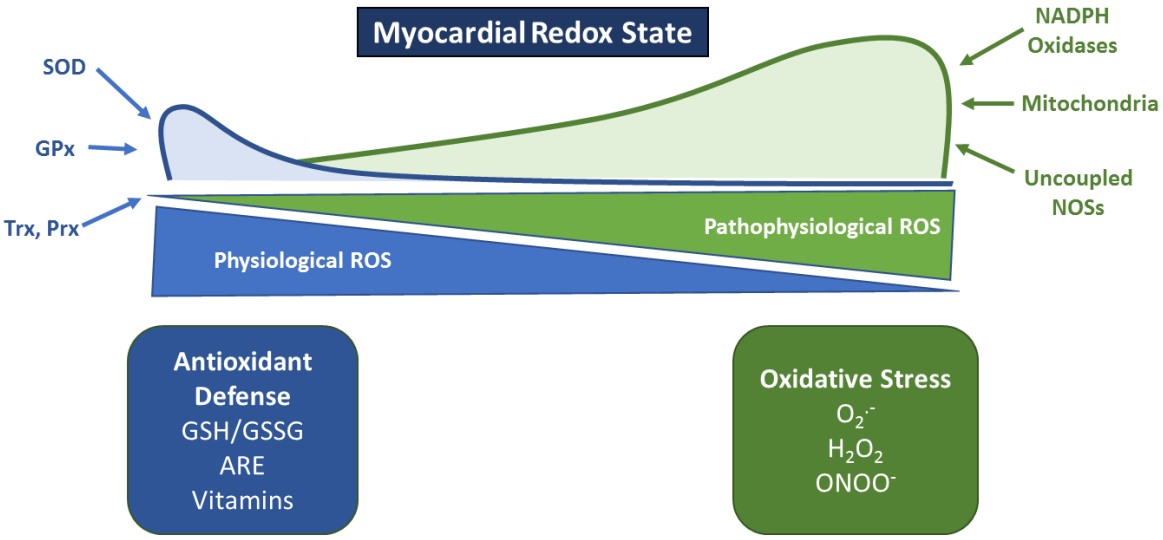


Figure 1.1 ROS Signalling, Antioxidant Defence, and Myocardial Oxidative Stress

While physiological ROS signalling is crucial to the function of the heart, uncontrolled ROS generation resulting in myocardial oxidative stress can contribute to disease pathogenesis. ROS in localized compartments of the cell regulate several physiological processes in the heart including contractility, proliferation, differentiation, apoptosis, immune defences, and more. However, uncontrolled ROS production leads to myocardial oxidative stress, which can interfere with fundamental biomolecules in the heart including DNA, lipids, and proteins. Antioxidant defence systems in the heart that attempt to balance the uncontrolled production of ROS include vitamins (e.g. vitamin A, E), enzymatic systems (e.g. superoxide dismutase), and molecules like glutathione (GSH). These systems when overwhelmed by ROS production cannot maintain a balanced myocardial redox state, contributing to disease. Oxidative stress can contribute to inflammatory processes in the heart, which can in turn increase oxidative stress in a vicious cycle. These modifications ultimately interfere with the heart's ability to function, leading to fibrosis, impaired contractility, hypertrophy, and other disease mechanisms. The balance between physiological ROS signalling and reducing pathophysiological oxidative stress is key for myocardial redox state balance. Figure was created based on several papers.[13,17]

1.1.3 Enzymatic sources of $O_2^{\cdot-}$ in the human heart

Several key enzymes are involved in the production of ROS and particularly myocardial $O_2^{\cdot-}$ which has been shown to be a significant player in cardiac pathology. Important sources of myocardial $O_2^{\cdot-}$ include pro-oxidant enzymatic systems like NADPH oxidases, mitochondrial oxidases, and uncoupled nitric oxide synthases (NOSs).[12] Examining the regulation of $O_2^{\cdot-}$ production from these enzymatic sources may provide new therapeutic targets against myocardial oxidative stress contributing to cardiac disease.

NADPH Oxidases as a source of $O_2^{\cdot-}$ in the human heart

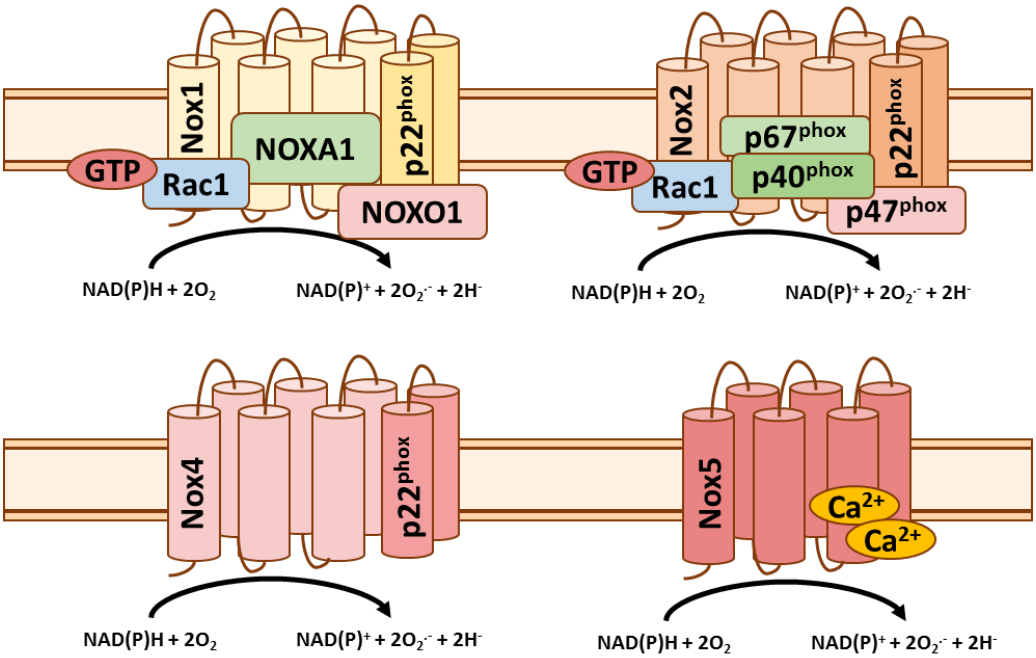


Figure 1.2 NADPH Oxidase Isoforms as a Source of $O_2^{\cdot-}$ in the Cardiovascular System

In the cardiovascular system, the isoforms of NADPH oxidases expressed are Nox1, 2, 4 and 5. In the heart, the isoforms of NADPH oxidases expressed are Nox1, 2, and 4, with the latter linked to both pathophysiological and protective roles. These isoforms assemble at the membrane (e.g. membrane translocation of subunit Rac1) and transfer electrons from substrate NADPH to molecular O_2 to form $O_2^{\cdot-}$. Activators of these isoforms include inflammatory cytokines like tumor necrosis factor-alpha and suppressors include adiponectin. Known SNPs in the subunits can contribute to increased NADPH oxidase activity. Better understanding of what regulates NADPH oxidases and what causes its dysregulation in disease might suggest new therapeutic approaches. Figure was recreated from two papers.[18,19]

NADPH oxidases are part of a unique family of Nox enzymes whose primary role is to produce $O_2^{\cdot-}$ through the assembly of a catalytic subunit (Nox or dual oxidase isoforms) and oxidase subunits (e.g. $p47^{phox}$, $p67^{phox}$, $p40^{phox}$, Rac1, and $p22^{phox}$).[12] The Nox family contains seven members: Nox1, 2, 3, 4, 5, Duox1, and Duox2.[7,8] Of these seven members of this family, only Nox 1, 2, 4, and 5 are known to be expressed in cardiovascular tissues and it is known that Nox 1, 2, and 4 are expressed in cardiomyocytes (Figure 1.2).[7,8,12,20]

NADPH oxidases play a key role in the heart through their production of $O_2^{\cdot-}$. NADPH oxidase activity has been shown to be increased in the hearts of patients with end-stage heart failure compared to the hearts of individual without heart failure.[21] This study provided the first evidence of the importance of NADPH oxidases in heart failure in

humans. Furthermore, NADPH oxidase activity has been independently associated with post-operative atrial fibrillation.[22] Studies into specific isoforms have more recently taken place and Nox2 and 4 have been predominantly studied in the heart.[12]

Nox2: Nox2-NADPH oxidase derived $O_2^{\cdot-}$ contributes to early stages of atrial fibrillation.[23,24] Moreover, the gene expression of Nox2 is highly correlated with myocardial $O_2^{\cdot-}$ in a large cohort of patients undergoing coronary artery bypass grafting or valve replacement.[20] Thus, several studies have now implicated the Nox2 isoform in cardiac pathology. Nox2 generates $O_2^{\cdot-}$ by reducing O_2 using electrons from NADPH that travel through flavin and heme moieties and is activated by various stimuli including angiotensin II, cytokines like tumor necrosis factor-alpha (TNF-α), and mechanical forces.[12]

Nox4: The literature on Nox4, in contrast to Nox2, remains controversial regarding its role as pathological or cardioprotective: a recent study, for example, has shown that Nox4 is a source of $O_2^{\cdot-}$ from cardiac mitochondria, leading to increased cardiac damage after pressure overload[25] while another study has shown Nox4 to be cardioprotective in a murine model of heart failure.[26] The former study examines mitochondrial function in particular while the latter study examines changes in redox signalling including Nrf2 activation.[26] The differences in these studies may be attributed to methodological differences and the model of heart failure but more research is needed to tease apart the differences. Nox4 is considered constitutively active, a key source of H_2O_2 instead of $O_2^{\cdot-}$, and uniquely does not require regulatory subunits like Rac1 and its translocation.[12,27] Although Nox4 has continuous activity, stress like hypoxia and ischemia can further stimulate Nox4.[26]

Mitochondrial Oxidases as a source of $O_2^{\cdot-}$ in the human heart

Mitochondria, which are abundant in cardiomyocytes, are not only a source of adenosine triphosphate (ATP) but also a major source of $O_2^{\cdot-}$.[28] Under physiological conditions, electrons move from NADH and $FADH_2$ to O_2 (forward flow of electrons) via electron carriers (complex I, II, III, IV and ubiquinone and cytochrome C) while, simultaneously, protons are pumped from the mitochondrial matrix into the intermembrane space (Figure 1.3).[28] This pump generates a proton motive force, a result of both a membrane potential and a proton gradient, that is then coupled with ATP production through F_0F_1ATPase.[28] Electrons occasionally move from complex II back to complex I (reverse flow of electrons) as well.[28]

While this flow of electrons coupled to ATP production is tightly regulated in the mitochondria, there are several opportunities for $O_2^{\cdot-}$ production. Broadly, mitochondrial electron transport chain (ETC) complexes I and III have been particularly recognized as key sources of $O_2^{\cdot-}$, with complex I-derived $O_2^{\cdot-}$ released into the mitochondrial matrix and complex III-derived $O_2^{\cdot-}$ released into the mitochondrial matrix as well as the intermembrane space.[11,29] Within these complexes, there are particular moieties and domains that are suggested to be sources of $O_2^{\cdot-}$ from the mitochondria.[28] For example, the ubiquinone-binding domain and iron-sulfur clusters of complex I and the Q-cycle regulated by complex III may be specific sources of $O_2^{\cdot-}$.[28] It is thought that NADH dehydrogenase of complex I leaks electrons that can lead to $O_2^{\cdot-}$ while complex III leaks electrons through the flow of electrons between ubisemiquinone and cytochrome b.[28] In addition to complex I and III, complex II and IV have also been suggested to play a role in $O_2^{\cdot-}$ production but whether these mechanisms exist in the human myocardium is not clear.[28] In addition to ETC complexes, other proteins in the mitochondria have been recognized as sources of $O_2^{\cdot-}$, including monoamine oxidase and $p66^{Shc}$ protein.[11]

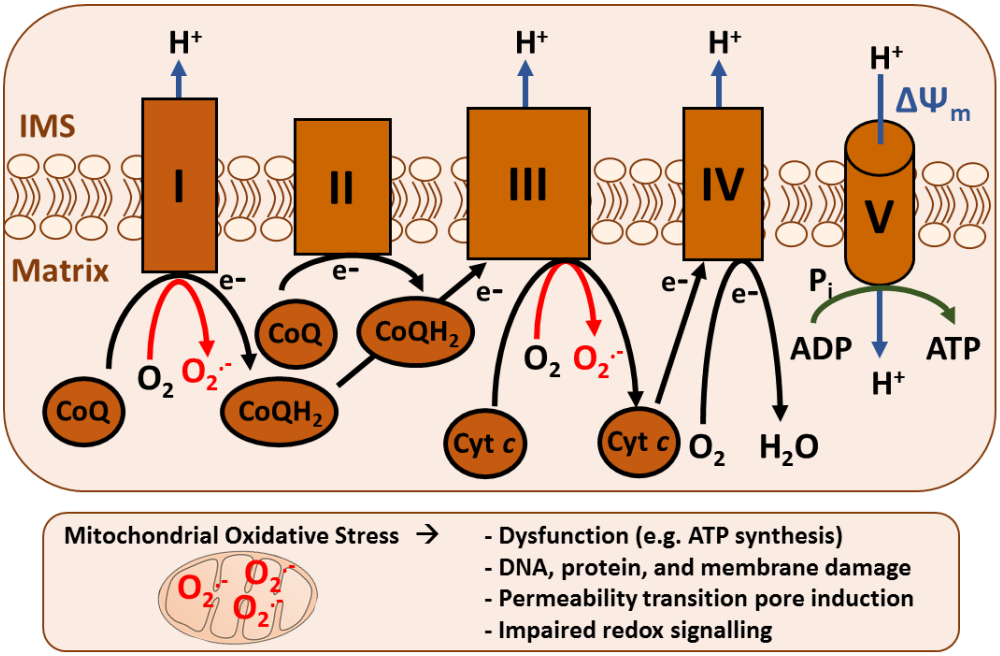


Figure 1.3 Mitochondrial Electron Transport Chain in Myocardial Oxidative Stress

Mitochondria, which are abundant in the heart, are key sources of myocardial $O_2^{\cdot-}$. In physiological conditions, electrons flow from complex I to II to III to IV via differences in redox potential between the complex, and the electrons are taken to the final electron acceptor O_2. However, in cardiac disease, this flow is disrupted and electrons are known to leak from different complexes. As a result, mitochondria become a source of $O_2^{\cdot-}$ that contributes to oxidative stress. Specifically, electrons (from NADH and $FADH_2$) are transferred from complex I and II to CoQ (forming $CoQH_2$) which transfers electrons to complex III. Electrons are then transferred from complex III to IV, but via a single-electron carrier Cyt *c*. Finally, electrons are transferred from Cyt *c* to Complex IV to the final electron acceptor, O_2, to form H_2O. Complex I, III, and IV pump protons from the matrix to the intermembrane space, from the energetically favorable electron transfers, generating a proton motive force ($\Delta\Psi_m$) or electrochemical gradient that channels complex V (ATP synthase) to phosphorylate ADP to form ATP as protons move back to the mitochondrial matrix. O_2 also accepts a single electron to form $O_2^{\cdot-}$ and this occurs primarily at complex I and complex III (both in forward and reverse electron transport). Excess $O_2^{\cdot-}$ or mitochondrial oxidative stress can lead to mitochondrial dysfunction and dysregulate ATP synthesis, as well as damage DNA, proteins, and membranes of the mitochondria. Furthermore, mitochondrial oxidative stress can lead to increased permeability via induction of the permeability transition pore and impaired redox signaling. Only a few cardiovascular medications target the mitochondria but extensive research is taking place for the development of new targets (e.g. mitochondria-targeted antioxidants and DNA repair). Better understanding of what regulates mitochondrial oxidases and what causes its dysregulation in disease might suggest new therapeutic approaches. All black and red arrows represent electron transfers with red arrows specifically representing electron transfer to O_2 to form $O_2^{\cdot-}$. Blue arrows represent movement between matrix and IMS. Figure created on basis of several mitochondrial papers.[30-32] CoQ: Coenzyme Q; Cyt *c*: Cytochrome C; H^+: Proton; H_2O: Water; IMS: Intermembrane Space; O_2: Oxygen; $O_2^{\cdot-}$: Superoxide; P_i: Inorganic phosphate.

Experimental models have shown that mitochondrial $O_2^{\cdot-}$ generation may play a role in redox-dependent cardiac pathogenesis. In an *in vivo* model, for example, reperfusion after myocardial ischemia provides myocardial mitochondria with the substrate needed to increase mitochondrial ROS production that can lead to further damage of the electron

transport chain, occasionally referred to as ROS-induced ROS release.[28] Understanding the molecular mechanisms that regulate mitochondrial $O_2^{\cdot-}$ production, including gating of mitochondrial proteins like the mitochondrial permeability transition pore (mPTP),[33] may provide more insight into the underlying mechanisms of mitochondrial $O_2^{\cdot-}$ production that contributes to cardiac disease pathogenesis.

Uncoupled NOSs as a source of $O_2^{\cdot-}$ in the human heart

NOSs are enzymes known to exist in two states, coupled or uncoupled, and exist as homodimers with monomers consisting of a reductase and oxygenase domain each (Figure 1.4).[34] In a coupled state, NOSs catalyse the conversion of L-arginine to L-citrulline by transferring electrons from flavins on the reductase domain to heme iron on the oxygenase domain, generating NO which plays an important role in signalling.[34] On the other hand, NOSs can be uncoupled, in which case the electrons that were coupled to L-arginine oxidation instead are transferred from the reductase domain to O_2 (one-electron reduction), turning NOS into a source of $O_2^{\cdot-}$ rather than NO.[34] Uncoupled NOSs are another crucial enzymatic source of $O_2^{\cdot-}$ in the heart in disease states.

NOS Isoforms

In addition to the coupling status of NOSs determining its role in physiological signalling versus disease mechanisms, isoforms of NOS exist in the heart with distinct roles that are being explored in the regulation and localization of myocardial redox signalling. Two isoforms, endothelial (NOS1, eNOS) and neuronal (NOS3, nNOS), are constitutively expressed in cardiomyocytes, with eNOS primarily localized to caveolae of the sarcolemma membrane and nNOS predominantly to the sarcoplasmic reticulium.[34-36] eNOS is also found largely in endothelial cells. Another isoform of NOS, inducible (NOS2, iNOS), has been detected in the failing heart and other disease states, activated by inflammatory cytokines.[36]

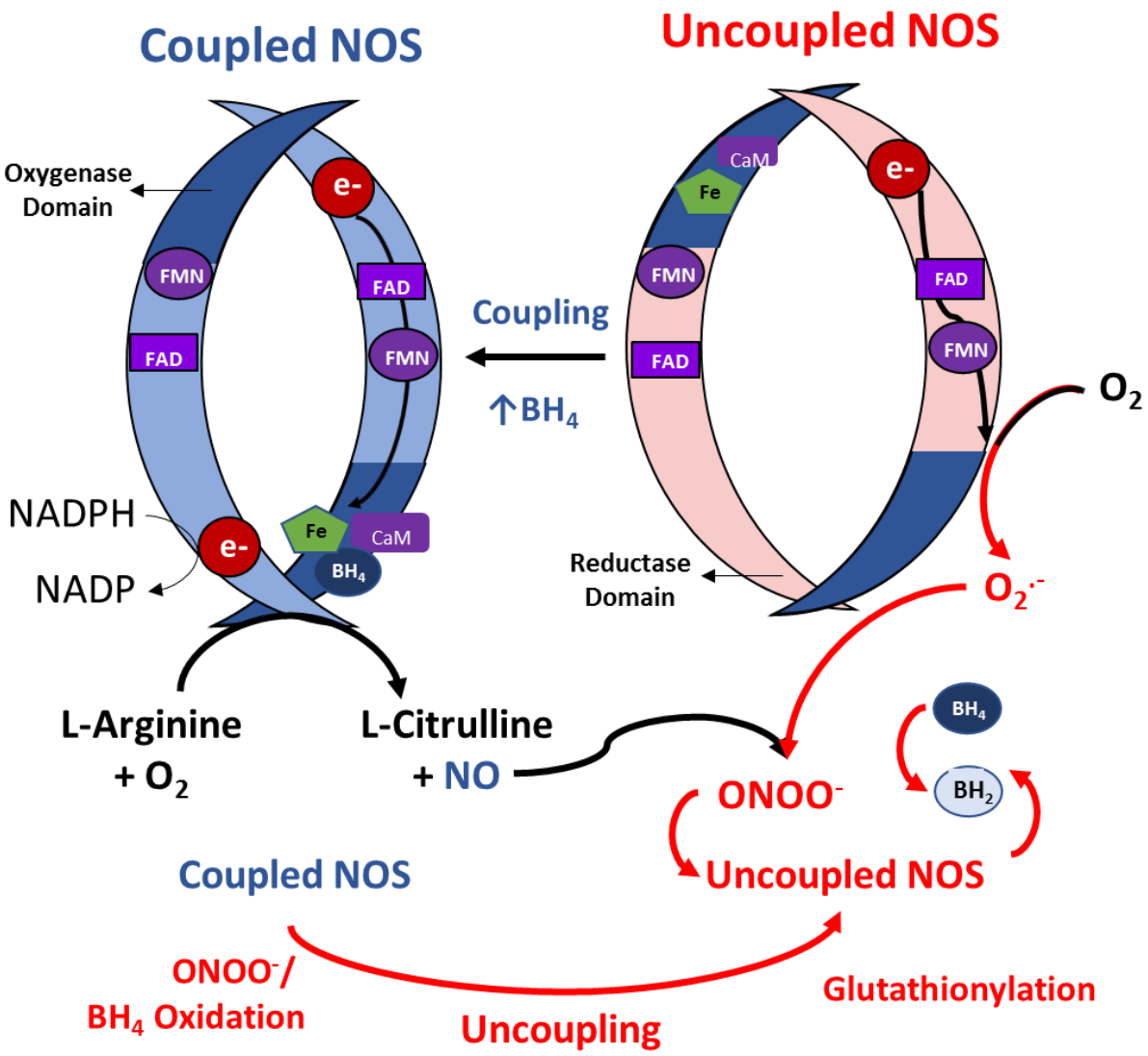


Figure 1.4 Uncoupled Nitric Oxide Synthases in Myocardial Oxidative Stress

Nitric Oxide Synthases (NOSs) are key enzymes in physiological signaling in the heart, generating NO as a by-product of the conversion of L-arginine to L-citrulline. NOS-derived NO is an important signaling molecule in the heart. However, NOSs can contribute to myocardial oxidative stress when they are 'uncoupled', turning NOSs into a source of $O_2^{\cdot-}$ rather than NO. NOS uncoupling is known to mediated by a few different mechanisms including oxidation of BH_4 or posttranslational modification S-glutathionylation. These processes in some cases are reversible and uncoupled NOSs can become coupled again. However, the scavenging of $O_2^{\cdot-}$ by NO leads to the generation of $ONOO^-$ which can also oxidize BH_4 and induce uncoupling of NOSs in a vicious cycle. The key NOS isoforms expressed in the heart include nNOS, eNOS, iNOS in the heart which have localization in different cells. Current cardiovascular therapeutics targeting NOS biology include sapropterin and better understanding of NOS biology may open new avenues for cardiovascular medicine. Figure recreated based on several NOS-based papers.[19,34,37,38]

The distinct role of these different isoforms in cardiac disease are still being explored.[36] Of the different NOS isoforms, nNOS (NOS3) in particular has been shown to have a protective role in the heart.[28] For example after myocardial infarction, the presence

of NOS3 in wildtype mice (compared to $NOS3^{-/-}$ mice) led to improved LV dilation and contractility.[28] Furthermore, reduced nNOS gene expression (a result of upregulation of micro-RNA 31) contributes to atrial fibrillation mechanisms including electrical remodelling.[39] The subcellular presence of nNOS in the sarcolemma membrane has been shown to have potential protective effects, corroborating early findings that NO diffusion is limited and its local production mediates its targets.[40] The isoform, nNOS, may in turn regulate beneficial effects of eNOS through posttranslational modifications, further implicating these enzymes as potential therapeutic targets.[41,42]

Regulation of NOSs: Several mechanisms are known to regulate NOS uncoupling which leads to the generation of $O_2^{\cdot-}$. Oxidation of NOS cofactor tetrahydrobiopterin (BH_4) into dihydrobiopterin (BH_2), as indicated by altered BH_4 levels and BH_4:BH_2 ratios, is one such uncoupling mechanism.[34] As a critical cofactor that binds to NOS at its intersection, BH_4 stabilizes NOS dimers while also facilitating electron transfer; therefore its oxidation prevents electrons from flowing to the oxygenase domain.[34] This oxidation of BH_4 cofactor uncouples NOS and turns it into a source of $O_2^{\cdot-}$; $O_2^{\cdot-}$ in combination with NO can form $ONOO^-$ which can oxidize BH_4 in a vicious cycle leading to increased oxidative stress, uncoupled NOSs, and further oxidation of BH_4. As such, the reduced state of BH_4 is critical to maintain. Improvement in NOS coupling in vessels has been demonstrated through scavenging of $ONOO^-$ (by 5-methyltetrahydrofolate, a circulating form of folate), protecting BH_4 from oxidation.[43] The generation of BH_4 is catalysed by several enzymes which may also may be mediated to influence the coupling status of NOSs. The rate-limiting enzyme in the generation of BH_4 is guanosine triphosphate cyclohydrolase I (GTPCH) which catalyses the conversion of guanosine-5'-triphosphate (GTP) to 7,8-dihydroneopterin triphosphate in what is known as the *de novo* synthesis of BH_4.[34,44] BH_4 can be recycled back from BH_2 by dihydrofolate reductase (DHFR).[44] An

alternative pathway for BH_4 generation is through sepiapterin reductase's (SPR) conversion of sepiapterin; however this latter pathway may be less important as the substrate sepiapterin is not considered to be endogenously synthesized by human cells in large amounts.[44]

In addition to oxidation of BH_4, there are other proposed mechanisms for uncoupling NOSs. One such mechanism of eNOS uncoupling is S-glutathionylation of cysteine residues, whereby a tripeptide glutathione (GSH) group attaches to cysteine residues on eNOS, leading to $O_2^{\cdot-}$ generation from NOS flavins;[34] how the posttranslational modification S-glutathionylation leads to $O_2^{\cdot-}$ generation from flavins is not entirely clear. It has also been shown that reduced substrate L-arginine, accumulation of asymmetric dimethylarginine (ADMA), and reduced Thr495 phosphorylation are associated with uncoupling of NOSs, but this has not been continued to be predominantly explored as major uncoupling mechanisms of NOSs.[45,46]

While utilizing mechanisms to couple NOSs *in vivo* would indeed seem to be a promising area of research for clinical application to target $O_2^{\cdot-}$ production in the heart and modulate myocardial redox state, there are limitations. For example, BH_4 (through treatment with sapropterin) in a small clinical trial in patients with coronary artery disease was not effective in increasing vascular BH_4:BH_2 levels or improving endothelial function; similarly in an experimental model of chronic heart failure, BH_4 supplementation did not improve myocardial BH_4:BH_2 ratios.[44,47] BH_4 given exogenously may have been oxidized before even exerting its effect with the oxidation preventing improvement in NOS coupling.[44] Therefore, an endogenous modulation to increase BH_4 (e.g. through increasing the expression of GTPCH, *unpublished Professor Casadei's laboratory*, or the endogenous production of a reducing molecule that reduces BH_4) may have beneficial effects.

Furthermore, activation of NOSs may provide another method of regulation of the enzyme. Activation of NOSs can occur regardless of coupling status (coupled or uncoupled NOSs) through increased phosphorylation at Ser1177 (or Ser1179) or reduced phosphorylation at Thr495. Activation of coupled NOSs lead to increased NO production while activation of uncoupled NOSs lead to greater generation of $O_2^{\cdot-}$. Thus, ideally, therapeutic strategies may aim at recoupling NOSs and activating these recoupled NOSs.

Importance of NOSs: Role of NO Signalling in the Healthy Myocardium and $O_2^{\cdot-}$ Production in Diseased Myocardium

Species like NO and/or the combination of $O_2^{\cdot-}$ and NO to generate $ONOO^-$ are crucial to monitor for a complete understanding of myocardial redox signalling. Indeed, NO bioavailability and signalling and changes in NOS expression, subcellular localization, or activity have been shown to play a role in heart failure, atrial fibrillation, ischemia-reperfusion injury, and other cardiac pathologies.[40,44] In addition to the important role of NOS-mediated NO production, $ONOO^-$ has also been shown to cause damage through reduced NO signalling and direct oxidative damage on cells (e.g. damage to cellular membranes), playing a role in myocardial ischemia-reperfusion injury and other cardiac pathologies.[48,49,50] In a clinical setting, myocardial redox state in humans has been shown to be relevant to cardiac disease: a study in humans demonstrated that basal myocardial $O_2^{\cdot-}$ and $ONOO^-$ are important predictors of post-operative atrial fibrillation and length of hospital stay.[6] Indeed, maintaining myocardial redox state balance would be beneficial for cardiac disease pathogenesis.

Other known sources of $O_2^{\cdot-}$ and ROS

In addition to the main sources of $O_2^{\cdot-}$ described above, other sources of $O_2^{\cdot-}$ and ROS include lipoxygenase, myeloperoxidase, xanthine oxidase, cytochrome P450 reductases, and cyclo-oxygenases.[7,16] Lipoxygenases catalyse the oxidation of fatty acids

and myeloperoxidases catalyse the formation of reactive hypohalous acids (Cl^-, Br^-, I^-) that can also contribute to the oxidation of lipids.[7] Xanthine oxidases (XO) are also key sources of $O_2^{\cdot-}$; XO generates $O_2^{\cdot-}$ as a by-product of catalysing the conversion of hypoxanthine to xanthine to uric acid and the enzyme itself is formed by the oxidation of the enzyme xanthine dehydrogenase.[7] This latter example suggests that sources of ROS and $O_2^{\cdot-}$ may be under redox-sensitive regulation and their function may vary in conditions of oxidative stress. Inflammatory cells are also a key source of $O_2^{\cdot-}$ and can contribute to myocardial oxidative stress, particularly when antioxidant defence mechanisms in the heart are overwhelmed.

1.1.4 Antioxidant Defence Mechanisms and Biomarkers of Oxidative Damage

Antioxidant defence systems in the heart help regulate myocardial redox state; however, when these defences are not working properly or are overwhelmed due to uncontrolled ROS production by prooxidant sources, this may contribute to oxidative stress and disease pathogenesis. In the heart, antioxidant systems include both non-enzymatic and enzymatic systems.[27] Non-enzymatic antioxidant defence systems include antioxidants themselves, like vitamins C and E, uric acid, and glutathione (GSH).[27] The ratio of glutathione in its reduced form to oxidized from (GSH:GSSG) is particularly indicative of the redox status of the cell and myocardium.[9]

Enzymatic antioxidant defence systems in the heart include SOD, catalase, thioredoxins (Trx), peroxiredoxins (Prx) and glutathione peroxidases (GPx).[27] SOD which catalyses the conversion of $O_2^{\cdot-}$ to H_2O_2 has several known isoforms (SOD1-3) located in various parts of the cell.[7] SOD1 is located in the intermembrane space of the mitochondria and the cytosol, SOD2 is located in the mitochondrial matrix, and SOD3 is connected to the extracellular matrix.[51] Due to the important biological role SOD plays,

SOD mimetics have been tested in experimental models and have met with success, particularly in reducing injury after myocardial ischemia-reperfusion injury.[52] Another antioxidant enzyme, catalase, rapidly metabolizes H_2O_2 to water (H_2O); thioredoxins and glutathione peroxidases also catalyse the conversion of H_2O_2 to H_2O.[11] The interconversion of ROS is also catalysed by chemical reactions; for example, H_2O_2 can also generate $HO^{\cdot}$ through the Fenton reaction.[7] Heme oxygenase may also mediate antioxidant defence mechanisms.

These members of the antioxidant defence try to maintain a balance in ROS. What is the maximum capacity of these defence systems? At what point they will be overwhelmed? In disease, do they have a reduced capacity that leads to oxidative stress contributing to disease? These questions are being explored to better understand if targeting antioxidant systems in the body may prove beneficial. Non-enzymatic systems have been targeted (e.g. increasing vitamins and GSH through antioxidant treatments) but with little success, possibly due to the lack of specificity to regional increases in ROS production (Section 1.1.5). A more nuanced approach examining and targeting the sources of ROS that overwhelm the antioxidant defence may be one approach to solving this problem. Oxidative damage in the cardiovascular system can be assessed by changes in stable oxidation products like 4-HNE, MDA, isoprostanes, and GSH:GSSG ratios.

1.1.5 Potential Therapeutic Targets in Cardiac Disease

Given the importance of myocardial redox state, among the numerous therapeutic strategies that have been developed thus far to target cardiac disease mechanisms, several have aimed at targeting myocardial redox state in clinical practice. Medications that have become widespread in the therapeutic strategy against cardiac disease include statins, angiotensin converting enzyme inhibitors (ACEi), angiotensin II receptor blockers (ARB) and recently angiotensin receptor-neprilysin inhibitor (ARNI), many of which have

indirect effects on myocardial redox state (Figure 1.5). Cardiovascular medications particularly aimed at myocardial redox state include BH_4, scavengers of $O_2^{\cdot -}$, folate fortification, and antioxidant vitamins.

Conventional medications and redox state: Statins, ACEi, and ARBs

Statins are lipid-lowering drugs with anti-inflammatory and antioxidant properties. They are known for their important role in lowering low-density-lipoprotein (LDL) cholesterol through inhibition of 3-hydroxy-3-methylglutaryl coenzyme A (HMG-CoA).[53] This lowering of LDL cholesterol modulating lipoprotein metabolism has beneficial effects; however, it is statins' pleiotropic effects, particularly its anti-inflammatory proprieties and effects on the mevalonate pathway independent of its lipid lowering related effects, that have been shown to be important in redox state.[53] Prevention of isoprenylation of small guanosine triphosphate (GTP)-binding proteins (e.g. Rac) has been shown to prevent Rac1 activation and lower $O_2^{\cdot -}$ production from NADPH oxidases (Nox2) in human atria.[23,53] Statins were shown to exert similar effects when administered pre-operatively, suppressing NADPH oxidase-derived myocardial $O_2^{\cdot -}$ production, likely through Rac-1 inhibition.[6] Statins have also been considered to possibly increase BH_4 bioavailability and reduce ADMA levels, thereby improving NOS function and possibly reducing risk for atrial fibrillation.[54] In terms of inflammatory effects, statins also reduce expression of pro-inflammatory cytokines (e.g. TNF-α, IFN-γ) while increasing expression of anti-inflammatory cytokines (e.g. IL-10) in the heart, possibly contributing to prevention of fibrotic and hypertrophic cardiac pathogenesis.[53] However, a recent trial (the STICS trial) has shown statin therapy given up to eight days before cardiac surgery and five days after to be ineffective at reducing primary or secondary cardiovascular outcomes, suggesting more understanding is needed of statins' perioperative effect.[55]

ACEi (e.g. enalapril) and ARBs belong to a class of renin-angiotensin system (RAS) targeting drugs that have been used as a first line of defence against cardiac disease pathogenesis, particularly heart failure, and affect inflammation-related and redox-sensitive pathways.[56,57] ACEi, which inhibits the enzymatic conversion of angiotensin I to angiotensin II (AngII), aim to prevent production of AngII due to its pleiotropic effects on activation of pro-oxidant enzymes like NADPH oxidases, apoptotic signalling through ASK1, and effects on hypertrophy signalling pathways.[58] However, it has been shown that AngII is produced through an alternate pathway despite ACE inhibition, known as the "angiotensin escape phenomenon."[56] As such, antagonists against downstream angiotensin receptors (AT_1-receptors) have been developed, known as angiotensin receptor blockers (ARBs).[56] ARBs targeting AT-receptors also have been shown to modulate PPAR-γ which is important in signalling in the heart and thus may partly mediate therapeutic effects of ARBs.[56] Both ACEi and ARBs have been shown to be effective in randomized clinical trials, with ACEi reducing total and cardiovascular mortality in patients with heart failure and ARB therapy reducing cardiovascular risk.[56,59]

Medications aimed at myocardial redox state: BH_4, scavengers of $O_2^{\cdot -}$, and antioxidants

BH_4 has recently been examined as a potential therapeutic for cardiac disease due to its crucial role in NOS uncoupling as an essential cofactor for NOSs. Acute and chronic treatments of BH_4 have been tested in clinical trials; acute treatment has been shown to improve vasorelaxation properties of the endothelium and acute forms using supra-physiological concentrations have suggested that BH_4 has nonspecific scavenging effects, particularly scavenging ROS.[60] These findings suggest that BH_4 supplementation acutely may exert beneficial effects. On the other hand, chronic supplementation of BH_4 has also been tested in clinical trials and has not proven very effective. Indeed, long-term BH_4 supplementation (in the form of sapropterin hydrochloride, or 6R-BH_4 or Kuvan) did not

exert beneficial effects in several clinical trials, including those examining its role in peripheral artery disease.[61] There are several explanations as to why the effects of long-term BH_4 were limited, including increases in BH_4 also led to increases in BH_2 particularly due to BH_4 oxidation and BH_4 was oxidized in the long-term before it could exert its effects.[61] As such, while the approach to target NOSs and myocardial redox state are indeed possible therapeutic strategies, chemical obstacles need to be overcome. BH_4 has been shown to be increased by drugs currently used including statins and folic acid.[61]

Scavengers of $O_2^{\cdot-}$ and $ONOO^-$ including *N*-acetyl-*L*-cysteine (NAC), Tempol (and mitochondria specific Mito-Tempol), 1,2-dihydroxybenzene-3,5-disulfonate (Tiron), and uric acid have been used to target oxidative stress.[62] While NAC has been shown to be effective at reducing oxidative stress in the heart evidenced by changes in 8-iso-prostaglandin-$F_2\alpha$,[63] NAC did not show beneficial effects in clinical outcome (e.g. myocardial infarction, duration of hospital stay) post-cardiac surgery,[64] suggesting its limitations. Tempol has also been shown to have some beneficial effects in the heart, reducing infarct size after myocardial ischemia-reperfusion, but it is not clear if tempol exerts these effects through the direct scavenging of $O_2^{\cdot-}$ or $OH^{-}\cdot$.[65] Part of the reason these scavengers may not be potential therapeutic strategies returns to the idea that ROS play an important role in signalling so scavenging all ROS may actually lead to harmful signalling effects. Rather than scavenging all ROS production given the physiological role of ROS signalling, understanding and targeting what regulates the enzymatic sources of $O_2^{\cdot-}$ in localized compartments may result in a plausible therapeutic approach. Increasing antioxidant defence via vitamins (mimicking endogenous antioxidant defence systems that may get overwhelmed) was also examined as a potential target.

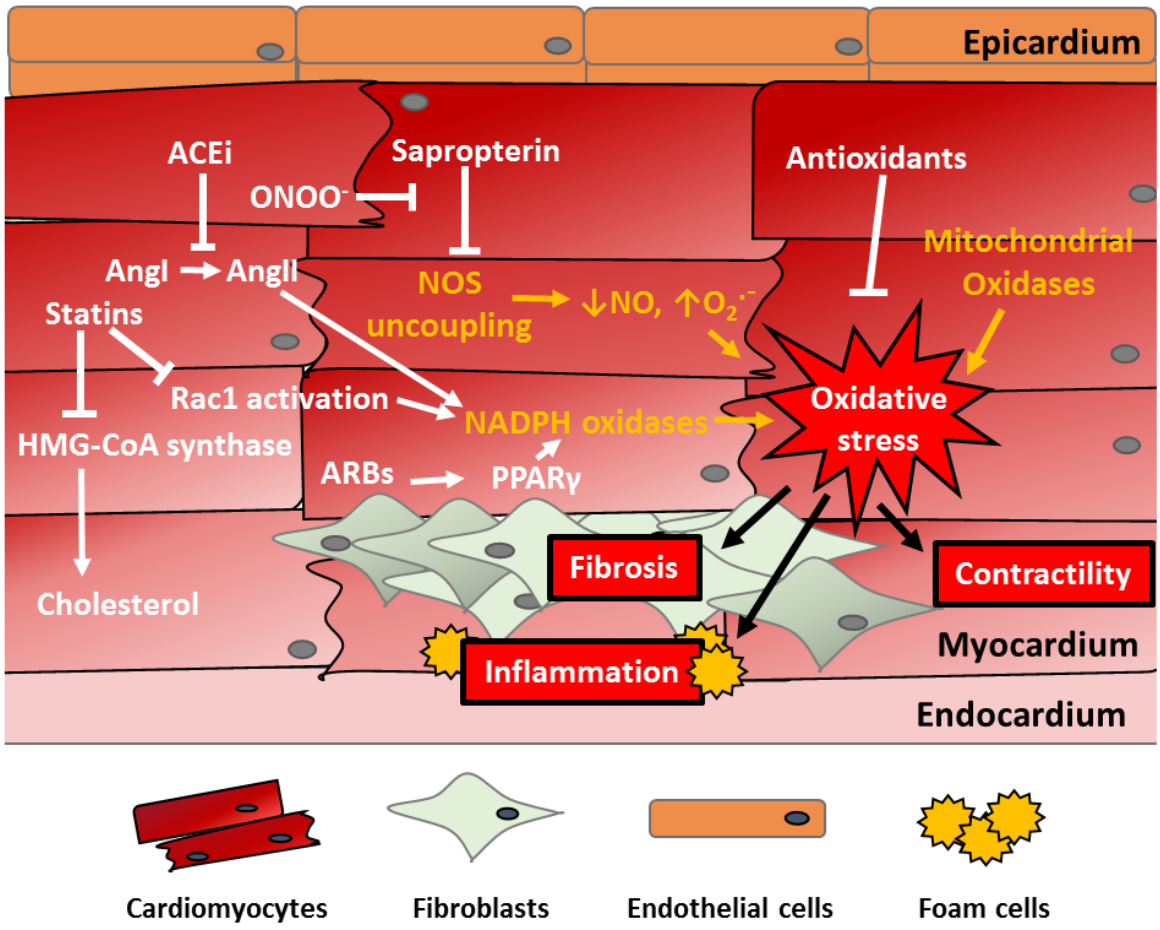


Figure 1.5 Proposed Therapeutic Strategies Targeting Myocardial Oxidative Stress

The 'reduction-oxidation' environment described by ROS is known as myocardial 'redox' state, and this state takes into account pathological, or excess, ROS accumulation known as oxidative stress as well.[7,12] The balance of ROS and antioxidants determines the redox state of the heart. Increases in ROS, compartmentalized or from particular sources, or overwhelming antioxidant defence systems can lead to myocardial oxidative stress. Myocardial oxidative stress contributes to a variety of cardiac disease pathologies including heart failure, hypertrophy, and arrhythmias. Impaired ROS (and RNS signalling) in the heart contributes to cardiac disease pathogenesis. ROS, and particularly $O_2^{\cdot-}$, from sources like uncoupled NOSs, NADPH oxidases, and the mitochondria in turn affect processes like metabolism and contractility. Antioxidants play a role in modulating ROS levels but these systems can be overwhelmed. Previously proposed therapeutic strategies against myocardial oxidative stress are also described. ACEi, Sapropterin/Tetrahydrobiopterin (BH_4), antioxidants, folic acid, statins, and ARBs have all been proposed as possible strategies to target oxidative stress in the myocardium. These therapeautic strategies may affect key processes in the heart including fibrosis, contractility, and inflammatory response, through the modulation of oxidative stress in the heart. Epicardium or the visceral pericardium is shown anterior to the myocardium while the endocardium is depicted posterior. *ACEi: Angiotensin converting enzyme inhibitor; ARB: angiotensin receptor blocker; Ang I: Angiotensin I; Ang II: Angiotensin II; HMG-CoA synthase: Hydroxymethylglutaryl-CoA synthase; ROS: reactive oxygen species; PPARγ: Peroxisome proliferator-activated receptor gamma.*

Vitamins/Antioxidants and Why "Antioxidants" have not worked

In the past few decades, it is antioxidant vitamins that may have raised the most hopes as therapeutic targets against myocardial oxidative stress but have been the most disappointing in clinical trials (Figure 1.6). Various vitamins, include Vitamin A, B (B_6 and B_{12}), C (ascorbic acid), D, E, and Beta-carotene, have been tested and have not shown promising results.[66] Vitamin C has not been shown to be associated with reduced cardiovascular events though it was suggested to have antioxidant effects that may affect cardiovascular outcome.[1] Vitamin E has eight different forms and its efficacy may be related to which form is tested but it seems more unstable forms have been used in studies.[1] Beta carotene supplementation also has largely been ineffective, despite natural foods with beta carotene being associated with positive outcomes,[1] suggesting an important difference between antioxidant supplementation and antioxidants coming from natural foods. Meta-analyses have largely concluded that antioxidant vitamins may not be the optimal therapeutic approach against myocardial oxidative stress.

Modulation of oxidative stress has been shown to be effective in basic science research while failing in large scale clinical trials. Does this mean oxidative stress does not play a causal role in cardiovascular disease that can be modified to reduce risk and outcomes? It has been hypothesized that the antioxidants in these clinical trials have not worked for various reasons: first, using general antioxidants may impair physiological redox signalling in the heart. It has more recently been thought that vitamins likely do not scavenge $O_2^{\cdot -}$ with kinetics fast enough to prevent $O_2^{\cdot -}$ from reacting with NO to product $ONOO^{-}$.[27] Moreover, these vitamins are likely not targeted to the major sources of ROS like the mitochondria, also preventing their ability to reduce oxidative stress.[27]

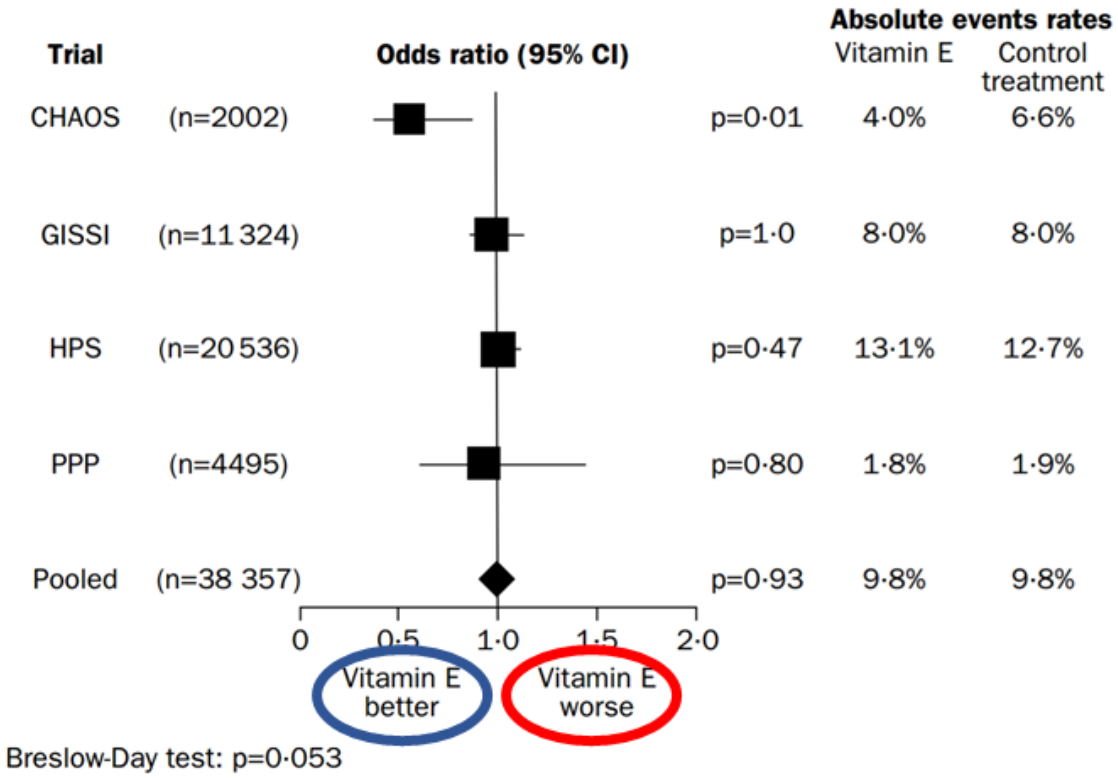


Figure 1.6 Meta-Analysis of Antioxidants in Cardiovascular Clinical Trials

The forest plot indicating odd ratio of antioxidants in a variety of studies occurring between years 1990 and 2006 assessing cardiovascular risk is shown in a meta-analysis. The odds ratios of Vitamin E on cardiovascular outcome and myocardial infarction in several trials is pooled and suggests there is no clear benefit of Vitamin E in these outcomes.[67]

In addition, it is thought that the patients included in most trials were patients with advanced stages of disease, and these advanced stages may lead to irreversible changes, masking potential benefits of antioxidants.[18] Antioxidants may have beneficial effects in primary prevention. Moreover, the literature varies in terms of the dosages of antioxidants given and this may also play a role.[18] Finally, it is also hypothesized that the scavenging of ROS may lead to the generation of other ROS, still corroborating to the problem of an overwhelmed endogenous antioxidant defence system.[18] New knowledge of the importance of physiological ROS signalling suggests that a more nuanced approach in modulating sources of oxidative stress locally and specifically may have beneficial effects. While antioxidants may mimic endogenous antioxidant defence systems, it is not

clear if the antioxidants reach the local increased production of $O_2^{\cdot-}$ or get overwhelmed, suggesting a potential need to target ROS sources directly.

1.1.6 The Unmet Need: To Target Myocardial Redox State using Novel Approaches

While myocardial oxidative stress has been shown to be implicated and contribute to cardiac disease, and certain therapeutic targets as mentioned have shown beneficial effects, large-scale clinical trials of antioxidants to reduce ROS have not been tremendously successful in lowering cardiac disease risk and prognosis,[9] suggesting our approach needs additional nuance. Moreover, a recent trial (the STICS trial) has shown statin therapy given perioperatively to be ineffective at reducing primary or secondary cardiovascular outcomes, as described earlier in Section 1.1.5.[55] Indeed, it is now clear that new strategies are needed to target myocardial redox state as very few of the above strategies tested in randomized clinical trials have been effective. It is clear that targeting myocardial redox state as suggested by experimental models may need to be far more nuanced. To identify novel therapeutic strategies to target cardiac disease pathogenesis, however, a better understanding of endogenous mechanisms regulating myocardial redox state are needed.

Understanding better the endogenous mechanisms regulating myocardial redox state

Current tools to begin addressing cardiac pathologies beyond antioxidants and statins include interventions ranging from multidrug regimens described earlier (e.g. β-blockers, ACEi) to surgeries (e.g. coronary artery bypass graft) to implantation of devices (e.g. defibrillators).[1] These specific tools, however, are limited by our understanding of the underlying mechanisms of cardiac disease, like arrhythmias and heart failure.

For example, arrhythmias, which are characterized by an irregular rhythm of the heart, are thought to be regulated by the heart's electrical system: electrical signals, which

pass from the sinoatrial node to the right and left atria through the atrioventricular node, bundle of His, to the ventricles, are thought to mediate the contraction and relaxation of the heart's four chambers.[68] As such, when the electrical system is disorganized or disrupted as is the case in arrhythmias, medical procedures like electrical cardioversion, catheter ablation, implantation of a pacemaker or implantable cardioverter defibrillator (ICD), or Maze surgery aim to restore the electrical signals and rhythm of the heart.[68] Furthermore, medications like calcium channel blockers (CCB) and β-blockers aim to interfere with the flow of calcium in the heart and reduce heart rate, respectively.[68] While these tools have brought about positive outcomes, they do not necessarily target the root cause of arrhythmias and more specific tools can be developed when we better understand their cause.[69]

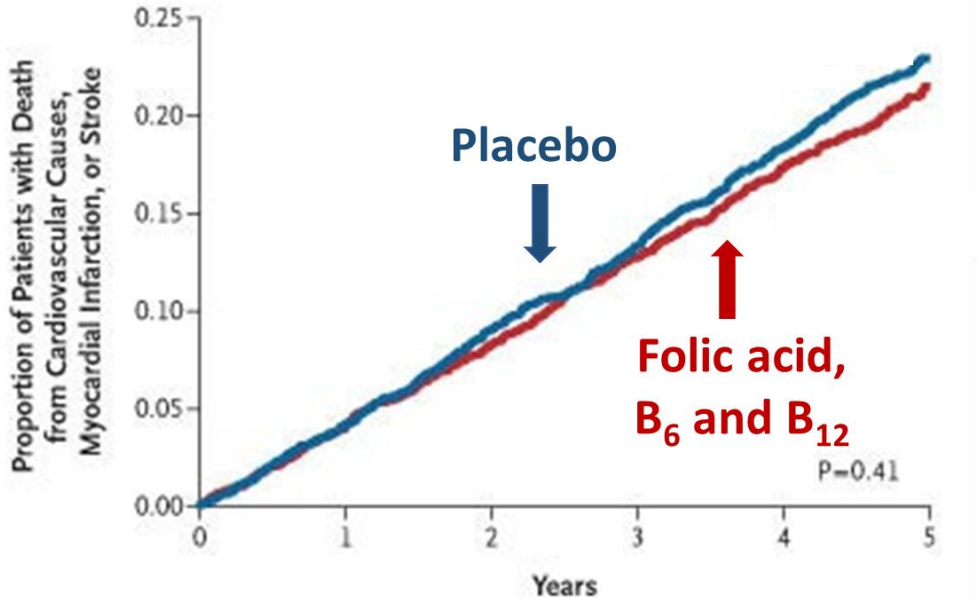
Indeed, like arrhythmias, the underlying mechanisms that lead to heart failure or weakening of the heart's ability to fill or contract are still unknown. Drugs like ACEi, angiotensin receptor blockers (ARBs), and aldosterone antagonists are used to reduce the workload of the heart,[68] yet, again, these current treatments are limited by our understanding of the disease. In order to develop further treatment options (both cost-effective and targeted) and to prevent these diseases, we crucially need a better and more clear understanding of the pathophysiology and the mechanisms behind these diseases: how do they develop, how are they sustained, what exacerbates their conditions? Thus, we need new strategies to target myocardial redox state because current strategies as evidenced by clinical trials are not sufficient.

1.2 Hydrogen Sulfide (H_2S) as a Regulator of Redox Signalling

In observational clinical trials, homocysteine (Hcy) has been shown to be a strong risk factor for cardiovascular disease, and it was thought that reducing plasma Hcy levels with Folic Acid/Vitamin B_9 (and other cofactors) may have beneficial effects.[1,70] Corroborating this hypothesis, in observational studies, lowering Hcy levels was associated with lower risk of coronary heart disease: specifically 25% lower Hcy was associated with approximately 11% reduced risk for coronary heart disease.[1]

However, folic acid supplementation has been shown to have limited associations with cardiovascular risk, despite its Hcy-lowering effects (Figure 1.7).[71-73] In one study, it has been shown that folic acid may lead to 19% lower Hcy levels, yet demonstrates little effect on cardiovascular risk, suggesting Hcy may be a biomarker but may not be a causative agent for the correlations seen between Hcy and cardiovascular risk or that folic acid may have additional effects that counterbalance the Hcy-lowering effects.[1] In a meta-analysis of twelve folic acid supplementation clinical trials taking place, folic acid supplementation did not improve cardiovascular risk.[73]

Basic science and translational experiments suggested that folic acid supplementation may have direct effects on vasculature that are not captured by the large randomized clinical trials conducted; for example, 5-MTHF, the circulating form of folate, scavenges $ONOO^-$ directly and leads to improved coupling of NOSs independent of Hcy.[43,74,75] Do these findings suggest homocysteine biology is not directly involved in cardiovascular disease (and is not a modifiable risk factor in cardiovascular disease that can lead to improved clinical outcomes)? Or is homocysteine a surrogate for another metabolite that plays a causal role in cardiovascular disease?



Number at Risk in Year	0	1	2	3	4	5
Placebo	2764	2633	2481	2327	2180	948
Folic acid, B_6, and B_{12}	2758	2633	2479	2330	2179	965

Figure 1.7 Folates, Vitamin B_6, and Vitamin B_{12} Treatment and Cardiovascular Death

The HOPE2 Clinical Trial was conducted to examine the effects of Folate, Vitamin B6, and Vitamin B12 on improving cardiovascular outcome. These Kaplan-Meier estimates show there was no benefit of this treatment compared to placebo. Cardiovascular clinical trials lowering homocysteine levels failed to reduce cardiovascular risk in patients. While many theories are proposed, the clinical trials suggest a better understanding of homocysteine biology is necessary. Figure modified from *New England Journal of Medicine.*[76]

To begin understanding this biology, it is important to first understand how folic acid lowers Hcy levels (Figure 1.8): Folic acid (or Vitamin B_9) is a key player in biosynthetic pathways in the body. It is known that dietary folic acid is reduced to dihydrofolate (DHF) and tetrahydrofolate (THF) by DHF reductase (DHFR).[77,78] THF, which is converted to N5,N10, methylene-THF can be converted back to DHF via thymidylate synthase or can be converted to 5'-methyl-THF by methylene tetrahydrofolate reductase (MTHFR).[77] The production of methyl-THF is important to homocysteine metabolism, as methyl-THF can be converted back to THF by vitamin B_{12}, which removes the methyl group from methyl-THF and adds it to homocysteine to

generate methionine.[77] As such, folic acid may reduce Hcy levels through its support of Hcy conversion to methionine. Homocysteine levels associated with increased cardiovascular risk in observational studies may be critically examined not for a causal relationship between homocysteine and cardiovascular risk but rather with homocysteine as a surrogate for other homocysteine-related metabolites (e.g. H_2S) playing a causal role in reduction in cardiovascular risk. H_2S biology may provide new insight into our understanding of cardiac disease pathogenesis.

1.2.1 H_2S as a Physiological Molecule in Humans and the Cardiovascular System

H_2S has been shown to play wide-ranging roles in numerous organs of the body, including the heart, vessels, adipose tissue, pancreas, brain, liver, kidneys, gastrointestinal tract, and brain. In the cardiovascular system, H_2S has specifically shown to play an important role in angiogenesis and vasorelaxation in vasculature and in metabolism of the heart. This widespread role of H_2S has been partly attributed to its biological and chemical properties that allows it to be a wide-ranging signalling molecule.

H_2S has unique biological and chemical properties that make it an important physiological signalling molecule (Table 1.1). In literature, H_2S is used to describe three species that exist in physiological conditions, namely H_2S, HS^-, and S^{2-}.[79] There are studies that attempt to distinguish these ionic species; for example one study suggests that hydrogen sulfide anion (HS^-) has distinct nucleophilic properties compared to H_2S and it is the anion that is responsible for posttranslational modifications.[80] However, further chemical examination of the monobromobimane and bis-S-bimane methods utilized in the study to measure these species are needed to determine whether the specific role of the anion can indeed be distinguished from the gaseous molecule H_2S.[80] In most cases, it is

broadly H_2S as the non-ionic species, in equilibrium with the other two species, that is recognized as a key gasotransmitter (or gaseous transmitter) alongside NO and CO.[79]

H_2S as a molecule is considered to be a small gas that is endogenously generated by key enzymes in the body, is able to cross membranes without relying on membrane receptors, and has specific physiological functions and specific cellular targets; these criteria which were used to define gasotransmitters NO and CO now define H_2S as one.[81] In particular, H_2S is unique in that it is able to cross lipid membranes and is soluble in aqueous solutions, with a half-life of minutes in biological systems.[79,82] It is these qualities that are considered to help define and recognize H_2S as a key signalling molecule. Although these chemical and biological properties allow H_2S to be a physiologically relevant molecule, it continues to be important to recognize that H_2S production and oxidation in biological environments may change rapidly, and monitoring H_2S poses its own challenges.

H_2S circulates as a gas but is also known to be stored in cells in two primary groups: (1) acid-labile sulfur and (2) sulfane sulfur.[82] In the former group, H_2S is considered to be bound as iron-sulfur complexes, and it is under acidic pH (pH<5) that these complexes release H_2S known as acid-labile sulfur.[82] Sulfane sulfur, on the other hand, is known as sulfur bound to sulfur (e.g. thiols on cysteine residues in protein).[83] Particular examples of sulfane sufur, or bound sulfane sulfur, include persulfides (R-S-SH), polsulfides, thiosulfate, elemental sulfur, and others.[82] Some of these stores release H_2S in changing environments, like reducing conditions.[82,83] As such, it is thought that the bound sulfane sulfur pool may be redox-sensitive, particularly releasing H_2S depending on the presence of redox-sensitive compounds like glutathione that create a reducing environment for the cell to release H_2S.[82] It is now more widely recognized that free H_2S

can be released to act as a signalling molecule through both of these stores. These stores are important sources of H_2S signalling molecule.

Table 1.1 Biologically-Relevant Physical, Chemical, & Toxicological H_2S Properties

H_2S Gaseous Properties		
Molecular mass	34.08 g/mol	Wang et al. (2012)
Half-life	12 – 37 h in air	Wang et al. (2012)
	Order of minutes In biological systems	Polhemus et al. (2014a)
Acid dissociation constant (pK_a)	pK_{a1} = 6.76 (at 37°C) pK_{a2} > 12 (at 37°C) $H_2S \longleftrightarrow HS^- + H^+ \longleftrightarrow S^{2-} + 2H^+$	Liu et al. (2012) Wang et al. (2012)
Ratio of H_2S/HS^-	50% H_2S: 50% HS^- (biological tissues) 20% H_2S: 80% HS^- (plasma, extracellular fluid)	(Wang, 2012)
Solubility	Amphipathic Lipophilic: 1g of H_2S in 94.2 mL ethanol (EtOH) 1g of H_2S in 48.5 mL diethyl ether $(C_2H_5)_2O$ Water-soluble: 1g of H_2S in 242 mL water (H_2O)	Liu et al. (2012) Wang et al. (2012)
Tolerance	0.1-1ppm: Threshold for sensing 10ppm: Eye irritation 27ppm: Strong odor toleration 50-100ppm: Serious symptoms (neurological, cardiovascular, respiratory) >320ppm: Serious complications and possible death	Wang et al. (2012)

1.2.2 Regulation of H_2S in the Heart: Endogenous, Enzymatic Sources

H_2S is known to be generated endogenously in the heart as a by-product of cystathionine γ-lyase (CSE), cystathionine β-synthase (CBS), and 3-mercaptopyruvate transulfurase (MST) enzymatic catalysis.[84] However, to date, it is thought that CSE may predominate in the cardiovascular system while CBS and MST contribute more prominently to H_2S production in the nervous system; as such, more focus has been given to CSE in recent years in the heart and vasculature.[85] CSE, also abbreviated occasionally in literature as CGL, is described in Section 1.3 in detail. Here we will focus briefly on CBS and MST as additional important enzymatic sources of H_2S.

CBS: CBS is a 252 kDa protein, a tetramer with subunits of 63 kDa in their non-truncated from; CBS catalyses the conversion of homocysteine and serine to cystathionine and water.[83,86] This reaction, although not responsible for generating H_2S as a by-product, is important as it is known as the 'first and committing step' of the transsulfuration pathway, an evolutionarily conserved pathway in humans.[83] Other reactions that CBS catalyzes include the catalysis of (1) cysteine and homocysteine to cystathionine and importantly H_2S, (2) two cysteine molecules to produce lanthionine and H_2S, and (3) cysteine and water to generate serine and H_2S.[83,87] Given the difference in K_m for CBS, serine 2mM and cysteine 6.8mM, CBS may have a likely preference for serine.[83] Trifluoroalanine, and aminooxyacetate (AOAA) are used for pharmacological inhibition of CBS but no selective inhibitors for CBS are currently known to have widespread use in cardiovascular clinical practice.[88,89]

CBS localization and protein regulation: CBS has been shown to be localized in the cytosol but also has been shown to be present in the mitochondria.[84] CBS may be localized in the nucleus dependent on whether it is post-translationally modified (sumolyation) by small ubiquitin-like modifier (SUMO).[83] As part of its regulation of activity, CBS uses heme as an essential cofactor, and like CSE, is also a pyridoxal-5-phosphate (PLP) dependent enzyme.[83,85] In particular, CBS heme interconverts between ferric and ferrous (Fe^{+3}/Fe^{+2}) states, with the ferrous state interacting with two other gasotransmitters NO and carbon monoxide (CO).[83] CBS activity may also be importantly modified by oxidative stress (in particular, NADPH may donate electrons to convert CBS from its ferric state to a ferrous state).[83] CBS may also be activated by donation of a methyl group to its C-terminal domain by S-adenosylmethionine (SAM, or AdoMet) and may also be stabilized by SAM.[83] CBS is encoded by its gene on chromosome 21 (21q22.3).[90]

Studies have demonstrated that CBS expression and activity is under redox-sensitive regulation. In particular, a recent study in cells has shown that CBS activity is increased by S-glutathionylation at Cys346 under conditions of oxidative stress (while protein levels were unchanged).[91] SP1 also binds to CBS promoter regions[92] and human CBS has a redox-sensitive cofactor heme.[93] Further understanding of the regulation of human CBS will also provide important insight into the regulation of endogenous H_2S.

MST: MST is a 33 kDa protein (murine) that transfers sulfur from 3-mercaptopyruvate to other groups, which can then later be released as H_2S.[84,94] In order for this transfer to occur, MST utilizes zinc as a cofactor.[84] MST is often paired with cysteine aminotransferase (CAT)/aspartate aminotransferase (AAT); CAT/AAT catalyzes the conversion of cysteine to 3-mercaptopyruvate for MST to further metabolize to pyruvate with H_2S as a by-product.[83] As such, MST and CAT, which are found in both the cytosol and the mitochondria, are considered important in H_2S metabolism as a facilitator of H_2S generation.[84] In a less well-known pathway than CAT/AAT to MST, D-amino acid oxidase (DAO) can also generate 3-mercaptopyruvate by metabolizing D-cysteine; MST metabolizes 3-mercaptopyurvate to pyruvate with the by-product of H_2S.[95] Hypotaurine, phenylpyruvate, and oxybutyrate have been used in experimental models for pharmacological inhibition of MST.[88,89,96] Selective inhibitors for mouse MST have also been recently identified in a comprehensive screening of chemical compounds, and these inhibitors lay a path forward for identification of human MST inhibitors.[97,98] Currently, no selective inhibitors for MST are known to be used in cardiovascular clinical practice.

Taken together, these enzymatic systems, primarily CSE, CBS, and MST form part of a larger signalling pathway, playing a role in reverse transsulfuration pathway and the methionine and folate cycle; methionine, homocysteine, and cysteine are key substrates with H_2S as a key by-product. They may be targets for cardiovascular

therapeutics in the future, particularly if they are dysregulated in expression or activity in cardiovascular disease. At the same time, given the prolific role of these enzymes that generate H_2S as a by-product, inhibitors of these enzymatic sources may not be specific to modulation of H_2S and may modulate other related metabolites, suggesting a more nuanced approach may be needed to target H_2S signalling.

1.2.3 Non-Enzymatic Sources and Catabolic Processes of H_2S in the Heart

In addition to enzymatic sources of H_2S in the heart, non-enzymatic sources play a minor role in the endogenous production of H_2S and catabolic processes also play a role in regulating H_2S in the heart. Specifically, it has been suggested that H_2S may be generated through the reduction of elemental sulfur (release of H_2S from sulfur-containing sources).[82] The reduction of elemental sulfur may be coupled with the oxidation of molecules like glucose and glutathione oxidation to generate H_2S.[81] In addition, H_2S may be generated by sulfur donating molecules like sulfur dioxide or sulfenic acids.[99] Dietary sources of sulfur and the metabolism of related-molecules may also be used to generate endogenous H_2S, including naturally occurring compounds like garlic and garlic-based polysulfides.[82,99,100] Bacteria have also been shown to generate H_2S.[101]

H_2S in the heart is also regulated by the catabolism of H_2S. Three key mechanisms known for the catabolism of H_2S include the oxidation, methylation, and/or scavenging of H_2S.[82] These mechanisms regulate H_2S bioavailability in the heart but it is not clear if these systems are overactive in cardiovascular disease.

Oxidation: H_2S can be oxidized to various molecules including SO_2, SO_3^{2-}, and SO_4^{2-}. Mitochondria have been shown to be a key organelle involved in the oxidation of H_2S. In particular, in the mitochondria, it is known that sulfide quinone oxidoreductase

(SQR) can initiate the first step in oxidizing H_2S through a two-electron oxidation (known as the 'canonical sulfide oxidation pathway') and ferric-heme may also mediate H_2S oxidation (known as 'heme-dependent sulfide oxidation pathway'), with both pathways leading to reduced H_2S bioavailability.[79] The mechanisms involve H_2S being oxidized to thiosulfate and then sulfite (SO_3^{2-}) and sulfate (SO_4^{2-}).[82] It is also suggested that NADPH oxidases may oxidize H_2S, leading to the production of sulfur dioxide (SO_2).[102] The importance of this latter mechanism requires further exploration.

Methylation: H_2S can be metabolized into methanethiol (CH_3SH) through an addition of a methyl group by thiol S-methyltransferase;[85] methanethiol can be further methylated to form demethylsulfide (CH_3SCH_3) by the same enzyme.[87] This mechanism also leads to reduced bioavailability of H_2S.

Scavenging: H_2S can also be used to form sulfhemoglobin from methemoglobin.[82] H_2S may also be scavenged by different ROS[103] but the kinetics, weight, and relevance of these mechanisms need further investigation in cardiac tissues.[104] It is also thought that H_2S may be scavenged by metallo-containing compounds or disulfide-containing compounds.[105]

H_2S catabolism has also been shown to relate to O_2 levels, and several hypotheses exist about the exact relationship between these two molecules. H_2S is being increasingly recognized as an evolutionarily conserved sensor of O_2, and O_2 may be a regulator of H_2S catabolism.[106] For example, one study has demonstrated that the bioavailability of H_2S negatively correlates with the partial pressure of O_2: when P_{O2} is low, there is an increase in H_2S bioavailability.[82,106] Further studies have examined a causal relationship and have suggested that, under hypoxic conditions, H_2S production is increased by CSE, and that this increase in CSE-derived H_2S is dependent on heme oxygenase-2 (HO-2).[107] Moreover, increases in H_2S production are also observed under intermittent hypoxic

conditions.[108] In addition to HO-2-dependent changes, H_2S may be reduced in the presence of O_2 as a result of increased conversion of H_2S to sulfate in the mitochondria.[109] H_2S may also be directly oxidized by O_2 but the biological significance of this reaction may be limited by kinetics.[104] These findings suggest that O_2 is intricately involved in H_2S catabolism and this process requires further exploration in physiology.[106] Taken together, several key mechanisms are in place to remove H_2S from local systems. These catabolic mechanisms may be targeted for modulating the bioavailability of H_2S with more research on these processes.

1.2.4 Modulating H_2S in the Heart via Pharmacological Donors

Currently, several pharmacological tools are implemented to provide H_2S exogenously in biological systems. H_2S donors in particular span a wide variety of categories, some representing more physiological conditions than others. Due to the volatile nature of H_2S, the specific donors used may affect the results of investigations; therefore, the specific pharmacological tool used must be taken into account when interpreting results. This will also allow for better, more accurate, and nuanced understanding of H_2S as an endogenous mediator of cardiovascular risk, cardioprotection, and disease.

Three broad categories of H_2S donors include inorganic salts, synthetic donors, and organic compounds. Inorganic salts including NaHS and Na_2S are used to increase H_2S concentrations rapidly in numerous model systems in literature, both *in vivo* and *in vitro*; these salts however are considered to be at least partially imprecise because (1) commercially sold salts have impurities that lead to polysulfide formation which may reduce H_2S concentrations and (2) the volatility of H_2S suggests these salts may provide very different concentrations of H_2S.[110] Slow-releasing synthetic donors have been developed like morpholin-4-ium 4 methoxyphenyl(morpholino) phosphinodithioate

(GYY4137), which is water-soluble and releases H_2S through a hydrolysis reaction.[110] GYY4137's structural analog which lacks sulfur (ZYJ1122)[110] is not commercially available. Organic compounds have also been developed for the release of H_2S, and these compounds include diallyl sulfide (DAS), diallyl disulfide (DADS), and diallyl trisulfide (DATS).[110] An H_2S donor specific for mitochondria (AP39) has also been developed along with a donor that increases bioavailability of circulating H_2S in humans (SG-1002).[84] The kinetic profiles of many of these donors have not yet been characterized though in use. Given the developing knowledge regarding H_2S donors, donors with different kinetics should be utilized for a nuanced understanding of H_2S modulation and H_2S effects.

It is also important to note that several drugs used in the cardiovascular field may exert their effects partially through H_2S. For example, sulfhydrated ACEi like zofenopril and non-steroid anti-inflammatory drugs (NSAIDs) have been suggested to exert their effects at least partially through H_2S.[84] Similar to currently used drugs, modulating H_2S via established drugs or newly designed H_2S donors may provide tremendous values in cardiovascular therapeutics.

1.2.5 Detecting and Quantifying H_2S Levels in the Cardiovascular System

Current methods of detecting and quantifying H_2S vary and include methods like methylene blue,[87] amperometry,[87] gas chromatography with sulfur chemiluminescence detection,[111] reversed-phase high-performance liquid chromatography (RP-HPLC) with monobromobimane (MBB),[112] and fluorescent probes.[113]

Of these methods to measure H_2S, a commonly used method in the literature to date has been methylene blue, which however, has limitations. Importantly this method utilizes zinc or lead to trap H_2S and acidic conditions to liberate it, but it is these acidic

conditions that result in H_2S release from bound stores, thus approximating H_2S as higher than would be detected by a method detecting only free H_2S.[87] It is also believed to lack sensitivity for low concentrations of H_2S and susceptible to interference by the components of the environment, like O_2.[114] Despite this limitation of methylene blue, it may be possible to make relative comparisons between sulphide levels in samples (both free and bound H_2S, or H_2S/Sulfide) through this method.

Amperometry is also a more recently utilized technique for measuring H_2S. Its major advantage is its ability to detect H_2S in real-time, dynamically, but it is not clear if this technique can be used with biological fluids (including supernatants) or in cells and tissue though this possibility is suggested.[87,115] In this technique, H_2S passes through a selective permeable membrane on a electrochemical sensor and H_2S reduces the molecules of the electrode (e.g. $Fe(CN)_6^{3-}$); as the molecules on the electrode are re-oxidized, this reduction-oxidation reaction generates a current which is proportional to the amount of H_2S gas in the sample.[95,115] H_2S can further be quantified in samples with unknown concentrations of H_2S on the basis of a standard curve of known concentrations from salt donors like NaHS and pH of the solution.[95]

Gas chromatography with chemiluminescence sulfur detection is another technique used to measure H_2S, particularly in biological fluids like plasma.[87,116] This technique has been implemented in several ways and relies on the distinct elution time of H_2S to separate it from other sulfur-containing compounds.[111,117] In one implementation of this method, samples are incubated with sodium citrate to release free H_2S gas; this gas is then eluted by gas chromatography (e.g. 7890 Series GC, Agilent Technologies)[116] and then detected in a chemiluminescence detector (e.g. G660XA Series Chemiluminescence Detector, Agilent Technologies[116]).[111,117] This technique has been used to measure free

H_2S in micromolar concentrations in plasma from healthy individuals and heart failure patients.[116]

With each method having advantages, disadvantages, and variability, it is important to recognize which method is used and the molecule(s) being detected before interpretation. This is especially important as it is not clear whether these methods have been validated against each other, and to better understand and make use of current findings, it may be crucial to see if the various methods of H_2S detection do indeed correlate.

1.2.6 Direct Signalling Effects of H_2S: Posttranslational Modifications & Scavenging

H_2S has been shown to exert biological effects through several mechanisms. One key mechanism among these is the direct posttranslational modification of cysteine residues by H_2S known as S-sulfhydration or persulfidation.[87] This modification is a result of the addition of a sulfhydryl group (-SH) to a cysteine residue, which largely depends on the protonation status of the cysteine residue that varies with the local pH and environment.[87]

One reason that this posttranslational modification S-sulfhydration or persulfidation may have wide-ranging effects is because of the prevalence of cysteine residues on key molecules, like transcription factors (e.g. NF-κB), receptors and ion channels (e.g. K_{ATP} channels and LTCC), kinases and proteins.[87] Moreover, it has been postulated that H_2S may exert these posttranslational modifications in favor of other well-known posttranslational modifications like S-nitrosylation by NO and glutathionylation.[118] S-nitrosylation in particular is the addition of an NO group to cysteine residues to form S-nitrothiols (SNO).[118]

Through comparison of S-nitrosylation and S-sulfhydration in particular, it has been suggested that the covalent bond established by S-sulfhydration is stronger than that established by S-nitrosylation, suggesting that S-sulfhydration may be able to replace S-nitrosylation but not vice versa.[118] Moreover, it is thought, at least based on particular models like glyceraldehyde-3-phosphate dehydrogenase (GAPDH), that S-nitrosylation and S-sulfhydration have opposing effects; indeed, it has been suggested that S-nitrosylation may be responsible for modifying proteins to inhibit their activity while S-sulfhydration may be responsible for modifying proteins to increase their activity.[87] It is not yet clear how this may occur.

Another key mechanism by which H_2S may also its biological effects is through possible scavenging. In particular, H_2S may also exert effects through its ability to scavenge $O_2^{\cdot -}$.[79] Studies seem to be inconclusive regarding the interaction of H_2S with $ONOO^-$, with some studies suggesting H_2S may inhibit $ONOO^-$ mediated processes with more recent studies suggesting a direct scavenging reaction between the two molecules may occur; the kinetics may even be relevant in a biological system with a rate constant of $8\times10^3\ M^{-1}\cdot s^{-1}$ at 37°C.[119-121] This rate constant is higher than H_2S reacting with $O_2^{\cdot -}$.

In addition to scavenging and posttranslational modifications, H_2S may also exert its signalling effects indirectly; for example, through the formation of more stable polysulfides from H_2S, H_2S may exert effects. There is also evidence that the interaction between H_2S and other molecules may be bidirectional; indeed studies like the one conducted in mice show that sodium nitrite ($NaNO_2$) therapy (an NO donor) increases the bioavailability of H_2S, suggesting H_2S generation may be sensitive to NO.[122] Other mechanisms of H_2S's effects include an interplay with other molecules relevant in redox balance in the heart (e.g. SNO formation). Crucially, more investigation is needed regarding H_2S's direct mechanistic effects.

1.2.7 Importance of H_2S in the Heart and Redox State

H_2S has recently been shown to play a major role in cardiac disease in experimental models: in fact, it has been shown to have a positive cytoprotective effect in myocardial ischemia-reperfusion injury and in transverse aortic constriction (TAC)-induced heart failure. These experimental models have begun to elucidate the effects of H_2S on myocardial disease. These recent studies have identified H_2S as an important physiological signalling molecule, independent of homocysteine, through both exogenous and endogenous H_2S alterations.[84] H_2S can specifically exert effects on the myocardium through non-redox central pathways and redox-sensitive pathways.

H_2S has been shown to be involved in the regulation of oxidative stress[84,123-125] and may regulate key enzymatic sources of $O_2^{\cdot-}$ (and $ONOO^-$) pertinent in cardiac disease: mitochondrial $O_2^{\cdot-}$,[126,127] NADPH oxidases,[128-130] and NOSs.[118,124,128,131,132] Effects of H_2S in the heart are specifically discussed below.

1.2.7.1 Protective Effects of H_2S on Cardiac Function and Structure

Several studies have helped elucidate the key role of H_2S in the heart as a possible protective molecule in cardiac function. Specifically, several H_2S donors have been shown to have beneficial roles in the heart after heart failure. Prior to the more recent development of controlled-H_2S release, NaHS and Na_2S were given exogenously to animals to evaluate changes in function of the heart and cardiac dimensions. In a study of ischemia-induced heart failure, exogenous H_2S was given by Na_2S to mice; while Na_2S given only at the time of reperfusion did not yield protective effects in terms of LV function (ejection fraction) or cardiac dilatation (left ventricular end-systolic diameter, LVESD; left ventricular end-diastolic diameter, LVEDD), continuous application of Na_2S through daily administration for seven days from the start of reperfusion was protective for both LV function and dilation.[123] This study gave some of the first indications of

indeed the potential role of long-lasting H_2S in protecting against LV dysfunction and dilation in ischemia-induced heart failure.

More recent donors have also shown similar protective effects of H_2S: SG1002 and diallyl trisulfide (DATS, found in garlic) were able to decrease LVESD and improve cardiac ejection fraction after TAC-induced heart failure.[128,133] In the TAC-induced heart failure model, SG1002 demonstrated further protective effects of H_2S, beyond direct measurements of LV function and dilation, indicated by a reduction in BNP. [128] Both SG1002 and DATS showed significant reduction in fibrosis as indicated by histological analysis of the mice hearts after TAC-induced heart failure.[128,133] Moreover, SG1002 and DATS led to a significant increase in vascular density and a significant reduction in heart weight after TAC-induced heart failure (which increased heart weight significantly).[128,133] These studies demonstrate the relevance of more recent H_2S donors and the wide-ranging potential of H_2S in protecting the heart. The exact mechanisms by which H_2S exerts these beneficial effects are still being explored.

1.2.7.2 Potential Mechanisms of H_2S: Effects on Oxidative Stress (Global)

Oxidative Stress: Furthermore, H_2S (by Na_2S) reduced cardiac oxidative stress as measured by lipid hydroperoxidation after ischemia-induced heart failure (with Na_2S + procedure having higher oxidative stress than WT/sham and procedure animals).[123] Moreover, in a TAC-induced model of heart failure, H_2S (from SG1002) was able to reduce oxidative stress in the plasma and mice hearts as indicated by 8-isoprotane levels (a result of arachidonic acid peroxidation), suggesting H_2S may have a role in reducing global oxidative stress after challenging conditions like heart failure.[128,134] However, it is not clear from these studies whether oxidative stress is reduced by H_2S in the absence of heart failure. In addition to effects on global oxidative stress, the effects of H_2S on specific sources of myocardial oxidative stress have been explored.

1.2.7.3 Effects of H_2S on NADPH Oxidases

H_2S (through SG1002) has been shown to reduce the expression of NOX4 that is elevated after transverse aortic constriction (TAC) in mice hearts; it was not clear if SG1002 reduces NOX4 expression in the absence of TAC-induced heart failure.[128] This finding on NOX4 was further corroborated by studies in cardiac and non-cardiac cells where H_2S reduced the expression of NOX4.[130,135] Cell models in the vascular system suggest H_2S may mediate changes not only in the expression of NADPH oxidases but also in Rac1 activation.[136]

1.2.7.4 Effects of H_2S on Mitochondrial Oxidative Stress and Function

One of the first indications that H_2S may have a functional role in the mitochondria was from findings in a study conducted in mice that revealed that H_2S can induce a reversible 'hibernation' state in which core body temperature and O_2 consumption were reduced by inhaling H_2S; these effects were likely mediated by inhibition of the mitochondrial respiratory chain, specifically through H_2S's inhibition of cytochrome C oxidase (complex IV of the electron transport chain).[137-139] Whether these effects also affect mitochondrial-dependent processes in the heart like contractility (including changes in mitochondrial K_{ATP} channels) is still being explored.

Through its effects *in vivo* in an ischemia-induced heart failure model, H_2S (from Na_2S) has also been shown to improve mitochondrial function as indicated by improved O_2 consumption (V_{O2}) and ATP synthesis; mitochondrial oxidative stress in these hearts before or after daily H_2S administration was not specifically examined which could be of potential interest.[123] Similarly in a TAC-induced heart failure model, SG1002 was able to influence mitochondrial respiration at certain states of respiration but mitochondrial oxidative stress was not specifically examined.[128] Moreover, H_2S shown to protect mitochondrial function after I/R injury as seen by preservation of mitochondrial

respiration, structure, and function.[137] Mice overexpressing CSE were also seen to be protected against MI/R injury, possibly though similar protection of mitochondrial function.[137]

Mitochondrial Oxidative Stress: Although H_2S has been shown to affect mitochondrial function, changes in $O_2^{\cdot-}$ from mitochondrial oxidases by H_2S has not been clearly explored in myocardial tissue. Given O_2 from the respiratory chain plays a key role in the production of $O_2^{\cdot-}$ in the mitochondria, improved mitochondrial respiration may indeed lead to a reduction in $O_2^{\cdot-}$ but further investigation is required to explore this hypothesis.

1.2.7.5 Effects of H_2S on NOS Biology

NOS Biology: Part of H_2S's protective effects may be mediated by alterations in NOS biology. In a TAC-induced model of heart failure, both SG1002 and DATS increased phosphorylation of eNOS at Ser1177 suggesting H_2S activates eNOS.[128,133] It is not clear if this is mediated by Akt: in the TAC-induced model of heart failure, SG1002 led to increased phosphorylation of Akt at Thr308 and Ser473 and increased cGMP levels, while DATS had no effect on the phosphorylation of Akt or AMPK.[128,133] Further indication however of H_2S's role in NOS biology, both SG1002 and DATS also increased NO bioavailability as indicated by increased myocardial nitrites after induction of heart failure.[128,133] Given the protective effects of SG1002 in terms of BNP, LVESD, and ejection fraction were absent in eNOS KO mice further suggested the importance of NOS biology in mediating at least partly H_2S from SG1002's protective effects.[128] It was not clear from these studies what role H_2S has in NOS biology in the absence of cardiac disease.

The role of H_2S has been explored in CSE knockout mice (in the absence of cardiac disease).[124] CSE knockout mice with no compensation by CBS or MST had

elevated myocardial malondialdehyde content, reduced plasma nitrite levels, reduced phosphorylation at eNOS activation site Ser1177, increased phosphorylation at eNOS inhibition site Thr495, reduced BH_4:BH_2 levels, and increased injury in response to myocardial ischemia-reperfusion.[124] H_2S donor given to the knockout mice reversed several of these markers, including the effects of I/R injury.[124] In eNOS mutant mice, H_2S donor did not exert protective effects against myocardial I/R injury, suggesting an eNOS-dependent mechanism.[124]

Despite these findings, there are still crucial questions that have not been addressed regarding H_2S's role in NOS biology as a method of protection. First, it is not clear if similar increased posttranslational modifications would be seen in the absence of heart failure as SG1002 and DATS were not given without challenge or in the absence of CSE knockout.[124,128,133] Important posttranslational modifications like persulfidation or changes in S-glutathionylation and S-nitrosylation have also not been examined. Second, it is not clear what effect H_2S has on the coupling status of NOSs (production of $O_2^{\cdot-}$ versus NO). Whether H_2S directly affects $O_2^{\cdot-}$ from myocardial NOSs is not known and would be beneficial. Furthermore, NOSs in the heart have been indicated to come not only from eNOS but also from neuronal NOS (nNOS), which may be the predominant NOS in the heart. Therefore, phosphorylation sites and activation of nNOS would be beneficial to understand. Lastly, understanding H_2S's effects on human NOS biology would be important.

1.2.7.6 Effects of H_2S on Antioxidant Pathways

In a model of ischemia-induced heart failure, H_2S (from Na_2S) increased the localization of transcription factor nuclear factor-E2–related factor (Nrf2) to the nucleus from the cytosol and, in a separate study, H_2S (from DATS) increased the expression of antioxidant enzymes glutathione peroxidase 1 (GPx-1) and heme oxygenase 1 (HO-1)

after TAC-induced heart failure.[123,133] These finding suggest that H_2S has protective effects against disease potentially via a diverse set of antioxidant response pathways.

There is also substantial evidence that H_2S (from Na_2S) reduces infarct size after ischemia-reperfusion injury (I/R injury) in the myocardium.[140] For example, a study conducted in mice demonstrated that H_2S (from Na_2S) given during preconditioning led to increased expression of antioxidant elements through increased localization of Nrf2 in early stages and led to increased activation of PKCε and antiapoptotic pathways in late stages.[140]

1.2.8 The Unmet Need: Role of H_2S as a Regulator of Myocardial Redox Signalling

It will be crucial to understand H_2S's direct effects on $O_2^{\cdot-}$ from sources like NADPH oxidases, NOSs, and mitochondrial oxidases in the heart. Given numerous H_2S donors in literature, it will be crucial to explore H_2S's effects on these redox-mechanisms in human myocardium through both fast-releasing and slow-releasing donors.

1.3 Cystathionine γ-Lyase (CSE) and Redox State

CSE is a small 44.5kDa protein that is produced in the human body and cardiovascular system.[141] Its emerging role in cardiac disease makes it an enzyme of great interest.

1.3.1 CSE in Transsulfuration Pathway and 'Switching' Reactions

Long before its now more well-known role as a contributor of H_2S, CSE was examined for the important role it plays in the evolutionarily conserved transsulfuration pathway, a known route for both the removal of homocysteine and the generation of L-cysteine and antioxidants like glutathione.[141]

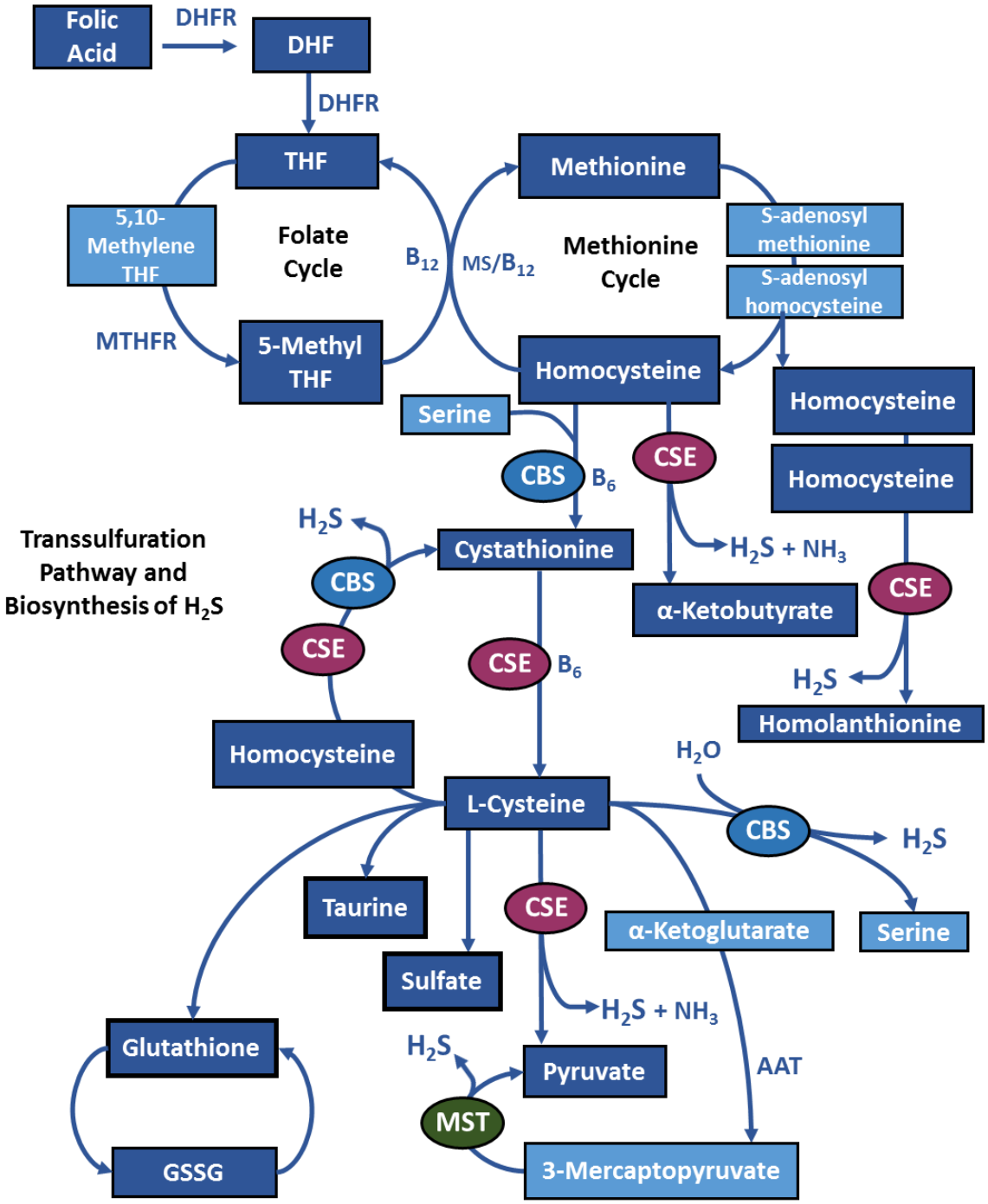


Figure 1.8 Enzymatic Reactions Important in the Generation of By-Product H_2S

Observational studies demonstrated that homocysteine levels were a strong predictor of cardiovascular risk. The transsulfuration pathway, folate cycle, and methionine cycle are all involved in the metabolism of homocysteine. Homocysteine levels are reduced through (1) the transsulfuration pathway in which CBS converts homocysteine to cystathionine and through (2) the methionine cycle by remethylation forming methionine; the remethylation is facilitated by the folate cycle as 5-MTHF is converted to THF. CSE plays a crucial role as the second enzyme in this pathway. Dietary folic acid can be converted to THF through DHFR. THF in its methylated form, methyl-THF, can provide vitamin B_{12} with a methylene moiety to transfer to homocysteine, leading to the generation of methionine. In addition to its conversion to methionine, homocysteine can also be converted to cystathionine through the enzyme CBS. Despite this understanding, it is not clear of there is a causal link between homocysteine levels and cardiovascular

disease or if homocysteine serves a surrogate for a separate causal mechanism. Three key enzymatic sources of H_2S in the heart are CSE, CBS and MST. CBS is a crucial enzyme in the metabolism of homocysteine, combining homocysteine and serine to form cystathionine. Cystathionine is then further metabolized to cysteine with the catalysis of CSE. In addition to these fundamental reactions, CBS also catalyzes several reactions that generate H_2S as a by-product: (1) cysteine and homocysteine to form cystathionine and H_2S; (2) cysteine and water to form serine and H_2S. CSE also catalyzes several reactions that generate H_2S as a by-product: (1) homocysteine to alpha-ketobutyrate and H_2S; (2) homocysteine and homocysteine to form homolanthionine and H_2S; (3) cysteine and homocysteine to form cystathionine and H_2S; (4) cysteine to form ammonia, pyruvate and H_2S. MST catalyses 3-mercaptopyruvate and glutamate to pyruvate and H_2S. Figure created on the basis of several papers.[77,87,95,142,143] *3-MST: 3-mercaptopyruvate sulfurtransferase; 5-MTHF: 5-methyltetrahydrofolate; AAT: Aspartate Aminotransferase; CBS: cystathionine β-synthase; CSE: Cystathionine γ-lyase; DHFR: dihydrofolate reductase; DHF: dihydrofolate; H_2S: hydrogen sulfide; THF: tetrahydrofolate.*

CSE is the second enzyme in the transsulfuration pathway, following CBS's catalysis of the conversion of substrates homocysteine and serine to cystathionine (Figure 1.8).[141] CSE specifically catalyses the conversion of cystathionine to L-cysteine leading to by-products ammonia and α-ketobutyrate (Figure 1.8).[141] This reaction forms the basis of the enzyme's name, and though this reaction does not directly generate H_2S, L-cysteine remains an important substrate for H_2S generation.[87] The generated L-cysteine can be used as a substrate by several enzymes to generate H_2S (including CSE in a further reaction) as well as to generate glutathione.[141,144]

Switching Responses: More recent understandings of CSE in the transsulfuration pathway suggest that CSE must commit to the transsulfuration pathway.[144] CSE has an affinity for a variety of substrates; it is known to catalyze substrate L-cysteine to pyruvate and ammonia, with H_2S as a product.[87,145] It also catalyses the conversion of cysteine and homocysteine to cystathionine and homocysteine to homolanthionine or α-ketobutyrate, both reactions generating H_2S as a by-product.[87] However, it is not clear when CSE catalyses which reaction. Thus similar to the dual role several enzymes play, like uncoupled and coupled NOSs, CSE may too importantly catalyse different reactions depending on its environment or 'status.' It is now known that the byproduct of this reaction, H_2S, may act as an important signalling molecule. As such, in addition to its main role in the evolutionary conserved pathways in metabolizing amino acids like L-

Cysteine and generating homocysteine, more novel roles for CSE have been emerging. In fact, CSE is thought to be an important enzyme in the cardiovascular system, perhaps even the main contributor of H_2S and altering oxidized:reduced glutathione ratios in the cardiovascular system. Further comparison of the expression and contribution of the H_2S generating enzymes are required. Given CSE's potential importance, a better understanding of the transcriptional and enzymatic regulation of CSE and its localization is crucial in addition to examining its specific role in the heart.

1.3.2 Transcriptional Regulation of CSE

CSE is encoded by its gene cystathionase (CTH) on chromosome 1 (1p31.1, Table 1.2).[90,145] Several redox-sensitive transcription factors have been identified for transcriptional regulation of CSE, including transcription factors specificity protein 1 (SP1) and activating transcription factor 4 (ATF4).[146] SP1 in particular has been shown in non-cardiac models to increase CSE expression (e.g. in Huntington's disease) and may be involved in upregulation of CSE in chronic models of oxidative stress (e.g. in response to TNF-α mediated inflammation) while ATF4 may increase CSE in response to both acute and chronic forms of oxidative stress.[83,146] A recent study has also shown that CSE expression is increased in NOX4 transgenic mice, further suggesting CSE to be under redox-sensitive regulation.[147]

Myeloid zinc finger 1 may be involved in the transcriptional regulation of CSE as well.[82] The promoter region of human CSE is known to have two SP1 binding sites to regulate transcription of CSE.[82] The causal role of SP1 has been tested in cells through the use of inhibitor Mithramycin which inhibits SP1 binding and knockdown of SP1.[82] MicroRNA-21 (miR-21) may also regulate CSE expression (and SP1 expression), as evidenced in smooth muscle cells.[82]

1.3.3 Regulation of CSE Enzyme and CSE Enzyme Localization

CSE Enzyme, Cofactor Pyridoxal-5-Phosphate (PLP), and Redox-Sensitivity: Human CSE is a small 44.5 kDa protein that combines to form a 178 kDa tetramer (Table 1.2).[83,141] As revealed by its three-dimensional crystal structure, CSE is a tetramer with two monomers contributing to form the active sites of the dimer and those dimers joining to form a tetramer.[141] CSE is dependent on PLP as a cofactor, with PLP and CSE subunits in a 1:1 ratio.[85,141] Cofactor PLP is bound to CSE's active site by surrounding hydrogen bonding in addition to direct hydrogen bonding interactions; PLP's binding leads to a conformational change in CSE, forming a stronger tetramer complex than the apoprotein.[148] Each subunit has two CXXC motifs, which are two cysteine residues separated by two other residues, and these motifs may importantly be redox-sensitive.[83] CSE protein may also be regulated by direct posttranslational modifications (like sumolyation).[83] A better understanding of the regulation of CSE is crucial.

Homology and CSE Localization: Human CSE shares homology with rodent CSE: mouse CSE which is 43.6kDa and 398 amino acids is similar to rat CSE which is 43.6 kDa and 398 amino acids (93.5% homology between mouse and rat) and human CSE which is 44.5 kDa and 405 amino acids (85.6% homology between human and mouse).[145] CSE has been shown to be expressed in the heart[128] along with many other tissues. Within the cell, CSE is predominantly located in the cytosol, but it may also be translocated to the mitochondria.[84] The exact conditions in which CSE translocates to the mitochondria are not well-understood.

Targeting CSE via inhibitors: In addition to the donation of H_2S exogenously, endogenous H_2S can be modulated by targeting endogenous sources of H_2S like H_2S-generating enzymes. Chemical inhibitors provide a unique opportunity to modulate these enzymes' functions, particularly in the short term if the inhibition is reversible. One

important advantage is that these pharmacological tools do not require expensive and specialized molecular techniques like genetic manipulation.[88] Indeed, given the importance of pharmacological inhibitors, several have been developed to inhibit CSE to affect H_2S biology.[89] DL-proparylglycine (PAG) or B-cyanoalanine are commonly used as pharmacological inhibitors for CSE.[88,89] Current screening of molecules are being conducted to find more specific and more potent inhibitors for H_2S's enzymatic sources.[89] There are to-date no selective inhibitors of CSE used today in cardiovascular clinical practice.

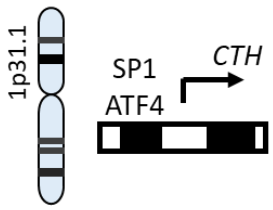
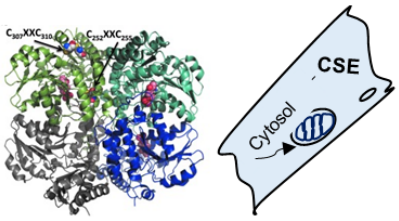
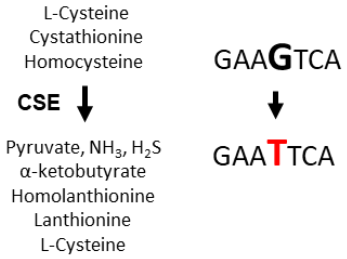
1.3.4 Importance of CSE in the Heart and Redox State

What has made CSE rise from its traditional role to prominence in the cardiovascular system? A large part of this rise in importance is due to animal models of CSE demonstrating it has an important role to play in cardiac function. In particular there are two key animal models of CSE demonstrating such effects: (1) Global CSE Knockout and (2) Cardiac-specific CSE overexpressing mice. Through these models, it has been shown that CSE (1) contributes to functional changes in the heart and can improve heart function, (2) can affect and increase NO bioavailability and (3) potentially improves certain global oxidative stress markers. These findings are detailed below.

1.3.4.1 CSE's importance in heart function

CSE's importance in heart function has been demonstrated through several animal models. In one study, after ischemia-induced heart failure, wildtype versus cardiac-specific CSE overexpressing mice were compared for cardiac dilatation and function.[123] CSE overexpression led to reduced left ventricular dilatation, as indicated by LVESD and LVEDD, both after permanent left coronary artery (LCA) occlusion and short-term LCA occlusion followed by reperfusion.[123]

Table 1.2 Cystathionine γ-Lyase (CSE): Gene, Protein, Function

GENE	PROTEIN	FUNCTION
		
Gene • **Chromosome 1 (1p31.1) and gene CTH** • **Under transcriptional regulation of specificity protein 1 (SP1) and activating transcription factor 4 (ATF4)** Paul et *al.* (2012)	**Protein** • **44.5 kDa/subunit and 178 kDa homotetramer** • **Depends on pyridoxal-5-phosphate (PLP) cofactor** • **Localization in cytosol** • **Translocation to mitochondria** Zhu et *al.* (2008)	**Function** • **CSE catalyzes conversion of several substrates with H_2S as a byproduct** • **rs1021737T SNP in CSE (Ser403Ile) associated with ↑Homocysteine** Hartle et *al.* (2016) Paul et *al.* (2012) Donnarumma et *al.* (2017)

While CSE overexpression did not protect against loss of LV function after permanent LCA occlusion as indicated by measurements of ejection fraction, CSE demonstrated protective effects in LV function in short-term LCA occlusion followed by reperfusion.[123] This study, one of the first in the field, gave indication that CSE may be important in protecting against loss of LV function in non-permanent ischemia-induced heart failure. Importantly, this study also demonstrates that overexpression of CSE improves survival after permanent LCA occlusion, suggesting CSE may also play a larger role in heart failure in the long-term that is not clear from simple measurements of LV function.[123]

In line with these findings of improved LV function in short-term ischemia-induced heart failure, in another study in mice, heart function was evaluated after heart

failure was induced by a different method, namely transverse aortic constriction (TAC); in this study, wildtype, CSE knockout, and cardiac-specific CSE transgenic mice were examined.[128] This study found that LVESD and LVEDD, indicative of LV dilatation, were both significantly increased in CSE knockout mice after TAC compared to wildtype mice after TAC, suggesting the absence of CSE led to more cardiac dilatation.[128,149] Moreover, in cardiac-specific CSE transgenic mice, LVESD and LVEDD were lower following TAC compared to wildype mice following TAC, suggesting CSE indeed had a protective effect against cardiac dilation.[128] Direct measurement of LV function showed similar importance of CSE, with ejection fraction significantly reduced in CSE knockout mice after TAC compared to wildtype mice after TAC, and cardiac-specific CSE transgenic mice showing a preservation in ejection fraction.[128] This study was one of the first in the field to thoroughly describe the importance of CSE in cardiac function and dimensions through both a knockout and overexpressing CSE animal model.[128]

1.3.4.2 CSE improves NO bioavailability and global markers of oxidative stress

In addition to heart function, the role of CSE in oxidative stress and NOS biology has been more recently explored. It has been shown that cardiac-specific overexpression of CSE led to increased nuclear localization of Nrf2 from the cytosol.[140] Effects of CSE may indeed be related to H_2S pathways as described earlier as well as antioxidant pathways. As described in support of H_2S's role in NOS signalling, it has also been shown that CSE knockout mice have elevated myocardial malondialdehyde (MDA) content, reduced plasma nitrite levels, reduced phosphorylation at Ser1177, increased phosphorylation at Thr495, reduced BH_4:BH_2 levels, while leading to increased myocardial I/R injury.[124]

1.3.5 Regulation of CSE Gene and Protein Expression

CSE expression may indeed be altered in the conditions of oxidative stress. Evidence for this possibility comes from indirect studies including a study in mice demonstrating that TAC-induced heart failure (on wildtype mice) led to a significant increase in CSE protein expression, a significant reduction in MST protein expression, and no change in CBS protein expression.[128] Interestingly, H_2S reduced CSE expression after TAC-induced heart failure, suggesting there may be a feedback mechanism that regulates CSE expression via H_2S.[128] While not specific to the heart, Professor Ajay Shah's group has shown that CSE is under the regulation of NOX4-dependent regulation in endothelial cells, suggesting a further line of investigation into CSE's redox-sensitive expression.[147] A recent study has also suggested CSE is upregulated by increased homocysteine levels while CSE is downregulated by H_2S treatment.[150]

1.3.6 CSE Single Nucleotide Polymorphism and Homocysteinemia

As described briefly earlier, in early, large-scale clinical trials, homocysteine levels in plasma were associated with mortality in patients with coronary artery disease and, in fact, homocysteine was a strong predictor of such mortality.[151] However, it was shown that while homocysteine levels could be significantly lowered by supplementation of B vitamins and folic acid, these supplements did not alter cardiovascular causes or events in patients with vascular disease or after acute myocardial infarction.[76,152] The literature on homocysteine is controversial. A possible explanation for these clinical trials is that elevated homocysteine levels may not be the direct cause of the increased risk of cardiovascular disease. That is, homocysteine accumulation may be a result of reduced CSE activity with CSE being an evolutionarily conserved enzyme in humans that catalyses the conversion of homocysteine to products (like homolanthionine and cystathionine); Reduced CSE activity may lead to not only an accumulation of substrate

homocysteine but a reduction in H_2S, one of CSE's major by-products.[87] As such, a possible explanation for these clinical trials is that elevated homocysteine levels may not be the direct cause but serves as a surrogate: reduced H_2S may mediate the negative effects of increased homocysteine and therapeutic strategies should aim at altering H_2S signalling rather than lowering homocysteine, suggesting H_2S and CSE's role in cardiovascular disease presents an exciting opportunity for research.[75,84]

CSE has been studied in the context of several disease states including homocysteinemia as well as cystathioninuria (an accumulation of substrate cystathionine). Two missense mutations in CSE (rs28941785, 70415987C>T, Thr67Ile; rs28941786, 70430388C>G, Gln240Glu) are known to contribute to cystathioninuria and result in differences in CSE activity *in vitro*; this latter property suggests these mutations could be important tools to better understand the role of CSE activity in the cardiovascular system.[141] However, this examination may be potentially independent of the context of homocysteinemia.[141] There is also a known SNP in CSE that leads to an amino acid substitution (rs1021737, 70439117G>T, Ser403Ile), which varies in prevalence in different ethnic groups and is correlated with "mild hyperhomocysteinemia under homozygous conditions."[141] Specifically, CSE SNP 70439117G>T was found to be associated with higher plasma homocysteine levels in a cohort of 496 individuals (Homozygous TT: Hcy 13.3 ± 8.6 μmol/L, MAF 0.3014).[153,154] This SNP may be more relevant to study CSE in the context of cardiovascular disease given that homocysteine has been indicated as an independent risk factor for cardiovascular disease.[141] The CSE SNP 70439117G>T associated with homocysteinemia and may lead to alterations in H_2S is of particular interest.

CSE SNP 70439117G>T is located in exon 12 and the amino acid substitution position 403 is located at the C-terminus of the protein, two amino acids from the end of

the protein in a coding region.[141] This C-terminus location suggests that the variant does not modify the active site of the enzyme.[141] To examine differences in the activity of S403 and I403, differences in cystathionine cleavage and H_2S generation from substrates homocysteine and cysteine by the purified proteins of these two variants were measured *in vitro*.[141] The study found no changes in activity between the two variants.[141] The variants also had similar cofactor PLP content as assessed by PLP absorbance and similar kinetic properties, including K_m, $k_{cat,}$, V_{max}, and k_{cat}/K_m ratio.[141] There have been cases where, although no *in vitro* differences in enzymatic activity were detected between variants, variants *in vivo* had differences in enzymatic activity.[141] As such, the SNP could potentially be used in line with a Mendelian randomization approach to better understand the role of endogenous CSE and CSE-derived H_2S in humans and *in vivo*.

Key H_2S-producing enzymes like CBS also have functional SNPs (i.e. related to disease, possibly through SNP-mediated changes in enzymatic activity) that may be used to study changes in the role of homocysteine/H_2S. CBS SNP (rs2851391, 43067294C>T) was found to be located in a noncoding region, but it may exert effects on CBS through potentially epigenetic changes; the SNP is related to homocysteine (Homozygous TT: Hcy 5.075 ± 0.172 μmol/L, Minor Allele Frequency/MAF .289).[155-157] Another CBS SNP (rs234709, 43066854C>T, intron variant) may also be of interest as it has been associated with homocysteine levels (in unconditioned analysis).[157] These SNPS can provide evidence of the enzyme's role in regulating myocardial redox state. Thus, using genetic models and further clinical trials, it will be crucial to explore in humans whether CSE (or CBS) mediated changes in H_2S play a role in cardiac disease as the evidence remains limited. The emerging clinical and human evidence regarding H_2S and CSE's role in cardiovascular disease suggests that further clinical studies on H_2S and CSE and the

myocardium and myocardial redox state are warranted. The SNPs may lead to a change in activity of the enzymes in humans.[141]

1.4 Clinical Importance of H_2S and CSE Biology

While H_2S biology has only recently begun to be examined in the human heart and through H_2S-donors in clinical trials, the first evidence suggests H_2S biology is relevant in human cardiovascular disease and its biological promise is tremendous (Table 1.3).

1.4.1 Human Plasma H_2S/Sulfide levels in Cardiovascular Disease

Plasma H_2S/Sulfide levels have been measured in healthy individuals as well as in different cohorts of patients, and interestingly, patients with cardiovascular disease have different circulating levels of H_2S gas (measured by gas chromatography chemiluminescence sulfur detection or RP-HPLC with MBB) or H_2S/Sulfide (measured by methylene blue) compared to healthy individuals and matched controls.

Heart Failure: In fact, in two key studies, small in sample size but the first in the field, it has been shown that heart failure patients have reduced circulating levels of H_2S. Kovacic et al. demonstrate that in fifty-seven patients with congestive heart failure, H_2S/Sulfide is reduced in each NYHA Class II, III, and IV compared to eighteen healthy individuals as age and gender-matched controls, with H_2S/Sulfide being lowest in NYHA Class IV patients.[158] H_2S/Sulfide in this study was measured by methylene blue.[158] More recently, Polhemus et al. have similarly demonstrated that compared to twenty-four age-matched control individuals, twenty patients with heart failure had lower plasma H_2S levels, while patients were not divided by NYHA class.[159] H_2S was measured by gas chromatography-chemiluminescence in this latter study.[159] These findings thus far demonstrate that heart failure patients have lower circulating levels of H_2S compared to their healthy counterparts. This is important because if indeed these lower H_2S levels are

a result of disease state or lower levels are even a cause of pathogenesis, compensation of this potentially protective molecule may have beneficial effects.

Type 2 Diabetes: In other cardiovascular related-disease states like type 2 diabetes mellitus, similar to the reduced levels of plasma H_2S/Sulfide seen in patients with heart failure, several studies have shown that patients with type 2 diabetes have reduced plasma H_2S/Sulfide levels compared to non-diabetic individuals, with H_2S/Sulfide measured by methylene blue.[160-162] Furthermore, within those patients that had type 2 diabetes, one recent study suggests that individuals with cardiovascular disease (coronary and peripheral artery disease, and cerebrovascular disease) have significantly lower plasma H_2S/Sulfide levels compared to diabetic individuals without cardiovascular disease.[160] These studies suggest a link between reduced plasma H_2S/Sulfide and metabolic disorders and provide further insight into the links between H_2S/Sulfide and cardiovascular disease.

Vascular Disease: However, in vascular disease, without regard to diabetes, different studies have demonstrated both elevated and reduced circulating H_2S levels in patients. Peter et al. have reported that in men with vascular disease, plasma H_2S levels are highest in individuals with peripheral artery disease compared to individuals with coronary artery disease.[112] This observational study and further studies from this group have further suggested that plasma H_2S may be a biomarker for vascular disease in men, measuring H_2S by RP-HPLC and MBB (NCT01407172, PCT/US2013/066012).[112] This elevated plasma H_2S compared to the lowered plasma H_2S in patients with heart failure has been a point of controversy that has been discussed in reviews.[159] According to Polhemus et al., the differences may be due in part to biological differences arising from these different cardiovascular diseases.[159] The specific disease state seems to make a difference as individuals with coronary artery disease and a more severe phenotype have also been shown to have lower circulating H_2S levels.[163] Further insight may also be

provided in each disease state by looking at H_2S in relation to other circulating metabolites.

H_2S:NO and H_2S:Hcy Ratios: In addition to examining circulating H_2S alone, several studies have indeed examined the ratio of H_2S to NO or H_2S to Hcy levels which have provided further insight into disease state. One study, for example, found that plasma H_2S levels and plasma total NO levels were significantly altered in individuals with vascular disease.[112] However, neither plasma H_2S nor plasma total NO levels could be used alone to separate individuals with peripheral artery disease (PAD) versus individuals with coronary artery disease (CAD).[112] Examining the ratio of H_2S:NO in individuals, however, provided differences in individuals with PAD alone compared to those individuals with CAD alone.[112] This study therefore suggests that the ratio of H_2S:NO may provide additional insight into differences in disease state, for example between individuals with PAD versus CAD. The ratio of H_2S:Hcy has also been examined in the context of disease. In one study examining this ratio, H_2S:Hcy was found to be significantly lower in children with hypertension compared to healthy children: plasma H_2S was reduced and plasma Hcy levels were increased in children with hypertension.[164] This study suggests H_2S:Hcy may also provide additional value through its use of several metabolites to characterize the underlying biology in hypertension. Taken together, these findings begin to suggest that in addition to examining H_2S levels alone, ratios of circulating metabolites may provide distinct insight into disease state than any one circulating metabolite alone.

Together, these studies in various cardiovascular and related disease states highlight the deep complexity of H_2S biology in humans. These studies examine plasma H_2S in different states and suggest that circulating H_2S differs, while it is not clear if the differences in levels of H_2S are a result of disease or lower or higher levels serve as a

contributor to the disease state. To clarify this role, it will be important to know if circulating H_2S levels do not simply differ in disease state but whether H_2S levels are correlated with more mechanistic insight into disease state. What is not yet known for example is whether circulating H_2S levels is correlated with myocardial redox state and oxidative stress in humans, but a robust examination of this type may yield more insight into the relationship between circulating H_2S and disease state. In this study, using a large cohort of patients undergoing cardiac surgery, we examine closely the relationship between circulating H_2S, myocardial redox state, and cardiovascular disease states.

1.4.2 H_2S-releasing drugs and Randomized Clinical Trials

Given the tremendous insight into H_2S in experimental models and further identification of circulating H_2S levels being altered in cardiovascular disease states, there is clear motivations to test whether H_2S can have beneficial effects in humans.

To date, H_2S-releasing drugs are being tested as a therapy in clinical trials, primarily through an H_2S-releasing drug known as SG1002. In particular, following the observations of reduced plasma H_2S in heart failure patients and SG1002's efficacy in preclinical models to improve cardiac dysfunction, a Phase I clinical trial (NCT01989208) has been conducted demonstrating the safety of donor SG1002 and its ability to raise H_2S levels in healthy individuals and heart failure patients.[116,128,159] This study further demonstrates that SG1002 increases NO bioavailability as indicated by nitrites in NYHA Class II and III heart failure patients and healthy individuals.[116] In order to assess whether SG1002 has beneficial effects in cardiovascular disease, this work is being taken to the next phase as a randomized, placebo-controlled Phase II clinical trial (NCT02278276) to examine whether indeed H_2S improves heart function assessed by echocardiograms and reduces oxidative stress and inflammation examined by biomarkers after administration of SG1002.[116]

Table 1.3 H_2S and CSE Biology in the Human Cardiovascular System

Importance of H_2S and CSE in the Human Cardiovascular System			
Plasma H_2S	Heart Failure Patients	↓↓ H_2S	Polhemus et al. (2014) Kovacic et al. (2012)
	Type 2 Diabetes Patients	↓↓ H_2S	Whiteman et al. (2010) Suzuki et al. (2017)
	Vascular Disease Patients	↓↑ H_2S	Peter et al. (2013) Kanagy et al. (2017) Rajpal et al. (2018)
H_2S-releasing drugs in clinical practice	Zofenopril	Releases H_2S	Bucci et al. (2014) Donnarumma et al. (2016)
	NSAIDs	Releases H_2S	Wallace et al. (2017)
Randomized Clinical Trials	Phase I	SG1002 Safe in Humans	Polhemus et al. (2015) NCT01989208
	Phase II	SG1002 on Cardiac Function	NCT02278276 (Ongoing)
CSE, CBS, MST Expression	Unstable Atherosclerotic Plaques	↑CSE and CBS protein expression	Sigala et al. (2017)
Outcomes, Hospitalizations	Higher mortality rate	↓↓ H_2S	Kovacic et al. (2012)

In addition to these clinical trials, several cardiovascular drugs administered routinely have an H_2S-releasing moiety that may mediate the beneficial effects of these drugs. Some of these drugs include angiotensin-converting enzyme (ACE) inhibitors like zofenopril and H_2S-releasing non-steroidal anti-inflammatory drugs (NSAIDs); the former have been shown to have protective effects through increasing NO bioavailability.[84,165] Zofenopril has been shown to reduce infarct size post-acute myocardial infarction (AMI)[166,167] and, in separate studies, beneficial effects of zofenopril have been attributed at least partially to the release of H_2S.[168,169]

1.4.3 Key Questions in the Field

Although circulating H_2S/Sulfide levels have been examined in several cohorts of patients, whether there are alterations in expression of CSE, CBS and MST in human cardiovascular diseases are less well known. A recent study demonstrates that CSE

protein expression is increased in unstable plaques in humans[170] but further study is required to understand and determine whether alterations in the expression of these enzymes occur in the heart with disease. Moreover, very little is known regarding H_2S biology (both circulating H_2S/Sulfide levels and the expression of these enzymes) and clinical risk factors. A small study has demonstrated that lower plasma H_2S predicts mortality in patients with heart failure suggesting a potential role for H_2S biology in prognostic tools;[158] however further study is warranted. Key questions remaining in the cardiovascular H_2S field and gaps remaining in the field in light of the emerging importance of CSE include the following:

1) What the relationship is, if any, between circulating H_2S/Sulfide and myocardial redox state
2) Is myocardial CSE, CBS, MST expression associated with myocardial redox state
3) Can a CSE SNP associated with homocysteinemia give further insight into CSE's role in cardiovascular disease and further insight into the role of endogenous H_2S biology in regulating myocardial redox state
4) Is H_2S biology (circulating levels of H_2S/Sulfide and expression of CSE/CBS/MST) related to clinical risk factors (e.g. diabetes, obesity, hypertension)
5) Does CSE have an effect on sources of $O_2^{\cdot -}$ and $ONOO^-$
6) What is CSE's functional role in myocardial redox state in the absence of advanced cardiac disease
7) Is the expression of CSE in the heart redox-sensitive?

Given that myocardial oxidative stress is a key contributor to cardiac disease pathogenesis, it is crucial to understand what regulates myocardial redox state and particularly what regulates the generation of $O_2^{\cdot -}$ in the heart.[6] NADPH oxidases,

mitochondrial oxidases, and uncoupled nitric oxide synthases are well-known enzymatic sources of $O_2^{\cdot-}$ in the heart that may serve as therapeutic targets in primary and secondary prevention.[20,23,27] It is not clear if H_2S/CSE biology plays a role in regulating $O_2^{\cdot-}$ generation directly from enzymatic sources like NADPH oxidases, mitochondrial oxidases, and uncoupled nitric oxide synthases in the human heart in advanced stages of cardiac disease.

H_2S and its generating enzymes have been shown to have beneficial roles in various models of cardiac disease including heart failure and ischemia-reperfusion injury and part of their effects have been shown to be mediated by changes in activation of NOSs. However, the direct role of this gaseous molecule and these enzymes in regulating myocardial redox state are still poorly understood and knowledge of their roles in the human heart is virtually non-existent.

Studies elucidating a possible role of H_2S/CSE in regulating human myocardial redox state and the underlying mechanisms would have tremendous value for understanding redox-dependent and -related cardiac disease. Crucial will be understanding H_2S and CSE's role in regulating myocardial redox state in humans through changes in $O_2^{\cdot-}$ production from NADPH oxidases, mitochondria, and uncoupled NOSs, and the underlying mechanisms behind these effects. H_2S/CSE biology may serve as a novel method to target myocardial redox state. The hypothesis and aims of our study are described in Section 1.5.

1.5 Hypothesis and Aims

1.5.1 Hypothesis

In this study, we hypothesize that H_2S specifically protects the human myocardium in three ways: H_2S a) prevents myocardial NOS uncoupling through

prevention of cofactor BH_4 oxidation, b) reduces myocardial $ONOO^-$, and c) suppresses $O_2^{\cdot-}$ generation from NADPH oxidases and mitochondrial oxidases.

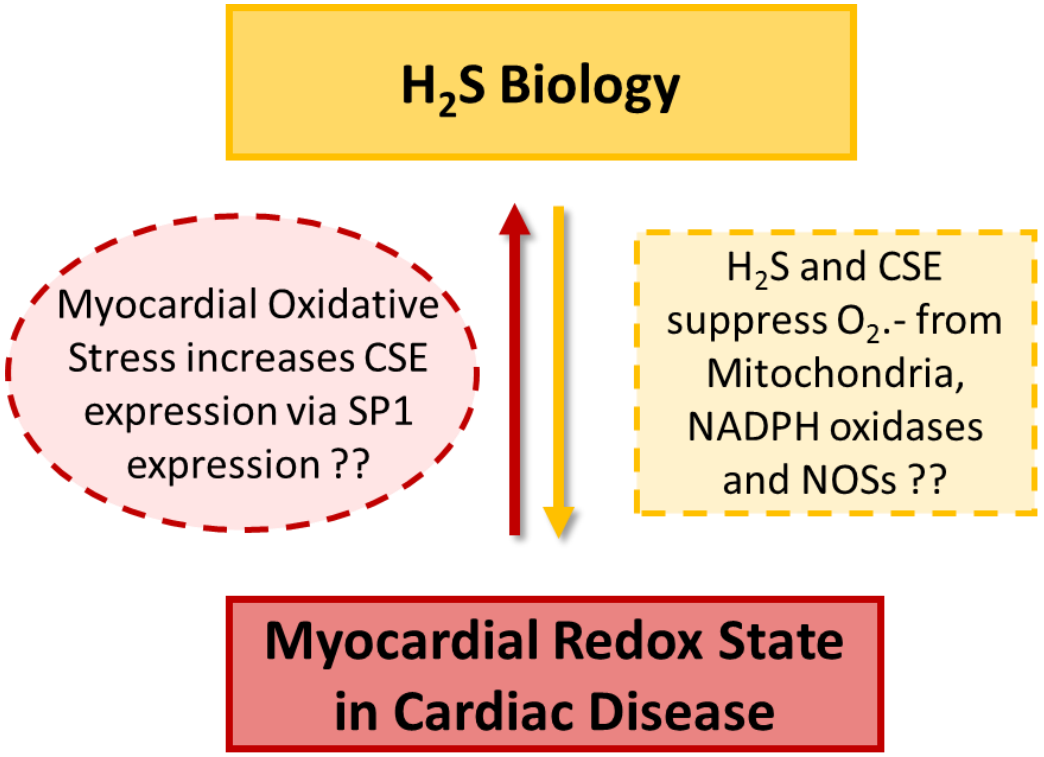


Figure 1.9 Overview of Original DPhil Hypothesis

We hypothesized that H_2S biology and myocardial redox state have a bidirectional interaction.

We further hypothesize that plasma H_2S/Sulfide and myocardial CSE gene expression are inversely correlated with myocardial redox state in patients with advanced stages of cardiac disease. We lastly hypothesize that CSE plays a role in suppressing myocardial $O_2^{\cdot-}$ generation and CSE is upregulated in response to increased myocardial $O_2^{\cdot-}$ generation.

1.5.2 Aims

The specific aims of this thesis are to investigate the following:

Aim 1 ─ To examine the role of H_2S/Sulfide in regulating myocardial $O_2^{\cdot-}$ generation

a) To examine whether H_2S/Sulfide is linked to clinical risk factors and demographics (e.g. cardiac function, metabolic syndrome, hypertension)

b) To determine whether H_2S/Sulfide levels are linked to myocardial redox state, specifically $O_2^{\cdot-}$ generation from NOSs, NADPH oxidases, and mitochondria

c) To determine the direct effects of H_2S from fast and slow-releasing donors on $O_2^{\cdot-}$ generation from NOSs, NADPH oxidases and mitochondria, levels of $ONOO^-$, and oxidation of BH_4

Aim 2 ─ To examine the bidirectional relationship between myocardial CSE, CBS, and MST gene expression and myocardial oxidative stress

a) To evaluate the relationship of myocardial CSE, CBS, or MST expression and clinical risk factors and demographics (e.g. cardiac function, metabolic syndrome, hypertension)

b) To determine if myocardial CSE, CBS, MST gene expression is associated with myocardial redox state, specifically $O_2^{\cdot-}$ generation from NOSs, NADPH oxidases, and mitochondria

c) To examine the direct effects of oxidative stress on myocardial CSE, CBS, and MST gene expression

Aim 3 ─ To examine the causal role of CSE in regulating myocardial redox state

a) To examine the role of CSE in regulating basal $O_2^{\cdot-}$ and $O_2^{\cdot-}$ from NOSs and $ONOO^-$ (in the absence of challenge)

d) To examine whether myocardial CSE and CBS SNPs are related to clinical risk factors and demographics (e.g. cardiac function, metabolic syndrome, hypertension)

e) To examine the role of CSE and CBS SNPs on myocardial redox state, specifically $O_2^{\cdot-}$ generation from NOSs, NADPH oxidases, and mitochondria

These aims are explored in Chapters 4, Chapter 5, and Chapter 6, respectively. Methods and Development of Methods are described in Chapter 2 and Chapter 3.

Chapter 2 Experimental Design and Methods

2.1 Study Design

This DPhil study is composed of four types of study:

I. Clinical Association Studies

II. Human Myocardium *Ex Vivo* Models

III. Cell Culture Models

IV. Animal Model

2.1.1 Clinical Study Design: The Oxford Heart-Vessels-Fat (Ox-HVF) Cohort

In a large part of this study, Clinical Associations, human samples including right atrial appendages and whole blood samples were obtained from patients undergoing cardiac surgery from the Oxford Heart-Vessels-Fat (Ox-HVF) cohort (Figure 2.1, https://oxhvf.com).[6,20] These patient samples were characterized for myocardial H_2S biology. By combining previously conducted phenotyping of myocardial redox state and demographics of this cohort with new phenotyping of myocardial H_2S biology from the same patients, we were able to conduct important paired analyses to understand the relationship between myocardial redox state and H_2S/CSE biology.[6,20]

Overview: As we have previously described, our group has developed the Ox-HVF Cohort, a cohort of more than one thousand five hundred participants with extensive non-invasive cardiovascular phenotyping and collection of a wide variety of human samples (https://oxhvf.com, Figure 2.1).[6,20,171,172] To this cohort, we specifically recruit patients undergoing elective coronary artery bypass graft (CABG) or valve replacement at the John Radcliffe Hospital (Oxford University Hospitals, NHS Foundation Trust).[6,20,172]

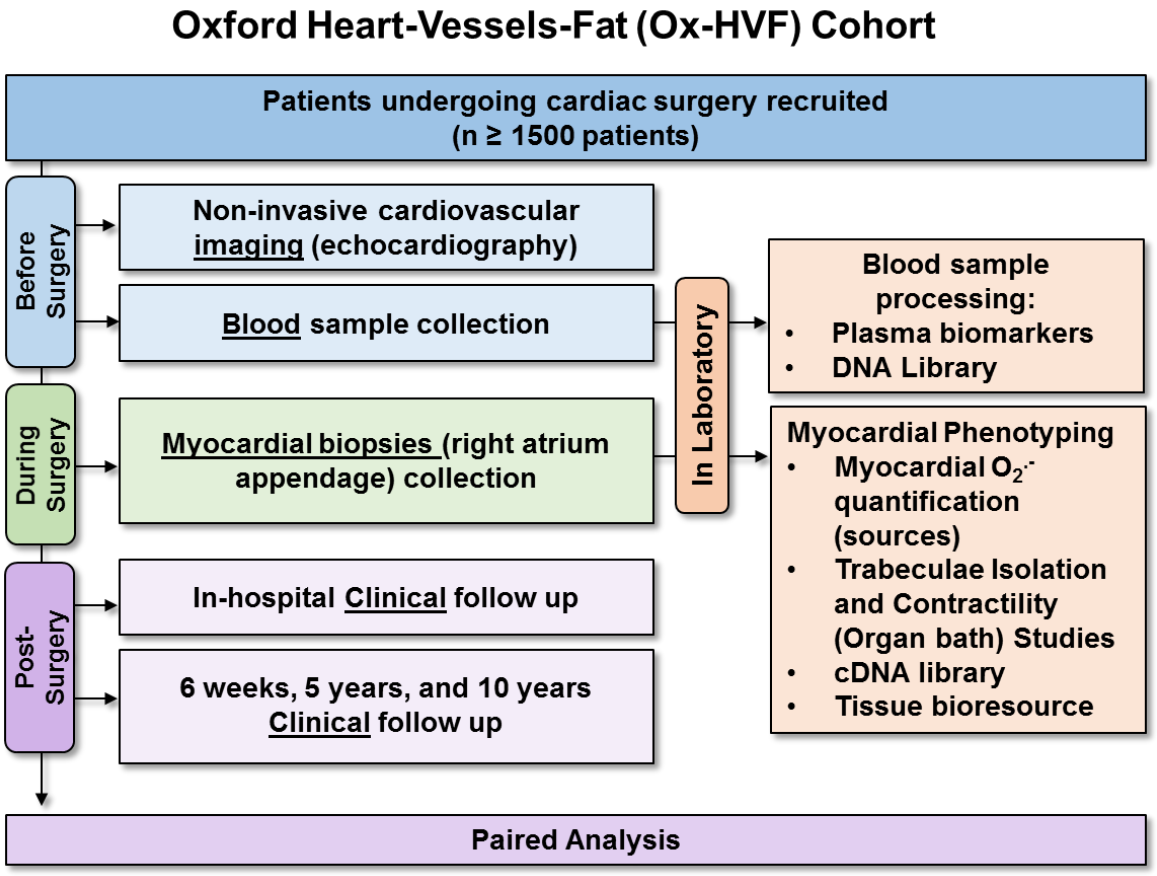


Figure 2.1 Clinical Study with the Oxford Heart-Vessels-Fat (Ox-HVF) Cohort

The Ox-HVF Cohort is a cohort of patients who are undergoing elective CABG or mitral/aortic valve replacement at the John Radcliffe Hospital (Oxford University Hospitals, NHS Foundation Trust). Cardiac non-invasive imaging via echocardiography takes place pre-operatively. Whole blood samples are also collected pre-operatively, creating a plasma bio-resource and DNA library. Human myocardial tissues are used to assess myocardial redox state and contractility. All tissues for each patient are stored as part of a tissue biobank for tissue-specific measurements and are processed to from a cDNA library and gene expression studies. After surgery, patients are followed up for in hospital events (e.g. atrial fibrillation, length of hospital stay) and cardiac imaging takes places in long-term follow-up (six weeks, five years, and ten years after surgery). The *ex vivo* findings are combined with demographic characteristics, clinical outcomes, and non-invasive cardiovascular phenotyping for paired analysis of this cohort. Information regarding our cohort and phenotyping was found on our website (https://oxhvf.com) and in several papers.[6,20,173] CABG, Coronary Artery Bypass Grafting. cDNA, Complementary DNA. NHS, National Health Service. $O_2^{\cdot-}$, Superoxide. Ox-HVF, Oxford Cohort of Heart, Vessels, and Fat.

Exclusion criteria for patient recruitment included cancer, chronic inflammatory disease, use of anti-inflammatory drugs, active infections, severe renal failure, or acute coronary events in the last thirty days (directly from Oxford-HVF exclusion criteria).[6,20,172] Patients are coded with a unique patient ID that is used to identify the

individual and an individual's samples throughout the study (e.g. R001 for patients undergoing CABG, and B001 for patients undergoing valve replacement).

Sample Collection, Phenotyping, and Follow up: From these patients, preoperatively, blood samples are collected and ultrasound (echocardiography) scans are taken for structural and functional myocardial assessment.[6,20] Whole blood sampling is used to create a plasma bioresource and DNA library.[6,20]

During surgery, we collect myocardial tissue where possible, that are in surgical excess.[6,20] The samples collected during surgery are used to further characterize the tissues of the patient and to conduct *ex vivo* experiments in the laboratory.[6,20] Human myocardium is examined for myocardial redox state.[6,20] All tissues for each patient are stored as part of a tissue biobank and cDNA library for specific interventions and gene expression studies.[6,20]

After surgery, patients are followed up for in-hospital events and clinical outcomes (e.g. mortality) over five to ten years as part of this ongoing cohort, and cardiac imaging takes places in long-term follow-up.[6,20,173] The *ex vivo* findings and experimental characterizations are combined with non-invasive imaging, clinical risk factors, clinical outcomes and demographics of these patients for paired analysis.[6,20,173] A schematic of the work flow of the Ox-HVF Cohort relevant to this project is shown (Figure 2.1).[6,20]

2.1.2 Technical Aims

The technical aims of Chapter 3 were specifically as follows:

I. Develop a method for real-time H_2S monitoring and determine the kinetics of fast and slow-releasing H_2S donors (these exogenous donors were used *ex vivo*)
II. Optimize the methylene blue technique to quantify H_2S/Sulfide in human plasma
III. Develop and validate a CSE knockdown cell line model (H9C2 cells) via shRNA
IV. Develop an *in vitro* model of oxidative stress

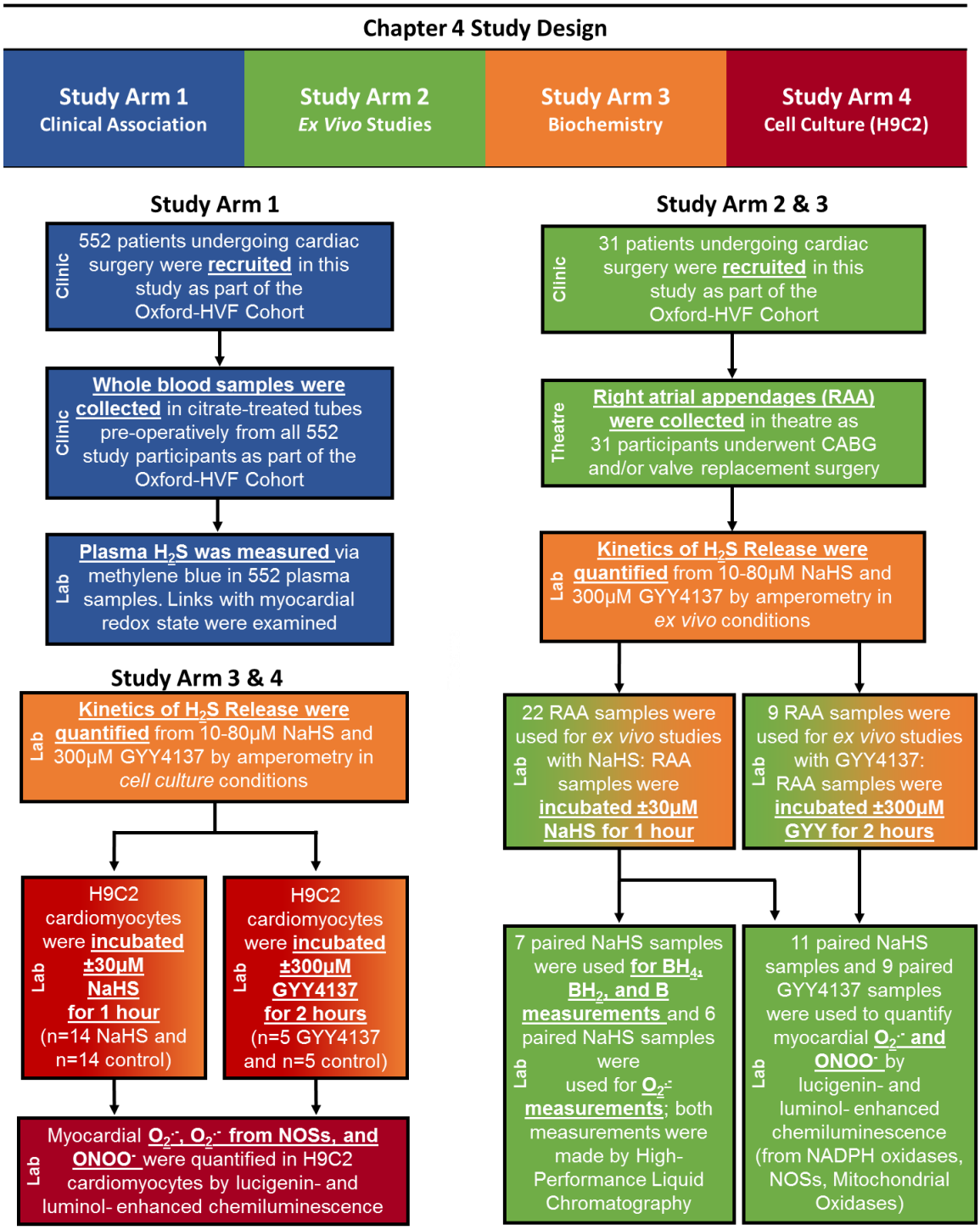


Figure 2.2 Study Design to Address Chapter 4 Aims

The technical aims of Chapter 4 (Figure 2.2) were specifically as follows:

I. Examine whether plasma H_2S/Sulfide was associated with patient demographics

II. Examine whether plasma H_2S/Sulfide (systemic) was associated with myocardial redox state ($O_2^{\bullet-}$ from NADPH oxidases, mitochondrial oxidases, and NOSs)

III. Examine the kinetics of H_2S release from two H_2S donors NaHS and GYY4137 in *ex vivo* conditions (to determine an appropriate incubation time for *ex vivo* incubations with H_2S donors) and three additional physiological conditions each

IV. Examine the effects of NaHS on myocardial redox state with a focus on NOSs

   a. Examine in healthy rat cardiomyocytes (H9C2 cell line) the effects of H_2S donor NaHS on NOS coupling and $ONOO^-$ levels

   b. Examine the effects of NaHS on myocardial sources of $O_2^{\cdot-}$ (NOSs and $ONOO^-$) in myocardium from patients undergoing cardiac surgery

   c. Examine the specificity of the effects of NaHS on basal $O_2^{\cdot-}$ using two methods to measure $O_2^{\cdot-}$ and effects on other enzymatic sources of $O_2^{\cdot-}$ (NADPH oxidases, mitochondrial oxidases)

   d. Explore potential underlying mechanisms for H_2S mediated-changes in NOS coupling and $ONOO^-$ by examining changes in tetrahydrobiopterin (BH_4) oxidation

V. Examine the effects of GYY4137 on myocardial redox state with a focus on NOSs

   a. Examine in healthy rat cardiomyocytes (H9C2 cell line) the effects of H_2S donor GYY4137 on NOS coupling and $ONOO^-$ levels

   b. Examine the effects of GYY4137 on myocardial sources of $O_2^{\cdot-}$ (NOSs and $ONOO^-$) in myocardium from patients undergoing cardiac surgery

   c. Examine the specificity of the effects of GYY4137 on basal $O_2^{\cdot-}$ and effects on other enzymatic sources of $O_2^{\cdot-}$ (NADPH oxidases, mitochondrial oxidases)

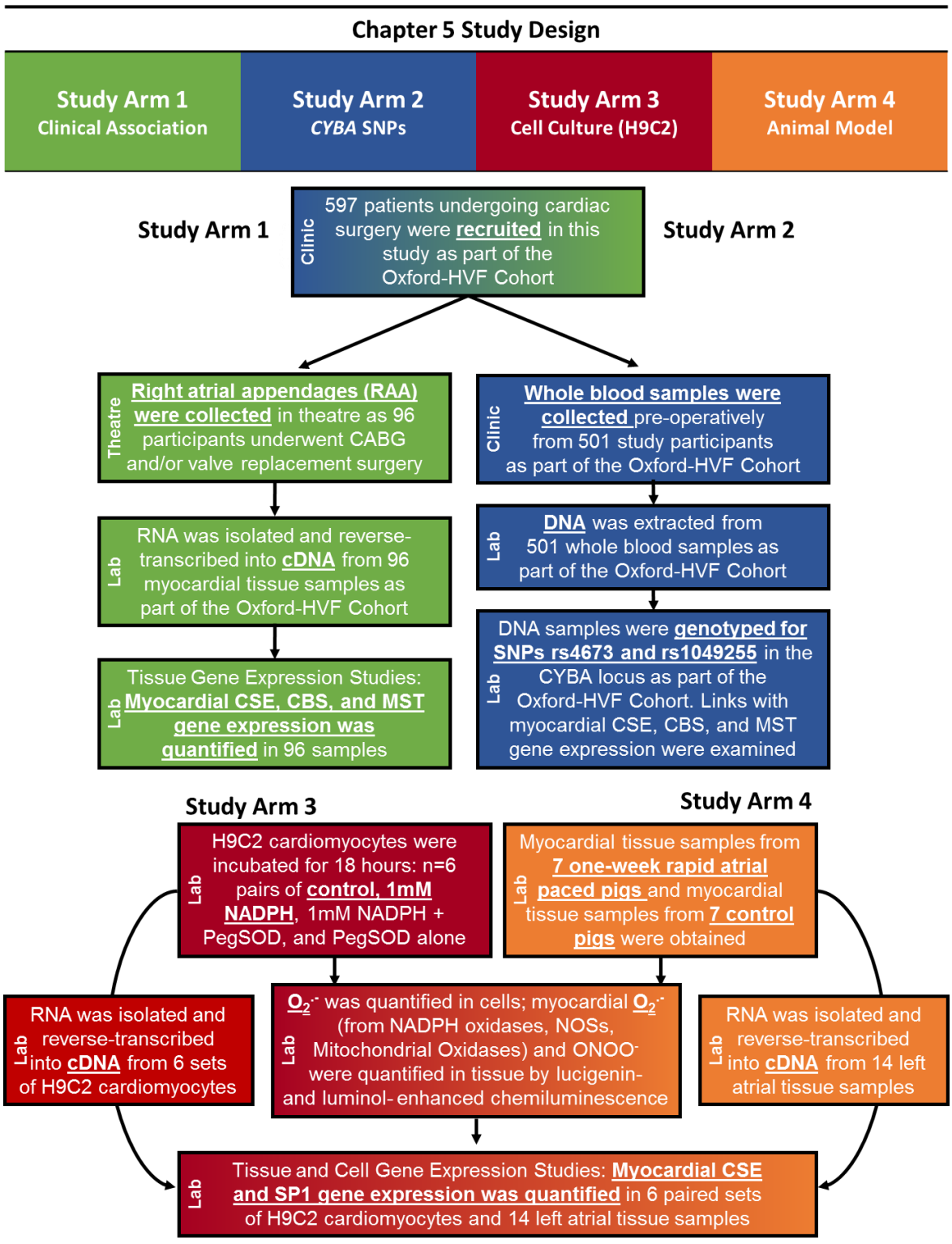


Figure 2.3 Study Design to Address Chapter 5 Aims

The technical aims of Chapter 5 (Figure 2.3) were specifically as follows:

I. Determine whether myocardial CSE, CBS, and MST expression was associated with myocardial redox state in a large cohort of patients with cardiac disease

a. Quantify myocardial CSE expression in large cohort
b. Determine whether myocardial CSE, CBS, and MST gene expression was related to patient demographics and cardiac disease
c. Determine whether myocardial CSE, CBS, and MST gene expression was related to $O_2^{\cdot -}$ from NADPH oxidases, mitochondrial oxidases, and NOSs

II. Determine whether oxidative stress reduces gene expression of myocardial CSE, CBS, MST, and Specificity protein 1 (SP1, a redox-sensitive transcription factor that may regulate CSE) *in vitro* and *in vivo*
    a. Characterize an *in vitro* model of oxidative stress and examine changes in gene expression
    b. Characterize an *in vivo* pig model of oxidative stress and examine changes in gene expression

III. Explore the redox-sensitivity of myocardial CSE expression in humans
    a. Determine whether the additive SNPs in CYBA $p22^{phox}$ can be used as a model of human myocardial oxidative stress
    b. Examine additive SNPs in CYBA $p22^{phox}$ related to increased oxidative stress and their associations with the expression of myocardial CSE and circulating H_2S levels

The technical aims of Chapter 6 (Figure 2.4) were specifically as follows:

I. Determine the role of CSE, if any, in regulating myocardial redox balance *in vitro* by characterizing NOS biology in CSE knockdown H9C2 cells

II. Explore a known functional variant in CSE's causal role in regulating myocardial redox state
    a. Determine associations between SNPs (CSE SNP rs1021737 and 2 SNPs in CBS) and patient demographics and cardiac disease

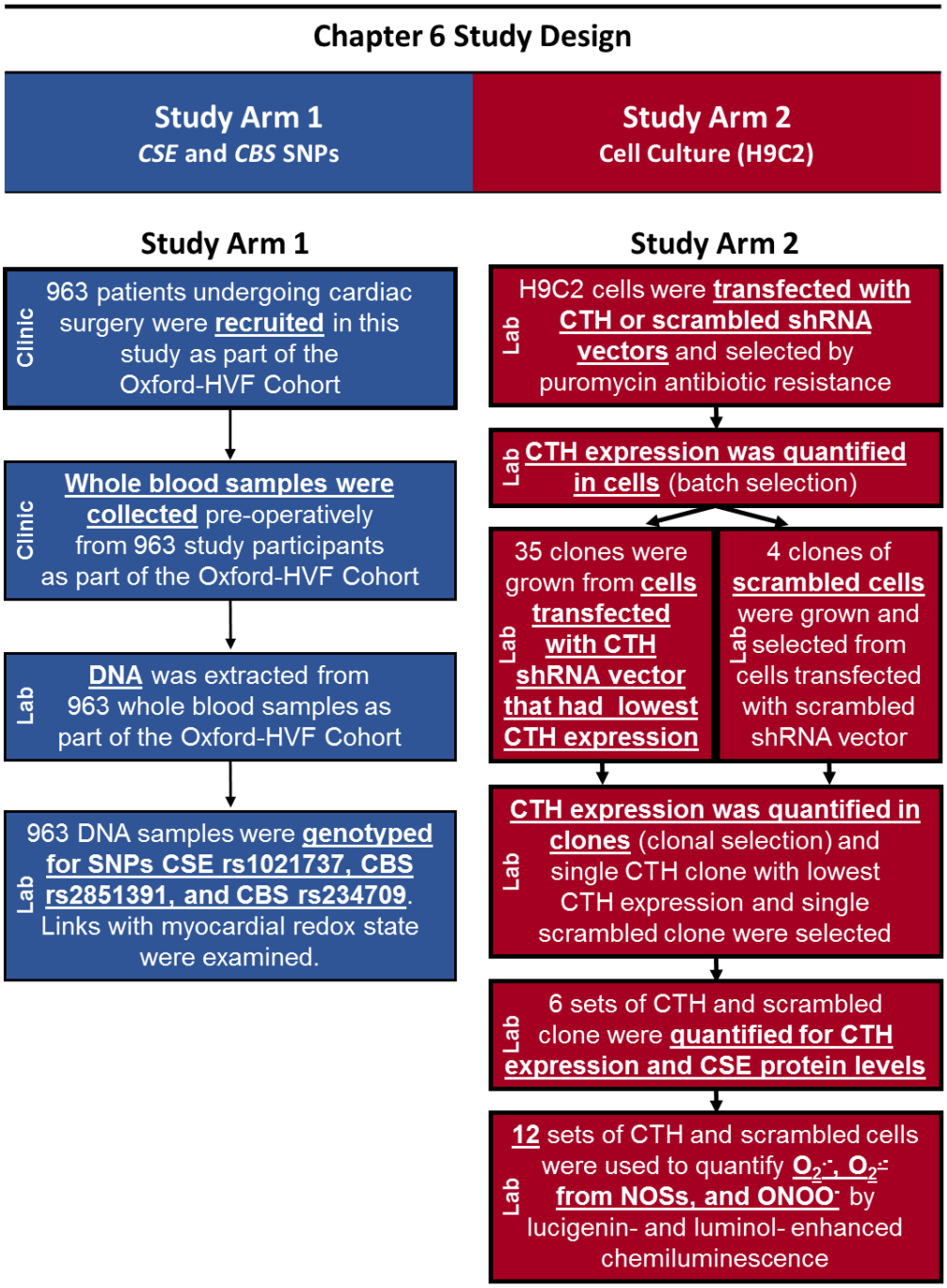


Figure 2.4 Study Design to Address Chapter 6 Aims

b. Examine whether a SNP in CSE demonstrates a causal relationship between CSE and myocardial oxidative stress

c. Examine whether two SNPs in CBS demonstrate a causal relationship between CBS and myocardial oxidative stress.

2.2 Clinical Measurements

2.2.1 DNA Extraction and Genotyping

Knowledge of variants in CSE and CBS allowed for further causal analysis of effects of H_2S/CSE biology on myocardial redox state. Single nucleotide polymorphisms (SNPs) in CSE and CBS genes were identified through the National Institute of Health (NIH) website database of genomic wide association studies (GWAS, genome.gov/gwastudies). SNPs that were associated with cardiovascular related diseases such as homocysteinemia were identified; through this selection process, 2 CBS SNPs (rs234709 and rs2851391)[155-157] and 1 CSE SNP (rs1021737)[153,154] were selected.

DNA extracted from whole blood was genotyped for these SNPs in CSE and CBS. As we have previously described, DNA was purified from whole blood using the QIAamp DNA Blood Midi Kit and the manufacturer's protocol.[20,75,174] Briefly, human blood was lysed and then added to QIAamp spin column which attracts the DNA.[175] The column was washed with buffers to remove protein and other contaminants and the purified DNA was eluted.[175]

DNA was genotyped for these functional SNPs on Applied Biosystems StepOne Plus polymerase chain reaction (PCR) system using Applied Biosystems TaqMan probes according to the manufacturer's protocol as we have previously described.[20,176] The specific cycles and temperatures of the PCR program are shown below (Table 2.1).

Table 2.1 Genotyping Program by Applied Biosystems for PCR Conditions

Step No.	Time (sec, min)	Temperature (◦C)	Cycle repeats
1	30 sec	60	1x
2	10 min	95	1x
3	15 sec	95	40x
4	1 min	60	
5	30 sec	60	1x

PCR, Polymerase Chain Reaction.

Briefly, a mastermix was made combining TaqMan Genotyping Master Mix (ABiosystems), nuclease-free water, and TaqMan probes (VIC & FAM) according to manufacturer's protocol.[177] Mastermix was added to DNA (10-15 nanograms) in a ratio of 4:1.[177] Samples were run on an ABiosystems platform.[177] In the StepOne Software, SNP alleles were labelled with their reporter dye (e.g. VIC=C, FAM=T).[177] The intensity of the signal from each reporter dye determined the homozygosity or heterozygosity of the individual for the particular SNP (Figure 2.5, Figure 2.6, and Figure 2.7).[177]

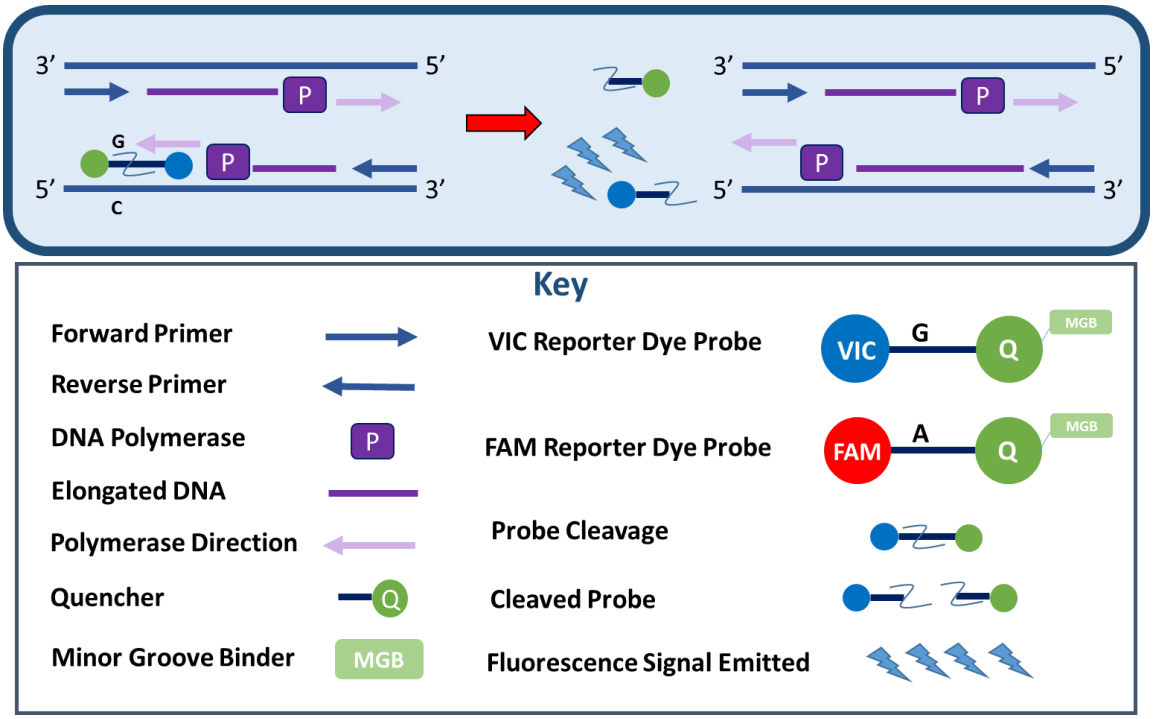


Figure 2.5 Genotyping using TaqMan® Probes

In a PCR reaction, the two strands of DNA are denatured and elongated, with specific forward and reverse primers as starting points for polymerization. In the TaqMan assay, in addition to primers, a probe is utilized that anneals specifically to a sequence located between the two primer binding sites including the allele of interest. The probe's minor groove binder helps the probe stay bound to the DNA strand until cleaved. When DNA polymerase elongates DNA strands and makes contact with the annealing/hybridizing probe, the polymerase cleaves the probe, separating the reporter dye (VIC/FAM) from the quencher. Before cleavage of the probe, the quencher 'quenched' the fluorescence of the reporter dye through FRET; however, in the cleaved state, the fluorescence signal is unquenched and can be monitored. The fluorescence intensity increases with DNA amplification. Therefore, as an example, if an individual is homozygous for the C allele, the VIC probe with the G allele will bind, be cleaved, and emit exponential fluorescence with DNA amplification. However, the FAM probe (with a different emission spectrum) will not bind, be cleaved, or emit signal if the individual does not have the T allele to which the FAM probe would bind. The intensity of the signal from each reporter dye, quantified and normalized, determines the homozygosity or heterozygosity of the individual for the SNP. Information from TaqMan® SNP Genotyping Assays User Guide.[177] PCR, Polymerase Chain Reaction.

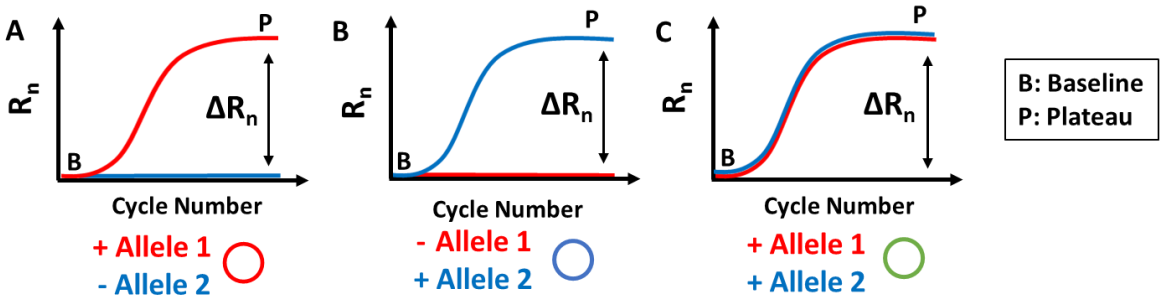


Figure 2.6 DNA Amplification Plot for Genotyping

Genotype of individuals for a particular SNP is determined by a DNA Amplification Plot. As cycles of PCR increase to 40 (on the x-axis), fluorescence of VIC (red) and FAM (blue) are plotted as Rn (on the y-axis). R_n (also known as the normalized reporter) is the fluorescence intensity of the VIC or FAM probe unquenched and normalized to a reference dye fluorescence (so changes in volume or concentration of the dye is negligible). ΔR_n is calculated as Rn_plateau (at a given cycle number, e.g. 40 or set threshold) – Rn_baseline (initial cycle numbers where fluorescence is not increasing significantly based on best fit line). Individuals who have an exponential increase in VIC fluorescence (red, $\uparrow\Delta R_n$) and no exponential increase in FAM fluorescence (blue) are homozygous for allele 1 (A). Individuals who have an exponential increase in FAM fluorescence (blue, $\uparrow\Delta R_n$) and no exponential increase in VIC fluorescence (red) are homozygous for allele 2 (B). Individuals who have an exponential increase in both VIC fluorescence (red, $\uparrow\Delta R_n$) and FAM fluorescence (blue, $\uparrow\Delta R_n$) are heterozygous for allele 1 and 2 (C). Information regarding DNA amplification from ABiosystems Guide.[178]

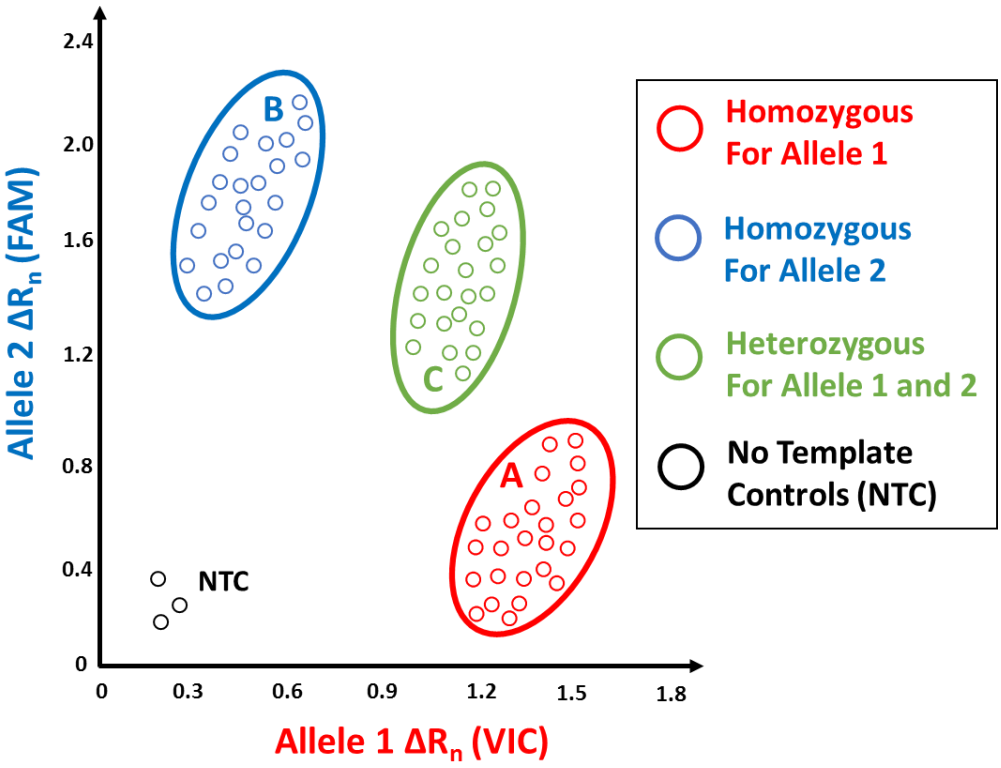


Figure 2.7 Analysis of Genotyping in an Allelic Discrimination Plot

The ΔR_n fluorescence of the VIC and FAM dyes in the DNA Amplification plot are plotted as ΔRn values in an allelic discrimination plot. Allele 1, represented by the fluorescence of VIC dye, is plotted on the x-axis while Allele 2, represented by the fluorescence of the FAM dye, is plotted on the y-axis. Individuals

homozygous for Allele 1 cluster in the bottom-right portion of the allelic discrimination plot where Allele 1 VIC fluorescence is highest and Allele 2 FAM fluorescence is lowest; this region is shown in red (A). Individuals homozygous for Allele 2 cluster in the top-left portion of the allelic discrimination plot where Allele 1 VIC fluorescence is lowest and Allele 2 FAM fluorescence is highest; this region is shown in blue (B). Individuals heterozygous for Allele 1 and 2 cluster in the top-right portion of the allelic discrimination plot where Allele 1 VIC fluorescence is highest and Allele 2 FAM fluorescence is highest; this region is shown in green (C). No Template controls are found in the bottom-left portion of the allelic discrimination plot (shown in black) where both Allele 1 VIC fluorescence and Allele 2 FAM fluorescence are lowest. Graph was made on the basis of information describing the TaqMan Assay.[177]

2.2.2 Human Myocardium *Ex Vivo* Models

In the second part of this study, *ex vivo* models, right atrial appendage samples (RAA, Figure 2.8) were incubated with H_2S donors NaHS and GYY4137 according to the experimental design described for Chapter 4 (Figure 2.2). Myocardial $O_2^{\cdot-}$ was quantified in these samples by lucigenin- and luminol-enhanced chemiluminescence as we have previously described (Section 2.3).[20] Changes in NOS cofactor tetrahydrobiopterin (BH_4) and its oxidizing partners (dihydrobiopterin, BH_2; biopterin, B) were also measured in RAA after incubation with H_2S from NaHS as previously described (Section 2.4).[179] The purpose of these measurements was to determine the effects of H_2S on the oxidation of BH_4, important for NOS coupling. Further quantification of $O_2^{\cdot-}$ was conducted by dihydroethidium high-performance liquid chromatography (DHE-HPLC), as previously described with some modifications (Section 2.4).[43,176]

2.2.2.1 *Ex Vivo* Myocardium Treatments

The method of *ex vivo* incubations of human myocardium is unique in that it allows us to determine the effects of NaHS (Sigma Catalog No. 161527) and GYY4137 (Sigma Catalog No. SML0100) on sources of $O_2^{\cdot-}$ in human myocardial tissue samples. This method enables us in particular to incubate human myocardial tissue in thin strips (which maximizes surface area and minimizes necrosis) in physiological conditions for up to two hours with our intervention and determine the effects of the intervention through experimentation (e.g. $O_2^{\cdot-}$ measurements) as we have previously described.[6,20]

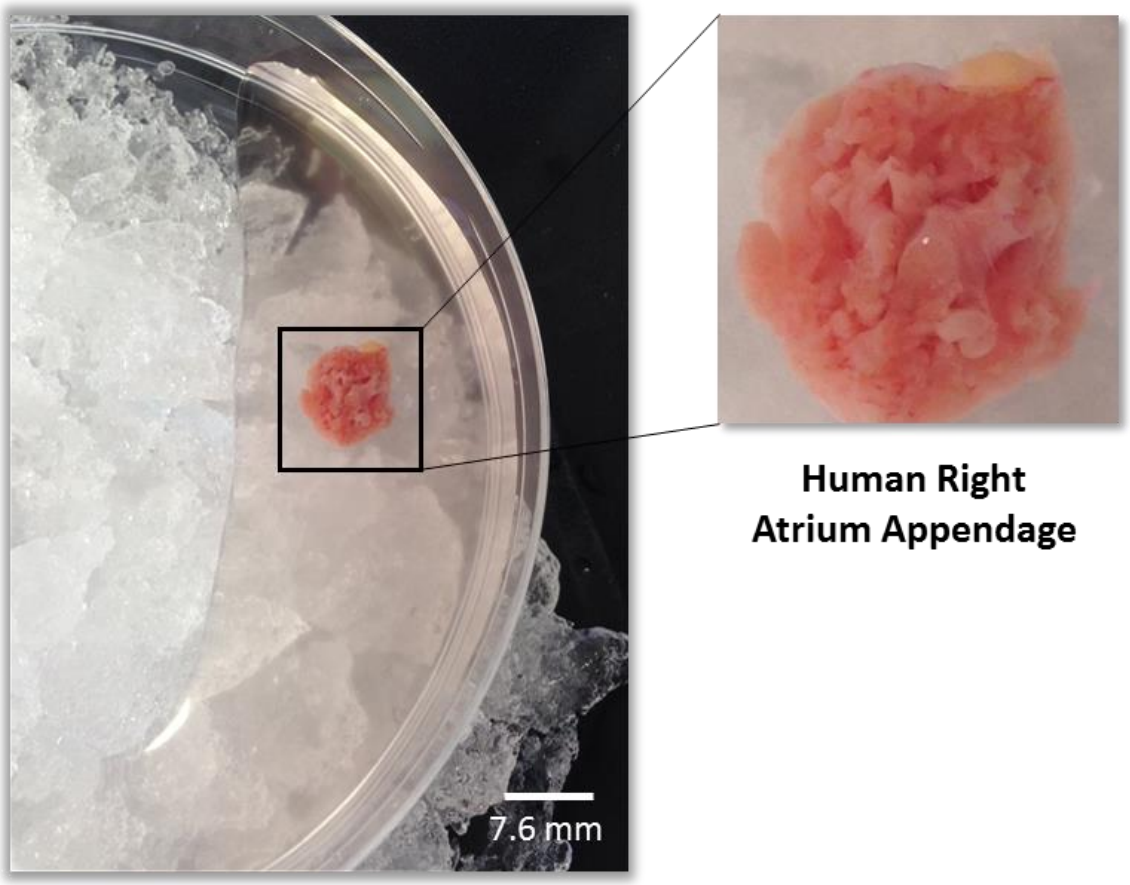


Figure 2.8 Human Myocardium (Right Atrial Appendage)

From patients undergoing surgery, a biopsy of the right atrial appendage is removed for cannulation. A sample is shown here. Scale bar is drawn (7.6mm).

Briefly, human myocardial tissue samples were washed in ice-cold Krebs HEPES buffer and then cut into thin strips containing all myocardial layers.[6,20] The myocardial samples were then equilibrated for 25 minutes in Krebs HEPES Buffer pH 7.35 at 37^{o}C, after which they were transferred to fresh Krebs HEPES buffer (equal number of strips) and incubated in the presence or absence of H_2S donors (incubated in a paired manner).[6,20] For NaHS treatments, human myocardial strips were incubated for 1hr in the presence or absence of 30μM NaHS. For GYY4137 treatments, myocardial strips were incubated for 2hrs in the presence or absence of 300μM GYY4137. GYY4137 was stored in concentrated aliquots at -80^{o}C while NaHS (salt) was stored at room temperature. Samples were briefly dried following incubation and immediately frozen for analysis.

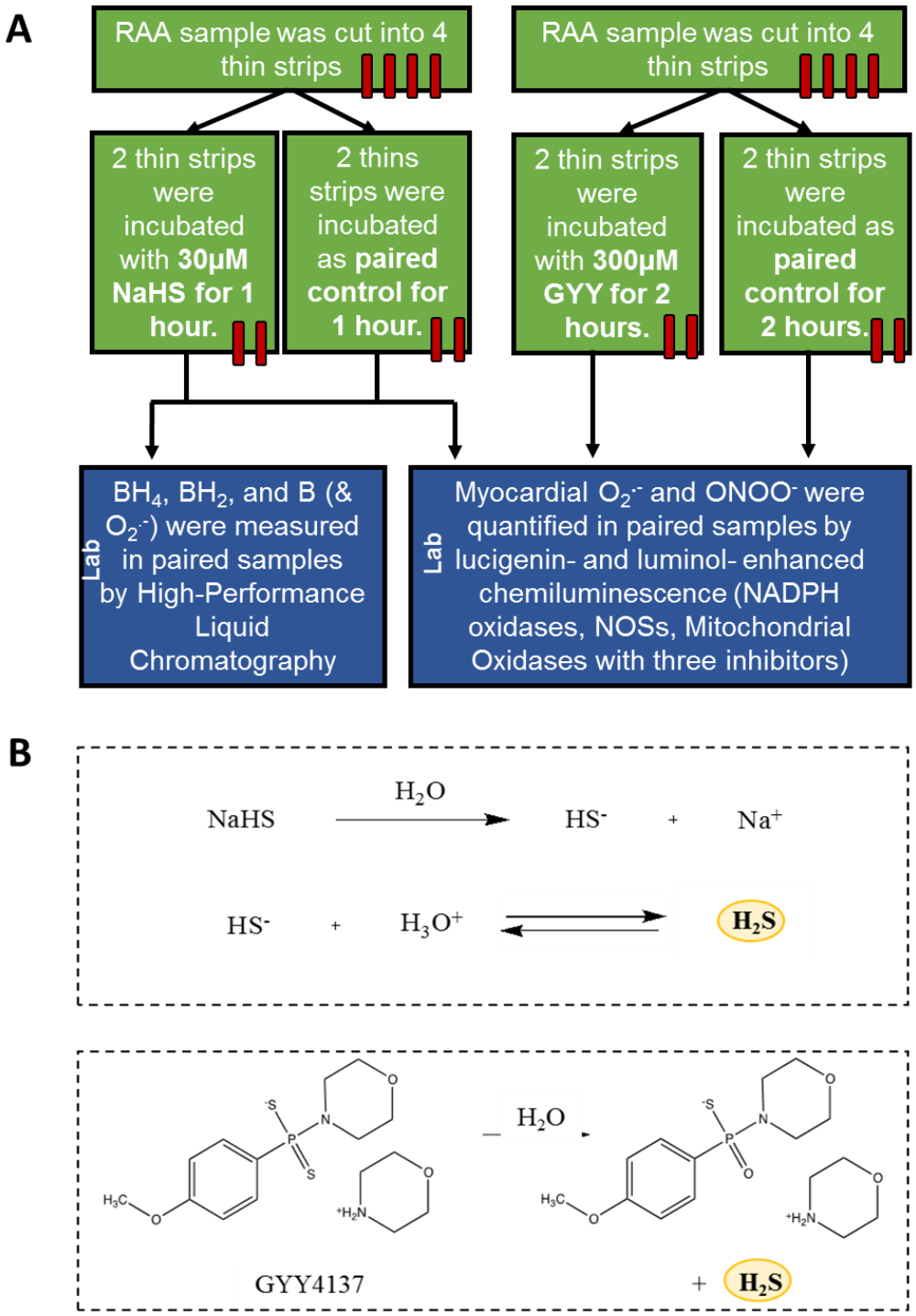


Figure 2.9 Experimental Design for *Ex Vivo* Studies and H_2S Donors

(**A**) Human myocardium is depicted, which is cut into thin strips and equilibrated, prior to (B) intervention. (**B**) The chemical structures of the H_2S donors used for *ex vivo* studies are shown.

Myocardial $O_2^{\cdot-}$ was quantified in these samples after incubation with H_2S donors (Figure 2.9). A known limitation of this *ex vivo* technique is that incubation time for human myocardium is limited to two hours as longer durations of incubation result in

non-physiological conditions for the tissue.[20] This limitation is important to note because, while using a long-lasting H_2S donor GYY4137, incubation time is limited to two hours.

2.3 Lucigenin- and Luminol-Enhanced Chemiluminescence

In this study, lucigenin- and/or luminol-enhanced chemiluminescence was utilized to quantify $O_2^{\cdot-}$ and $ONOO^-$ in right atrial appendages as part of the larger Ox-HVF cohort phenotyping (conducted by group members in our laboratory) and for *ex vivo* studies. In addition to human myocardial samples, lucigenin- and luminol-enhanced chemiluminescence was utilized in this study to quantify $O_2^{\cdot-}$ and $ONOO^-$ cell culture models and animal models.

To quantify myocardial $O_2^{\cdot-}$ generation in these samples, lucigenin- and luminol-enhanced chemiluminescence was used in conjunction with appropriate specific enzymatic inhibitors as we have previously described.[6,20] This method utilizes chemiluminescent probes lucigenin (bis-N-methylacridinium nitrate) and luminol (5-amino-2,3-dihydroxy-1,4-phthalayineidone) to detect ROS.[180,181] Lucigenin reacts with $O_2^{\cdot-}$ specifically and, in its reaction, releases a photon that is used to quantify $O_2^{\cdot-}$.[180] Luminol reacts with several ROS including $O_2^{\cdot-}$, $ONOO^-$, hydrogen peroxide (H_2O_2), and hydroxyl radical, but the use of scavengers can specify the species.[180] For example, the addition of uric acid (an $ONOO^-$ scavenger) to luminol-enhanced chemiluminescence can specify $ONOO^-$.[180]

This technique is unique in that it can measure source-specific $O_2^{\cdot-}$ by measuring the difference in $O_2^{\cdot-}$ with or without a source-specific inhibitor on the same sample in real-time.[6,20] That is, in a continuous manner, basal $O_2^{\cdot-}$ is recorded and then $O_2^{\cdot-}$ after the addition of an inhibitor is recorded, while in other techniques, a sample is split into two (with and without source-specific inhibitor) and this measurement as two different samples adds variability to the findings. As a limitation, it is known that lucigenin can

react with O_2 to generate $O_2^{\cdot -}$ itself, a phenomenon known as lucigenin-derived redox cycling which can lead to artificially raised $O_2^{\cdot -}$ measurements; however, this phenomenon is known to occur at 20 µM or higher concentrations of lucigenin.[180,182] Studies examining $O_2^{\cdot -}$ using 10 µM lucigenin or less did not result in this increase in stimulated $O_2^{\cdot -}$.[180] Our study uses 5 µM lucigenin, suggesting the lucigenin-derived redox cycling is not an apparent and obvious limitation here.[75] Another known limitation is that this technique cannot be used with cell culture media that contains phenol red as this increases lucigenin-enhanced chemiluminescence signal; buffers were used in all experiments.[183]

2.3.1 Sample Preparation and Measurements

Briefly, to prepare samples, as we have described previously,[6,20] ice-cold extraction buffer was prepared by mixing Krebs HEPES buffer (pH=7.40; components of buffer described in Section 0 below) with protease inhibitor and mixed buffer was kept on ice. Myocardial tissue frozen at -80°C was kept on dry ice and carefully weighed.[20] 35 µL/mg ice-cold extraction buffer was added to the myocardial sample and the sample was immediately homogenized and kept on ice.[20]

Protein in the tissue sample was quantified using the Bradford assay with BSA standards for equal loading.[20] Briefly, Bradford assay was added to all samples and standards and samples were briefly agitated before incubation at room temperature for 10 minutes.[20] Absorbance was read at 595 nanometers on a plate-reading spectrophotometer.[20] Standard curve was graphed based on known protein content in standards. Protein concentration in the samples were estimated based on the standard curve (estimated line of best fit). Volume of tissue homogenate in extraction buffer to load in luminometer was calculated based on protein content and desired protein to load (0.2 mg if possible for tissue samples).[20]

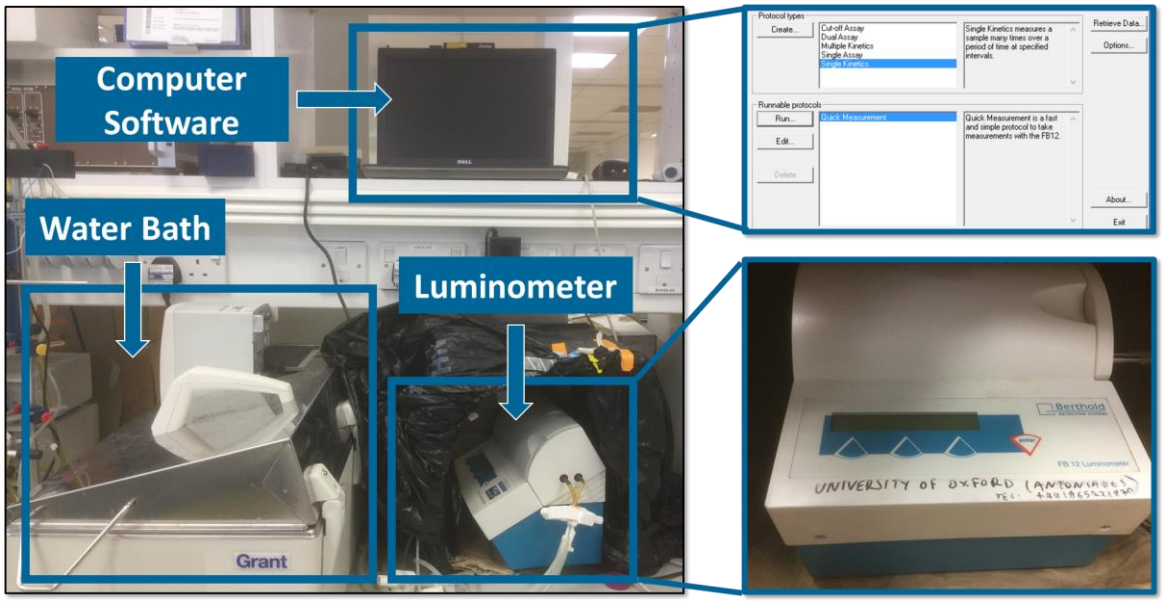


Figure 2.10 Lucigenin- and Luminol-Enhanced Chemiluminescence Setup

Lucigenin- and luminol-enhanced chemiluminescence, or luminometry, was used to measure reactive oxygen species in samples via light-sensitive probes (lucigenin and luminol) in instrument FB12 Titertek-Berthold single-tube luminometer. The luminometer, which was stored in a dark box to protect samples from light, maintains the sample at a physiological temperature through its connection to a water bath which circulates water through the luminometer. The measured light signal (in RLU/second) is recorded in a table and graphed on a laptop on FB12 Single Kinetics Software developed by Softstep Corporation©. RLU, Relative Light Units.

For measurement of $O_2^{\cdot-}$ production, a FB12 Titertek-Berthold single-tube luminometer maintained in the dark was utilized (Figure 2.10). Samples were kept at 37°C via a connected water bath. Lucigenin- and luminol-enhanced chemiluminescence signal was recorded on FB12 software. Samples were measured in the presence of 5µM lucigenin or 100 mM luminol.[6,75] To record basal $O_2^{\cdot-}$ production in myocardial tissue, first Krebs HEPES buffer and lucigenin were added to the luminometry vial and background signal (in relative light units) was recorded.[20] Following an achieved stable background, sample was added with the volume calculated previously for approximately 0.2 mg protein.[20] Stable tissue signal was achieved and this tissue signal with background subtracted provided the basal $O_2^{\cdot-}$ signal, which was adjusted for the amount of protein loaded, resulting in relative light units/mg protein.[20] This basal $O_2^{\cdot-}$ indicates total $O_2^{\cdot-}$ from myocardial sources at rest (non-stimulated).[20]

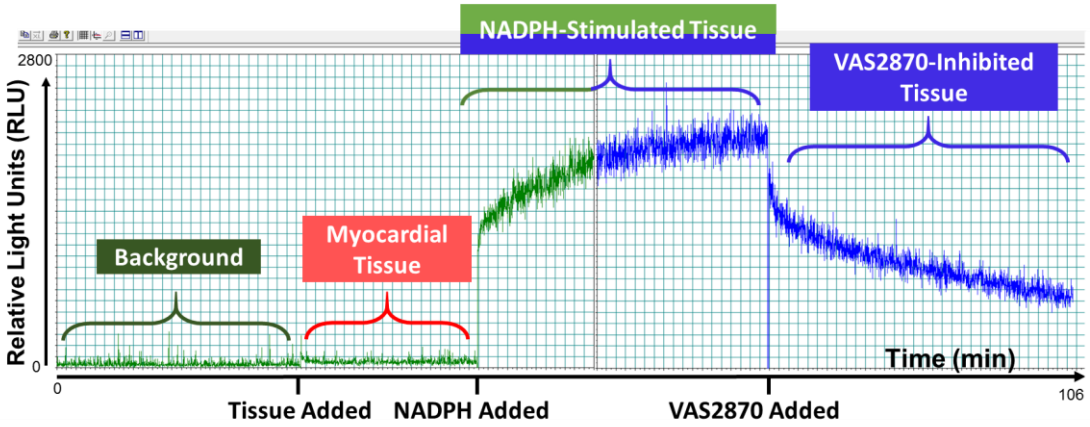


Figure 2.11 Lucigenin-Enhanced Chemiluminescence Trace (NADPH Oxidases)

$O_2^{\cdot-}$ from NADPH oxidases in myocardial samples (RAA homogenates) were quantified by the NADPH-stimulated and VAS2870-inhibtable signal as shown. A representative lucigenin-enhanced chemiluminescence trace (two screenshots are combined side by side given the limited timeframe of each screen) is shown quantifying $O_2^{\cdot-}$ from NADPH oxidases in a human myocardial sample. In a lucigenin-enhanced chemiluminescence experiment, background with Krebs HEPES and lucigenin is recorded. Myocardial tissue homogenate is then added and signal is continuously recorded. When tissue reaches a stable baseline, 1mM NADPH is added and the NADPH-stimulated signal is recorded until plateau. VAS2870 is added and recorded until plateau or 30 minutes.

2.3.2 Source-Specific Inhibitors and Data Analysis

Single Kinetics Software was utilized for data capture and analysis.

2.3.2.1 Basal $O_2^{\cdot-}$ Measurements in Myocardial Tissue and Cells

Basal $O_2^{\cdot-}$ measurements were repeated and source-specific stimulation or inhibition was used to quantify $O_2^{\cdot-}$ from particular sources.[6]

2.3.2.2 NADPH-stimulated and VAS2870-inhibitable $O_2^{\cdot-}$ Measurements in Myocardial Tissue and Cells

NADPH was added after recording basal $O_2^{\cdot-}$ to stimulate NADPH oxidases; NADPH-simulated $O_2^{\cdot-}$ indicates $O_2^{\cdot-}$ from all sources after NADPH stimulation (primarily from NADPH oxidases).[6] Specific inhibitors were also used: VAS2870 (triazolo pyrimidine) is an inhibitor of NADPH oxidases[184] and VAS2870-inhibitable $O_2^{\cdot-}$ indicates $O_2^{\cdot-}$ derived from NADPH oxidases.[20] VAS2870 was used in the presence and

absence of NADPH stimulation to determine the contribution of NADPH oxidase-derived $O_2^{\cdot-}$.[20] An example trace is shown (Figure 2.11).

2.3.2.3 LNAME- inhibitable $O_2^{\cdot-}$ Measurements in Myocardial Tissue and Cells

LNAME-inhibitable $O_2^{\cdot-}$ indicates $O_2^{\cdot-}$ from nitric oxide synthases (NOSs).[75]

2.3.2.4 Uric Acid-inhibitable ROS Measurements in Myocardial Tissue and Cells

In place of lucigenin, luminol was used with uric acid (an $ONOO^-$ scavenger) to determine the contribution of $ONOO^-$.[6]

2.3.2.5 Rotenone-inhibitable $O_2^{\cdot-}$ Measurements in Myocardial Tissue

Rotenone (100μM)-inhibited $O_2^{\cdot-}$ indicates $O_2^{\cdot-}$ from mitochondria (at complex I or from sources using complex I electrons like complex III).[6]

2.3.2.6 Myxothiazol-inhibitable $O_2^{\cdot-}$ Measurements in Myocardial Tissue

Myxothiazol (5μM)-inhibited $O_2^{\cdot-}$ indicates $O_2^{\cdot-}$ from mitochondria (from sources using complex III electrons).[28,185-188]

2.3.2.7 Antimycin A-inhibitable $O_2^{\cdot-}$ Measurements in Myocardial Tissue

Antimycin A (10μM)-inhibited $O_2^{\cdot-}$ indicates $O_2^{\cdot-}$ from mitochondria (from sources using complex III electrons).[28,185,186] In some cases, mitochondrial inhibitors (Rotenone, Myxothiazol and Antimycin A) are reported to increase $O_2^{\cdot-}$ rather than suppress $O_2^{\cdot-}$.[28,189] Significant effects on mitochondrial $O_2^{\cdot-}$ generation by interventions may nonetheless be observed with the use of these inhibitors with proper control samples.[28] Control samples (without intervention and use of inhibitors) were used throughout this study.

2.4 Organic Chemistry Analytical Techniques

2.4.1 Dihydroethidium High-Performance Liquid Chromatography

There is a consensus in the redox biology field that $O_2^{\cdot -}$ should be measured by at least two methods to confirm the validity of the results. Here, we use DHE-HPLC to quantify $O_2^{\cdot -}$ for this purpose, as we have previously described with some modifications.[43,176] DHE is known to have non-specific reactions that may confound the specific measurements of $O_2^{\cdot -}$.[190] To overcome this, we use polyethylene glycol-superoxide dismutase (PEG-SOD) to quantify $O_2^{\cdot -}$ specifically using this technique.

Briefly, tissue samples were retrieved from -80°C and stored on ice. Myocardial tissue was homogenized in PBS. BCA protein assay was used to quantify proteins in the samples. To 25ug of protein, 100 units of PEG-SOD was added (or water as control). Samples were mixed by agitation and incubated ± PEG-SOD (100 U/ml) for 30 min at 37˚C. DHE was then added to a final concentration of 25µM and samples were incubated at 37˚C for 30 minutes in the dark (as DHE is light sensitive).

The incubation was followed by a spin at full speed for 5 minutes at 4˚C. The supernatant was discarded by pipet. 200µl of ice-cold methanol was added to break open the cells in the pellet and were mixed thoroughly. Samples were frozen at -80˚C until the day prior to measurement or next steps were begun directly. 50µl of ice-cold 0.1 N HCl was added to target any remaining intact cells. Samples were spun at full speed for 5 minutes at 4˚C. Then 150µL of supernatant was transferred into dark vials and run on the HPLC column. The steps described above were used previously in our laboratory with modifications and were kindly provided by postdoctoral fellows Dr. Fabio Sanna and Dr. Costas Psarros.[43,176] A sample chromatogram showing the elution peaks are shown (Figure 2.12).

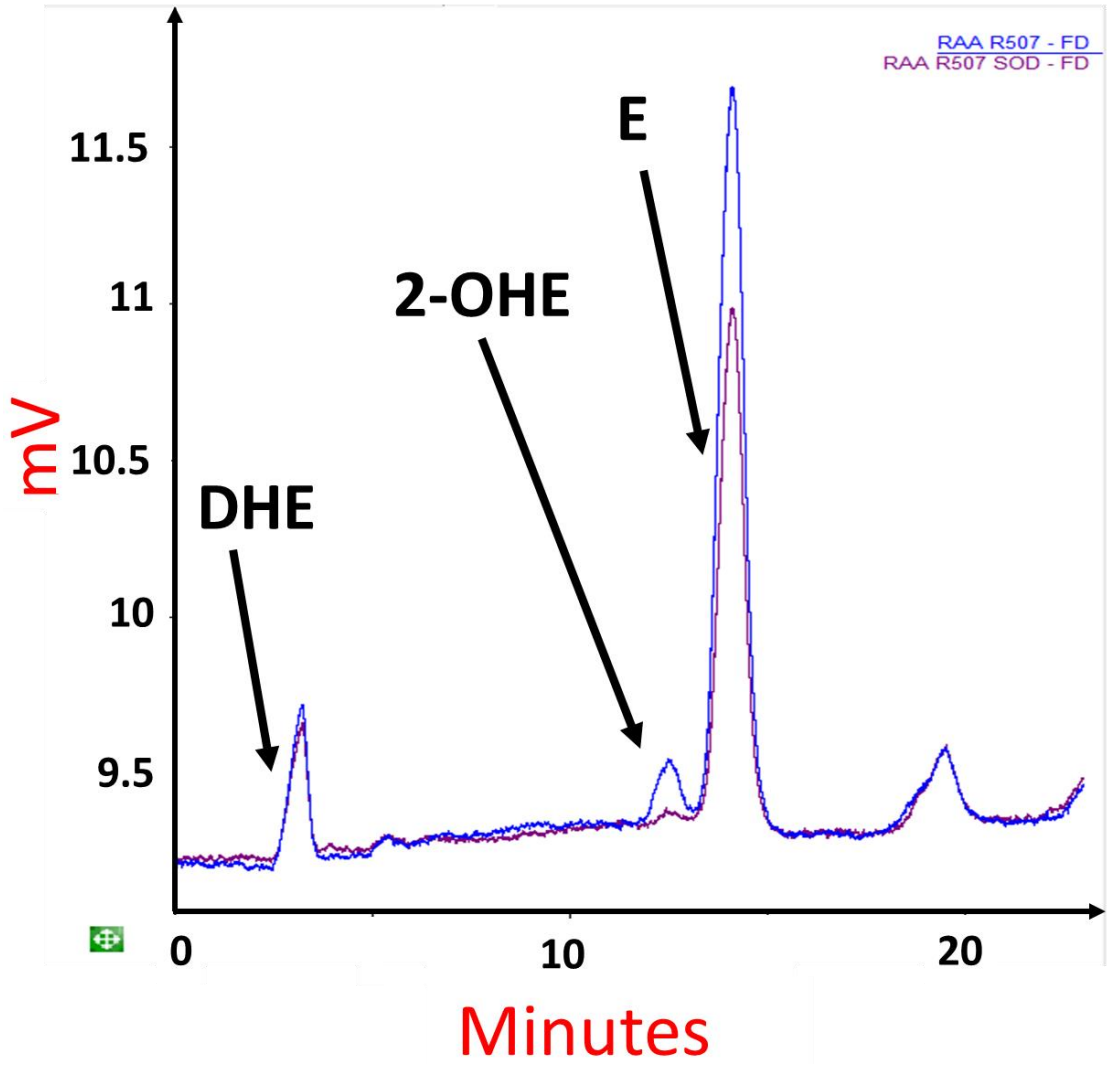


Figure 2.12 DHE-HPLC Chromatogram from RAA

Dihydroethidium (DHE) reacting with $O_2^{\cdot-}$ generates the highly fluorescent product 2-hydroxyethidium (2-OHE), which is quantified for $O_2^{\cdot-}$ measurements.[182] DHE, 2-OHE, and ethidium (another byproduct of DHE reactions) are shown in a chromatogram quantifying $O_2^{\cdot-}$ in RAA with (purple) and without (blue) PEG-SOD, a scavenger of $O_2^{\cdot-}$. With PEG-SOD, the 2-OHE peak quantifying $O_2^{\cdot-}$ is significantly reduced.

2.4.2 Reversed-Phase High-Performance Liquid Chromatography for Biopterins

RP-HPLC is a chemical technique used to measure tetrahydrobiopterin (BH_4), as well as its oxidized partners dihydrobiopterin (BH_2) and Biopterin (B), as we have previously described.[179] These molecules are distinguished by retention time in an HPLC column.[179]

Table 2.2 Mobile Phase Components for HPLC Column

Compound	Concentration	Molar Mass (g/mol)	g/L
Sodium Acetate (HPLC grade)	50 mM	82.03	6.8
Citric Acid	5 mM	192.12	1.05
Ethylenediaminetetraacetic acid (EDTA)	48 µM	292.24	$18 * 10^{-3}$
1,4-Dithioerythritol (DTE)	160 µM	154.25	$24.7 * 10^{-3}$
pH 5.22			

Given that the time of departure from the HPLC column is unique to each molecule, this relayed information is used to both identify the molecule and determine the quantity of the molecule (specifically using the area under the corresponding peak on the HPLC chromatogram). Here, this technique was used to determine if H_2S affects NOSs through effects on the essential cofactor BH_4. A limitation of this technique can be the oxidation of BH_4 before it is measured, which has been documented in previous studies. To overcome this limitation, antioxidants are used in the resuspension buffer in which the tissue is homogenized. Furthermore, samples are quantified in small batches to minimize the time between processing the samples and measurements by HPLC. The steps described from an established protocol and used for this study below were kindly provided by postdoctoral fellow Dr. Surawee Chuaiphichai in Professor Keith Channon's laboratory with the support and advice of Dr. Ricardo Carnicer, Dr. Mark Crabtree, and Dr. Svetlana Reilly; the steps were used previously in our laboratory with modifications here for myocardial tissue.[179]

HPLC Setup and Sample Preparation: The ^{18}C (Carbon) column was washed with 50% methanol/water and water prior to experimentation with a flow rate of 0.1 mL/min.[179] Flow rate of the mobile phase was set to 0.3 mL/min with electrodes running for 1 hour prior to experiment.[191] Components of the mobile phase are described in Table 2.2.[191] Myocardial samples frozen at -80°C were processed by adding resuspension buffer followed by homogenization.[179] Samples underwent one freeze-thaw cycle (dry ice 5-10 min and then thawed) to lyse cells in the resuspension buffer containing antioxidants.[179]

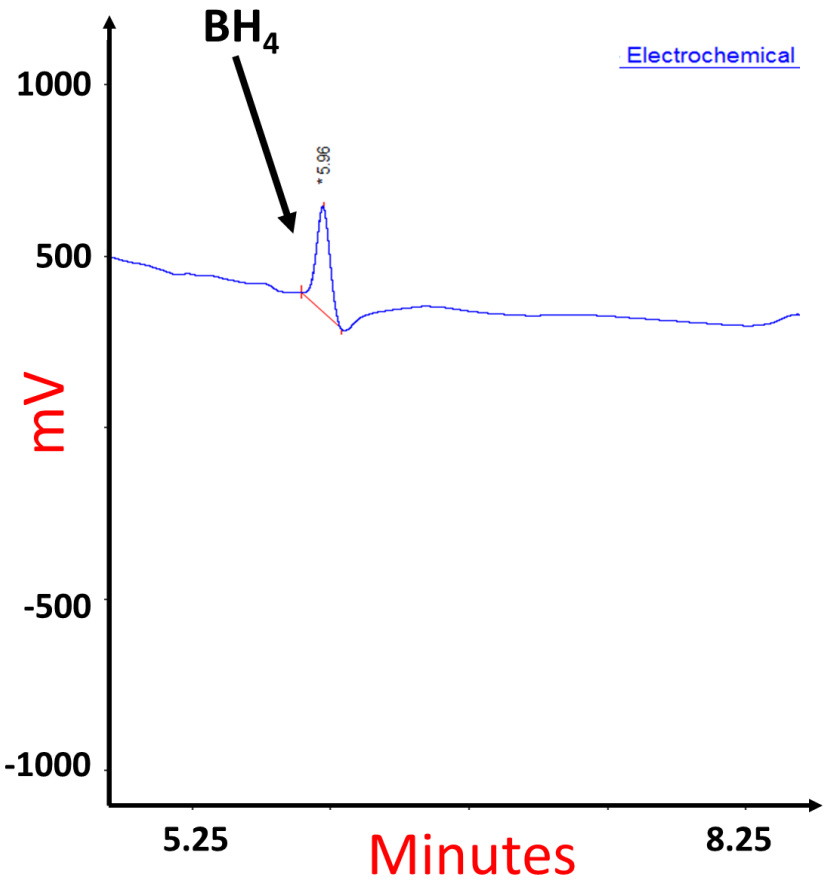


Figure 2.13 Electrochemical Chromatogram for Quantification of BH_4

Representative electrochemical chromatogram for BH_4 is shown. The identifiable peak is near six minutes and is determined by known standards and their elution times prior to each run.

Ice-cold resuspension buffer was prepared in Phosphate Buffer Saline (PBS, 50mM, pH 7.4) with 1mM DTE and 1:100 of 100µM EDTA and kept ice-cold.[179] Precipitation buffer was prepared as a 10X stock in PBS with 1M phosphoric acid, 2M trichloroacetic acid, and 1mM DTE.[179] The samples were then vortexed and spun at 13,200 RPM for 5 min at 4°C.[179] Supernatant was collected and precipitation buffer was added in a 1:10 ratio to precipitate proteins, while a small aliquot of supernatant was reserved for protein quantification using a BCA Protein Assay kit (following manufacturer's protocol).[191] Sample combined with precipitation buffer was spun at 13,200 RPM for 5 minutes at 4°C and a constant volume of supernatant was used for measurement.[191] Standards of BH_4, BH_2, and B were also prepared in resuspension buffer (10µM BH_4, 10µM BH_2, and 10µM B).

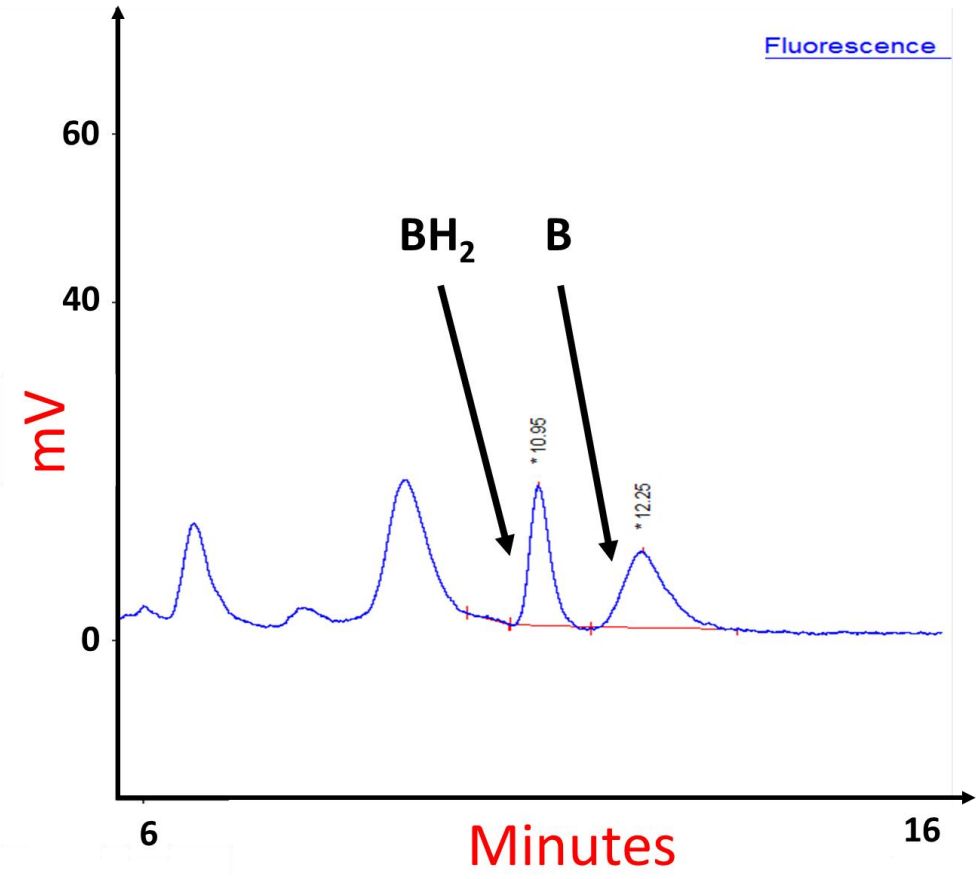


Figure 2.14 Fluorescence Chromatogram for Quantification of BH_2 and B

Representative fluorescence chromatogram for BH_2 and B is shown. The identifiable peak for BH_2 is approximately eleven minutes and the identifiable peak for B is approximately 12 minutes. The peaks are identified based on known standards and their elution times prior to each sample run.

Serial dilutions were used to prepare standards of concentrations 10^{-7} M, $5*10^{-8}$ M, 10^{-8} M, $5*10^{-9}$ M, 10^{-9} M, $5*10^{-10}$ M, and 10^{-10} M.[191] Precipitation buffer was added in a ratio of 1:10, spun and supernatant in a constant volume used for measurement.[191] All samples and standards were stored on ice prior to the run.

Sample run: Standards and samples were run on column RP-HPLC: 100uL of sample was injected by the autosampler for analysis.[191] Flow rate of the mobile phase throughout the run was 1.3 mL/min.[179] Electrochemical electrodes were used to detect BH_4 (Figure 2.13) and fluorescence was used to detect BH_2 and B (Figure 2.14) after the sample was separated in the column by polarity.[179] BH_4 species were detected by oxidizing them into their respective counterparts and reducing them to generate a current.[191]

2.5 General Molecular Biology Techniques

2.5.1 Nucleic Acid Gel Electrophoresis

Nucleic acid gel electrophoresis was used in multiple instances, including the verification of purified shRNA plasmids that had been amplified and purified from bacteria. Samples of DNA (1µg) were prepared with loading dye (1:6). Agarose gels of various percentages (depending on the size of DNA expected) were prepared. For shRNA constructs, a 1% agarose gel was prepared in TBE buffer (1g agarose in 100mL TBE). The mixture was heated in a microwave for a few minutes (until boiling) and was allowed to cool for a few minutes. GelRed was added (1uL in 50 mL) and this mixture was poured into a casting gel. Bubbles were removed and a comb was added to form wells. Following solidification of the gel, the comb was carefully removed, and TBE buffer was poured to cover the gel. Samples were added to the wells and the gel was run at 80V until the loading dye front reached the end of the gel. Gel image was captured on ImageLab Software with GelRed feature selected.

2.5.2 RNA Extraction, Reverse Transcription, and Quantitative-PCR

RNA Extraction: For RNA extraction by columns, Qiagen Kit (Cat. No. 74106) was used following manufacturer's protocol as previously described.[20] Briefly, cells or tissue are lysed and loaded onto a column for on-column DNAse digestion with DNAse enzymes. RNA was purified in the column and eluted.[20]

For non-column extraction, samples with QIAzol were thawed on ice from -80°C (or QIAzol was added and samples were placed on ice) and then homogenized for 30 seconds. Chloroform was added (200µL or 20% of the QIAzol volume used) and samples were shaken vigorously by hand for at least 15 seconds. Samples were kept at room temperature for 2-3 minutes (RNA is stable in QIAzol) and then centrifuged for 15 min at 14000 rpm at 4°C. The aqueous phase including RNA was carefully transferred to a new

Eppendorf without touching the opaque or pink layers containing DNA and protein respectively. 2µl Glyco Blue was added to visualize the RNA in the aqueous phase when precipitated. Isopropanol was added in equal volume as the aqueous phase. Samples were vortexed and stored at -20°C for 1 hour or overnight. Following this, samples were centrifuged for 15 min at 14000 rpm at 4°C.

Supernatant was removed and a washing step with 1 ml of 70% ethanol was used to eliminate last traces of phenol. The samples were vortexed gently and incubated at room temperature for 20 minutes. Samples were once again centrifuged for 15 min at 14000 rpm at 4°C. The majority of ethanol was removed carefully by pipette and the pellet was allowed to dry at room temperature without over-drying (over-drying results in visible white zones around the pellet). 30µl RNAase free water was added (or larger volume for larger pellet) and pellet was resuspended. Samples were stored at 4°C for four hours or overnight before quantification.

The NanoDrop spectrophotometer and software were used to quantify RNA. The "Nucleic Acids" and "RNA" specifications were selected, and NanoDrop was calibrated and blanked before loading sample. Following quantification, RNA samples were stored at -80°C and/or reverse-transcribed.

Reverse Transcription: Extracted RNA was reverse-transcribed into cDNA using Bio-Rad iScript cDNA Synthesis Kit (Cat. No. 170-8891) using standard manufacturer's protocol with the same principle as previously described (Table 2.3).[20] Briefly, 1µg of RNA (or 500ng where appropriate) was combined with RNAse-free water, iScript Master Mix, and reverse transcriptase. This mixture was then run through the denaturing, annealing, and extending program described in Table 2.3. cDNA was used for quantitative PCR.

Table 2.3 Reverse Transcription Program by Applied Biosystems

Step Number	Time (Minutes)	Temperature (◦C)
1	5	25
2	30	42
3	5	85
4	∞	4

Quantitative PCR (qPCR): TaqMan gene expression assays work on the same principle as the genotyping assays described in Section 2.2.1. As explained by TaqMan Video Guides, in addition to sequence-specific primers used in any PCR reaction, Applied Biosystems TaqMan probe is used to quantify product specifically in these assays. This probe has a reporter dye on one end and a quencher dye on the other end. When the probe is in-tact (i.e. unbound to nucleic acid) and the two ends are able to associate, the reporter dye releases energy which is transferred to the quencher by Förster resonance energy transfer (FRET). With the quenching of the energy, no signal is detected. However, when the probe binds to product, the DNA polymerase that is extending the nucleic acid cleaves the probe such that the two ends, reporter and quencher, are permanently separated. This results in a signal by the reporter that can be quantified and corresponds to the amount of product.

The qPCR reactions were performed using 5ng of cDNA per reaction.[20] Specifically, 10ng/µL of cDNA stock was created and samples were mixed. To 50ng of cDNA (5µL of 10ng/µL), 5µL of TaqMan Gene Expression Master Mix and 0.5µL probe (Housekeeping, or Gene of Interest). Samples were run using standard ABI StepOne software on an Applied Biosystems Real-Time PCR System and threshold for Ct cycles was specified as 0.2.[20] For cohort measurements of gene expression, standards from pooled myocardial cDNA were utilized. Pooled cDNA from all samples were then diluted

1:1 and 1:10, 1:25, 1:50. 1:100, 1:200. PGK1 (Phosphoglycerate kinase 1) was used as the housekeeping gene and the Pfaffl method was used to calculate relative expression of CBS and CSE as previously described.[20] In cell culture experiments, CSE gene expression was graphed as $2^{\Delta\Delta Ct}$ (e.g. ΔCt=CTH-GAPDH; ΔΔCt= $(CTH\text{-}GAPDH)_{Sample}$ - $Avg(CTH\text{-}GAPDH)_{Scrambled}$).

Table 2.4 Gene Expression Probes

Gene Expression	Species	Assay ID
CSE (CTH)	Human	Hs00542284_m1
CBS	Human	Hs00163925_m1
MST (MPST)	Human	Hs00560401_m1
SP1	Human	Hs00916521_m1
CSE	Rat	Rn00567128_m1
CBS	Rat	Rn00560948_m1
MST (MPST)	Rat	Rn00593744_m1
SP1	Rat	Rn00561953_m1
GAPDH	Rat	Rn99999916_s1

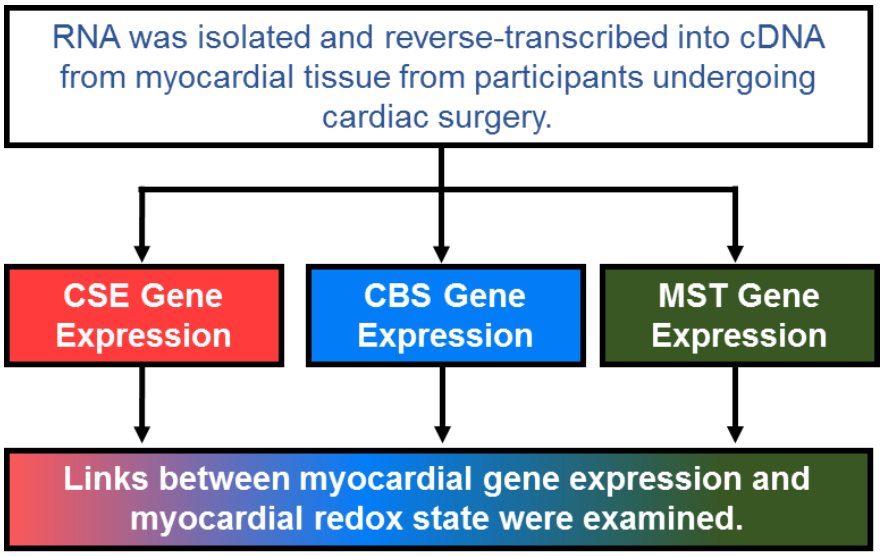


Figure 2.15 Study Design for Quantifying CSE, CBS, and MST Gene Expression

2.5.3 Western Blot and Antibodies

Western blotting in this study was used as we have previously described with some modifications for cells.[20] To prepare samples from H9C2 cells for western blotting, cells were washed two times with ice-cold PBS and then lysed with RIPA buffer containing phosphatase and protease inhibitors, 1:100). 150uL RIPA buffer was used per 6-well. The samples were sonicated three times for 15-20 seconds each and then centrifuged for 15 minutes at 14000 rpm at 4◦C. Supernatants were collected and placed in new eppendorfs on ice and protein was quantified by BCA protein assay below. Samples were frozen at -80◦C.

Protein quantification using BCA Protein Assay kit (Catalog #23227): Standards were made combining water and BSA in a serial dilution. Standards and samples were loaded onto a 96-well plate. Working reagent is added that includes copper ions that change oxidation state and color in the presence of proteins (Assay kit introduction). Samples with working reagent are agitated and then incubated at 37◦C for 30minutes. Absorbance is read at 562 nm on a spectrophotometer. Standards of known concentrations of BSA are used to create a standard curve and protein concentrations of samples are extrapolated from this curve.

Western Blot-specific buffers: 20% sodium dodecyl sulphate (SDS) was made by combining 100mL water with 20 grams SDS (Fisher BPE9738) and were mixed with heat to dissolve completely. 10x Tris-Glycine Running Buffer was formed using 30.28 g Tris-base (T1503 Sigma), 144 g Glycine, 25mL 20% SDS, and volume was raised to 1L by water. 1x Tris-Glycine Running Buffer was made from 10X by combining 900 mL water with 100mL of 10x Running Buffer. 10X Transfer Buffer was formed using 30.28 g Tris Base and 144 g Glycine and volume of water was raised to 1L. 1X Transfer Buffer from

10X stock was formed by combining 700 mL cold water, 100 mL 10X Transfer buffer, and 200 mL methanol.

Western Blot and Transfer: To run the western blot, samples with loading dye (4X or 6X added to sample) were boiled at 100°C for 8-10 min. Samples were briefly centrifuged to to bring down the condensation. 4-20% Thermoscientific Tris-Glycine (Catalog No. 0025264) were used and placed in cast. Running buffer was filled in the apparatus tank and wells of gel were washed with buffer by pipetting. Ladder (Biorad 161-03751) was loaded and then samples were loaded (usually 20µg). Western blot was run at constant 90 Volts for approximately 1.5 to 2 hours or when loading dye front reached the bottom of the gel. Cold transfer buffer (including methanol) was used to soak sponges, paper, and nitrocellulose membrane that would sandwich the gel. Sandwich was made with correct orientation so that the gel would transfer its proteins onto the nitrocellulose membrane. An ice pack was added to the transfer apparatus to maintain cold buffer. The transfer was run at constant 90 volts for approximately 1.5 hours. After transfer, nitrocellulose membrane was briefly stained with ponceau stain to ensure proteins had properly transferred onto the membrane and membrane was cut as needed for separate incubation with antibodies. Ponceau was washed off with TBS-Tween.

Blocking and Primary & Secondary Antibodies: Membranes were blocked with 5% milk (unless specified separately for the antibody) for 1 hr at room temperature. Blocking buffer was removed and primary CSE antibody was added in a ratio of 1:500 with 5% milk overnight at 4°C with agitation (Table 2.5). The following day, non-specific primary antibody was washed off with three washes with TBS-Tween for 10 minutes each. Secondary antibody that was HRP-conjugated was added to 5% milk for 1 hour at room temperature (Table 2.5). Non-specific secondary antibody was washed off with three washes with TBS-Tween for 10 minutes each.

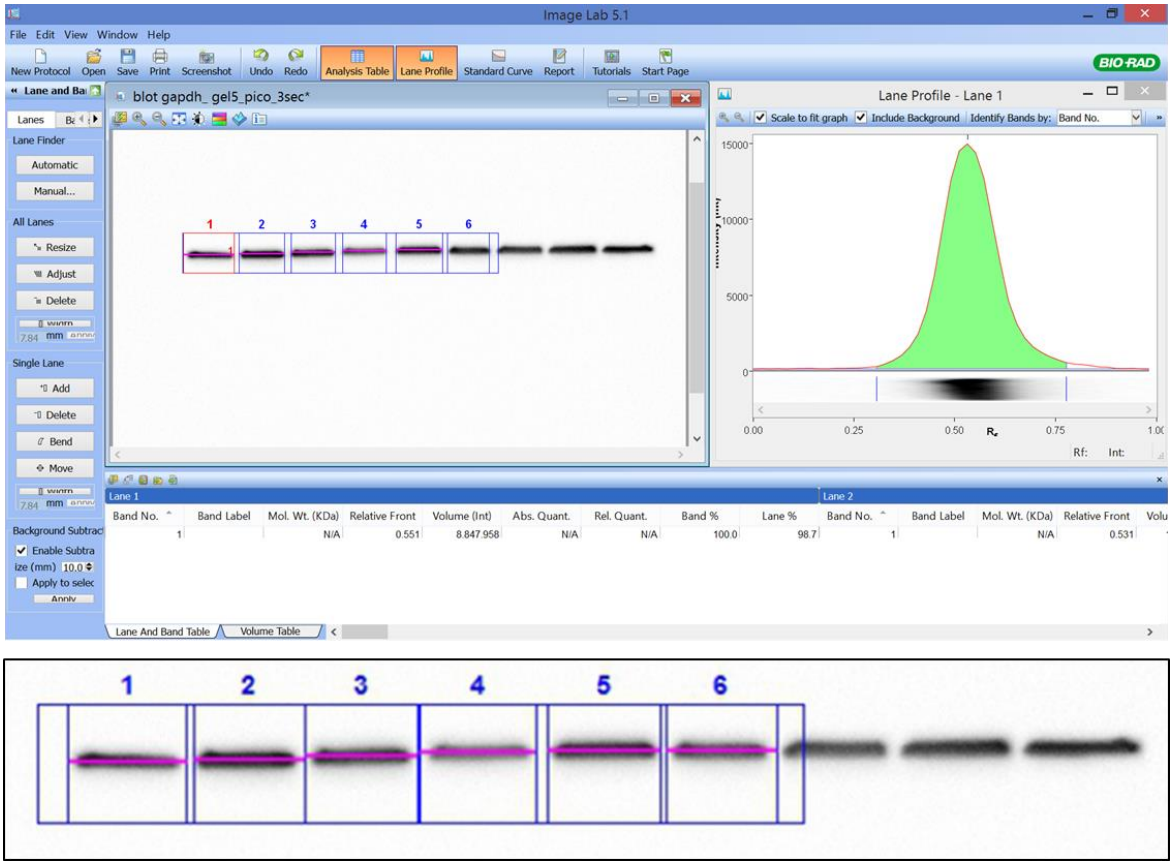


Figure 2.16 Image Analysis for Western Blotting

ChemiDoc™ MP (Serial Number 731BR02517) was used to acquire image and images were processed on ImageLab Software. Lanes (in blue; 6 lanes) and bands (in pink; 6 bands) were detected manually. Volume or the intensity of each band was graphed as shown by the intensity peak of band 1 in green. The numerical volume quantified is noted in the table below blot and lane peak.

Imaging and Imaging Analysis: Membrane was covered with ECL and allowed to rest on membrane for one minute and then liquid was tapped off membrane and imaged in the ChemiDoc System. Settings for imaging include blots with specific "Chemi" selection. Images at specified or automatic exposure times are taken and saved. Blot was imaged with specific "Colorimetric" selection to obtain image of ladder. The images are also merged and saved. Membrane was also incubated with GAPDH secondary antibody in 5% milk for 1 hour at room temperature (Table 2.5). Non-specific secondary antibody was washed off with three washes with TBS-Tween for 10 minutes each and GAPDH was also imaged as described above for other proteins. Bands from western blot were imaged on ImageLab Software.

Table 2.5 Primary and Secondary Antibodies for Western Blotting

Protein/Target	Antibody Type	Concentration	Source	Manufacturer	Catalog Number
CSE	Primary	1:500	Rabbit	Abcam	Ab80643
GAPDH	HRP-Conjugated	1:10,000	Mouse	Sigma-Aldrich	G9295
Anti-Rabbit IgG	Secondary	1:10,000	Goat	Sigma-Aldrich	A9169

CSE, Cystathionine γ-lyase. GAPDH, Glyceraldehyde-3-phosphate dehydrogenase. HRP, Horseradish peroxidase.

CSE protein was identified by both size in kilodaltons (compared to ladder) as well as by a positive control for CSE (293 lysate, Cat No. SC-112203). The .scn file was opened in the software and in the analysis tool box, "Lane and Bands" was selected. In the "Lanes" tab, "Manual" was chosen and number of lanes to quantify were selected. "Move" was selected on the left panel to move lanes around the bands and select bands to quantify. "Width" was selected to adjust the width of the selection area. Following the selection of the band area, in the "Bands" tab, "Add" and "Adjust" was selected to adjust the height of the lanes. The Lane profile demonstrated the selected bands and "Analysis Table" allowed for analysis to be exported. The "Volume (intensity)" for each band was compared after normalization to control (e.g. GAPDH).

2.5.4 Pig Model of Oxidative Stress

To characterize an *in vivo* model of oxidative stress in a large animal model, we assessed myocardial redox state in the left atria of pigs that underwent rapid atrial pacing for one week compared to their controls. Pig hearts were obtained from collaborators Prof. Sander Verheule, Dr. Hussein M. Nasrallah, and Dr. Dragan Opacic at Maastricht University (The Netherlands). As we have previously described with some modifications, briefly, 14 Dutch Landrace pigs were studied with 7 pigs undergoing one week of rapid atrial pacing (RAP) and 7 pigs used as healthy controls.[20] At Maastricht University, complying with animal procedure guidelines as confirmed by Dr. Dragan Opacic, 7 RAP

pigs received a pacemaker (CapSureFix 5568 and Itrel II, Medtronic Inc.) and were allowed to recover after the implantation for one week.

Table 2.6 Pig Primers for Myocardial Gene Expression Quantification

Gene	Forward / Reverse Primer	Primer Sequence	Product Length (Base Pairs)
CSE	Forward	5' TCGAAGCTCAACATGCAGGA 3'	190
	Reverse	5' ACTCAAAACCCGAGTGCTGT 3'	
CBS	Forward	5' AGATGGTGTTCGGGGTCGT 3'	82
	Reverse	5' CCTGGCTTCGTCTTCTGGAT 3'	
MST (MPST)	Forward	5' TTGAGGCTTCTCGTGCAACA 3'	97
	Reverse	5' TGAGTCCTCCCTAGTTGCCA 3'	
SP1	Forward	5' AATGGGGGCAGTGGTAATGG 3'	278
	Reverse	5' GTAGCCCCAGAGGAGGAAGA 3'	
GAPDH	Forward	5' CACTGAGCACCAGGTTGTGT 3'	142
	Reverse	5' CCTGTTGCTGTAGCCAAATTC 3'	

RAP pigs were then paced for one week by pacemakers at 600 beats per minute (pacing protocol was described by Dr. Dragan Opacic). Hearts from RAP pigs and controls were excised and rinsed in modified cardioplegic solution; samples were snap-frozen in liquid nitrogen and stored at -80◦C (information provided by Dr. Dragan Opacic). These methodological steps from pacemaker implantation to storage of frozen heart samples were kindly provided by Dr. Dragan Opacic and conducted in Professor Sander Verheule's laboratory.[20]

In this study, we quantified basal $O_2^{\cdot-}$ and $O_2^{\cdot-}$ from NADPH oxidases, NOSs, and mitochondrial oxidases form the left atria of pigs that underwent one week of rapid atrial pacing and their respective controls. We also extracted RNA from left atrial samples by a combined trizol and column method. RNA was reverse transcribed by the Quantitect

Reverse Transcription kit with genomic DNA wipe-out (Catalog No. 205311) following the manufacturer's protocol. Myocardial CSE and CBS gene expression was quantified using primers (Table 2.6) and SSOAdvanced Universal Sybr Green Supermix (Catalog No. 172-5270) following manufacturer's protocol to determine the redox-sensitivity of the gene expression of these enzymes *in vivo*.

2.5.5 General Buffers and Probes

Buffers components are below, as previously described.[20,43,192,193]

Table 2.7 Krebs HEPES Buffer Components

Compound	Concentration (mM)	Molar Mass (g/mol)	g/L
NaCl	99	58.4	5.78
KCl	4.7	74.6	0.35
$MgSO_4$	1.2	246.5	0.30
KH_2PO_4	1	136.1	0.14
$CaCl_2$	1.9	147	0.28
$NaHCO_3$	25	84	2.1
Glucose	11.1	180.1	2
NaHEPES	20	238.3	4.77
pH 7.35			

Table 2.8 Tyrode's Buffer Components

Compound	Concentration (mM)	Molar Mass (g/mol)	g/L
NaCl	118.5	58.44	6.93
$NaHCO_3$	24.8	84.01	2.08
KCl	4.7	74.55	0.36
$MgSO_4.7H_2O$	1.44	246.77	0.36
KH_2PO_4	1.2	136.09	0.16
$CaCl_2$	1.8	147	0.27
Glucose	10	180.16	1.8
Sodium Pyruvate	10	110	1.1
Bubble with Oxygen (O_2) for 5 minutes; pH 7.4 Formula optimized by Alexis Antonopoulos			

Table 2.9 Krebs Henseleit Buffer Components

Compound	Concentration (mM)	Molar Mass (g/mol)	g/L
Krebs Part A			
NaCl	120	58.4	7.01
KCl	4.7	74.6	0.35
$MgSO_4$	1.2	246.5	0.30
KH_2PO_4	1.2	136.1	0.16
$NaHCO_3$	25	84	2.10
Combine 200mL Krebs Part A + 1600 mL H_2O; Bubble with Oxygen (O_2) for 5 minutes			
Krebs Part B			
Glucose	5.5	180.15	0.99
$CaCl_2$	2.5	147	0.37
Add 200mL Krebs Part B to give 2L total volume			

Table 2.10 Genotyping Probes

Gene	SNP ID	Assay ID
CSE (CTH)	rs1021737	C___8369524_10
CBS	rs2851391	C___1605450_1_
CBS	rs234709	C___1605447_10
CYBA Locus ($p22^{phox}$)	rs4673	C___2038_20
	rs1049255	C___7516913_10

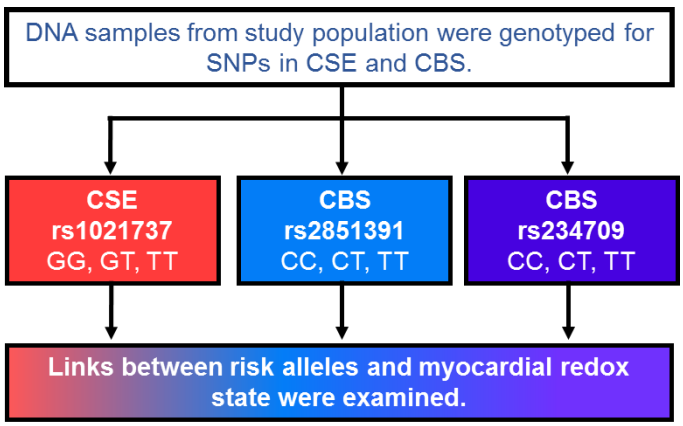


Figure 2.17 Study Design for Genotyping CSE and CBS SNPs

2.6 Statistical Analysis

2.6.1 *Ex Vivo*, *In Vitro*, and *In Vivo* Studies

Statistical analysis was performed by methods as we have previously described,[20,171,173] with some modifications. Differences between two groups that were non-normally distributed were compared by non-parametric tests: two unpaired groups (e.g. cells incubated with or without H_2S) were compared by the Mann-Whitney rank test (which ranks values and compares the means and is sensitive to differences in medians based on the GraphPad Statistics Guide). Two paired groups were compared by Wilcoxon matched-pairs signed-rank test (e.g. for *ex vivo* experiments in which segments from the same right atrial appendage were incubated as pairs).

Differences among three or more groups that were non-normally distributed were compared by non-parametric 1-way ANOVA: three or more unpaired groups (e.g. viability in media versus Krebs HEPES buffer versus Tyrode's buffer) were compared by the Kruskal-Wallis test followed by Dunn's post hoc correction for multiple comparisons. Three or more paired groups (e.g. snap-frozen, control, and NaHS incubated segments of right atrial appendage for BH_4 measurements) were compared by Friedman's test followed by Dunn's post hoc correction for multiple comparisons. Variables were examined for normal distribution by the D'Agostino & Pearson normality test.

For the methylene blue assay and comparison of standards, a linear regression model was used to determine the line of best fit for standards. Slopes of these lines of best fit were compared by analysis of covariance (ANCOVA).

Data with group sample size fewer than 15 are presented as mean ± SEM (individual dots, with paired samples in two or three groups connected by a line). Samples specifically calculated as fold change of paired controls are presented as mean ± SEM (bars). Data examining differences in range are presented as median with range.

2.6.2 Clinical Correlations and Power Calculations

Clinical associations were also examined by methods as we have previously described,[20,171,173] with some modifications. Differences between two groups that were non-normally distributed were compared by non-parametric t-tests: two unpaired groups (e.g. males and females) were compared by the Mann-Whitney rank test. Differences among three or more groups that were non-normally distributed were compared by non-parametric 1-way ANOVA: three or more unpaired groups (e.g. individuals with different number of risk alleles of CSE SNP rs1021737) were compared by the Kruskal-Wallis test followed by Dunn's post hoc correction for multiple comparisons. Three or more paired groups (e.g. quantification of myocardial CSE, CBS and MST expression in the same individuals) were compared by Friedman's test followed by Dunn's post hoc correction for multiple comparisons. Correlations between continuous variables with no expected threshold effect (e.g. age and plasma H_2S) were examined by bivariate analysis and non-parametric Spearman's correlation coefficient ρ(rho) estimation is presented. Variables were examined for normal distribution by the D'Agostino & Pearson normality test.

Data with group sample size greater than 15 are presented as box-and-whisker plots with median (25^{th} to 75^{th} percentile) and whiskers (Tukey), unless otherwise noted in individual panels. Some panels are presented as median (25^{th} to 75^{th} percentile) and whiskers (10^{th} to 90^{th} percentile) to better visualize differences and similarities between medians and these panels are noted in figure legends.

Power analysis used for clinical correlations studies are described in complete detail in Chapter 7 (Discussion). G*$_{POWER}$ (Version 3.1.9.2) was used to perform all power calculations. G*Power 3.1 Manual was used as guide for types of power analyses.

$P<0.05$ was statistically significant. IBMS SPSS Statistics Version 22 and 25 and GraphPad Prism 7.01 were used for graphing and statistical analysis.

Chapter 3 Development of Methods and Models

3.1 Human Plasma H_2S by Methylene Blue Assay

To measure H_2S in plasma, the methylene blue assay was utilized, a technique commonly used in literature.[194] This technique provides useful information regarding sulfide levels in the plasma broadly. Given that this technique uses acid that lowers the pH and results in acid-labile pools of sulfur to be released, the measurement of H_2S is a sulfur pool we refer to as H_2S/Sulfide to depict the trapped H_2S gas measured as well as the acid labile pools. To better understand the principles behind this technique, a simplified version of the methylene blue assay is shown (Figure 3.1).

In this method, zinc acetate (ZnAc, aqueous) is added to the sample which H_2S reduces to form a stable storage for H_2S known as Zinc Sulfide (ZnS), which is more stable in the presence of air.[195,196] The dye (DMPD), which can be reduced by H_2S to methylene blue, is then added to the mixture with the stable form of ZnS.[195] To catalyse the reaction, $FeCl_3$ is added to the reaction mixture, and is added after being reconstituted in highly acidic hydrochloric acid.[195] The strong acidic conditions of $FeCl_3$ lead to ZnS's release of H_2S which can reduce DMPD to methylene blue.[195] Methylene blue formation results in a color change that can be quantified at the wavelength of approximately 668 nanometers.[197]

3.1.1 Standards, Sample Preparation, and Measurements

In order to establish this technique in the laboratory, I first set up standards of Sodium Hydrosulfide Hydrate (NaHS, Sigma Catalog No. 161527, MW 56.06) from 0-250µM which was a wide range that could encompass the concentrations of H_2S described in literature. I then measured the H_2S in these standards after 30-minute and 2-hour incubation times to determine their stability over course of the experiment.

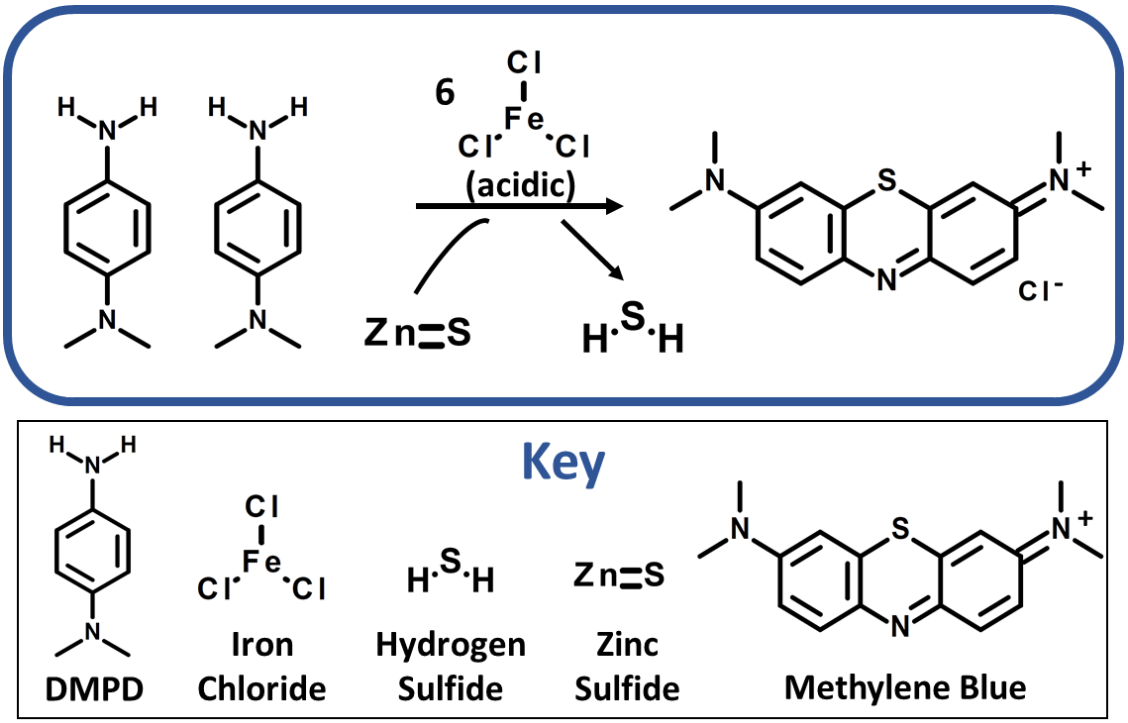


Figure 3.1 Methylene Blue Reaction for Measuring H_2S/Sulfide

A simplified representation of the methylene blue reaction for measuring H_2S is shown. DMPD (a dye solution, shown) forms methylene blue (a heterocyclic thiazine dye) when H_2S reduces DMPD. H_2S present in the sample and H_2S after being released under strong acidic conditions from a stable storage for H_2S (sulfide) can lead to this reaction. To preserve H_2S in the sample, Zinc acetate is added to from ZnS which releases H_2S under acidic conditions of $FeCl_3$. The reaction is catalyzed by the presence of $FeCl_3$ (regenerated). The color change produced by methylene blue can be measured by spectrophotometry. Chemical structures made in PubChem Sketcher V2.4 and structures drawn based on NIH National Center for Biotechnology Information and Open Chemistry Database (https://pubchem.ncbi.nlm.nih.gov/). Chemical reaction drawn and simplified on the basis of several papers.[195-197] DMPD, N,N-dimethyl-p-phenylenediamine. ZnS, Zinc Sulfide.

After finding similarities in stability, I proceeded with measuring plasma samples with 30-minute incubation times. With regard to whole blood processing for measurements (conducted by group members as part of the Oxford HVF Cohort), plasma was obtained from whole blood by adding whole blood to anti-coagulants (heparin, citrate, or EDTA). Serum was obtained by allowing blood coagulants to coagulate in whole blood before spinning; both plasma and serum samples were spun at 4°C for 15 minutes at 3000 rcf and aliquoted. Aliquots stored at -80°C were used for measurements.

Method (modified from literature[194]): To measure H_2S in samples, 10% trichloroacetic acid was added to samples and NaHS standards to precipitate proteins.

Samples were spun for 5min at 5000g at room temperature. Supernatants were transferred into new eppendorfs. 1% ZnAc was added to trap H_2S. Samples were sealed and shaken. 20mM DMPD was added and samples were shaken and set to rest for 1min. 30mM $FeCl_3$ was added and samples were kept in the dark for 30min. Samples were then vortexed briefly and transferred to a 96-well plate where absorbance was read at 668 nanometers on the spectrophotometer (Omega Software). Solutions were first prepared each day as following: 20 mM N,N-Dimethyl-p-phenylenediamine sulfate (DMPD, Fluka # 07770, MW 209.12) was prepared in 7.2 M HCl. Zinc acetate (ZnAc, ALDRICH #383317, MW 183.48) was prepared in water. 30 mM iron chloride ($FeCl_3$, SIGMA #157740, MW 162.20) was prepared in 1.2M HCl. ZnAc and $FeCl_3$ solutions were prepared fresh for each experiment.

3.1.2 Data Analysis

The absorbance reading for the blank was subtracted from the readings for all samples and standards. The readings of the standards were plotted against the concentrations of NaHS (known). A linear regression was performed to determine the line of best fit (displaying a linear equation describing the standard curve and an estimate of R^2 to determine how close the points are to the line). Finally, the plasma samples were plotted against the standard curve to estimate the H_2S in the plasma of individual patients relative to NaHS standards.

3.1.3 Validation for Human Plasma H_2S Measurements

To investigate the potential importance of systemic, circulating H_2S and associations with myocardial $O_2^{\cdot -}$ production from specific sources, circulating H_2S was measured by methylene blue in plasma (citrate). While for known biomarkers, there are readily available kits and ELISAs for their measurement, the H_2S field is still emergent

and methylene blue for H_2S measurements is still a home-made laboratory assay that needs to be internally validated.

For assessment and calibration of the methylene blue assay to plasma or serum, plasma and serum from 6 patients was measured (heparin, citrate, EDTA, and serum samples from each of these 6 patients). No appreciable or significant differences were detected in the average H_2S measured in heparin, citrate, EDTA and serum samples (Figure 3.2). From citrate and serum which had lowest intra-patient variability, citrate samples which were in abundance were used from -80°C for cohort-wide methylene blue measurements (Figure 3.2).

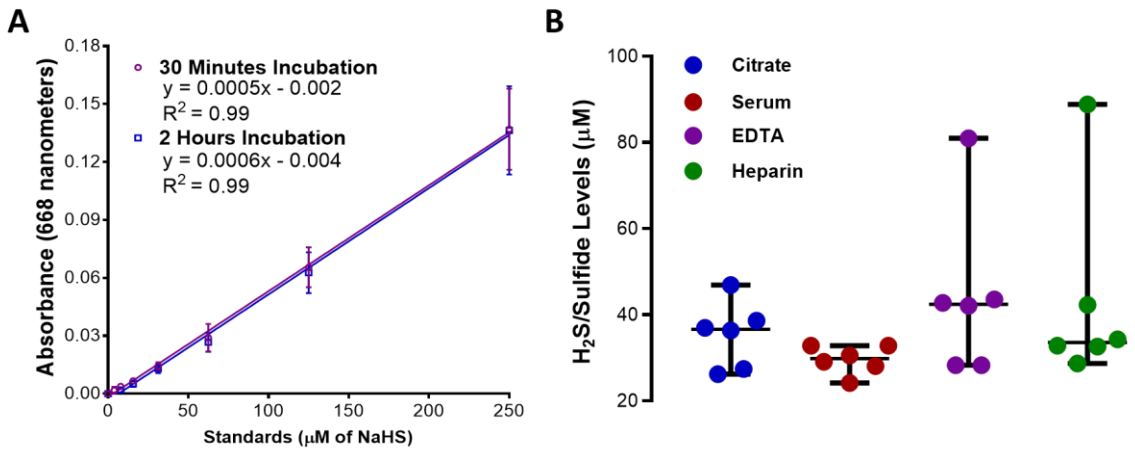


Figure 3.2. Methylene Blue Standard Stability & Comparison of Plasma and Serum

To determine the stability of standards used for experimentation, standards including concentrations of 250, 125, 62.5, 31.3, 15.6, 7.8, 3.9 µM NaHS and Blank (0 µM) were quantified by the methylene blue assay after 30-minute and 2-hour incubation times (**A**). Using a linear regression model, a line of best fit was plotted for the standards at each time point. Standard curves remained relatively stable with no significant difference between the slopes of the 30-minute incubation and 2-hour incubation time points. n=3 independent experiments at 30 minutes and n=3 independent experiments at 2 hours were conducted. Slopes were compared by ANCOVA (P=0.9). Measurements of H_2S/Sulfide were compared in anticoagulants and serum (**B**). H_2S/Sulfide levels were quantified for 6 patients and largest intra-patient variability was in EDTA and Heparin samples. Citrate and Serum demonstrated lowest intra-patient variability. ANCOVA, Analysis of Covariance. EDTA, Ethylenediaminetetraacetic acid. H_2S, Hydrogen Sulfide. NaHS, Sodium Hydrogen Sulfide. Values are presented as mean ± SEM in Panel *A* and as median with range in Panel *B*.

Citrate plasma samples were also collected for quality control from a few patients and were included in each run. Using quality controls, H_2S/Sulfide levels were measured

cohort-wide. Cohort-wide plasma H_2S/Sulfide levels were measured against NaHS Standards and distribution of plasma H_2S/Sulfide levels in the cohort was examined. H_2S/Sulfide levels in the cohort compared to NaHS standards were distributed with a concentration of 43.7±1.3μM (mean ± SEM). As this measurement via methylene blue is not a direct measurement of the gaseous levels of H_2S/Sulfide, we believe our findings indicate the correlation between 'sulfide state' of the individual relates to demographics, mitochondrial redox state in the heart. This mean concentration of plasma H_2S/Sulfide was used to later determine the concentration of NaHS applied to human myocardium.

3.2 Amperometric Sensor Set-Up for Real-Time H_2S Measurement

Overview: The electrochemical H_2S sensor (World Precision Instruments (WPI), ISO H2S-2) with a membrane permeable only to H_2S gas was connected to an analog detector (WPI TBR4100/1025) was set-up and developed according to the instrument instruction manual and guidance from World Precision Instruments.[198] The sensor was allowed to polarize for 24+ hours in PBS and was then immersed in distilled water for 30min.[198] Stable baseline was recorded for 1h in experimental conditions. H_2S donor was added and real-time signal recording continued. Following recording and between experiments, the probe was immersed in distilled water to remove salts and particles which may have accumulated on the membrane.

3.2.1 Set-up and Development of Real-time H_2S Monitoring

In order to determine whether H_2S affects myocardial sources of $O_2^{\cdot-}$, we first examined the kinetics of H_2S release from donors NaHS and GYY4137.

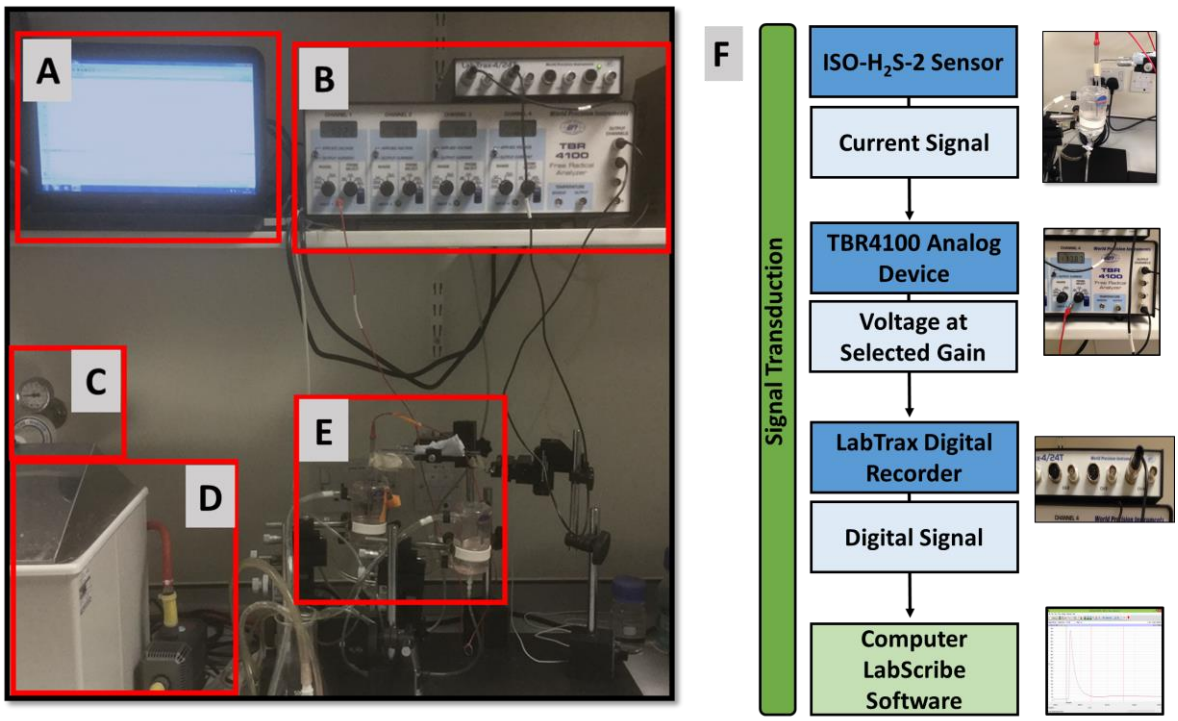


Figure 3.3. Experimental and Schematic Set-up of Amperometric H_2S Sensor

A diagram of the actual experimental set-up is shown: (**A**) LabScribe Software on laptop is shown where visual graphs of the H_2S release is monitored. (**B**) TBR4100 Free Radical Analyzer is connected to the LabTrax Digital recorder shown above it where current signal is processed and converted to digital signal for the computer to process. (**C**) 95% O_2/CO_2 and (**D**) water bath used to maintain physiological conditions for the organ bath where the H_2S donors would be added to physiological conditions are shown. Lastly, (**E**) the ISO-H_2S-2 sensor where H_2S passes the H_2S-permeable membrane on the sensor is shown. (**F**) A schematic diagram of signal processing for the amperometric sensor method is also shown. H_2S passage through amperometric sensor's selective H_2S permeable membrane and reaction with electrodes generates current. Current signal is transmitted to analog device (TBR4100) and amplified by selected gain and signal is sent to LabTrax for conversion to a digital signal that can be processed on the computer in the LabScribe software. A more detailed diagram of the software is shown in Figure 3.4. All information regarding signal processing is provided by World Precision Instruments Instruction Manual and Customer Support.

Understanding these kinetics would allow us to design experiments incubating human myocardium with these donors and examine potentially distinct effects of fast- and slow-releasing H_2S donors. To measure the kinetics of these two donors, we set up an amperometric sensor of H_2S and made measurements of H_2S in real-time in four physiological conditions.

In this method, H_2S passes through amperometric sensor's selective H_2S permeable membrane and its redox reaction with electrodes generates current. Current signal is transmitted to analog device (TBR4100) and amplified by selected gain and

signal is sent to LabTrax for conversion to a digital signal that can be processed on the computer in the LabScribe software (Figure 3.3 and Figure 3.4).[198] All information regarding signal processing is provided by World Precision Instruments Instruction Manual and Customer Support.

3.2.1.1 Setting up a method of Amperometry for monitoring H_2S release

First, to set up this method of amperometry, we assembled the H_2S sensor (Figure 3.3) developed by World Precision Instruments (ISO-H_2S-2).[198] The electrode, which was a combination of working/counter electrodes, was placed carefully inside a membrane sleeve which had a H_2S gas-permeable membrane whose material composition was proprietary.[198] This membrane sleeve was filled with electrolyte solution and the electrode was placed to slightly stretch the H_2S gas-permeable membrane on the sleeve.[198] The sleeve with the electrode was then connected to the probe handle with a lock cap and the probe handle was connected to the TBR4100 Free radical analyser.[198] The TBR4100 Free radical analyser's channels were then connected to the LabTrax Digital recorder.[198]

For analysis, appropriate parameters (e.g. gain) were set on the TBR4100.[198] In particular, the range on the TBR4100 analog device, which corresponds to the maximum current measured, was set at 100 nano-amperes (nA).[198] This was the optimal range to maximize gain and increase signal-to-noise ratio of the H_2S signal while maintaining a necessary range of recording. Briefly, gain determines the factor by which the signal is amplified – higher gain means higher signals and higher signal-to-noise ratios.[198] The gain is limited by the voltage of the analog device; that is, the voltage that the device can input or supply is the voltage that the device can output.[198] Therefore, higher gains should amplify current within the analog device's capacity to output voltage; otherwise, the

amplified signal will be considered 'out-of-range' and thus, the amplification of signal to improve signal-to-noise ratio is balanced with the optimal range of detection.[198]

A concrete example is provided by WPI: briefly, if a signal of 2mV is recorded and a gain of $X10^4$ is used, the signal is amplified to 20V.[198] If the noise signal is 1mV, then this gain improves the signal-to-noise ratio from 2mV:1mV or 2:1 to 20:1.[198] Although the signal-to-noise ratio is improved significantly, this 20V signal exceeds the supply voltage (supposing the analog device has a supply voltage of ±5V, 20V exceeds this maximum voltage that can be supplied) and will therefore be read as 'over-ranged.'[198] A gain of $X10^4$ narrows the range of detection (supply voltage/gain = maximum signal detected): ±5V / 10^4 gain = ±0.5 mV that can be detected.[198] Thus, the higher signal-to-noise ratio is balanced with a narrow range to detect signal.[198]

3.2.1.2 Testing functionality of the device

After selecting the appropriate range for H_2S detection, the functionality of the TBR4100 and ISO-H2S-2 sensor was determined. Five tests were conducted to ensure the functionality of the equipment prior to polarization and use in accordance with WPI technical advice.[198]

Assembly Test resistor[198]: The purpose of this test was to confirm the proper functioning of the TBR4100. The assembly test resistor (1G) was placed in the TBR4100 channels. The "output current" would read the actual voltage being applied if the TBR4100 was functioning properly; that is, this 'output current' should match the voltage that is said is being applied (i.e. 0.150 V or 150 mV). Some error (e.g. 2%) was permitted. Indeed, 0.130-0.170 was the 'output current' when the test resistor was in placed in each TBR4100 channel.

Dry Test[198]: The purpose of this test was to identify whether electrodes in the sensor are connected properly; the test is dry meaning there is no electrolyte solution to

connect the electrodes and therefore the electrodes should not form a circuit. The electrode was dipped in distilled water and wiped clean and further allowed to dry in the air. The electrode's connecting end (probe handle) was connected to the TBR4100, which should read close to zero in any range. Indeed, the device read .0017 in the 10 nA range. This value is close to zero, indicating the electrodes are not short circuiting each other.

Wet Test[198]: The wet test identifies if the electrodes can communicate when electrolyte solution in-between connects them. The electrode was placed in H_2S filling solution and monitored on the 100 nA range; values should rise in the positive direction (e.g. 116.60 in 100 nA range which is saturated). This was indeed the case and indicated that the electrodes can communicate with each other with electrolyte solution to connect them.

Partial Polarization[198]: In this test, the electrode was held above a small confined container to polarize. Prior, new filling solution was placed in the membrane sleeve and the membrane sleeve was placed around the electrode slightly loosely and gently. The sensor was then held in distilled water with a stirring magnet and left for 2-3+ hours. The current was to read approximately 0.834 in the 10 uA range and this range was confirmed.

Full Polarization[198]: The membrane sleeve was tightened against the electrode and monitor. The 0.834 on the 10uA range would lower to 0.22 or 0.120 after some adjustments over time. The sensor was allowed to stabilize for another 6+ hours to have a stable baseline below 0.1 in the 10 uA range or below 100 on the 100 nA range. The sensor was left in water with a magnetic bar stirring and the sensor was not deep in the water but indeed inside the liquid and centered as best possible.

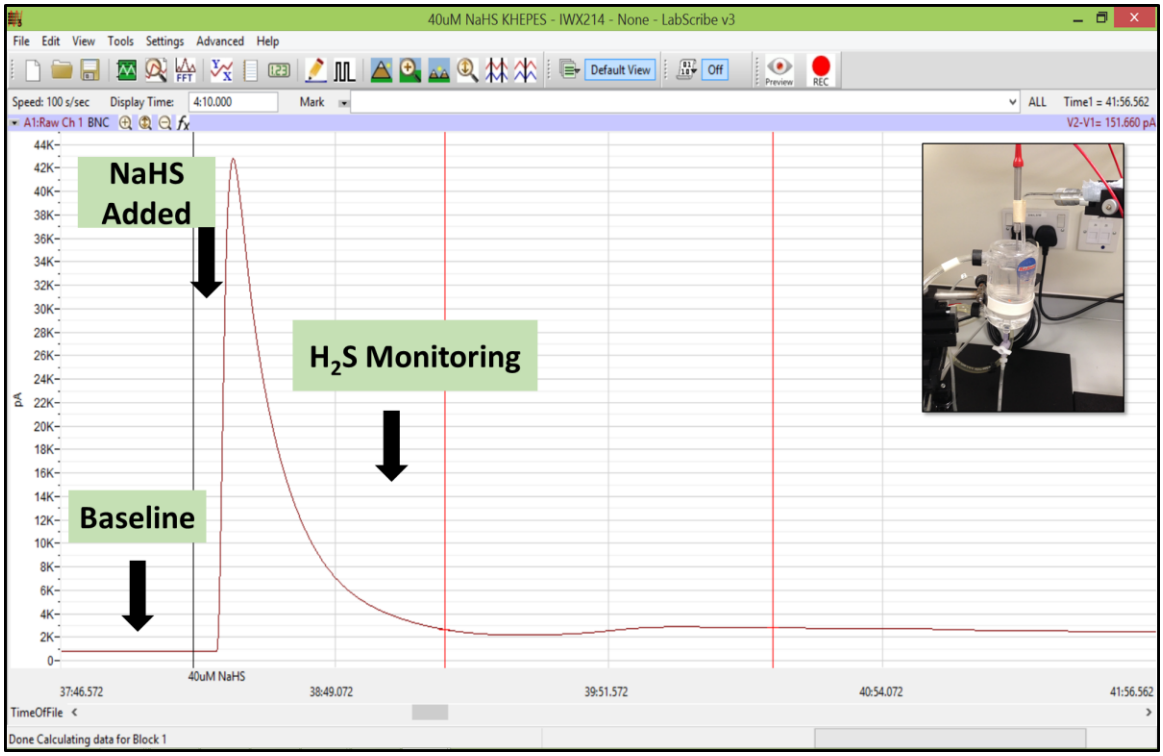


Figure 3.4 LabScribe Software: Trace of 40 µM NaHS

LabScribe Software was used to monitor H_2S release from different donors. Here a trace is shown for 40 µM NaHS in Krebs HEPES buffer. First a baseline was recorded. When NaHS was added, a sharp peak was observed. Continuous monitoring of H_2S continued after NaHS was added. H_2S, Hydrogen Sulfide. NaHS, Sodium Hydrogen Sulfide.

Polarization prior to baseline collection: The aim of these polarization steps was to have the sensor read below 100 nA (on the 100nA range) or below 0.1 uA (on the 1uA or 10 uA range). The sensor was initially polarized by immersion in water for 24+ hours prior to recording baseline. Between experiments, the sensor was immersed in distilled water for 30 minutes to remove salts and particles which may have accumulated on the membrane between experiments.

3.2.2 Measuring H_2S in Experimental Conditions

To investigate the kinetics of H_2S release from NaHS, a stable baseline was recorded by the amperometric sensor in an organ bath set-up before NaHS was added. On the LabScribe software, the time at which NaHS was added was marked and NaHS was added. H_2S release was monitored in these *ex vivo* conditions as well as Tyrode's buffer,

Krebs Henseleit buffer, and H9C2 cell culture media to further validate the results. This was repeated for GYY4137. The primary purpose of this quantification of the kinetics of H_2S donors was to design the conditions of the *ex vivo* incubations of human myocardium, specifically the time of incubation with each H_2S donor.

3.3 Model of Oxidative Stress in Cell Culture

3.3.1 H9C2 Rat Cell Line Proliferation and Differentiation

An H9C2 myoblast immortalized cell line from rat left ventricles was utilized as these cells have been utilized in our laboratory previously.[20] Mouse HL1 cells are expensive to maintain, while H9C2 cells also differentiate into cardiomyocytes in an established and phenotyped protocol.[20] While isolating human cardiomyocytes may be the ideal cardiomyocyte cell model, isolation of human cardiomyocytes from tissue yields very low numbers and make these primary cells difficult to work with on a regular basis.

Following a protocol already established in our laboratory, briefly, H9C2 cells were grown in media (Catalog No: FG 0435) supplemented with 10% Fetal Bovine Serum (FBS) Superior (Catalog No: S0615) and 0.5% Penicillin/Streptomycin (Catalog No: 15140-122).[20] Cells were maintained at 50-60% confluency, as further confluency would allow cells to cluster and signal between each other beginning their differentiation. Cells were split to maintain this confluency using low-percentage trypsin (0.05%, Catalog No: 25300-054) to maintain cell integrity while still de-attaching cells from the surface.[20]

After seeding cells in wells or flasks required for the experiment, cells were grown to confluency. To catalyse the differentiation of these H9C2 myoblasts, maintenance media was replaced by differentiation media which was media (Catalog No: FG 0435) supplemented with 2% horse serum (Catalog No: 16050-130) and 0.5% Penicillin/Streptomycin.[20] Cells typically showed cardiomyocyte characteristics in 4-5

days (depending on whether the cells had already initiated their differentiation process) and differentiation media was replenished every 2 days during differentiation.[20] On day 4 or 5 of differentiation, cells were harvested for experimentation.[20] Tissue-culture treated flasks and wells were used for both growth and differentiation of cells and cells were maintained and differentiated at 37°C in the 95% O_2/5% CO_2 incubator. When required for seeding, cells were counted using a haemocytometer. 150,000 cells were typically seeded per well of 6-wells and flasks were typically split 1:3.

3.3.2 Development of acute model of oxidative stress in H9C2 cardiomyocytes

Building from our previous work, I first generated an acute model of oxidative stress in H9C2 cells in which I could examine changes in gene expression of CSE. We have shown previously that exposure to exogenous NADPH (100µM), a key substrate of NADPH oxidases, stimulates $O_2^{\cdot-}$ production in H9C2 cells from NADPH oxidases (primarily Nox2) after 2 hours; furthermore, we have shown that exposure to NADPH (100µM) for 18 hours increased intracellular NADPH and NADP levels.[20] This earlier work suggested that exogenous NADPH could be used as a model of increased short-term $O_2^{\cdot-}$ generation by NADPH oxidases.

In order to further optimize this model of acute oxidative stress in H9C2 cells, $O_2^{\cdot-}$ was quantified and viability assessed in H9C2 cells grown on coverslips and exposed to 18 hours of 1mM NADPH. 1mM NADPH was chosen to prevent the need for replenishing over the course of 18 hours and incubation for 18 hours was chosen as a time in which changes in gene expression could be examined as our previous studies have demonstrated.[20]

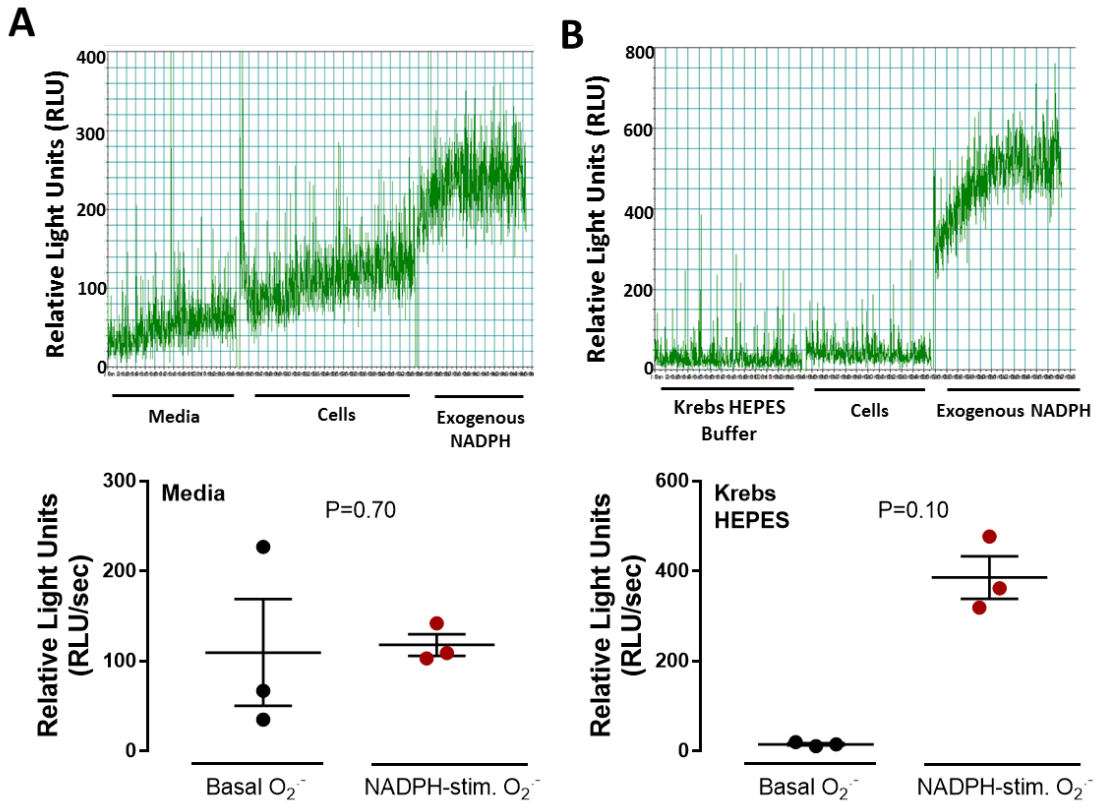


Figure 3.5 Development of Acute Oxidative Stress Model in H9C2 Cells

To develop a model of acute oxidative stress in H9C2 cells, $O_2^{\cdot-}$ was quantified and viability assessed in H9C2 cells grown on coverslips and exposed to 18 hours of 1mM NADPH. In media, a stable background and stable basal $O_2^{\cdot-}$ level were not achievable (**A**, representative trace for n=3) and exogenous NADPH did not increase $O_2^{\cdot-}$ (**A**, n=3 per group). However, in fresh Krebs HEPES buffer, a stable baseline was consistently achievable (**B**, representative trace for n=3) and cells responded to exogenous NADPH by a mean increase of 370 RLU per second (**B**, n=3 per group). RLU, Relative Light Units. Values are presented as mean ± SEM in Panels *A-B*. P-values from unpaired, non-parametric Mann-Whitney rank test.

The development of an acute oxidative stress model using H9C2 cells required cells to be grown on coverslips. Coverslips were coated with gelatin and grown in 12 well plates with gelatin coated coverslips. H9C2 cells were grown on coverslips to approximately 60-70% confluence in 10% FBS media.

Fresh Krebs HEPES Buffer in place of Media: Initially $O_2^{\cdot-}$ in H9C2 cells was quantified in fresh media without exposure to NADPH to determine whether a stable baseline was achievable. In media, a stable background and stable basal $O_2^{\cdot-}$ level using lucigenin-enhanced chemiluminescence was not achievable (Figure 3.5). Furthermore, the addition of exogenous NADPH that consistently yields a significant increase in $O_2^{\cdot-}$ did

not yield significant changes in $O_2^{\cdot-}$ in media, suggesting a possible interference of media's components (e.g. phenol) with $O_2^{\cdot-}$ and lucigenin reactivity (Figure 3.5). However, in fresh Krebs HEPES buffer, a stable baseline was consistently achievable and cells responded to exogenous NADPH by a mean increase of 370 relative light units (RLU/mg/protein) (Figure 3.5), suggesting Krebs HEPES could be used to measure $O_2^{\cdot-}$ in H9C2 cells. As I had previously shown that media could not be used for detection of $O_2^{\cdot-}$ by lucigenin-enhanced chemiluminescence, we needed to expose the cells to 1mM NADPH in Krebs HEPES buffer and use the buffer from 18h exposure as background. To explore this further, the viability of H9C2 cells was first examined and we explored whether FBS supplement increased viability of the cells.

3.3.3 MTT Assay for Cell Viability

The viability of cells was determined using the MTT assay. This assay works on the principle that viable cells have functioning mitochondrial dehydrogenase enzymes that can be used to reduce MTT (3-(4,5-dimethylthiazol-2-yl)-2,5-diphenyltetrazolium bromide) to a purple formazan.[199,200] This purple formazan is soluble and the color can be measured by absorbance using a spectrophotometer, with the colour of the well proportional to viability of cells.[199,200]

Briefly, MTT Assay was performed following manufacturer's protocol (Cat No: TOX1-1KT Sigma). Briefly, 10% by volume of MTT (5mg/mL in PBS) was added to cells that were replenished with fresh media (to remove debris and dead cells). A blank well with media but no cells was included as a negative control. Wells with MTT were allowed to incubate at 37°C for 1 hour and 45 minutes to 2 hours during which light-sensitive crystals were formed. Media was removed gently and washed 2 times with PBS. A constant volume of acidified isopropanol was added to dissolve crystals and were protected from light. Plate was gently mixed and then the dissolved crystal mixture was

loaded onto a 96 well in technical replicates. The absorbance was measured using a spectrophotometer at 570 and 690 nanometers. For analysis, absorbance at 690nm (background absorbance of the wells) was subtracted from the absorbance at 570nm and the intensities were compared. Higher intensity indicated increased mitochondrial activity and increased viability (decreased cytotoxicity) of cells compared to their counterparts.

Viability in Krebs HEPES alone and with 0.5% FBS: Incubating cells in Krebs HEPES buffer however significantly reduced viability of cells to 33% compared to cells grown in media; Tyrode's buffer, another physiological buffer, was consistent with Krebs HEPES and not an improved option, also reducing cell viability to 34% compared to those cells grown in media (Figure 3.6). To increase viability of the cells, while still having the capacity to measure $O_2^{\cdot-}$ by lucigenin-enhanced chemiluminescence, 0.5% FBS was added to Krebs HEPES buffer and viability increased to 66% compared to cells grown in media (Figure 3.6). Krebs HEPES buffer with 0.5% FBS also led to a stable background in lucigenin-enhanced chemiluminescence experiments (Figure 3.6) suggesting it could be utilized to measure $O_2^{\cdot-}$.

3.3.4 Characterization of oxidative stress in H9C2 cardiomyocytes

We also examined whether cells grown on coverslips incubated with 1mM NADPH for 18 hours but put into fresh Krebs HEPES in the luminometer would still allow for detection of increased basal $O_2^{\cdot-}$ generation in H9C2 cells after exposure to NADPH for 18 hours. However, no change in basal $O_2^{\cdot-}$ was detected after 18 hours of incubation (Figure 3.7). It was not clear whether (1) 1mM NADPH needed to be replenished during the 18 hours to see continued stimulation of H9C2 cells at endpoint or (2) whether placing the cells in fresh Krebs HEPES prevented cells from continually taking up or utilizing extracellular NADPH that was needed to generate $O_2^{\cdot-}$. We

hypothesized that $O_2^{\cdot-}$ generation required extracellular NADPH at 18 hours (continuous uptake) and using fresh Krebs HEPES buffer was not appropriate.

We hypothesized that excess NADPH from 1mM was in the original medium even after 18 hours and that the same medium the cells were incubated in for 18 hours should be utilized as the background for the cells. As such, we measured $O_2^{\cdot-}$ generation in H9C2 cells after recording background of the cells in the Krebs HEPES buffer (±1mM NADPH) that the cells were originally incubated in. Schematic of this final measurement is shown (Figure 3.8) and experimental results are shown in Chapter 5 as part of the final characterization of the acute model of oxidative stress.

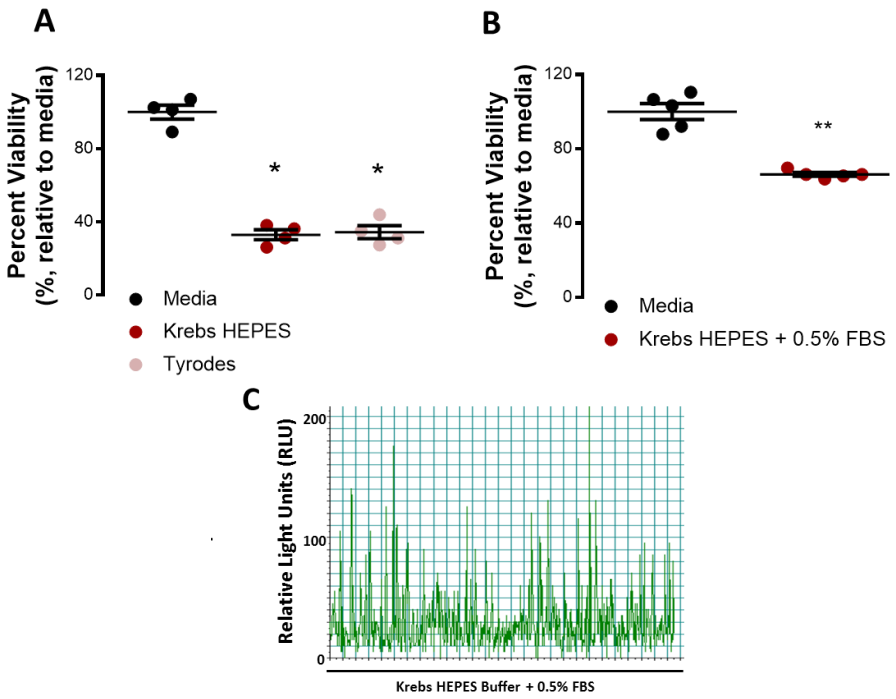


Figure 3.6 Viability of H9C2 Cells in Krebs HEPES Buffer with FBS

Viability of cells was significantly reduced in KHB (33%) and Tyrode's buffer (34%) compared to cells grown in media (**A**, n=4 per group). To increase viability of cells while still measuring $O_2^{\cdot-}$ by lucigenin-enhanced chemiluminescence, 0.5% FBS was added to KHB; viability of cells was 66% compared to cells grown in media (**B**, n=5 per group). KHB with 0.5% FBS also led to a stable background in lucigenin-enhanced chemiluminescence experiments (**C**, representative trace for n=5) suggesting this buffer system could be utilized to measure $O_2^{\cdot-}$. FBS, Fetal Bovine Serum. KHB, Krebs HEPES Buffer. Values are presented as mean ± SEM in Panels *A-B*. P-values from Kruskal-Wallis test followed by Dunn's post hoc correction for multiple comparisons in Panel *A* (comparisons only with media) and from unpaired, non-parametric Mann-Whitney rank test in Panel *B*. Adjusted P-values after post hoc correction are shown in Panel *A*. *P<0.05, **P<0.01 versus media.

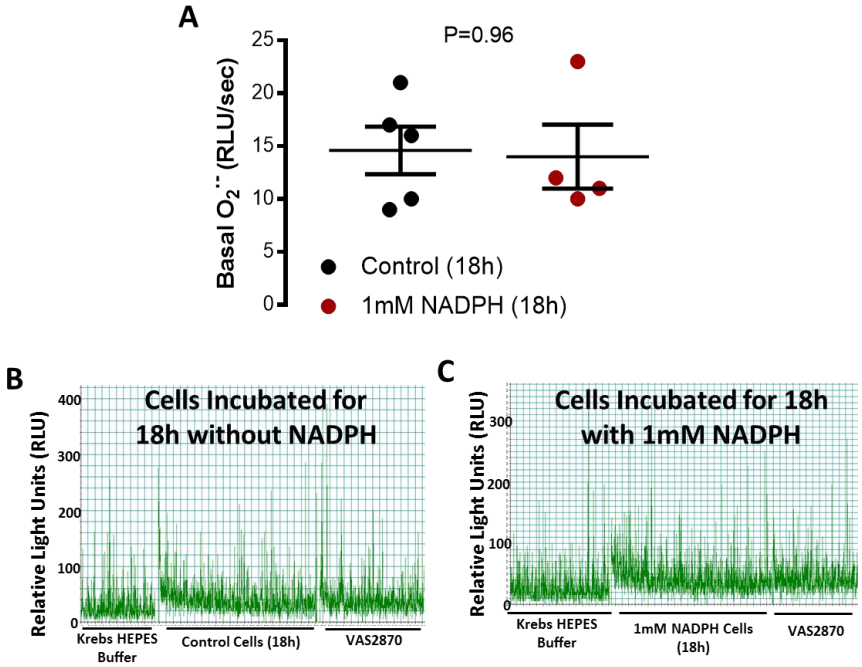


Figure 3.7 Cells Exposed to 1mM NADPH after placement in Fresh Krebs HEPES

When cells were exposed to 1mM NADPH for 18 hours and then placed in fresh Krebs HEPES buffer in the luminometer for $O_2^{\cdot-}$ quantification, no change in basal $O_2^{\cdot-}$ was detected (**A**, n=4-5), suggesting that using existing buffer the cells were exposed to as the background for $O_2^{\cdot-}$ quantification may be necessary. Representative lucigenin-enhanced chemiluminescence traces are shown for cells incubated in the absence of NADPH for 18 hours (**B**) and for cells incubated in the presence of 1mM NADPH for 18 hours (**C**). Values are presented as mean ± SEM in Panel *A*. P-value from unpaired, non-parametric Mann-Whitney rank test.

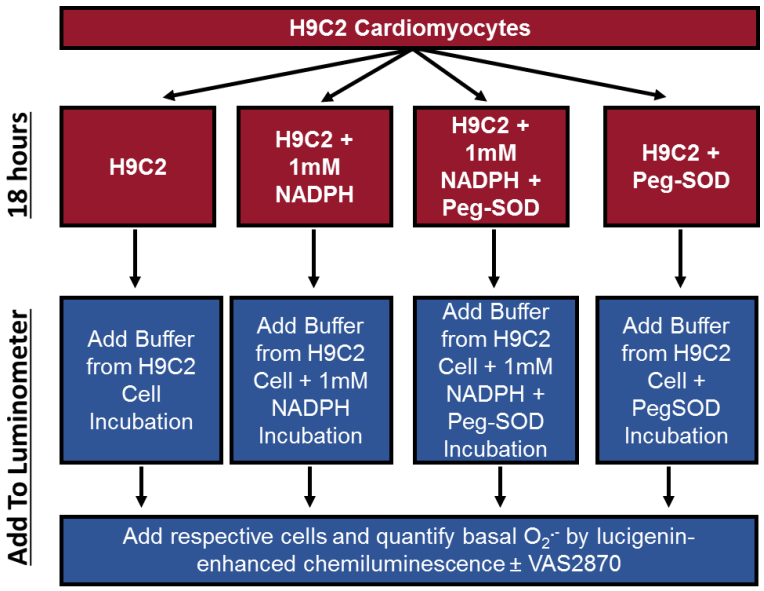


Figure 3.8 Schematic for Measuring $O_2^{\cdot-}$ in H9C2 Cells after NADPH Incubation

We hypothesized that $O_2^{\cdot-}$ generation required extracellular NADPH at 18 hours (continuous uptake) and therefore designed our luminometry experiment to include the original buffer in which cells were incubated.

3.4 CSE Knockdown in Cell Culture via shRNA

H9C2 cells were silenced with CTH shRNA or Scrambled shRNA and $O_2^{\cdot-}$ was quantified by lucigenin-enhanced chemiluminescence to determine the long-term effects of silencing CSE in healthy cardiomyocytes on basal myocardial redox state. A schematic for silencing H9C2 cells is shown (Figure 3.9).

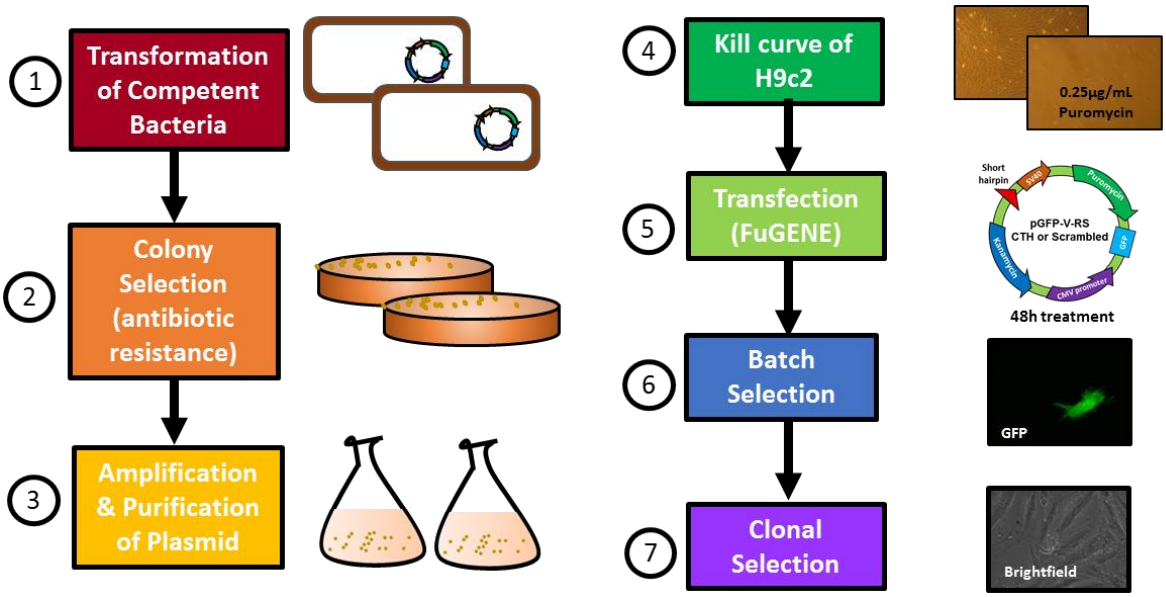


Figure 3.9 Schematic for the Generation of CSE Knockdown H9C2 Cells

Steps for the generation of CSE knockdown H9C2 cell line are shown. shRNA plasmid diagram created on basis of Origene shRNA guide. CSE, Cystathionine γ-Lyase. shRNA, Short-hairpin RNA.

3.4.1 Bacteria Transformation and Plasmid Amplification

Materials: Kanamycin (20-50µg/mL) agar plates were prepared: 14g of LB agar was mixed with 400 mL water and autoclaved immediately to prevent bacteria growth. The LB was equilibrated to 55°C in water bath with lid closed as antibiotics cannot be added to extremely high temperatures. Plates were laid near a Bunsen burner that created an updraft to remove bacteria from the area. Kanamycin was added to the LB agar (20-50ug/mL). The mixture was agitated and then poured into the plates (approximately 20-25mL per dish) and plates were left to solidify for 10 min with lid half open and Bunsen burner on. The lids were left half open to prevent condensation and water dripping and

mixing with the LB agar because this can be a source of contamination. When the kanamycin agar was solidified, the plates were wrapped tightly with parafilm and stored at 4°C, stored upside down to prevent condensation on the agar.

Transformation of Bacteria: Frozen (-80°C) DH10B competent bacteria were thawed on ice. shRNA vectors (pGFP-V-RS CTH and scrambled) were added (10ng total, from 5ng/μL mixture in nuclease-free water) to DH10B bacteria by pipetting and the mixture was left on ice for 30 minutes. A negative control of bacteria with no vector was also included throughout the steps. After the 30minute incubation on ice, bacteria mixtures were placed at 42°C for 45 seconds, and then were put back on ice for 5 minutes. This heat-shock allowed bacteria to uptake the plasmids. Approximately 200μL of sterile LB was pipetted under a sterile hood and added to each bacteria mixture. LB without kanamycin was added because the heat-shock was a stressful process for the bacteria which need recovery time. The LB, DH10B, and vector mixture was mixed with a pipette and incubated at 37°C for 1-1.5 hours to allow bacteria to grow. Lids were left loose to allow bacteria to receive O_2. Following this growth period, 100μL of the LB, DH10B, and vector mixture was plated on Kanamycin agar plates that had been equilibrated to room temperature. Bacteria were added in small amounts (approximately 30μL at a time) and spread until the plates were dry and a Bunsen burner was on during the spreading for updraft. Plates were left overnight at 37°C upside down.

Colony Selection: The following day, plates were equilibrated to room temperature for 1 hour so that colonies had an opportunity to spread out. The negative control plate had no colonies. Isolated colonies (singular colonies, large in size) were identified and selected by touching the individual colony with a filter tip and inoculating 1mL of LB with Kanamycin (50μg/mL final concentration) with the tip. Multiple colonies were selected. This mixture was then incubated at 37°C (150rpm) with agitation for

approximately 6 hours. The turbid 1mL mixtures were added to 100mL sterile LB with kanamycin (50ug/mL) and these larger mixtures were incubated at 37°C overnight with agitation.

Bacterial glycerol stocks: To prepare LB glycerol, 20mL glycerol was added to 30mL LB (40% glycerol in LB total volume) and autoclaved. The next day, LB glycerol and LB bacteria mixtures were added in a 1:1 ratio (e.g. 500µL each). These glycerol bacteria stocks were stored at -80°C immediately.

Plasmid Purification: The remaining LB bacteria was spun in an ultracentrifuge (rotor, JA25.50) after pre-cooling to 4°C for 15 minutes at 6000 x g (rcf) at 4°C. A midi prep kit (Catalog No: 12143) following manufacturer's protocol was used for the final steps of purification of the plasmids. Due to the shRNA structure, the shRNA construct was treated as low copy plasmid according to protocol. Briefly, supernatants were discarded after spinning and buffers were added to bacterial pellets to remove RNA and lyse bacteria, and precipitate proteins. The mixture was centrifuged at 20,000g for 30min a 4°C and added to an equilibrated column. DNA was eluted from the Qiagen tip and isopropanol was added. The DNA was then aliquoted and spun for 1 hour at maximum speed at 4°C. The supernatant was decanted and 70% ethanol was added for washing of the DNA and quickly decanted. Eppendorfs with DNA were placed in a speed vacuum for 20 min at 40-42°C to remove all traces of ethanol (and dehydrate DNA completely). DNA was rehydrated and resuspended in DNAse-free water and stored at 4°C overnight.

DNA Quantification and Verification by Nucleic Acid Gel Electrophoresis: The following day, the DNA from the eppendorfs were pooled together and quantified using the NanoDrop Nucleic Acids program. DNA stocks were made (1µg/µL). DNA samples were run on an agarose gel by gel electrophoresis (see gel electrophoresis for detailed methodology). DNA was identified as intact as opposed to degraded due to concrete

bands rather than a smear. DNA plasmid stocks were stored in aliquots at -80°C. This method was kindly explained by Dr. Fabio Sanna, and bacteria and reagents and guidance were also kindly provided by Dr. Paul Robinson.

3.4.2 Immunofluorescence and Staining Method

Imaging, transfection, and selection protocols that are discussed below were kindly explained with guidance by Dr. Costas Psarros. Green Fluorescent Protein (GFP) in the pGFP-V-RS shRNA vectors (CTH or Scrambled vectors) was used to visualize shRNA vector transfected H9C2 cells. Brightfield images were acquired to visualize cells, both transfected and non-transfected, and fluorescence was used to specifically visualize the GFP tag in transfected cells. Hoechst 33342 Solution (2'-[4-ethoxyphenyl]-5-[4-methyl-1-piperazinyl]-2,5'-bi-1H-benzimidazole trihydrochloride trihydrate; 20 mM, Catalog No. 62249) was used to visualize nuclei of all cells as the molecule is cell-permeable and specifically binds to DNA (ThermoFisher Product Overview).

Briefly, an Olympus inverted microscope (IX-71, Olympus UK), previously described,[201] was used with permission of Dr. Naveed Akbar from Prof. Choudhury's laboratory; the microscope was used with fluorescence filters (FITC for GFP; DAPI for Hoechst) to acquire images and microscope setup is shown (Figure 3.10). Acquisition times for FITC and DAPI were approximately 15 seconds and 2-3 seconds, respectively. ImagePro-Plus 6.3 (Media Cybernetic, Bethesda, USA) was specifically used as imaging software for acquisition.[201] For preparation of cells for imaging, cells were first washed with PBS after discarding media and 10µM of Hoechst 33342 Solution was added to cells in PBS before acquiring images. When image acquisition duration exceeded 10-15 minutes, excess Hoechst 33342 Solution was washed off with PBS and image acquisition continued. Images were analysed on Image J where brightness and contrast of the images were adjusted (Figure 3.11).

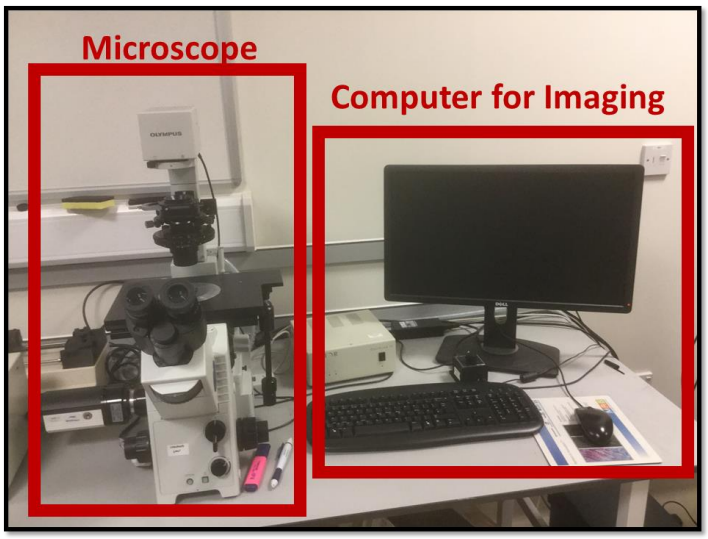


Figure 3.10 Microscopy for Imaging Fluorescent Cells

Using an Olympus inverted microscope (IX-71, Olympus UK) connected to a computer with Image Pro-Plus 6.3 software (Media Cybernetic, Bethesda, USA), non-transfected and transfected cells were located in brightfield and then imaged under fluorescence. Cells expressing green fluorescent protein, which was encoded in both the Scrambled and CTH plasmids, were observed under fluorescence. Detailed information regarding microscope was found in an imaging paper from Dr. Naveed Akbar in Professor Robin Choudhury's laboratory.[201] CTH, Cystathionine γ-Lyase Gene.

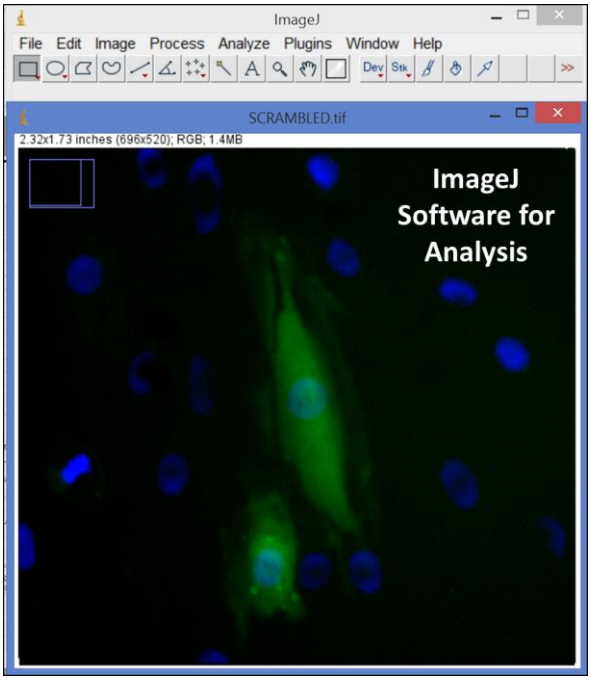


Figure 3.11 Screenshot of ImageJ Analysis

ImageJ software was used to analyse immunofluorescence images. The software allowed for adjustment of the brightness and contrast of the cells. GFP is shown in green and nuclei of cells are shown in blue. GFP, Green Fluorescent Protein.

3.4.3 Stable Transfection of Cell Line by shRNA Transfection

H9C2 cells were transfected with CTH and Scrambled shRNA constructs (Table 3.1), with FuGENE alone and non-transfected cells serving as negative controls. FuGENE, plasmid (1µg/µL), and media mixtures were prepared for transfection in a 1:3 or 2:6 DNA plasmid:FuGENE ratio. Media did not include FBS or antibiotics to reduce stress of the sensitive cells during the transfection process.

Table 3.1 Scrambled and CTH shRNA 29mer Construct Sequences

shRNA	29mer Construct Sequence
Scrambled	5' GCACTACCAGAGCTAACTCAGATAGTACT 3'
CTH 1	5' ATACAGCCGCTCTGGAAATCCGACGAGGA 3'
CTH 2	5' GGCTTAGTGTCTGTTACTTCCGATGACCT 3'
CTH 3	5' AAGACATCATTCTGGTTGTAGATAACACT 3'

29mer, 29 base pair sequence. CTH, Cystathionine γ-Lyase Gene. shRNA, Short-hairpin RNA.

As FuGENE is highly lipophilic, to make these mixtures, FuGENE was added directly into the media first without allowing adherence to plastic of the tube. FuGENE and media were mixed gently by hand or by vortex at the lowest speed. Media and FuGENE mixture was incubated at room temperature for 5 minutes. The corresponding amount of DNA plasmid was added and the mixture was again mixed gently by hand or by vortex at the lowest speed. This DNA Plasmid, FuGENE, and media mixture was incubated at room temperature for 15 minutes. H9C2 cells that were seeded into 6-well plates at approximately 50% confluency were replenished with fresh maintenance media without antibiotics (media with 10% FBS superior but no penicillin/streptomycin) during the 15-minute incubation. Following the incubation, 100 µL of the DNA plasmid, FuGENE, and Media mixture were added to each respective well. The mixture was added to the top of the media without touching the cells and carefully drop by drop to not

directly hit the cells. The 6-well plate was then moved in a cross-like motion for mixing and were incubated at 37°C in the 95% O_2/5% CO_2 incubator for 48 hours.

3.4.4 Imaging of Transfected Cells Transfected Cells

Immediately after 48 hours, transfection was confirmed by examining cells for green fluorescent protein (GFP) tag which was encoded for in both scrambled and CTH shRNA plasmids using immunofluorescence. GFP-expressing cells were visible in cells transfected with scrambled or CTH shRNA plasmids. Representative images of both GFP-tagged cells and their view in brightfield (amongst non-transfected cells) are shown (Figure 3.12).

Puromycin at 1-4 μg/mL for Selection of Silenced Cells

To generate a knockdown cell line, H9C2 cells transfected with shRNA (OriGene) needed to be selected from non-transfected cells using antibiotic puromycin whose resistance is encoded in the shRNA vector. To determine the appropriate and optimal concentration of puromycin prior to transfection, a kill curve was performed by growing H9C2 cells in the presence or absence of 1-4μg/mL puromycin for 5 days and determining which concentration kills the non-transfected cells slowly but completely by day 5.

At day 1, 1μg/mL of puromycin killed approximately 75% of the H9C2 cells and at day 2, all cells exposed to 1 μg/mL were dead (Figure 3.13). Concentrations higher than 1 μg/mL, namely 2-4 μg/mL killed the majority of the cells on day 1 itself so the experiment did not proceed past day 2 (Figure 3.13). Given the purpose of the kill curve was to determine a puromycin concentration in which the H9C2 cells were killed at day 5 and not earlier, these tested concentrations of 1-4μg/mL puromycin were determined to be too high.

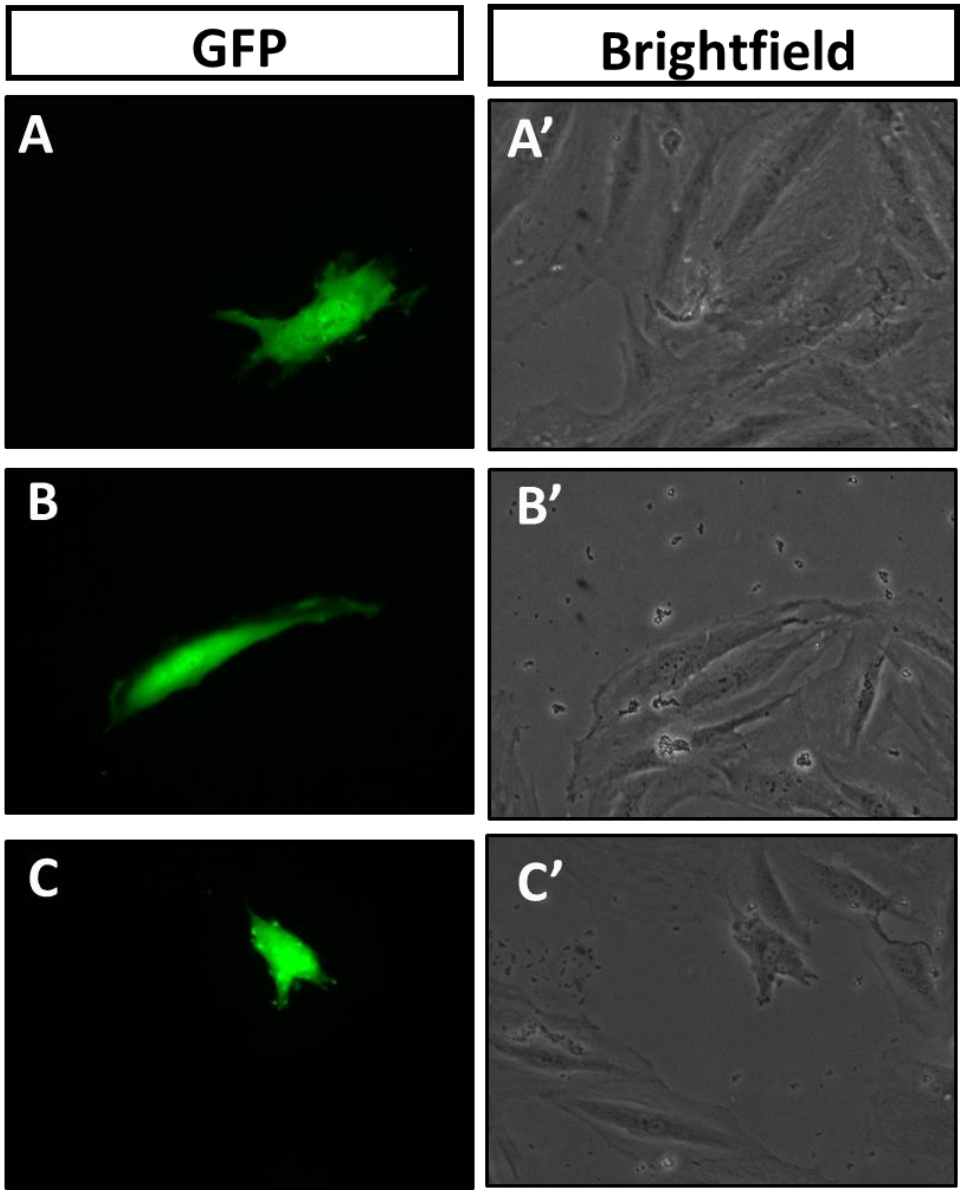


Figure 3.12 Immunofluorescence and Brightfield Images Post-Transfection

H9C2 cells were transfected with shRNA plasmid via FuGENE for 48 hours and presence of the GFP tag was detected by immunofluroscence 48-hours post-transfection. Cells expressed GFP tag present and GFP (**A-C**) and Brightfield (**A'-C'**) images of three different GFP-expressing H9C2 cells are shown. GFP, Green Fluorescent Protein.

Puromycin at 0.1-0.75 μg/mL for Selection of Silenced Cells

Lower concentrations of puromycin were then tested. In addition to control cells, cells were grown in 0.1, 0.25, 0.5, and 0.75 μg/mL of puromycin. 0.25 μg/mL of puromycin killed the majority of the H9C2 cells at day 5 and was thus chosen as the optimal and appropriate concentration of puromycin (Figure 3.14 and Figure 3.15).

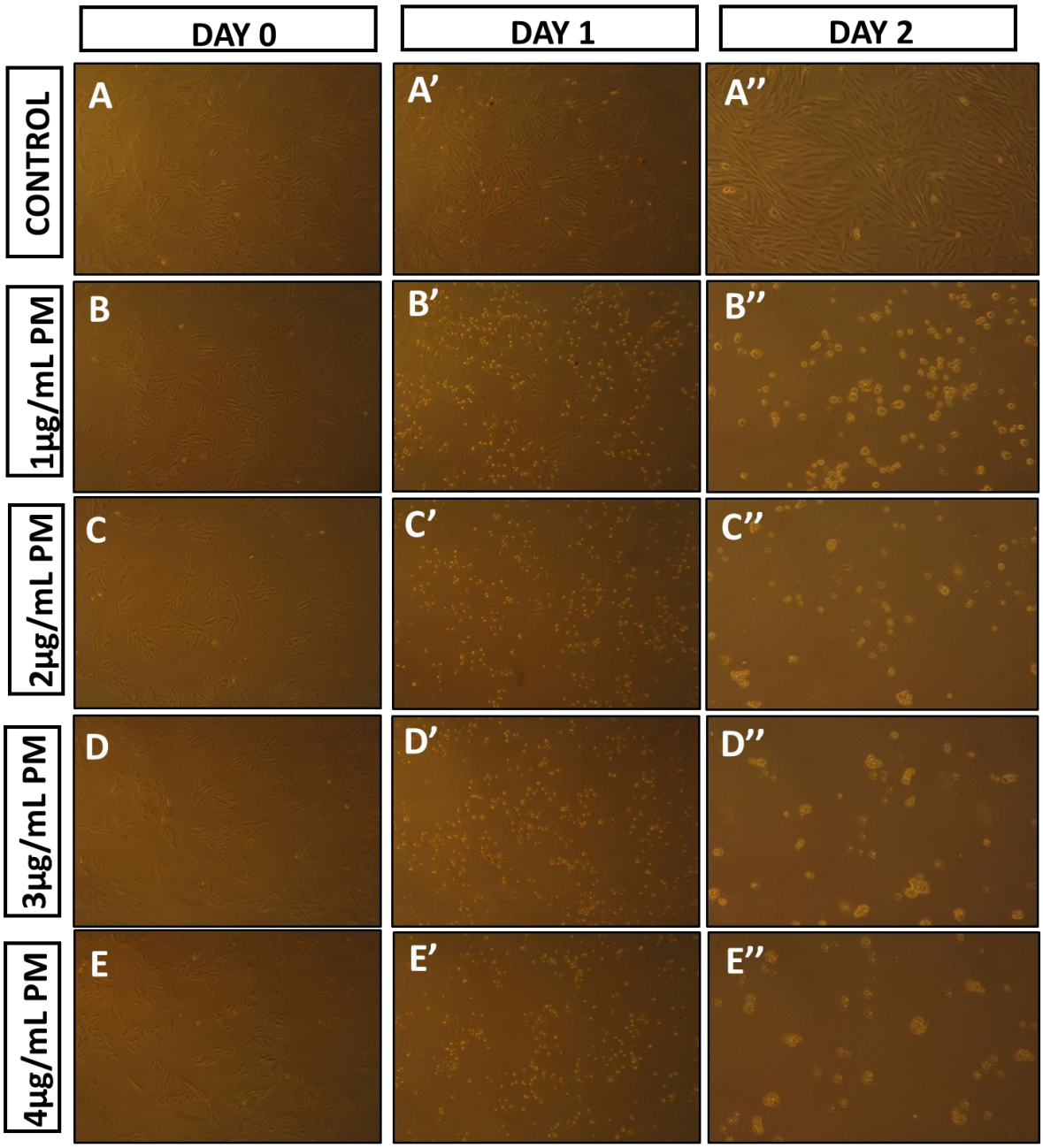


Figure 3.13 Puromycin Concentrations for H9C2 cells: 1-4 µg/mL, Day 0-2

To determine the optimal concentration of antibiotic puromycin that kills H9C2 cells at day 5 (the day of full differentiation), a kill curve was performed in which H9C2 cells were exposed to varying concentrations of puromycin and survival was monitored (1-4 µg/mL Puromycin, Day 0-2). Day 0, 1, and 2 of proliferation are shown for control cells (**A-A"**), 1 µg/mL puromycin (**B-B"**), 2 µg/mL puromycin (**C-C"**), 3 µg/mL puromycin (**D-D"**), and 4 µg/mL puromycin (**E-E"**). By day 2, all cells were dead for all concentrations of puromycin 1-4 µg/mL while control cells remained viable. PM, Puromycin.

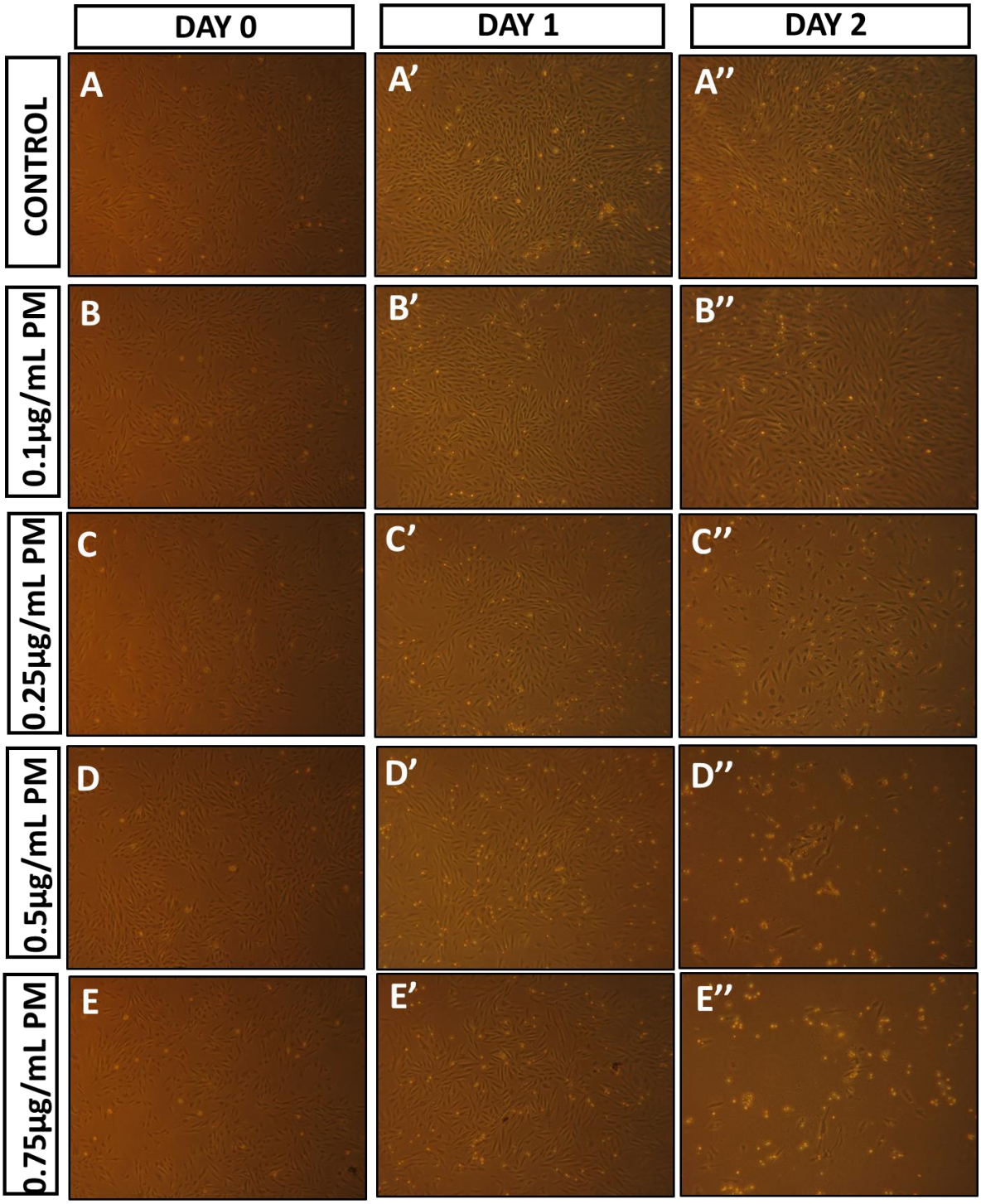


Figure 3.14 Puromycin Concentrations for H9C2 cells: 0.1-0.75 µg/mL, Day 0-2

To determine the optimal concentration of antibiotic puromycin that kills H9C2 cells at day 5 (the day of full differentiation), a kill curve was performed with concentrations of puromycin that were lower than 1 µg/mL. Day 0, 1 and 2 of proliferation are shown for control cells (**A-A"**), 0.1 µg/mL puromycin (**B-B"**), 0.25 µg/mL puromycin (**C-C"**), 0.5 µg/mL puromycin (**D-D"**) and 0.75 µg/mL puromycin (**E-E"**). The majority of cells were killed at day 2 with exposure to 0.5 and 0.75 µg/mL puromycin. Cells exposed to 0.1 and 0.25 µg/mL puromycin survived to day 2. PM, Puromycin.

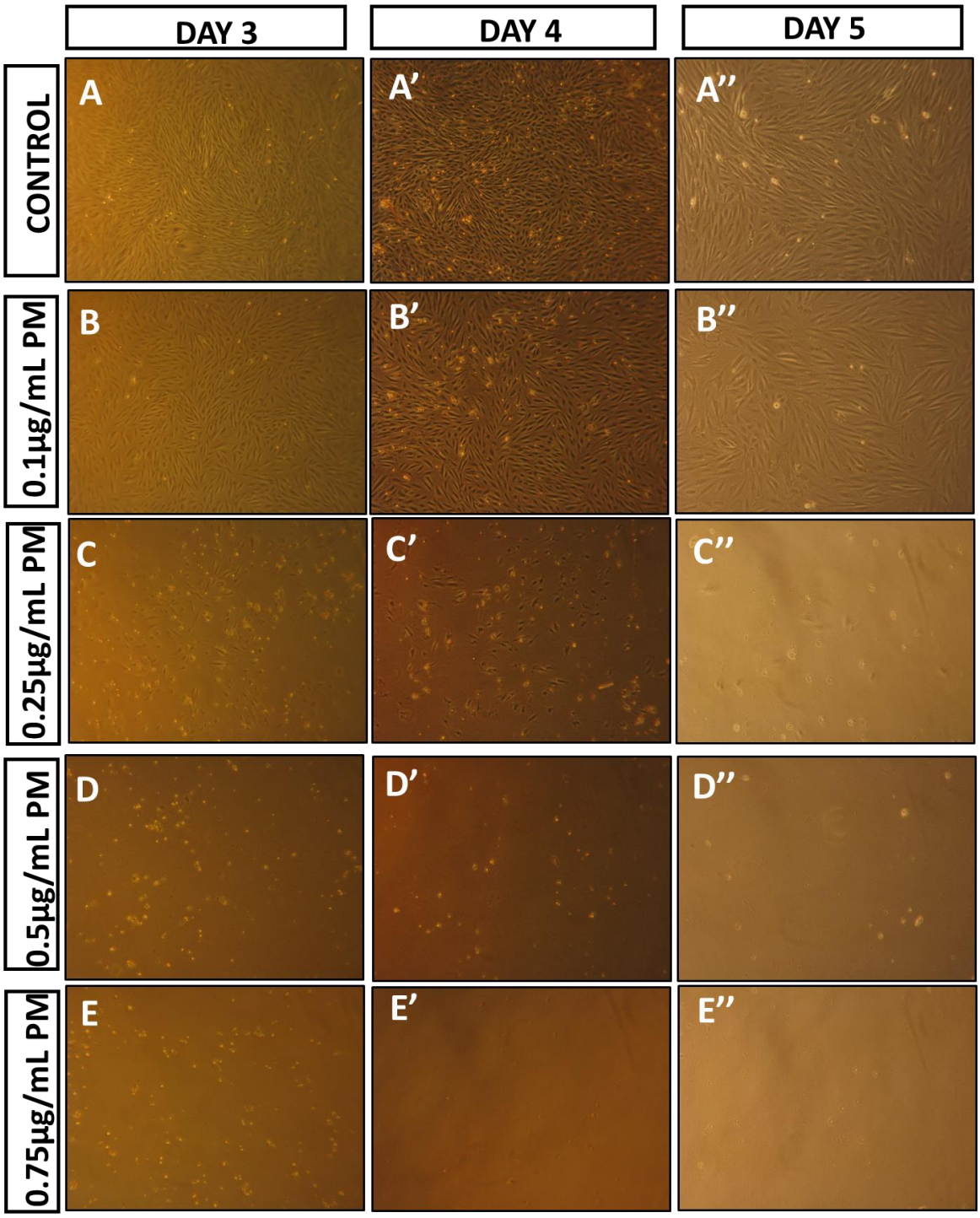


Figure 3.15 Puromycin Concentrations for H9C2 cells: 0.1-0.75µg/mL, Day 3-5

To determine the optimal concentration of antibiotic puromycin, a kill curve was performed with concentrations of puromycin that were lower than 1 µg/mL. Day 3-5 of proliferation are shown for control cells (**A-A"**), 0.1 µg/mL puromycin (**B-B"**), 0.25 µg/mL puromycin (**C-C"**), 0.5 µg/mL puromycin (**D-D"**) and 0.75 µg/mL puromycin (**E-E"**). 0.25 µg/mL puromycin killed the majority of cells at day 5 of proliferation and 0.25 µg/mL puromycin was the selected concentration. PM, Puromycin.

3.4.5 Characterization of Stably Transfected Cells after Batch and Clonal Selection

Batch Selection: Cells were grown in batches in selection media with puromycin (the concentration at which all cells were dead by day five on the H9C2 cell kill curve) and media was changed every 2-3 days for the following 10-14 days. The selection media allowed for the selection of transfected cells. These batches of cells were then assessed for CSE gene expression and silencing. After 10-14 days, cells were then grown in maintenance media with puromycin (the concentration at which cells were still approximately 25-30% confluency on day five on the H9C2 cell kill curve). During the entirety of this process, when cells were split, puromycin was not used on the day of split but media was changed to include puromycin the following day. Cells were split into separate 6-well plates from T75 flasks for qPCR and immunofluorescence.

Clonal Selection: Transfected H9C2 cells from the batches that had the most reduction in CSE expression were selected by clonal selection. For clonal selection, cells from batch selection were counted using a haemocytometer (e.g. 160,000 cells/mL). Cells were diluted in a serial dilution, first in a 1:50 ratio by adding 1mL of the original cells to 49mL of media (e.g. 160,000cells/mL / 50 = 3200 cells/mL). This 1:50 ratio dilution was repeated (e.g. 3200 cells/mL / 50 = 64 cells/mL). Finally, 200µL (one fifth of a mL) of this final dilution was added to each well of a 96-well plate (e.g. one fifth of 64 cells/mL = 13 cells/200uL plated). Cells were allowed to grow and media with puromycin was used the day after initial plating.

Increasing the quantity of cells derived from groups of 10-13 initial cells, scaling up from 96-wells took place. Cells before reaching 60-70% confluency were seeded from 96-well plates to 24-well plates, to 12-well plates, to 6-well plates, and finally to T25 flasks. In particular, when seeding from 12-well plates, cells were seeded into both 6wells

and T25 flasks as the 6wells were used to collect cells for CSE gene expression and T25 were maintained for freezing.

Cells were collected from 6-wells by washing 2x with ice-cold PBS. Cells were scraped and added to an Eppendorf. Then in the fume hood, trizol was added to the PBS and cell mixture and cells were frozen at -80°C through slow-freezing in bubble wrap or Mr. Frosty for RNA extraction. Cells from T25 flasks were spun down for 5 min at 1500 rpm, supernatant was removed and freezing medium (90% DMEM and 10% DMSO) was added to cell pellet. This mixture was frozen in cryovials (in bubble wrap or Mr. Frosty to slow down freezing). The cells were then placed into liquid nitrogen after at least one day in -80°C.

Following extraction, reverse transcription, and qPCR of the various clones, the clones with the best silencing were selected to grow and freeze in bulk and for experiments assessing myocardial redox state. For qPCR analysis for H9C2 cells, Ct values for CTH were normalized by Ct values for GAPDH (ΔCt). The difference between CTH and GAPDH Ct values were further normalized by subtracting the average difference between CTH and GAPDH for all the scrambled clones (undifferentiated or differentiated) (ΔΔCt). The negative of this difference was then raised to the power of 2 ($2^{-\Delta\Delta Ct}$) and graphed.

Characterization after Batch Selection of Silenced Cells

To grow the transfected cells and kill the non-transfected cells, H9C2 cells were then grown in selection media containing 0.25μg/mL of puromycin. Cells were than imaged for visual inspection of transfection efficiency (sufficient pictures could not be taken to quantify accurately transfection efficiency). Representative images of cells with stained nuclei are shown and GFP-expressing cells are visible (Figure 3.16). This

suggested H9C2 cells had successfully taken up the shRNA plasmids and were expressing its encoded protein GFP and demonstrating puromycin resistance.

Identification of Clonal Populations of Silenced Cells

After transfection and puromycin selection of H9C2 cells to obtain transfected H9C2 cells, the gene expression of CSE was quantified. Non-transfected cells and cells transfected with scrambled shRNA plasmid or 3 different CTH shRNA plasmid were compared. We found that cells transfected with CTH shRNA plasmid 1 had the lowest gene expression of CSE, with approximately 47% downregulation compared to scrambled controls (Figure 3.16). The scrambled plasmid itself upregulated CSE expression by approximately 20% compared to non-transfected controls (Figure 3.16). CTH shRNA plasmids 2 and 3 did not downregulate CSE by 47% as CTH shRNA plasmid 1 did (Figure 3.16) and therefore CTH shRNA plasmid 1 was selected as the transfection plasmid for future experiments.

To obtain cells with further downregulation of CTH, single cells transfected with scrambled shRNA plasmid or CTH shRNA plasmid 1 were isolated from the group of cells described above. In particular, 4 clones transfected with scrambled shRNA plasmid and 35 clones transfected with CTH shRNA plasmid 1 were grown. These isolated cells were grown into clonal populations and their gene expression of CSE was quantified. 2 clonal populations with the scrambled shRNA plasmid and 4 clonal populations with the lowest CSE expression transfected with CTH shRNA plasmid 1 were identified and grown for further examination. CSE gene expression and CSE protein levels were examined in final selected clones with comparisons made between scrambled clonal population and CTH clonal population, and this final characterization is described in Chapter 6.

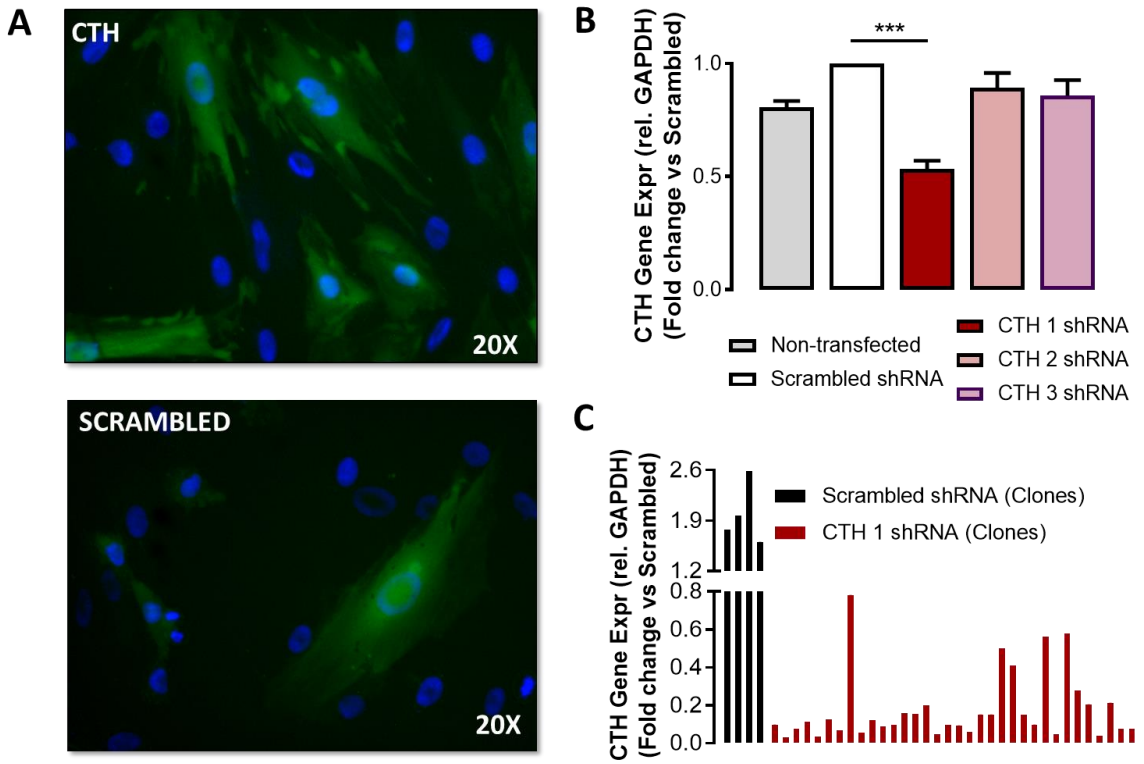


Figure 3.16 Immunofluorescence Images & Gene Expression Post-Batch Selection

Transfected H9C2 cells were grown in selection media with 0.25 µg/mL puromycin to allow growth of transfected cells only, excluding non-transfected cells. Images of cells transfected with CTH or Scrambled shRNA plasmids and selected in puromycin are shown; GFP is in green and nuclei of cells are in blue (**A**). H9C2 cells were transfected specifically with either scrambled shRNA or one of three different CTH shRNA plasmids (**B**). Gene expression of CSE was quantified in these 4 different cell lines as well as non-transfected controls. Shown as fold change compared to scrambled controls, CTH shRNA plasmid 1 had the lowest expression of CSE with approximately 47% downregulation compared to Scrambled (**B**, n=6 per group). Transfection itself increased CSE gene expression by approximately 20% (non-significant) compared to non-transfected controls. Single clones of cells were isolated from H9C2 cells transfected with CTH shRNA plasmid 1 or Scrambled shRNA plasmid and grown in 96-well plates and scaled up to 24-wells, 12-wells, 6-wells, and finally T25 flasks. CSE gene expression was examined in these clonal populations (**C**, n=1 per clonal population). 18 of 35 CTH shRNA plasmid 1 clones had less than 10% CSE gene expression compared to Scrambled controls, and 6 of 35 CTH shRNA plasmid 1 clones had less than 5% CSE gene expression compared to Scrambled controls (**C**). The 4 clonal populations with lowest CSE gene expression were selected along with 2 clonal populations with the Scrambled shRNA plasmid were selected for further examination. CSE, Cystathionine γ-Lyase. CTH, Cystathionine γ-Lyase Gene. GFP, Green Fluorescent Protein. shRNA, Short-hairpin RNA. Values are presented as mean ± SEM in Panel *B* and individual values are presented in Panel *C*. P-value from paired, non-parametric Friedman's test followed by Dunn's post hoc correction for multiple comparisons in Panel *B* (adjusted P-value between Scrambled and CTH 1 shRNA plasmids is shown; multiple comparisons were with Scrambled control only). ***P<0.001 vs Scrambled.

Chapter 4 H_2S and Myocardial Redox State

In this study, we explore the hypothesis that endogenous plasma H_2S/Sulfide levels are correlated with myocardial redox state and exogenous H_2S directly suppresses $O_2^{\cdot-}$ generation from enzymatic sources NADPH oxidases, mitochondrial oxidases, and uncoupled nitric oxide synthases in the myocardium from individuals with cardiac disease. Moreover, we explore these effects using distinct fast-releasing H_2S donor NaHS and slow-releasing H_2S donor GYY4137 whose H_2S profiles are characterized by an amperometric probe. The specific aims of the present study were to examine

I. Whether plasma H_2S/Sulfide was associated with patient demographics and myocardial redox state
II. The kinetics of H_2S release from two H_2S donors NaHS and GYY4137 *in vitro*
III. The effects of fast-releasing donor NaHS on myocardial redox state
IV. The effects of slow-releasing donor GYY4137 on myocardial redox state

This chapter therefore provides insight into the role of kinetically-distinct H_2S donors on myocardial redox state and specific sources of $O_2^{\cdot-}$ in the myocardium, further examining potential mechanisms for H_2S's effects on coupling status and providing insight into a link between H_2S/Sulfide and myocardial redox state.

4.1 Plasma H_2S/Sulfide, Demographics, & Myocardial Redox State

Several studies have measured H_2S/Sulfide in the circulation of patients (systemic) with heart failure or vascular disease and patents have been filed to use H_2S as a potential clinical marker.[159] However, while circulating H_2S/Sulfide has been measured in different disease states, studies have not examined whether circulating H_2S/Sulfide levels correlate with myocardial redox state.

Table 4.1 Demographics Characteristics of Study Participants in Chapter 4

Participant Demographic Characteristics		
	Study Arm 1 Clinical Associations	**Study Arm 2** *Ex Vivo* Studies
Demographics		
Participants (n)	**552**	**31**
Age (years)	**66.7±0.4**	**68.6±1.7**
Male gender (%)	**82.2**	**87.1**
Smoking (active/ex) (%)	**66.6**	**58.1**
Hypertension (%)	**74.7**	**77.4**
Hypercholesterolemia (%)	**75.4**	**90.3**
Diabetes mellitus (%)	**26.2**	**19.4**
BMI (kg/m^2)	**28.5±0.2**	**28.3±0.9**
Waist circumference (cm)	**93.3±1.2**	**99.9±2.3**
Waist:Hip ratio	**0.98±0.01**	**0.99±0.01**
Medications		
ACEi/ARBs (%)	**51.4/11.7**	**48.4/6.5**
β-blockers (%)	**68.9**	**67.7**
Aspirin/Clopidogrel (%)	**83.5/24.8**	**74.2/19.4**
Statins (%)	**84.8**	**96.8**
CCBs (%)	**30.1**	**22.6**
Diuretics (%)	**24.0**	**6.5**
Insulin/Oral hypoglycaemic (%)	**9.1/16.5**	**3.2/12.9**
Nitrates (%)	**36.5**	**48.4**

ACEi, Angiotensin Converting Enzyme inhibitors. ARB, Angiotensin Receptor Blockers. BMI, Body Mass Index. CCB, Calcium Channel Blockers. Values are presented as mean ± SEM.

To understand whether there is such a correlation between circulating H_2S and myocardial redox state, we measured plasma H_2S/Sulfide using the methylene blue assay validated above in a large cohort of patients undergoing cardiac surgery whose demographics have been recorded from medical charts and whose myocardial redox state has been characterized (Table 4.1).

4.1.1 Plasma H_2S/Sulfide and Patient Demographics

We found that individuals who were female had slightly elevated plasma H_2S/Sulfide levels compared to males (Figure 4.1). However, there was no difference in plasma H_2S/Sulfide levels (based on age, Figure 4.1). We further found that there was a

significant reduction in plasma H_2S/Sulfide levels for individuals with diabetes compared to individuals with no diabetes but HOMA-IR greater than 2.9 (Figure 4.2). There were no significant differences in plasma H_2S/Sulfide levels between individual with or without diabetes, hypertension, hypercholesterolemia (Figure 4.2). Furthermore, there was no difference in plasma H_2S/Sulfide levels between patients of different NYHA Classes (Figure 4.3). Moreover, there was no correlation between plasma H_2S/Sulfide levels and ejection fraction, LA diameter, LV mass, left ventricular end-diastolic volume, or days in hospital (Figure 4.3).

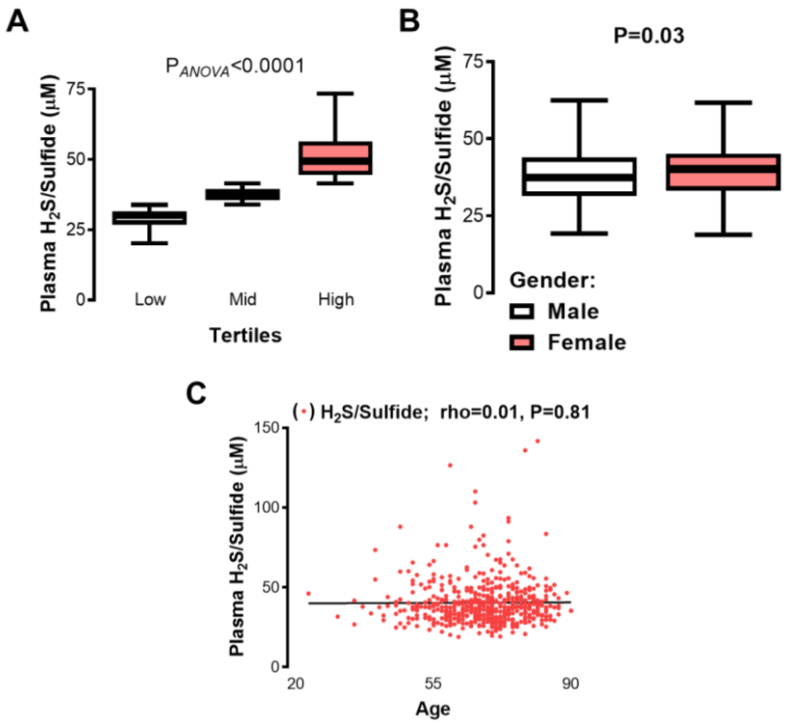


Figure 4.1 Plasma H_2S/Sulfide and Patient Demographics

Plasma H_2S/Sulfide levels were measured in the study population (552 individuals from the Ox-HVF cohort). Plasma H_2S/Sulfide in tertiles were significantly different with mean ± SEM of 29.0±0.2 for low tertile, 37.6±0.2 for middle tertile, and 54.1±1.2 µM H_2S/Sulfide for high tertile (**A**, P_{ANOVA}<0.0001; adjusted for multiple comparisons, P<0.001 for Low vs Mid, Mid vs High and Low vs High; n=184 per tertile). Plasma H_2S/Sulfide levels were marginally but significantly elevated in females compared to males (**B**, P=0.03; 40.0±0.6 µM in males versus 42.1±1.6 µM in females; n=449 males, 97 females) but plasma H_2S/Sulfide levels were not associated with patients' age in years (**C**, ρ(rho)=0.01, P=0.81; n=537). H_2S, Hydrogen Sulfide. Values are presented as median (25^{th} to 75^{th} percentile) and whiskers (Tukey) in Panels *A-B*. P-values from unpaired, non-parametric Kruskal-Wallis test followed by Dunn's post hoc correction for multiple comparisons in Panel *A* and from unpaired, non-parametric Mann-Whitney rank test in Panel *B*. Correlation assessed by bivariate analysis is presented with non-parametric Spearman's correlation coefficient ρ(rho) estimation in Panel *C*.

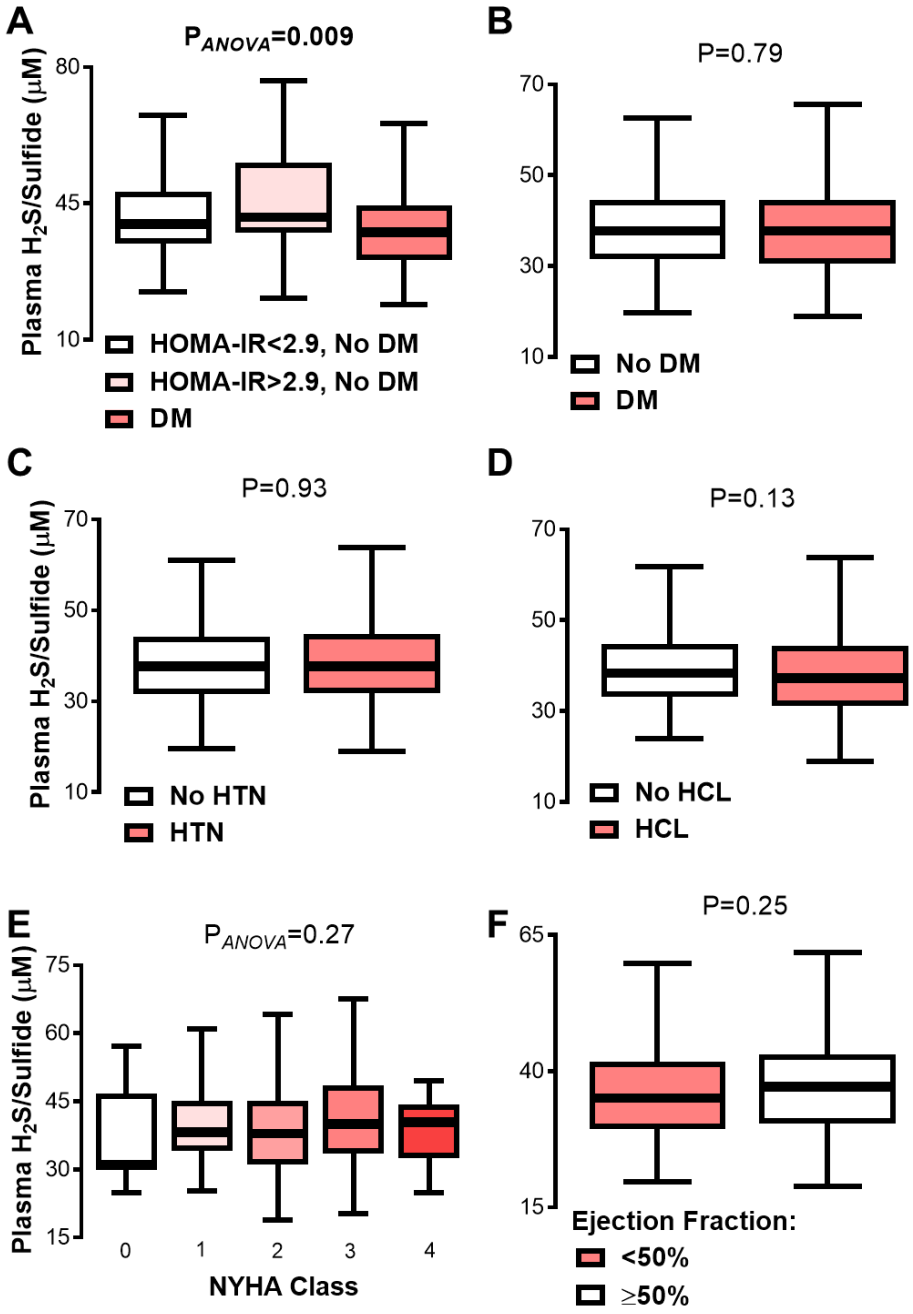


Figure 4.2 Plasma H_2S/Sulfide, Metabolic Profile, and Heart Failure

Plasma H_2S/Sulfide was significantly reduced in patients with DM compared to those with no diabetes but HOMA-IR>2.9 (**A**, P_{ANOVA}=0.0009, adjusted P=0.03 between No DM HOMA-IR>2.9 vs DM; n=232, 30, 142 per tertile). No differences in plasma H_2S/Sulfide were observed between patients with and without DM (**B**, P=0.79; n=399 No DM, n=142 DM), with and without HTN (**C**, P=0.93; n=395 HTN, n=134 No HTN), with and without HCL (**D**, P=0.13; n=408 HCL, n=133 No HCL). No differences in plasma H_2S/Sulfide levels were observed between patients of different NYHA Classes 0-4 (**E**, P_{ANOVA}=0.27; n=13, 128, 202, 125, 16) or between individuals with ejection fraction <50% and those with ejection faction ≥50% (**F**, P=0.25; n=94, 249). DM, Diabetes Mellitus. EF, Ejection Fraction. HCL, Hypercholesterolemia. HTN, Hypertension. HOMA-IR, Homeostatic model assessment of insulin resistance. Values are presented as median (25^{th} to 75^{th} percentile) and whiskers (Tukey) in Panels *A-F*. P-values from unpaired, non-parametric Kruskal-Wallis test followed by Dunn's post hoc correction for multiple comparisons in Panel *A* and *E* and from unpaired, non-parametric Mann-Whitney rank test in Panel *B-D* and *F*.

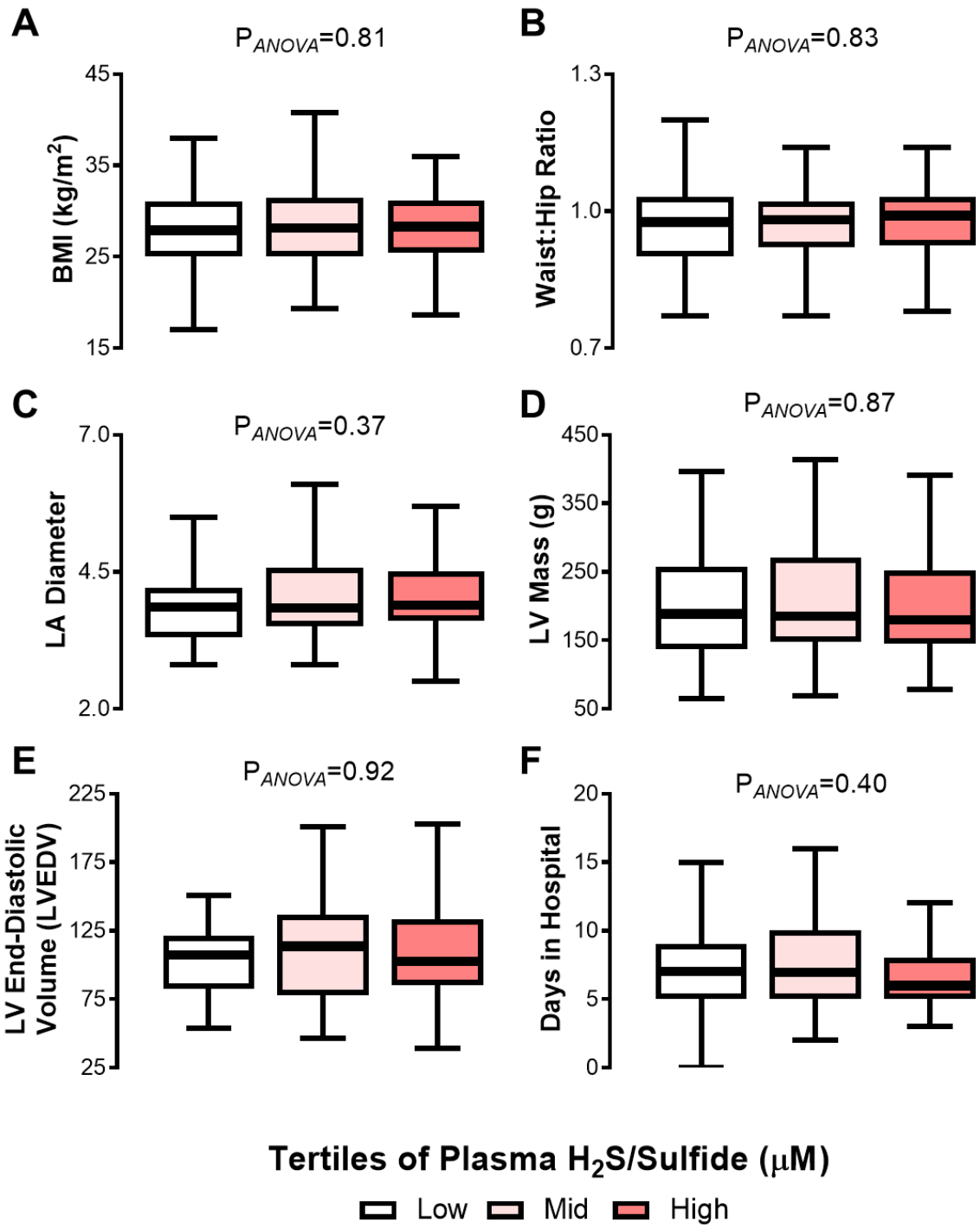


Figure 4.3 Plasma H_2S/Sulfide, Obesity, and Myocardial Function

Plasma H_2S/Sulfide was not associated with BMI (**A**, P=0.81; n=171 per tertile) or Waist:Hip ratio (**B**, P=0.83; n=108-109 per tertile). There was no correlation between plasma H_2S/Sulfide levels and LA diameter (**C**, P_{ANOVA}=0.37; n=44-45 per group), LV mass (**D**, P_{ANOVA}=0.87, n=57-58 per group), or LVEDV (**E**, P_{ANOVA}=0.92; n=52 per group) or days in hospital (**F**, P_{ANOVA}=0.40; n=162 per group). BMI, Body mass index. H_2S, Hydrogen Sulfide. LA, Left Atrium. LV, Left Ventricle. LVEDV, Left Ventricular End-Diastolic Volume. Values are presented as median (25^{th} to 75^{th} percentile) and whiskers (Tukey). P-values from unpaired, non-parametric Kruskal-Wallis test followed by Dunn's post hoc correction for multiple comparisons.

4.1.2 Plasma H_2S/Sulfide and Myocardial Redox State

After examining the relationship between plasma H_2S/Sulfide and the demographics of our cohort, we asked whether circulating H_2S/Sulfide levels were correlated with myocardial redox state. We found that circulating H_2S was significantly correlated with mitochondrial $O_2^{\cdot -}$ as measured by rotenone-inhibited $O_2^{\cdot -}$ (Figure 4.4). Rotenone-inhibited $O_2^{\cdot -}$ measured $O_2^{\cdot -}$ after rotenone blocks complex I, inhibiting the $O_2^{\cdot -}$ coming from downstream of the electron transport chain. H_2S correlated with this reduction in $O_2^{\cdot -}$ by rotenone suggesting a correlation with increased $O_2^{\cdot -}$ post-complex I. However, we found that circulating H_2S was not correlated with myocardial $O_2^{\cdot -}$ generation from NADPH oxidases or nitric oxide synthases (Figure 4.4). Our findings indicate circulating H_2S/Sulfide is not a correlate for myocardial redox state but is correlated with mitochondrial $O_2^{\cdot -}$ in the heart.

4.2 Kinetic Release Profiles of Fast- and Slow-Releasing H_2S Donors

Given that correlations do not determine causality, we next examined whether there was a direct effect of H_2S on myocardial redox state. In order to explore this question, following set-up of the amperometric sensor described in Chapter 3, we examined the H_2S release from both H_2S donors NaHS (10, 20, 40, 80μM) and GYY4137 (300μM) in four experimental conditions. The release of H_2S from the donors in experimental conditions similar to *ex vivo* experiments, namely in Krebs HEPES buffer at 37°C, was of particular interest as this was the condition in which *ex vivo* human myocardium would be incubated.

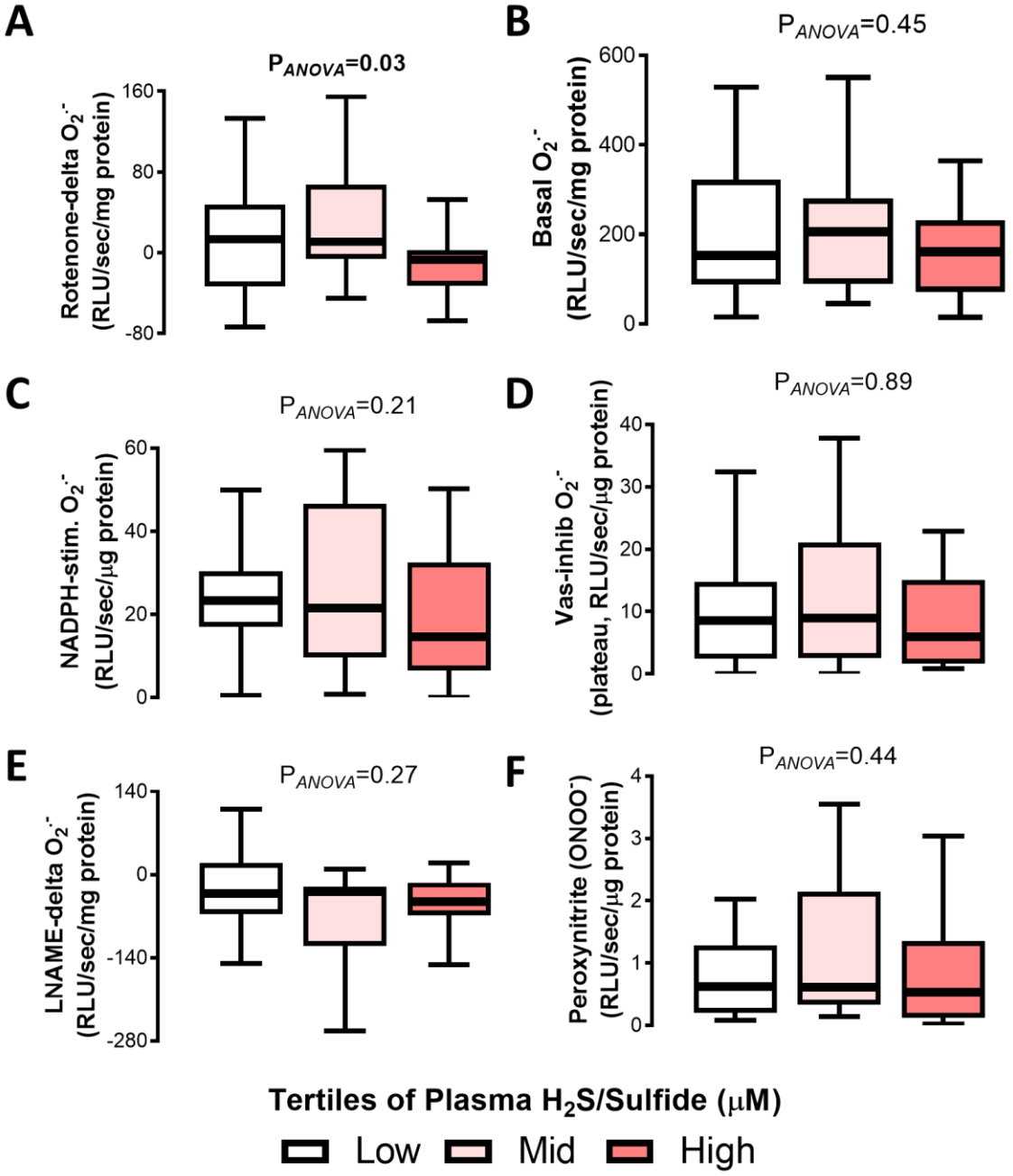


Figure 4.4 Plasma H_2S/Sulfide and Myocardial Redox State

Plasma H_2S/Sulfide levels were significantly correlated with mitochondrial $O_2^{\cdot-}$ generation in the heart as estimated by rotenone-inhibited $O_2^{\cdot-}$ (**A**, P_{ANOVA}=0.03; adjusted for multiple comparisons, P=0.03 between mid and high tertile groups; n=24 per group). Plasma H_2S/Sulfide was not correlated with basal $O_2^{\cdot-}$ in the heart (**B**, P_{ANOVA}=0.45; n=27 per group) or $O_2^{\cdot-}$ from myocardial NADPH oxidases as estimated by both NADPH-stimulated and VAS2870-inhibitable $O_2^{\cdot-}$ (**C**, P_{ANOVA}=0.21; n=27-28 per group. **D**, P_{ANOVA}=0.89; n=26-27 per group). Plasma H_2S levels were not correlated with $O_2^{\cdot-}$ from myocardial NOSs (**E**, P_{ANOVA}=0.27; n=26-27 per group) or myocardial $ONOO^-$ levels (**F**, P_{ANOVA}=0.44; n=26-27 per group). H_2S, Hydrogen sulfide. $O_2^{\cdot-}$, Superoxide. $ONOO^-$, Peroxynitrite. Values are presented as median (25^{th} to 75^{th} percentile) and whiskers (Tukey). P-values from unpaired, non-parametric Kruskal-Wallis test followed by Dunn's post hoc correction for multiple comparisons.

4.2.1 H_2S Release from NaHS in Physiological Conditions

The release of H_2S was monitored and NaHS was found to release H_2S in consistent time range of release in all four conditions (within 30 minutes), and notably, the release of H_2S peaked within the first few minutes in all concentrations (Figure 4.5). These results, consistent in different systems tested including Krebs Henseleit buffer, Tyrode's buffer, culture media, and Krebs HEPES buffer confirmed that NaHS released H_2S characteristic of a short-release, rapid H_2S donor (Figure 4.5).

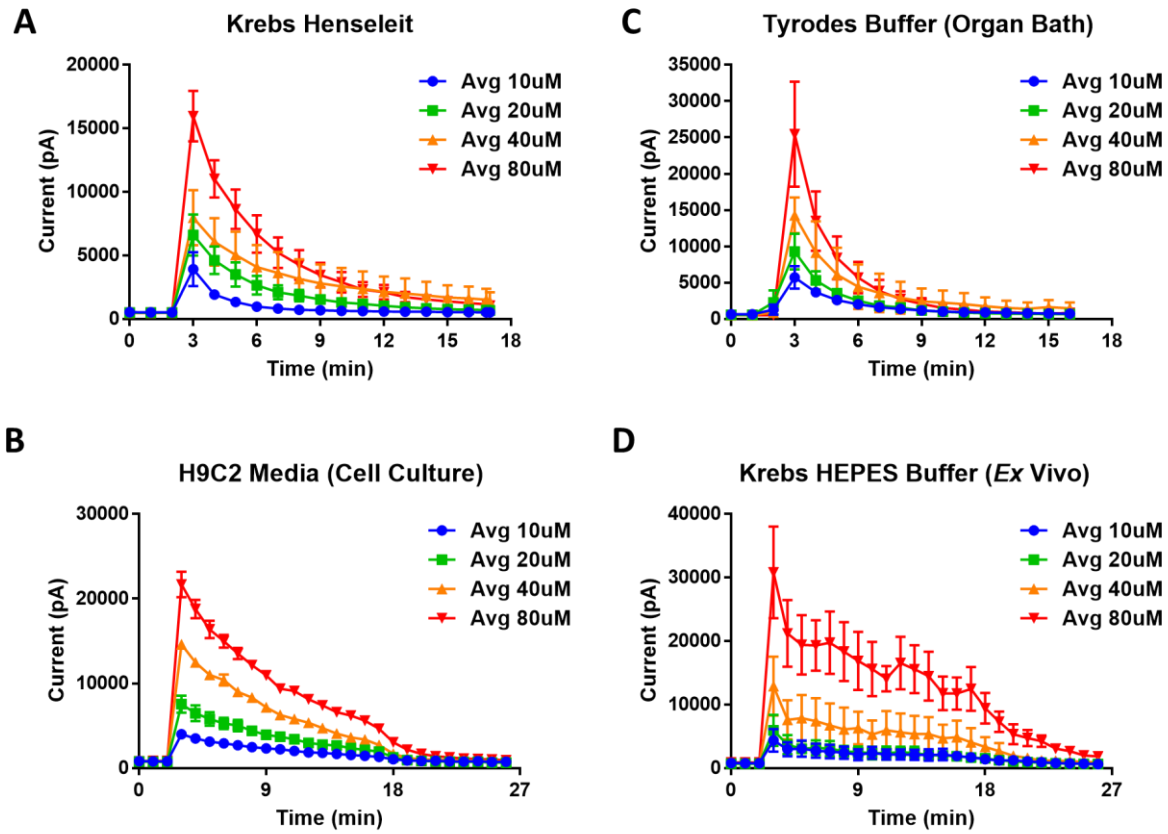


Figure 4.5 H_2S Release from NaHS (Four Physiological Conditions)

The release of H_2S from 10, 20, 40, and 80 µM NaHS is shown in (**A**) Krebs Henseleit buffer, (**B**) Tyrode's buffer, (**C**) H9C2 cell culture media, and (**D**) Krebs HEPES buffer. Each concentration was performed in triplicates (n=3) and all conditions were at 37◦C. NaHS, Sodium hydrogen sulfide. pA, picoamperes. Values are presented as mean ± SEM.

4.2.2 H_2S Release from GYY4137 in Physiological Conditions

Next, we examined the kinetics of GYY4137. A single concentration of 300µM GYY4137 was detectable by the amperometric sensor. With an interest in the release of

H_2S from this donor in experimental conditions similar to *ex vivo* experiments in which human myocardium would be incubated, GYY4137 kinetics were examined in Krebs HEPES and, for validity, three additional physiological conditions (Figure 4.6). Interestingly, the kinetics of the GYY4137 varied in different buffers: GYY4137 in Krebs Henseleit demonstrated a steady-state constant release, in Tyrode's buffer and Krebs HEPES demonstrated a parabolic decrease in release over time, and in cell culture media demonstrated a parabolic increase in release over time (Figure 4.6).

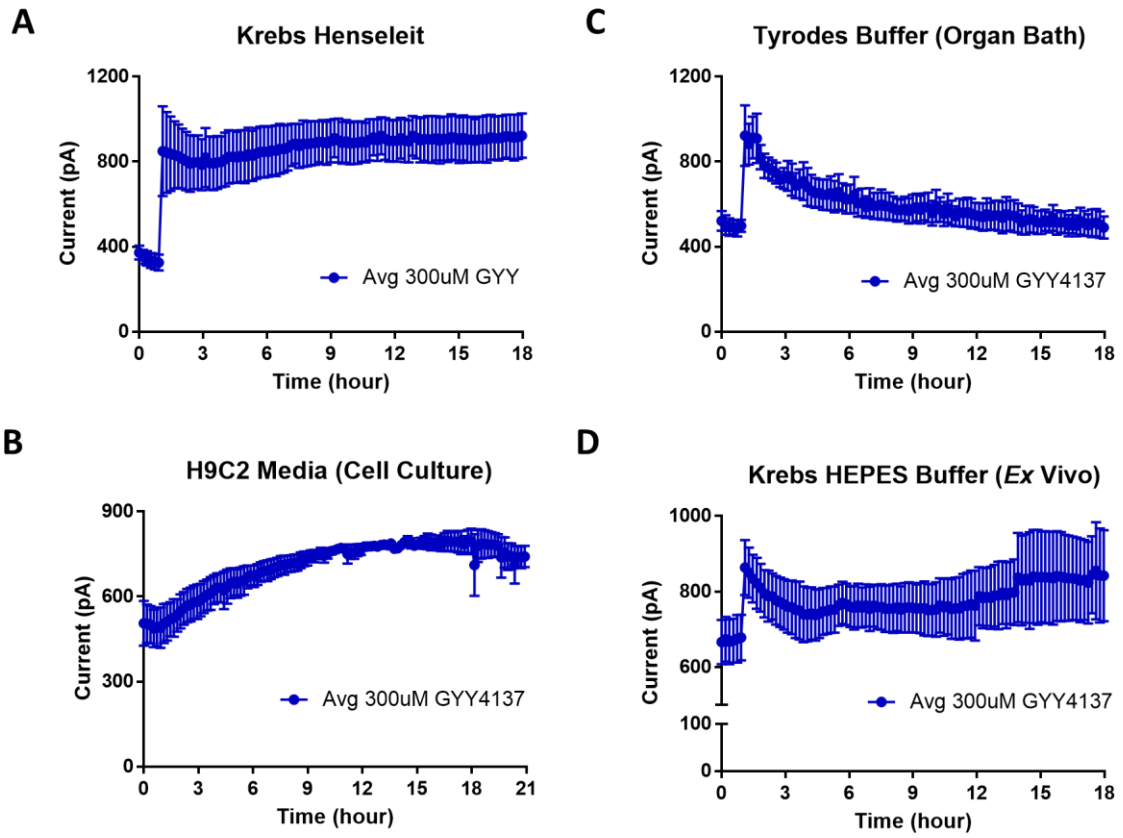


Figure 4.6 H_2S Release from GYY4137 (Four Physiological Conditions)

The release of H_2S from 300 µM GYY4137 is shown in (**A**) Krebs Henseleit buffer, (**B**) Tyrode's buffer, (**C**) H9C2 cell culture media without serum (with serum, noise only in the range of 0-1000 pA, not shown), and (**D**) Krebs HEPES buffer. GYY4137 release in each experimental condition was performed in triplicates (n=3) and all conditions were at 37◦C. pA, picoamperes. Values are presented as mean ± SEM.

Given 30µM NaHS would be used for *ex vivo* incubations of myocardium, we re-graphed the kinetics of NaHS removing 80µM NaHS and focusing on 10-40µM NaHS.

Furthermore, both NaHS and GYY4137 were re-graphed with current as a delta from the baseline (Figure 4.7). These graphs were used to determine the incubation times for human myocardium. While H_2S was released rapidly by NaHS as seen by amperometry, H_2S can be released at far lower concentrations for longer periods of time by other donors like GYY4137.

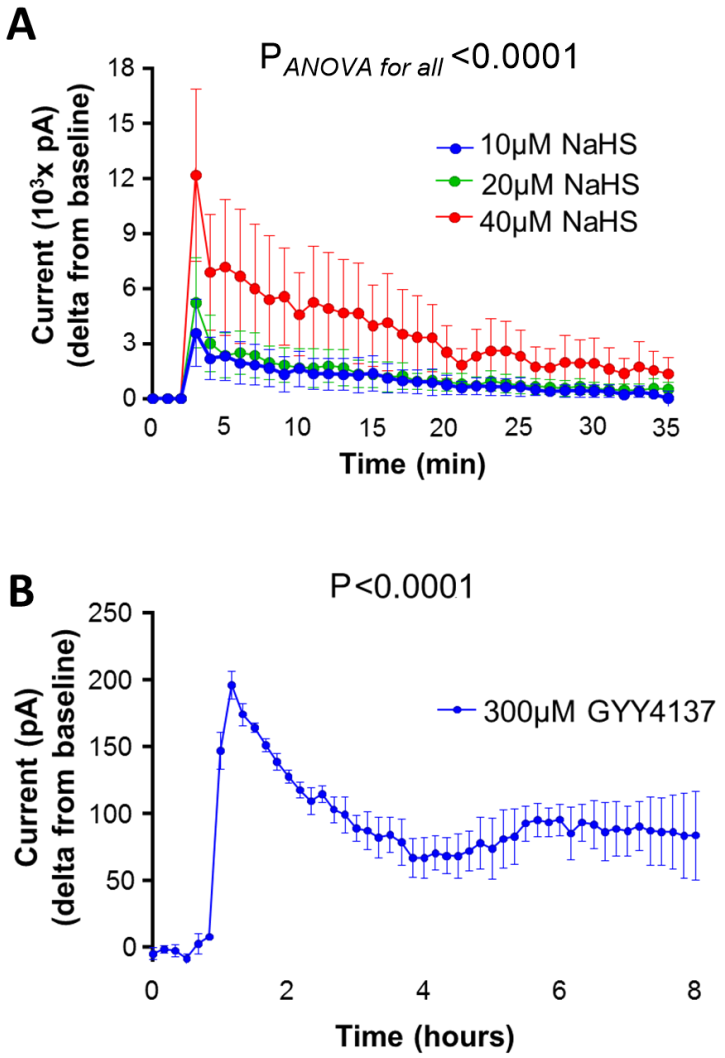


Figure 4.7 H_2S Release from NaHS and GYY4137 in Krebs HEPES Buffer

The release of H_2S from 10, 20, and 40 μM NaHS is shown in Krebs HEPES experimental conditions (**A**, P_{ANOVA}<0.0001 for all curves; adjusted P<0.0001, significant differences between any pair of NaHS curves). The release of H_2S from 300μM GYY4137 is also shown in Krebs HEPES experimental conditions (**B**, P_{ANOVA}<0.0001, significant differences between the average values of GYY4137 versus average values of baseline). Each concentration was performed in triplicates (n=3). H_2S, Hydrogen Sulfide. NaHS, Sodium hydrogen sulfide. Values are presented as mean ± SEM (delta current: difference from average baseline). P-values from unpaired, non-parametric Kruskal-Wallis test followed by Dunn's post hoc correction for multiple comparisons in Panel *A* (not compared across time) and from unpaired, non-parametric Mann-Whitney rank test in Panel *B*.

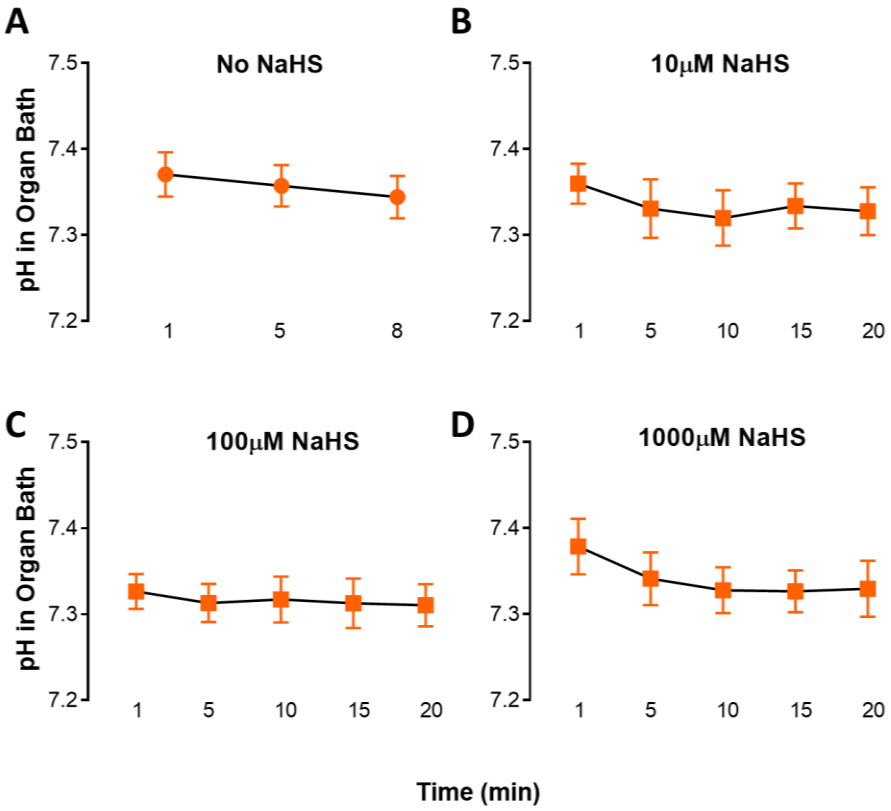


Figure 4.8 Effects of NaHS on pH in Physiological Conditions

Average pH was monitored in oxygenated Tyrode's buffer (**A**) in the organ bath system and with the addition of 10μM NaHS (**B**), 100μM NaHS (**C**), and 1000μM or 1mM NaHS (**D**) in three separate trials (n=3 each). The average pH remained in the buffer region of 7.2-7.5 with the addition of each concentration of NaHS. NaHS, Sodium hydrogen sulfide. pH, Power of hydrogen. Values are presented as mean ± SEM.

4.2.3 Effects of Elevated H_2S on pH in organ bath studies

Given the high concentration of H_2S release by NaHS, we examined whether NaHS altered pH in physiological conditions in order to determine whether changes in redox state were simply a result of differences in pH, NaHS at various concentrations was added to the organ bath set-up without tissue and pH was monitored along with temperature. Of particular interest was differences in pH due to the known dissociation of NaHS into Na^+ and HS^- which are in equilibrium with H_2S, S^{2-}, and H^+ and these H^+ ions could alter the pH if the protons are in an extreme range compared to the range of buffering capacity. No significant difference was observed in pH; pH (and temperature, tight range around 37°C) of the organ bath setup remained approximately between pH 7.3-7.4 (Figure 4.8).

4.3 The Effects of H_2S from NaHS on Myocardial Redox State

4.3.1 The Effects of NaHS on $O_2^{\cdot-}$ and $ONOO^-$ in H9C2 Cardiomyocytes

We asked what are the effects of H_2S under physiological conditions on myocardial redox state. Given the limited availability of healthy human myocardium, we used cells as a model system. We found that cells exposed to 30μM NaHS for 1h did not have altered $O_2^{\cdot-}$ production from NOSs, although there was a non-significant trend for increased coupling of NOSs (Figure 4.9). This suggests importantly that H_2S from NaHS may have more clear effects or improve coupling most clearly in a disease state when NOSs are uncoupled.

4.3.2 NaHS improves NOS Coupling and reduces $ONOO^-$ in Human Myocardium

We then asked what are the effects of H_2S in non-physiological, disease states. To explore this question, we utilized human myocardium *ex vivo* from patients with cardiac disease (undergoing CABG or valve replacement). We exposed human myocardium (strips of tissue) to 30uM NaHS for 1h and found that H_2S from fast releasing donor NaHS increased coupling of myocardial NOSs in humans (Figure 4.9). We further found that H_2S from NaHS reduced myocardial $ONOO^-$ (Figure 4.9). To determine whether H_2S from NaHS affected basal $O_2^{\cdot-}$, we quantified basal $O_2^{\cdot-}$ using lucigenin-enhanced chemiluminescence and found no significant differences (Figure 4.9).

4.3.3 The Effects of NaHS on Human Myocardial $O_2^{\cdot-}$ from Various Sources

We then asked whether the effects of H_2S on human myocardial NOSs was specific or whether H_2S altered basal $O_2^{\cdot-}$ and other enzymatic systems. To further examine H_2S's effects (from NaHS) on other sources of $O_2^{\cdot-}$ in human myocardium after exposure to NaHS, specific inhibitors of NADPH oxidases (VAS2870) and mitochondria

(rotenone, antimycin A, myxothiazol) were used. We found that H_2S from NaHS had no effects on $O_2^{\cdot-}$ from NADPH oxidases or mitochondrial oxidases (Figure 4.10). These finding suggested that H_2S could positively increase coupling of NOSs and reduce $ONOO^-$ without altering $O_2^{\cdot-}$ from other sources, providing insight that H_2S from NaHS could selectively target NOSs.

4.3.4 Mechanisms of NaHS's prevention of NOS Uncoupling in Human Myocardium

To further confirm whether H_2S from NaHS affected basal $O_2^{\cdot-}$, we quantified basal $O_2^{\cdot-}$ using DHE-HPLC. By both methods (lucigenin-enhanced chemiluminescence above and DHE-HPLC, here), myocardial basal $O_2^{\cdot-}$ was unchanged after exposure to 30uM NaHS for 1 hours (Figure 4.11).

Tetrahydrobiopterin (BH_4) is a key cofactor of NOSs and alterations in BH_4 and BH_4:BH_2 are a fundamental mechanism for regulating the coupling status of NOSs. We asked whether H_2S prevented uncoupling of NOSs (and promoted coupling) by altering BH_4 levels in human myocardium *ex vivo*.

We found that human myocardium exposed to NaHS for 1h had no change in BH_4, BH_2, biopterin, or the ratio of BH_4:BH_2 compared to paired human myocardium not exposed to exogenous H_2S (Figure 4.11). This finding suggested H_2S's prevention of NOS uncoupling in human myocardium is via a BH_4-independent mechanism and H_2S may have a more selective method for altering the coupling status of NOSs.

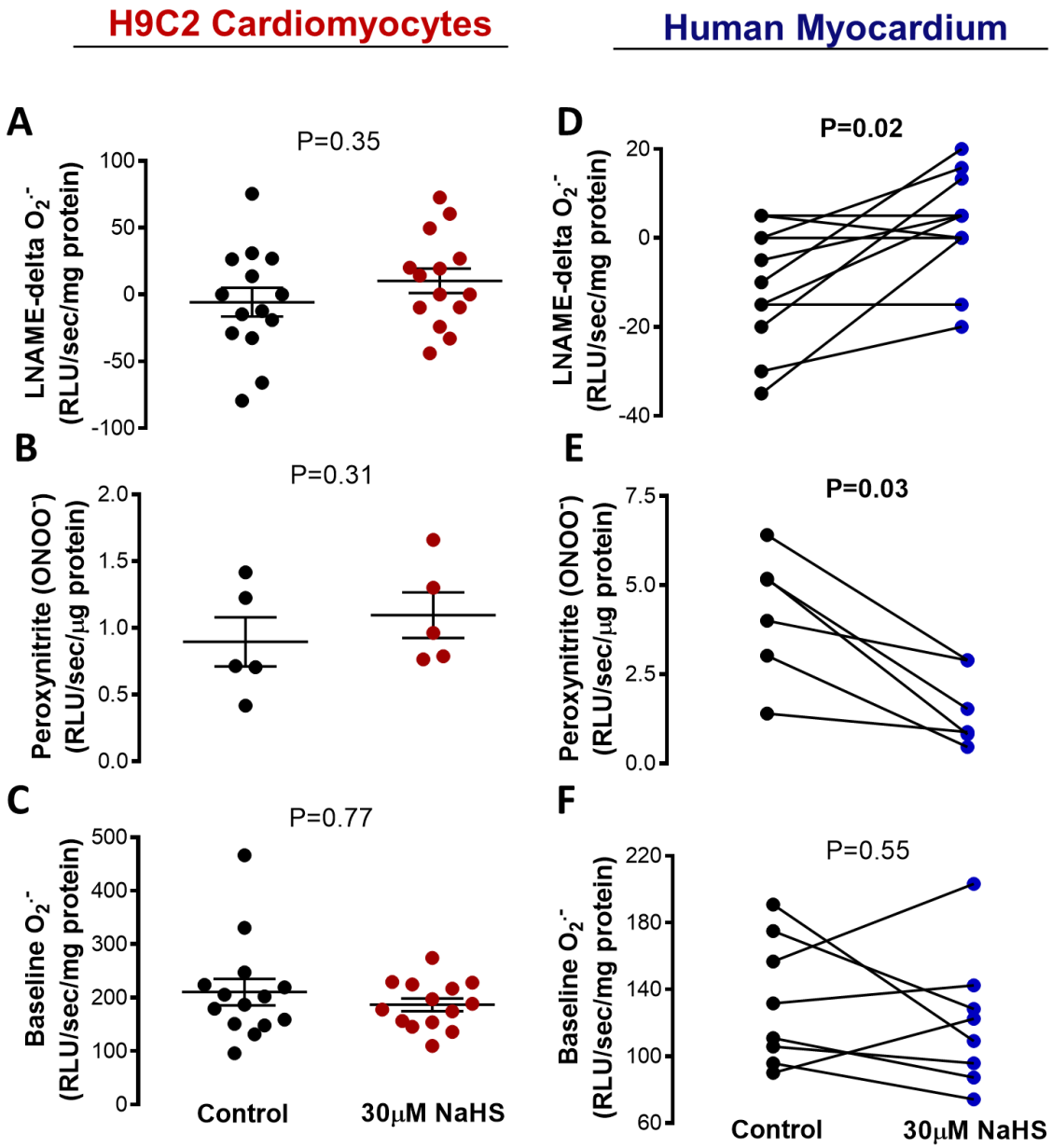


Figure 4.9 Effects of NaHS on $O_2^{\cdot-}$ from NOSs and $ONOO^-$ *in vitro* and *ex vivo*

No differences were observed in $O_2^{\cdot-}$ production from NOSs (**A**, P=0.35, n=14 per group, LNAME for 10 minutes) or $ONOO^-$ (**B**, P=0.31, n=5 per group) or basal $O_2^{\cdot-}$ (**C**, P=0.77, n=14 per group) after H9C2 cardiomyocytes were incubated with 30µM NaHS for 1 hour. Human Myocardium exposed to 30µM NaHS for 1 hour resulted in improvement in NOS coupling as seen by LNAME-delta $O_2^{\cdot-}$ (**D**, P=0.02, n=11 pairs) and significantly reduced $ONOO^-$ (**E**, P=0.03, n=6 pairs) with no change in basal $O_2^{\cdot-}$ (**F**, P=0.55, n=8 pairs). NaHS, Sodium hydrogen sulfide. NOS, Nitric oxide synthase. $O_2^{\cdot-}$, Superoxide. $ONOO^-$, Peroxynitrite. Values are presented as mean ± SEM in Panels *A-C* and as individual pairs (connected by lines) in Panels *D-F*. P-values from unpaired, non-parametric Mann-Whitney rank test in Panels *A-C* and from non-parametric, Wilcoxon matched-pairs signed-rank test in Panels *D-F*. Significant outliers were determined by two-tailed Grubb's test (alpha set at 0.01).

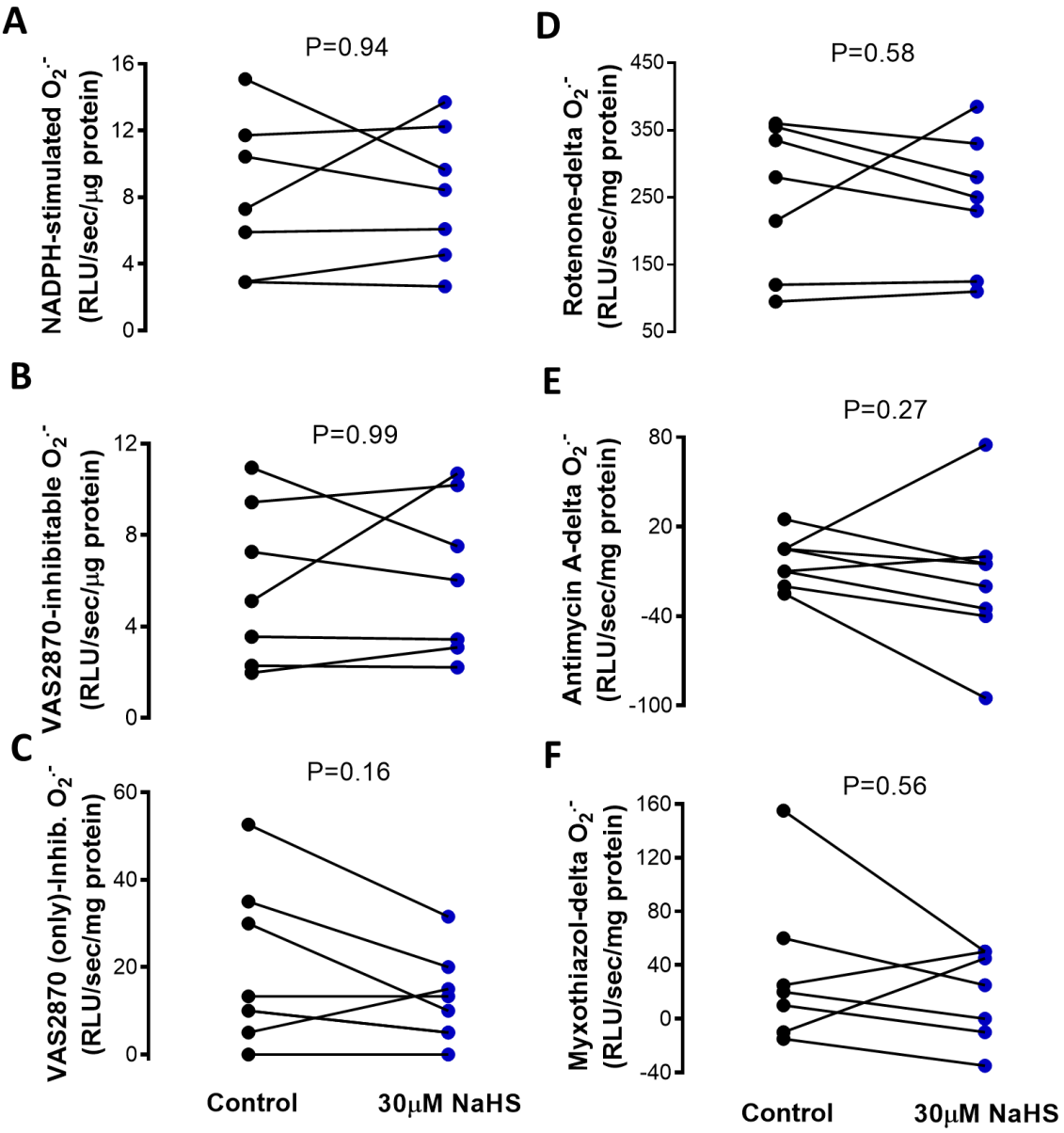


Figure 4.10 Effects of NaHS on NADPH oxidases and Mitochondrial Oxidases

Exposure to fast-releasing donor NaHS (30µM, 1 hour) had no effect on $O_2^{\cdot-}$ from NADPH oxidases as indicated by NADPH-stimulated $O_2^{\cdot-}$ (**A**, P=0.94, n=7 pairs), Vas2870-inhibitable $O_2^{\cdot-}$ after NADPH (**B**, P=0.99, n=7 pairs), and Vas2870-inhibitable $O_2^{\cdot-}$ without NADPH (**C**, P=0.16, n=8 pairs) in human myocardium. Incubation with 30µM NaHS also had no effect on $O_2^{\cdot-}$ from mitochondrial oxidases as seen by no difference in rotenone-inhibited $O_2^{\cdot-}$ (**D**, P=0.58, n=7 pairs, complex I), antimycin A-inhibited $O_2^{\cdot-}$ (**E**, P=0.27, n=8 pairs, complex III) and myxothiazol-inhibited $O_2^{\cdot-}$ (**F**, P=0.56, n=7 pairs, complex III) in human myocardium. NaHS, Sodium hydrogen sulfide. $O_2^{\cdot-}$, Superoxide. Values are presented as individual pairs (connected by lines). P-values from non-parametric, Wilcoxon matched-pairs signed-rank test. Significant outliers were determined by two-tailed Grubb's test (alpha set at 0.01).

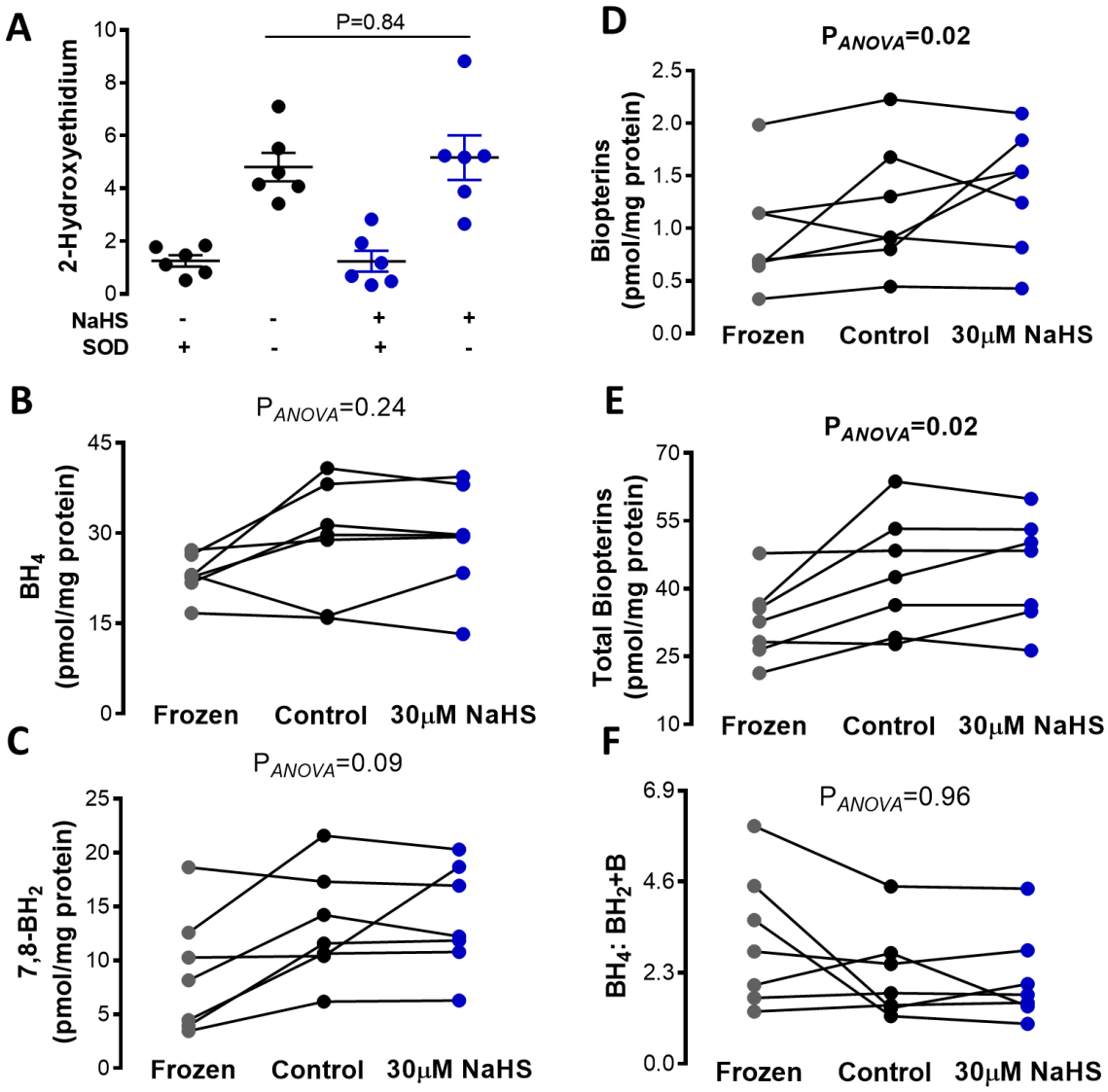


Figure 4.11 Effects of NaHS on Basal $O_2^{\cdot-}$ and Biopterins

Basal $O_2^{\cdot-}$ was measured by DHE-HPLC and H_2S from 30μM NaHS (1h) had no effect on basal $O_2^{\cdot-}$ (**A**, SOD-inhibitable $O_2^{\cdot-}$ with P=0.75, n=6 pairs). To explore whether H_2S mediated coupling effects by modifying biopterins, BH_4, or BH_2, these molecules were measured in paired human RAA samples that were snap-frozen, incubated for 1hour (Control), and incubated for 1 hour with 30μM NaHS. No differences were observed between paired samples exposed to 30μM NaHS (1h) compared to control (1h incubated) for BH_4 (**B**, P_{ANOVA}=0.24, n=7 pairs), BH_2 (**C**, P_{ANOVA}=0.09, n=7 pairs), or Biopterin (**D**, P_{ANOVA}=0.02, significance and adjusted P=0.03 between Snap-frozen and Control groups, n=7 pairs). No significant differences were observed in total biopterins (**E**, P_{ANOVA}=0.02, significance and adjusted P=0.02 between frozen and control groups, n=7 pairs) or the ratio of BH4:BH2 (**F**, P_{ANOVA}=0.96, n=7 pairs) between groups. Incubating myocardium *ex vivo* (1h) compared to frozen tissue increased Biopterin (**D**) and Total Biopterins (**E**) suggesting potentially increased oxidation of BH_4 to B. 7,8-BH_2, Dihydrobiopterin. BH_4, Tetrahydrobiopterin. DHE-HPLC, Dihydroethidium high-performance liquid chromatography. $O_2^{\cdot-}$, Superoxide. SOD, Superoxide Dismutase. Values are presented as mean ± SEM in Panel *A* and as individual pairs (connected by lines) in Panels *B-F*. P-value from non-parametric, Wilcoxon matched-pairs signed-rank test in Panel *A* (difference between control and 30μM NaHS groups in the absence of SOD). P-values from paired, non-parametric Friedman's test followed by Dunn's post hoc correction for multiple comparisons in Panels *B-F* (multiple comparisons were with control only).

4.4 The Effects of H_2S from GYY4137 on Myocardial Redox State

4.4.1 The Effects of GYY4137 on $O_2^{\cdot-}$ and $ONOO^-$ in H9C2 Cardiomyocytes

Given the large kinetic differences in H_2S donors NaHS and GYY4137, we asked what the effects of the slow-releasing donor GYY4137 under physiological conditions are on myocardial redox state. To explore this question, we examined the effects of H_2S from GYY4137 on $O_2^{\cdot-}$ from H9C2 cardiomyocytes given the limited availability of healthy human myocardium. We found that there was no clear effect of GYY4137 on the coupling status of NOSs or on $ONOO^-$ in H9C2 cardiomyocytes (Figure 4.12).

4.4.2 GYY4137 increases uncoupling of NOSs in Human Myocardium

We then asked what are the effects of H_2S in non-physiological, disease states. To explore this question, we utilized human myocardium *ex vivo* from patients with cardiac disease (undergoing CABG or valve replacement). We exposed human myocardium (strips of tissue) to 300uM GYY4137 for 2h. We found that human myocardium exposed to GYY4137 for two hours led to uncoupling of myocardial NOSs, suggesting that slow and longer duration of H_2S exposure may lead to detrimental effects (Figure 4.12). The control samples had similar range of variability as the control of the 30uM NaHS. This uncoupling is accompanied by no change in ONOO- or basal $O_2^{\cdot-}$ (Figure 4.12). There are currently no known mechanisms to explore these effects.

4.4.3 The Effects of GYY4137 on Human Myocardial $O_2^{\cdot-}$ from Various Sources

We then asked whether the effects of H_2S from GYY4137 on human myocardial NOSs was specific or whether H_2S altered basal $O_2^{\cdot-}$ and other enzymatic systems. To further examine H_2S's effects on other sources of $O_2^{\cdot-}$ in myocardium after exposure to GYY4137, specific inhibitors of NADPH oxidases and mitochondria were used.

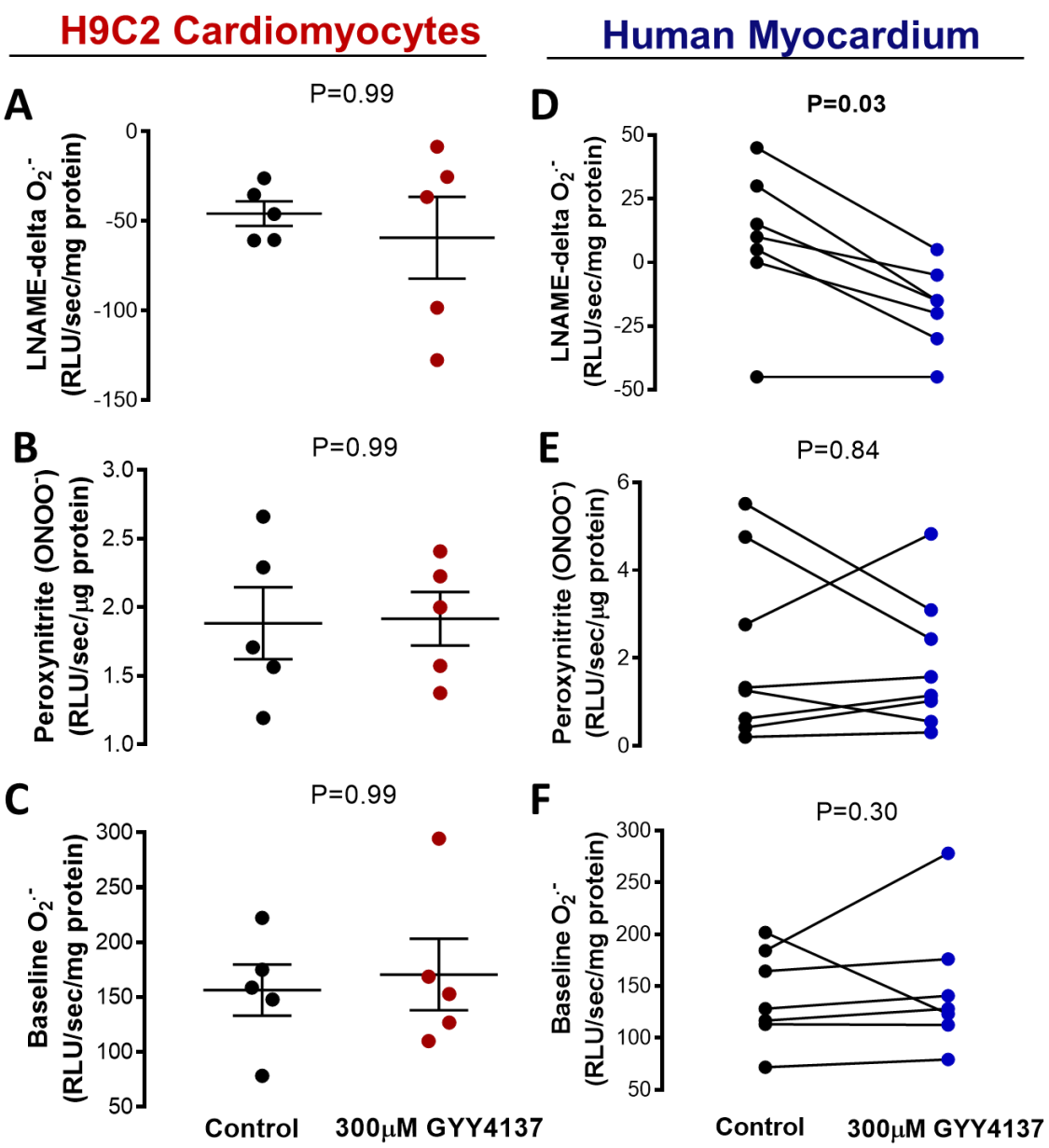


Figure 4.12 Effects of GYY4137 on $O_2^{\cdot-}$ from NOSs and $ONOO^-$ *in vitro* and *ex vivo*

To examine whether slow-releasing donor GYY4137 altered $O_2^{\cdot-}$ production from NOSs or $ONOO^-$ under physiological conditions, H9C2 cardiomyocytes were incubated in the presence or absence of 300µM GYY4137 for 2 hours. There was no difference in $O_2^{\cdot-}$ production from NOSs after incubation with GYY4137 as seen by LNAME-delta $O_2^{\cdot-}$ (**A**, P=0.99, n=5 per group, after incubation with LNAME for 30 minutes) in H9C2 cardiomyocytes. 300µM GYY4137 also had no effect on $ONOO^-$ (**B**, P=0.99, n=5 per group) or basal $O_2^{\cdot-}$ (**C**, P=0.99, n=5 per group) in H9C2 cardiomyocytes. To examine whether GYY4137 altered $O_2^{\cdot-}$ production from NOSs or $ONOO^-$ in disease states, human myocardium was incubated in the presence or absence of 300µM GYY4137 for 2 hours. Exposure to slow-releasing donor GYY4137 resulted in NOS uncoupling as seen by LNAME-delta $O_2^{\cdot-}$ (**D**, P=0.03, n=7 pairs, after incubation with LNAME for 30 minutes) in human myocardium. 300µM GYY4137 had no effect on $ONOO^-$ (**E**, P=0.84, n=8 pairs) or basal $O_2^{\cdot-}$ (**F**, P=0.30, n=7 pairs) in human myocardium. NOS, Nitric oxide synthase. $O_2^{\cdot-}$, Superoxide. $ONOO^-$, Peroxynitrite. Values are presented as mean ± SEM in Panels *A-C* and as individual pairs (connected by lines) in Panels *D-F*. P-values from unpaired, non-parametric Mann-Whitney rank test in Panels *A-C* and from non-parametric, Wilcoxon matched-pairs signed-rank test in Panels *D-F*.

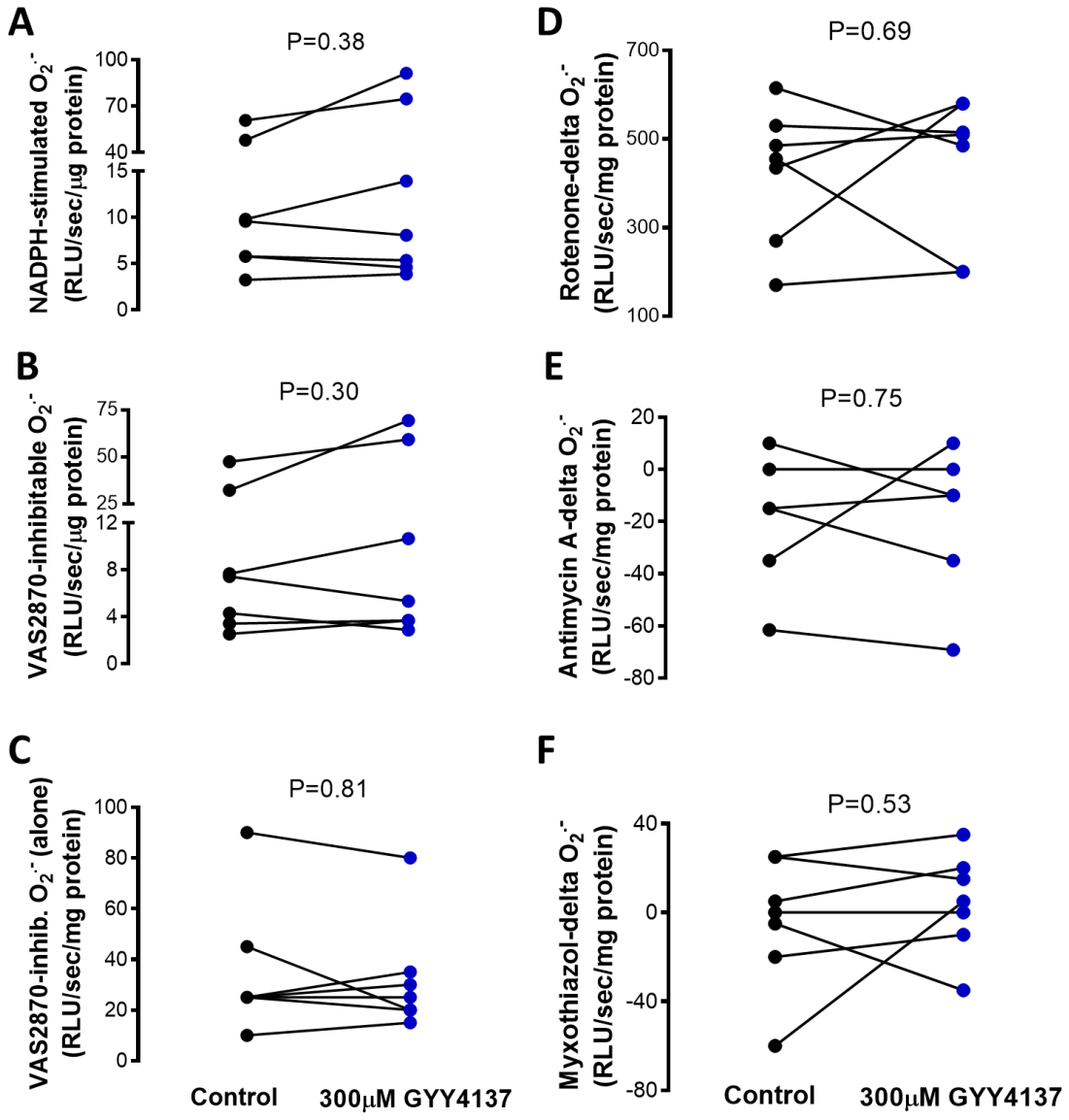


Figure 4.13 Effects of GYY4137 on NADPH Oxidases and Mitochondrial Oxidases

Exposure to slow-releasing donor GYY4137 (300µM, 2 hours) had no effect on $O_2^{\cdot-}$ from NADPH oxidases as indicated by no change in NADPH-stimulated $O_2^{\cdot-}$ (**A**, P=0.38, n=7 pairs), Vas2870-inhibitable $O_2^{\cdot-}$ after NADPH stimulation (**B**, P=0.30, n=7 pairs), and Vas2870-inhibitable $O_2^{\cdot-}$ without NADPH stimulation (**C**, P=0.81, n=7 pairs) in human myocardium. Incubation with GYY4137 also had no effect on $O_2^{\cdot-}$ from mitochondrial oxidases as seen by rotenone-inhibited $O_2^{\cdot-}$ (**D**, P=0.69, n=7 pairs, complex I), antimycin A-inhibited $O_2^{\cdot-}$ (**E**, P=0.75, n=6 pairs, complex III) and myxothiazol-inhibited $O_2^{\cdot-}$ (**F**, P=0.53, n=7 pairs, complex III) in human myocardium. $O_2^{\cdot-}$, Superoxide. Values are presented as individual pairs (connected by lines). P-values from non-parametric, Wilcoxon matched-pairs signed-rank test. Significant outliers were determined by two-tailed Grubb's test (alpha set at 0.01).

We found that H_2S from GYY4137 had no effects on $O_2^{\cdot-}$ from NADPH oxidases or mitochondrial oxidases (Figure 4.13). These findings suggest that GYY4137's effects on NOSs are specific and not attributed to or affecting other myocardial sources of $O_2^{\cdot-}$.

Chapter 5 Bidirectional Effects of CSE and Myocardial Oxidative Stress

A comprehensive examination of CSE, CBS, and MST gene expression in the heart and its relationship to patient demographics, cardiac disease, and myocardial redox state is lacking. Moreover, studies have suggested CSE expression may be redox-sensitive (under the transcriptional regulation of redox-sensitive SP1)[202-204] and several studies have suggested that CBS may be redox-sensitive particularly due to its redox-sensitive cofactor heme[205-207] but it is not clear whether CSE and CBS expression are indeed altered in models of oxidative stress. We hypothesize that the expression of myocardial CSE, CBS, and MST genes are related to cardiac disease (e.g. hypertension, NYHA class) and regulated by myocardial redox state. The aims of this study were to examine

I. The correlations between CSE, CBS, MST expression and patient demographics and myocardial redox state
II. Whether the CYBA SNP locus can be used as a model of myocardial oxidative stress in humans
III. Whether the expression of myocardial CSE, CBS, and MST gene in reduced in conditions of oxidative stress

5.1 CSE, CBS, and MST Gene Expression and Patient Demographics

The demographics of the study population are shown below (Table 5.1). To investigate whether the expression of myocardial CSE, CBS, and MST genes was correlated with cardiovascular disease in humans, we first quantified the gene expression of these enzymes in human myocardium.

Table 5.1 Demographics Characteristics of Study Participants in Chapter 5

Participant Demographic Characteristics		
	Study Arm 1 Clinical Associations	**Study Arm 2** *CYBA* SNPs
Demographics		
Participants (n)	**96**	**501**
Age (years)	**65.0±1.1**	**66.3±0.5**
Male gender (%)	**89.6**	**80.9**
Smoking (active/ex) (%)	**58.9**	**67.8**
Hypertension (%)	**75.5**	**72.8**
Hypercholesterolemia (%)	**79.2**	**67.2**
Diabetes mellitus (%)	**27.1**	**26.7**
HOMA-IR	**3.1±0.6**	**3.8±0.4**
BNP (pg/mL)	**152.2±42.9**	**153.6±19.0**
BMI (kg/m^2)	**28.6±0.4**	**28.1±0.2**
Waist circumference (cm)	**99.0±1.4**	**99.0±0.8**
Waist:Hip ratio	**0.98±0.01**	**1.01±0.01**
Medications		
ACEi/ARBs (%)	**49.0/11.5**	**50.3/12.4**
β-blockers (%)	**71.9**	**69.3**
Aspirin/Clopidogrel (%)	**89.6/24.0**	**80.4/28.0**
Statins (%)	**88.5**	**80.2**
CCBs (%)	**21.9**	**27.7**
Diuretics (%)	**13.5**	**24.0**
Insulin/Oral hypoglycaemic (%)	**10.4/15.6**	**6.0/20.0**
Nitrates (%)	**36.5**	**40.3**

ACEi, Angiotensin Converting Enzyme inhibitors. ARB, Angiotensin Receptor Blockers. BMI, Body Mass Index. BNP, B-Natriuretic Peptide. CCB, Calcium Channel Blockers. HOMA-IR, Homeostatic Model Assessment of Insulin Resistance. Values are presented as mean ± SEM.

Assessment of the relative gene expression of enzymes CSE, CBS, and MST in the human myocardium revealed all three enzymes are expressed in the human myocardium and we found that MST expression was highest in this patient population (Figure 5.1). We further examined whether there was a difference in expression of myocardial CSE, CBS, or MST in females compared to males or by age. We found there was no correlation between gender or age and myocardial CSE, CBS, or MST expression (Figure 5.1). We also examined whether myocardial CSE, CBS, or MST expression was correlated with days in the hospital. No significant correlations were observed between myocardial CSE, CBS, or MST and days in hospital (Figure 5.1).

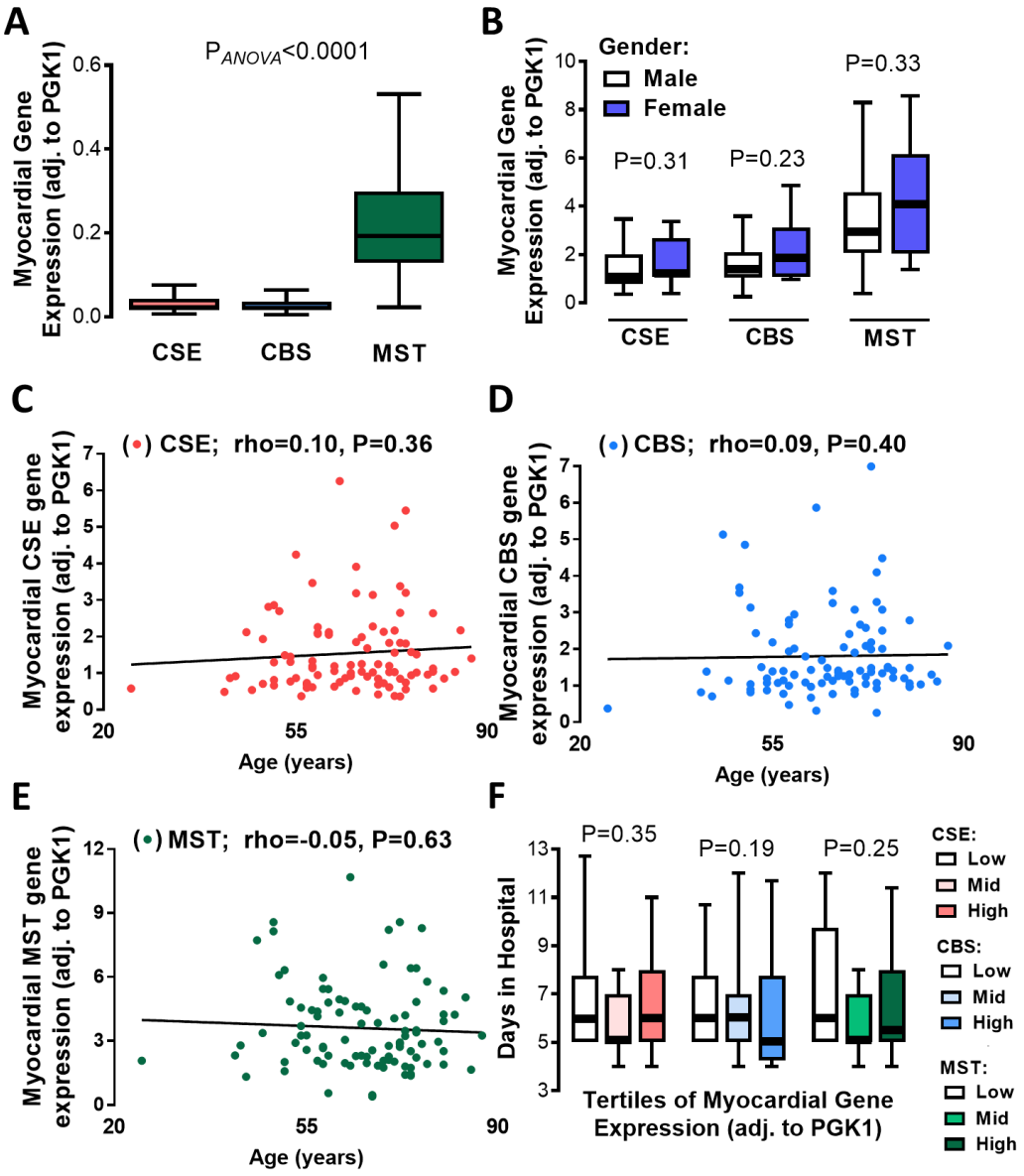


Figure 5.1 Myocardial CSE, CBS, and MST Gene Expression & Demographics

Myocardial MST gene expression is highest compared to myocardial CSE and CBS gene expression in our cohort (**A**, P_{ANOVA}<0.0001; adjusted for multiple comparisons, P=0.51 for CSE vs CBS, P<0.0001 for CSE vs MST, P<0.0001 CBS vs MST; n=96 individuals). No significant differences were observed in myocardial CSE, CBS, and MST expression between males and females (**B**, P=0.31 for CSE, P=0.23 for CBS, P=0.33 for MST; n=86 males, 10 females; comparison among females likely underpowered). There was also no significant association between age and expression of CSE, CBS, or MST (**C-E**, P_{ANOVA}=0.15 for CSE, P_{ANOVA}=0.39 for CBS, P_{ANOVA}=0.78 for MST; n=32 per tertile). Days in hospital were not correlated with myocardial CSE, CBS, or MST gene expression (**F**, P_{ANOVA}=0.35 for CSE, P_{ANOVA}=0.19 for CBS, P_{ANOVA}=0.25 for MST; n=32 per tertile). CSE, Cystathionine γ-Lyase. CBS, Cystathionine β-Synthase. MST, 3-Mercaptopyruvate Sulfurtransferase. Values are presented as median (25^{th} to 75^{th} percentile) and whiskers (Tukey) in Panels *A-B*; values are presented as median (25^{th} to 75^{th} percentile) and whiskers (10^{th} to 90^{th} percentile) in Panel *F*. P-values from paired, non-parametric Friedman's test followed by Dunn's post hoc correction for multiple comparisons in Panel *A*, unpaired, non-parametric Mann-Whitney rank test in Panel *B*, and unpaired, non-parametric Kruskal-Wallis test followed by Dunn's post hoc correction for multiple comparisons in Panel *F*. Correlation assessed by bivariate analysis is presented with non-parametric Spearman's correlation coefficient ρ(rho) estimation in Panels *C-E*.

5.1.1 Metabolic Profile and Hypertension

Given the increasing importance of obesity in cardiovascular disease, we next asked whether obesity and related metabolic profiles of individuals was related to myocardial CSE, CBS, or MST gene expression.

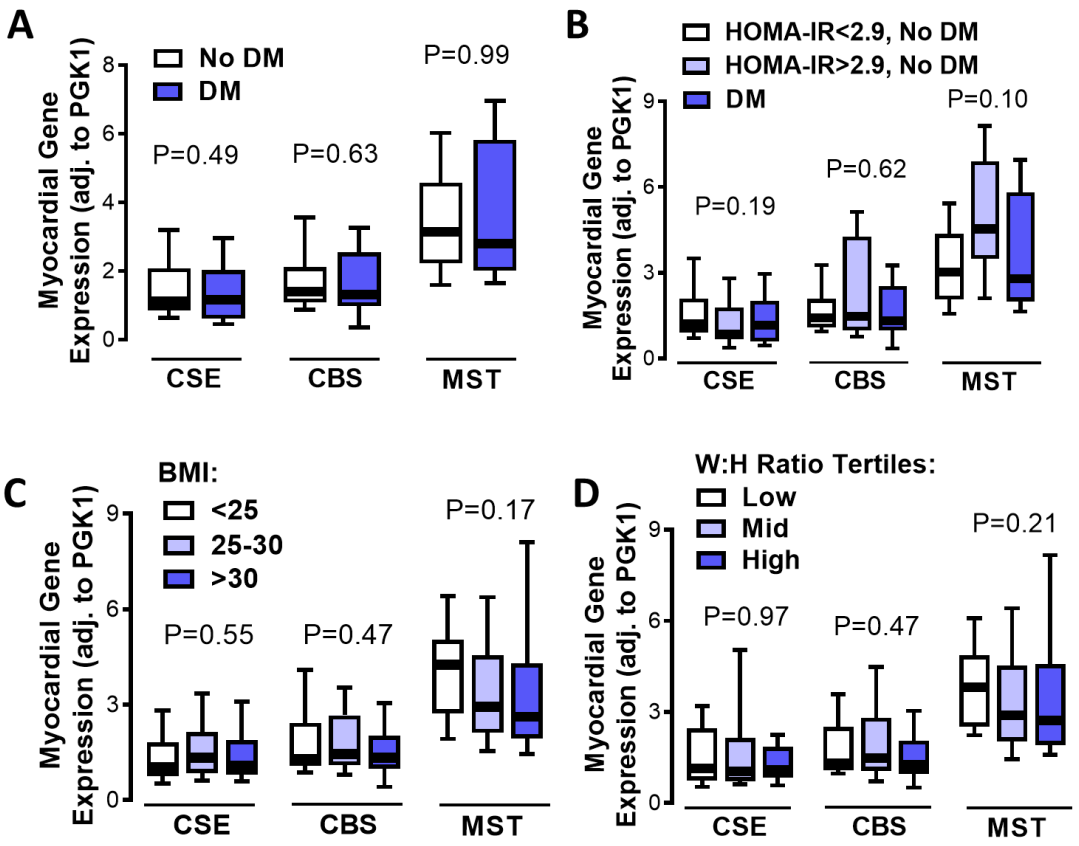


Figure 5.2 Myocardial CSE, CBS, and MST Gene Expression & Metabolic Profile

Expression of myocardial CSE, CBS, and MST in individuals with or without diabetes (**A**, P=0.49 for CSE, P=0.63 for CBS, P=0.99 for MST; n=70 no diabetes, n=26 with diabetes). IR status is not correlated with myocardial CSE, CBS, and MST gene expression (**B**, P_{ANOVA}=0.19 for CSE, P_{ANOVA}=0.62 for CBS, P_{ANOVA}=0.10 for MST; n=58 No DM, HOMA-IR<2.9, n=9 No DM, HOMA-IR>2.9, n=26 DM). There is no correlation with BMI and myocardial CSE, CBS, or MST expression, although a trend may be seen for reduced MST expression and BMI>30 (**C**, P_{ANOVA}=0.55 for CSE, P_{ANOVA}=0.47 for CBS, P_{ANOVA}=0.17 for MST; n=19 individuals with BMI<25, n=47 individuals with BMI between 25-40, n=30 individuals with BMI>30). There is no correlation with waist to hip ratio tertiles and myocardial CSE, CBS, or MST expression, although a trend is observed for reduced MST expression and high waist to hip ratios (**D**, P_{ANOVA}=0.97 for CSE, P_{ANOVA}=0.47 for CBS, P_{ANOVA}=0.21 for MST; n=29-30 individuals per tertile). BMI, Body Mass Index. CSE, Cystathionine γ-Lyase. CBS, Cystathionine β-Synthase. DM, Diabetes Mellitus. HOMA-IR, Homeostatic model assessment of insulin resistance. MST, 3-Mercaptopyruvate Sulfurtransferase. W:H Ratio, Waist to hip ratio. Values are presented as median (25^{th} to 75^{th} percentile) and whiskers (10^{th} to 90^{th} percentile). P-values from unpaired, non-parametric Mann-Whitney rank test in Panel *A* and from unpaired, non-parametric Kruskal-Wallis test followed by Dunn's post hoc correction for multiple comparisons in Panel *B-D*.

We found that individuals with diabetes mellitus had similar levels of myocardial CSE, CBS, and MST expression compared to individuals without diabetes (Figure 5.2). However, a clear trend was observed with lower myocardial MST expression in individuals with diabetes compared to individuals with no diabetes but HOMA-IR>2.9, but there were no significant correlations observed between insulin resistance status overall and myocardial CSE, CBS, or MST expression (Figure 5.2). To examine an underlying relationship between obesity and the expression of these enzymes, we examined individuals' body mass index (BMI; less than 25, 25-30 and greater than 30) and their waist-to-hip ratio (in tertiles) and found no relationship between BMI or waist-to-hip ratio and myocardial CSE, CBS, or MST expression (Figure 5.2). However, given the strong trend observed between reduced MST expression with increasing tertiles of BMI, we examined the relationship between MST expression and BMI as a continuous variable; in this further analysis, we found that myocardial MST expression was inversely correlated with BMI in our cohort with a Spearman correlation coefficient of -0.216 (Table 5.2). Taken together, these findings suggest a potential relationship between reduced myocardial MST in obesity.

With the guidelines and classification of hypertension prior to 2017, we further examined alterations in myocardial CSE, CBS, and MST expression in individuals with hypertension and hypercholesterolemia. We found that individuals with hypertension had significantly elevated myocardial MST expression but no differences in myocardial CSE or CBS expressions compared to individuals with no hypertension (Figure 5.3). Individuals with hypercholesterolemia had significantly reduced expression of myocardial CBS and a trend for reduced myocardial CSE expression but no differences in myocardial MST expression compared to individuals without hypercholesterolemia (Figure 5.3).

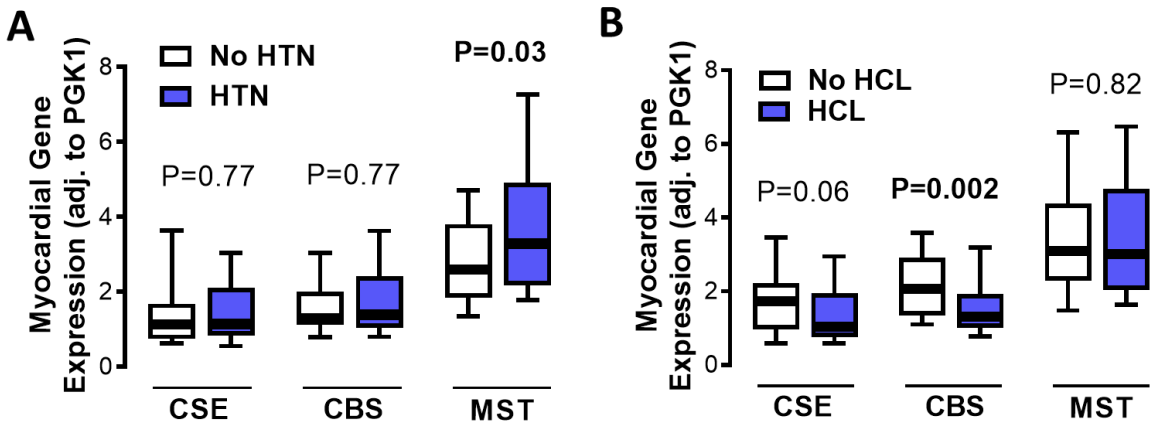


Figure 5.3 Myocardial CSE, CBS, and MST, Hypertension, & Hypercholesterolemia

Individuals with hypertension had increased myocardial MST expression with no differences observed in myocardial CSE and CBS expression compared to individuals without hypertension (**A**, P=0.77 for CSE, P=0.77 for CBS, P=0.03 for MST; n=23 no hypertension, n=73 with hypertension). Individuals with HCL had reduced myocardial CBS expression, a trend for reduced CSE expression, and no differences observed in myocardial MST expression compared to individuals without HCL (**B**, P=0.06 for CSE, P=0.002 for CBS, P=0.82 for MST; n=20 no HCL, n=76 with HCL). CSE, Cystathionine γ-Lyase. CBS, Cystathionine β-Synthase. HCL, Hypercholesterolemia. HTN, Hypertension. MST, 3-Mercaptopyruvate Sulfurtransferase. Values are presented as median (25th to 75th percentile) and whiskers (10th to 90th percentile). P-values from unpaired, non-parametric Mann-Whitney rank test.

These findings, while not excluding the potential role for CSE and CBS activity in hypertension, point towards a closer relationship between myocardial MST expression and hypertension than myocardial CSE or CBS expression and hypertension in individuals. These findings further suggest an additional relationship between myocardial CBS expression and hypercholesterolemia.

5.1.2 Cardiac Disease and Left Ventricular Function

We also asked whether there was a relationship between myocardial CSE, CBS, and MST gene expression and heart failure to examine whether these enzymes may be part of the autocrine/endogenous regulatory mechanisms regulating heart function. We first asked whether individuals belonging to different NYHA (heart failure) classes had differences in CSE, CBS, and MST expression. Our study was underpowered to examine NYHA Class 0 and 4 but between Class 1-3, we found no differences in myocardial gene expression of CSE, CBS or MST (Figure 5.4).

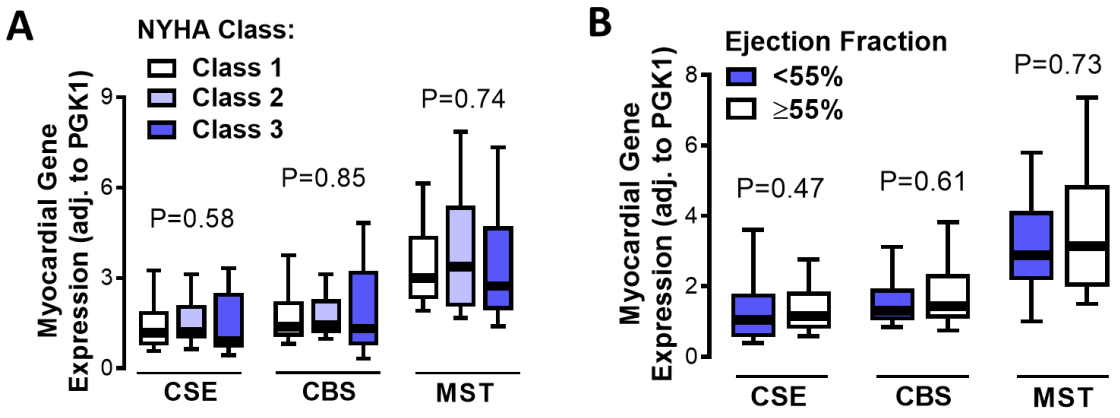


Figure 5.4 Myocardial CSE, CBS, and MST Gene Expression and Heart Failure

Individuals in NYHA Class 1-3 have similar myocardial gene expression of CSE, CBS, and MST (**A**, P_{ANOVA}=0.58 for CSE, P_{ANOVA}=0.85 for CBS, P_{ANOVA}=0.74 for MST; n=38 for NYHA Class 1, n= 41 for NYHA Class 2, n=12 for NYHA Class 3). NYHA Class 0 and 4 are underpowered (n=2 individuals in Class 0 and n=2 individuals in Class 4) and therefore not graphed. No differences were observed in CSE, CBS, or MST expression in the heart between individuals with ejection fraction <55% and those with ejection faction ≥55% (**B**, P=0.47 for CSE, P=0.61 for CBS, P=0.73 for MST; n=13 EF<55%, n=44 EF≥55%). CSE, Cystathionine γ-Lyase. CBS, Cystathionine β-Synthase. EF, Ejection Fraction. LA, Left Atrium. LV, Left Ventricle. MST, 3-Mercaptopyruvate Sulfurtransferase. Values are presented as median (25^{th} to 75^{th} percentile) and whiskers (10^{th} to 90^{th} percentile). P-values from unpaired, non-parametric Kruskal-Wallis test followed by Dunn's post hoc correction for multiple comparisons in Panel *A* and from unpaired, non-parametric Mann-Whitney rank test in Panel *B*.

We then asked whether myocardial function was associated with myocardial CSE, CBS, or MST expression. We found that individuals with left ventricular ejection fraction lower than 55% had similar expression of myocardial CSE, CBS, or MST compared to individuals with ejection fraction greater than or equal to 55% (Figure 5.4).

To further explore a possible relationship between heart function and gene expression, we used previously quantified parameters of the left atrium and left ventricle (by echocardiography) to also examine whether left atrial size and left ventricular size, mass, and volume/function were related to myocardial CSE, CBS, and MST expression. We found that individuals with the highest expression of MST had a significantly shorter left atrial diameter compared to individuals with middle tertile expression of MST, which may be due to statistical chance given multiple comparisons and that significance was not observed across all tertiles (Figure 5.5). CSE and CBS expression were unrelated to left

atrial diameter (Figure 5.5). Furthermore, we found that a trend for increased myocardial MST expression and reduced left ventricular mass, which was a significant inverse correlation in analysis with left ventricular mass as a continuous variable (a Spearman correlation coefficient of -0.273; Figure 5.5, Table 5.2).

To more closely characterize the left ventricle in terms of both size and function, we examined whether the was an association between myocardial CSE, CBS or MST expression and left ventricular end diastolic diameter (LVEDD), left ventricular end systolic diameter (LVESD), left ventricular end diastolic volume (LVEDV), and left ventricular end systolic volume (LVESV). While no clear differences were observed in myocardial CSE, CBS, or MST expression (tertiles) with these four parameters, a trend was observed for increased myocardial MST and CSE expression with reduced LVEDV and LVESV, respectively (Figure 5.5).

Furthermore, with LVEDV as a continuous variable, we found a significant inverse relationship between myocardial MST expression and LVEDV with a Spearman correlation coefficient of -0.396 (Table 5.2). Taken together, these findings uniquely suggest a relationship between myocardial MST and left atrial size and left ventricular mass and function with a potential role for CSE in left ventricular function as well. These findings highlight the difference in roles of CSE, CBS, and MST expression in the individual with heart failure and suggest that all three enzymes should not be considered to have the exact same role but distinct relationships with heart function.

5.1.3 Systemic Oxidative Stress and Inflammation

To examine the relationship between myocardial CSE, CBS, and MST and systemic markers of oxidative stress and inflammation, we asked whether myocardial CSE, CBS, and MST expression were correlated with malondialdehyde (MDA), high sensitivity C-reactive protein (hsCRP) or plasma B-natriuretic peptide.

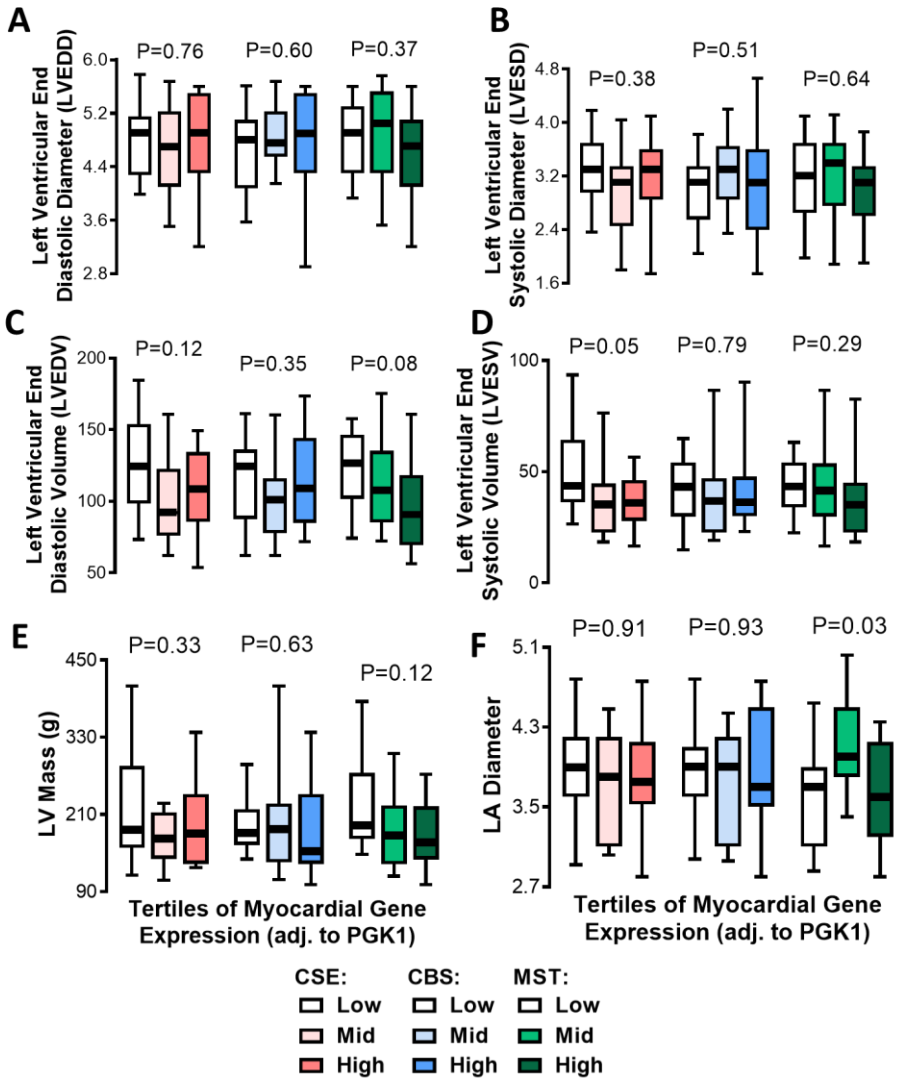


Figure 5.5 Myocardial CSE, CBS, and MST Expression and LV Function

LVEDD was not correlated with myocardial CSE, CBS, or MST gene expression (**A**, P_{ANOVA}=0.76 for CSE, P_{ANOVA}=0.60 for CBS, P_{ANOVA}=0.37 for MST; n=18-19 per tertile). LVESD was also not correlated with Myocardial CSE, CBS, or MST gene expression (**B**, P_{ANOVA}=0.38 for CSE, P_{ANOVA}=0.51 for CBS, P_{ANOVA}=0.64 for MST; n=17 per tertile). A strong trend is observed between MST gene expression and reduced LVEDV while no clear correlation is seen between myocardial CSE/CBS gene expression and LVEDV (**C**, P_{ANOVA}=0.12 for CSE, P_{ANOVA}=0.35 for CBS, P_{ANOVA}=0.08 for MST; n=15-16 per tertile). A strong trend is observed between CSE gene expression and reduced LVESV while no clear correlation is seen between myocardial CBS/MST gene expression and LVESV (**D**, P_{ANOVA}=0.05 for CSE, P_{ANOVA}=0.79 for CBS, P_{ANOVA}=0.29 for MST; n=15 per tertile). LV Mass was not correlated with CSE, CBS, or MST gene expression but a trend with MST expression was observed (**E**, P_{ANOVA}=0.33 for CSE, P_{ANOVA}=0.63 for CBS, P_{ANOVA}=0.12 for MST; n=19-20 per tertile). LA diameter was reduced in individuals with high myocardial MST gene expression compared to those with middle tertile of expression; LA diameter was not correlated with myocardial CSE and CBS gene expression (**F**, P_{ANOVA}=0.91 for CSE, P_{ANOVA}=0.93 for CBS, P_{ANOVA}=0.03 for MST; n=15-16 per tertile). CSE, Cystathionine γ-Lyase. CBS, Cystathionine β-Synthase. LA, Left Atrium. LV, Left Ventricle. LVEDD, Left Ventricular End Diastolic Diameter. LVEDV, Left Ventricular End Diastolic Volume. LVESD, Left Ventricular End Systolic Diameter. LVESV, Left Ventricular End Systolic Volume. MST, 3-Mercaptopyruvate Sulfurtransferase. Values are presented as median (25^{th} to 75^{th} percentile) and whiskers (10^{th} to 90^{th} percentile). P-values from unpaired, non-parametric Kruskal-Wallis test followed by Dunn's post hoc correction for multiple comparisons.

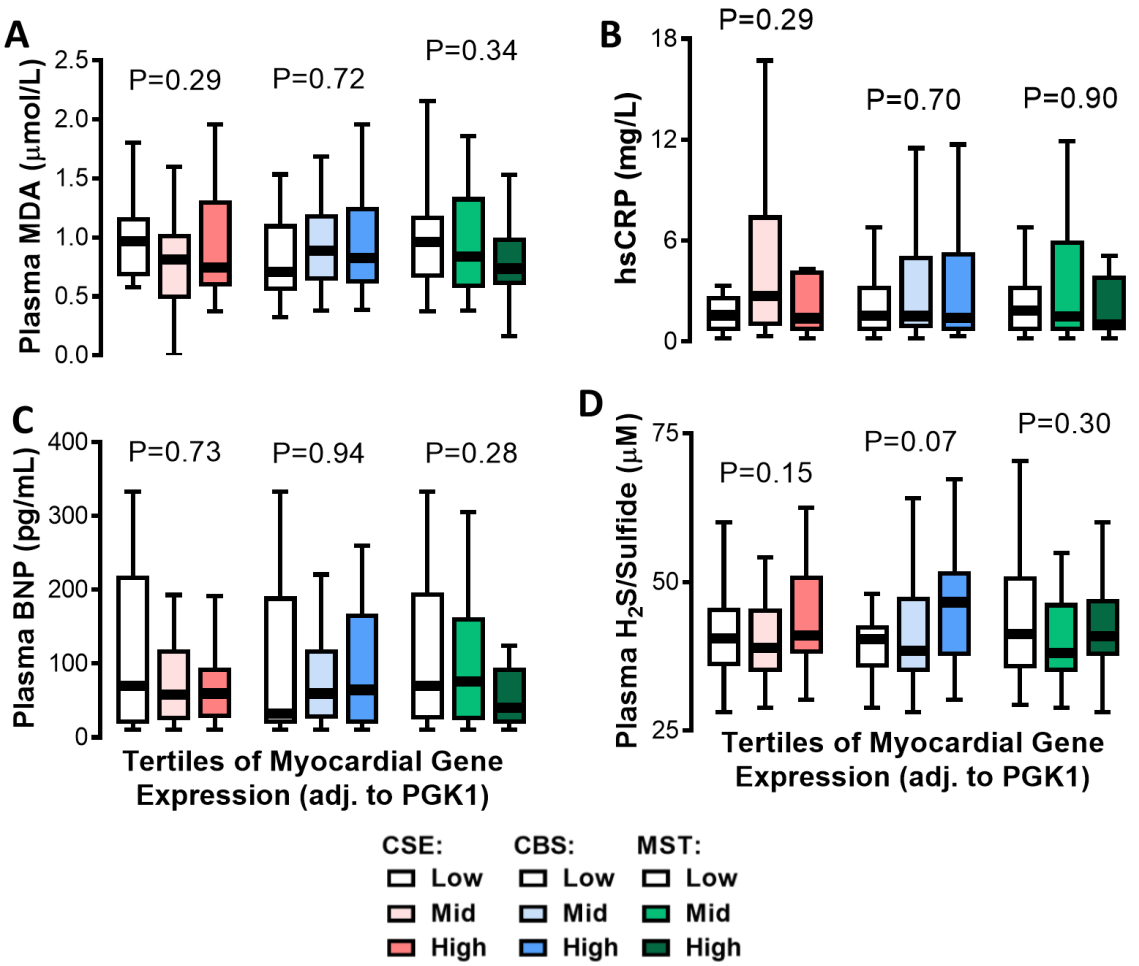


Figure 5.6 Myocardial CSE, CBS, and MST & Systemic Markers of Stress

We found there was also no correlation between endogenous myocardial CSE, CBS, or MST gene expression and plasma MDA (**A**, P_{ANOVA}=0.29 for CSE, P_{ANOVA}=0.72 for CBS, P_{ANOVA}=0.34 for MST; n=24-25 per tertile). There was also no correlation between hsCRP and myocardial expression of CSE, CBS, or MST genes (**B**, P_{ANOVA}=0.29 for CSE, P_{ANOVA}=0.70 for CBS, P_{ANOVA}=0.90 for MST; n=30-31 per tertile) or BNP and myocardial expression of CSE, CBS, or MST genes (**C**, P_{ANOVA}=0.73 for CSE, P_{ANOVA}=0.94 for CBS, P_{ANOVA}=0.28 for MST; n=28-29 per tertile). There was also no correlation between CSE, CBS, or MST gene expression in the heart and circulating H_2S/Sulfide levels (**D**, P_{ANOVA}=0.15 for CSE, P_{ANOVA}=0.07 for CBS, and P_{ANOVA}=0.30 for MST; n=31-32 per tertile). BNP, B-Natriuretic Peptide. CSE, Cystathionine γ-Lyase. CBS, Cystathionine β-Synthase. H_2S, Hydrogen Sulfide. hsCRP, High Sensitivity C-reactive protein. MDA, Malondialdehyde. MST, 3-Mercaptopyruvate Sulfurtransferase. Values are presented as median (25^{th} to 75^{th} percentile) and whiskers (10^{th} to 90^{th} percentile) in Panel *A* and as median (25^{th} to 75^{th} percentile) and whiskers (Tukey) in Panels *B-D*. P-values from unpaired, non-parametric Kruskal-Wallis test followed by Dunn's post hoc correction for multiple comparisons.

We found that there was no correlation between the myocardial expression of these enzymes and plasma MDA, hsCRP or plasma BNP (Figure 5.6). These findings provide further evidence that the relationship between these enzymes expression and oxidative stress and inflammation may be local rather than systemic.

Given the importance of these enzymes CSE, CBS, and MST in generating by-product H_2S/Sulfide, we also examined whether increased expression of myocardial CSE, CBS, and MST was correlated with increased plasma H_2S/Sulfide levels. While a strong trend was observed between increased myocardial CBS expression and circulating H_2S/Sulfide levels, there were no significant correlations observed between the expression of these enzymes and H_2S. This finding suggests that the relationship between these enzymes and H_2S may be local, and alterations in gene expression are not likely mediated by systemic changes in circulating H_2S or vice versa (Figure 5.6). Taken together, these findings suggest a possible importance of myocardial CSE, CBS, and MST gene expression in local, myocardial processes rather than a relationship with systemic phenomena.

5.2 CSE, CBS, and MST Gene Expression and Myocardial Redox State

After examining the relationship between myocardial CSE, CBS, and MST expression and the demographics of our patients, we examined whether there was a relationship between CSE, CBS, or MST expression and myocardial redox state.

5.2.1 CSE and Myocardial Redox State

We first examined associations between the expression of myocardial CSE and basal $O_2^{\cdot-}$ production as well as $O_2^{\cdot-}$ from NADPH oxidases, NOSs, and mitochondria in the heart. While myocardial CSE gene expression (in tertiles) was not correlated with basal, NADPH-stimulated, or VAS2870-inhibitable myocardial $O_2^{\cdot-}$ (VAS2870 being an inhibitor of NADPH-oxidases) or $O_2^{\cdot-}$ from mitochondria or NOSs, or $ONOO^-$ levels, trends were observed between $O_2^{\cdot-}$ from several of these sources and myocardial CSE expression (Figure 5.7). In particular, there was a strong positive trend between myocardial CSE expression and basal $O_2^{\cdot-}$, $O_2^{\cdot-}$ from NADPH oxidases, $ONOO^-$, and $O_2^{\cdot-}$

from NOSs (uncoupling of NOSs). In further univariate analysis of myocardial CSE gene expression as a continuous variable, we found significant positive correlations between myocardial CSE expression and NADPH-stimulated $O_2^{\cdot-}$ (ρ=0.232), VAS2870-inhibited $O_2^{\cdot-}$ (ρ=0.254) and ONOO- (ρ= 0.273) and a significant inverse correlation with LNAME-inhibitable $O_2^{\cdot-}$ (ρ= -0.241) (Table 5.2).

5.2.2 CBS and Myocardial Redox State

We also examined associations between the expression of myocardial CBS and $O_2^{\cdot-}$ production, both basal and from NADPH oxidases, NOSs, and mitochondria in the heart. Myocardial CBS gene expression was directly correlated with basal, NADPH-stimulated, and VAS2870-inhibitable myocardial $O_2^{\cdot-}$ (Figure 5.8). Myocardial CBS expression was also significantly associated with increased $O_2^{\cdot-}$ from NOSs (uncoupling of NOSs) (Figure 5.8). There were no significant correlations between myocardial CBS expression and $O_2^{\cdot-}$ from mitochondria or $ONOO^-$ levels (Figure 5.8).

Similar findings were observed with continuous variables (Table 5.2). Significant positive correlations were found between myocardial CBS gene expression and basal $O_2^{\cdot-}$ (ρ=0.310) and $O_2^{\cdot-}$ from NADPH oxidases (NAPDH-stimulated $O_2^{\cdot-}$, ρ=0.331; VAS2870-inhibited $O_2^{\cdot-}$, ρ=0.368) (Table 5.2). Increased expression of CBS was also associated with increased uncoupling of NOSs (significant inverse correlation with $O_2^{\cdot-}$ from NOSs, ρ= -0.306) (Table 5.2). These findings suggest, in corroboration with our previous findings with the direct effects of H_2S that CSE/CBS have an important relationship with NOS coupling. This paradoxical positive correlation between basal $O_2^{\cdot-}$ or NADPH-oxidase-derived $O_2^{\cdot-}$ and CSE/CBS expression may reflect an increase in expression of CBS/CSE as a novel defense mechanism.

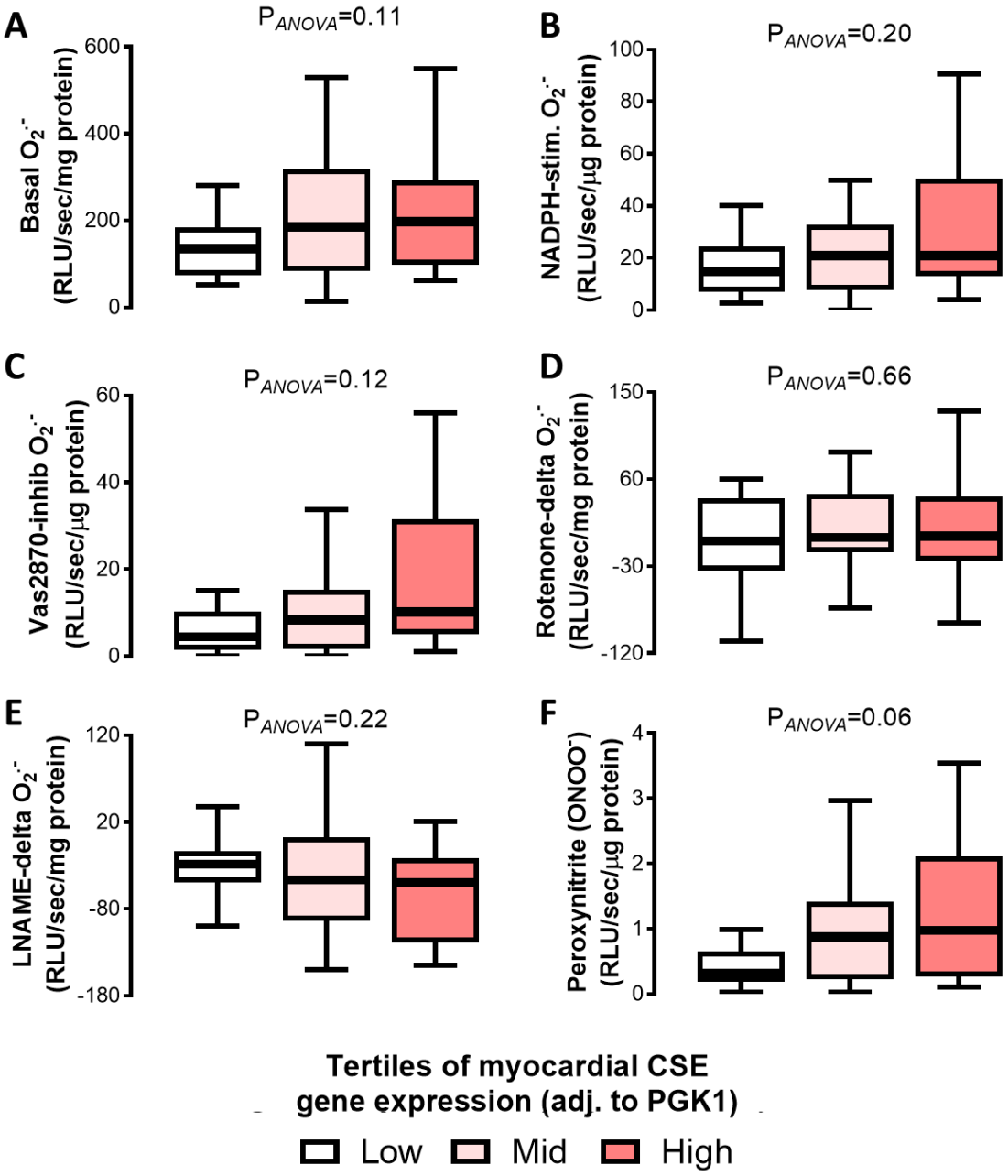


Figure 5.7 CSE Gene Expression and Myocardial Redox State

To further examine the role of local (myocardial) CSE biology in regulating myocardial redox state, we examined whether myocardial CSE expression was associated with $O_2^{\cdot-}$ generation. We found that there was a strong non-significant trend between myocardial CSE expression and basal $O_2^{\cdot-}$ (**A**). We found that myocardial CSE expression was not associated with $O_2^{\cdot-}$ from NADPH oxidases (**B-C**), mitochondrial $O_2^{\cdot-}$ generation as depicted by rotenone-inhibited $O_2^{\cdot-}$ (**D**), $O_2^{\cdot-}$ from NOSs (**E**) or $ONOO^-$ (**F**) in the myocardium. These finding suggest there is not a clear relationship between the local expression of CSE and these sources of $O_2^{\cdot-}$. n=21-26 per tertile. CSE, Cystathionine γ-Lyase. $O_2^{\cdot-}$, Superoxide. $ONOO^-$, Peroxynitrite. RLU: Relative Light Units. Values are presented as median (25^{th} to 75^{th} percentile) and whiskers (Tukey). P-values from unpaired, non-parametric Kruskal-Wallis test followed by Dunn's post hoc correction for multiple comparisons.

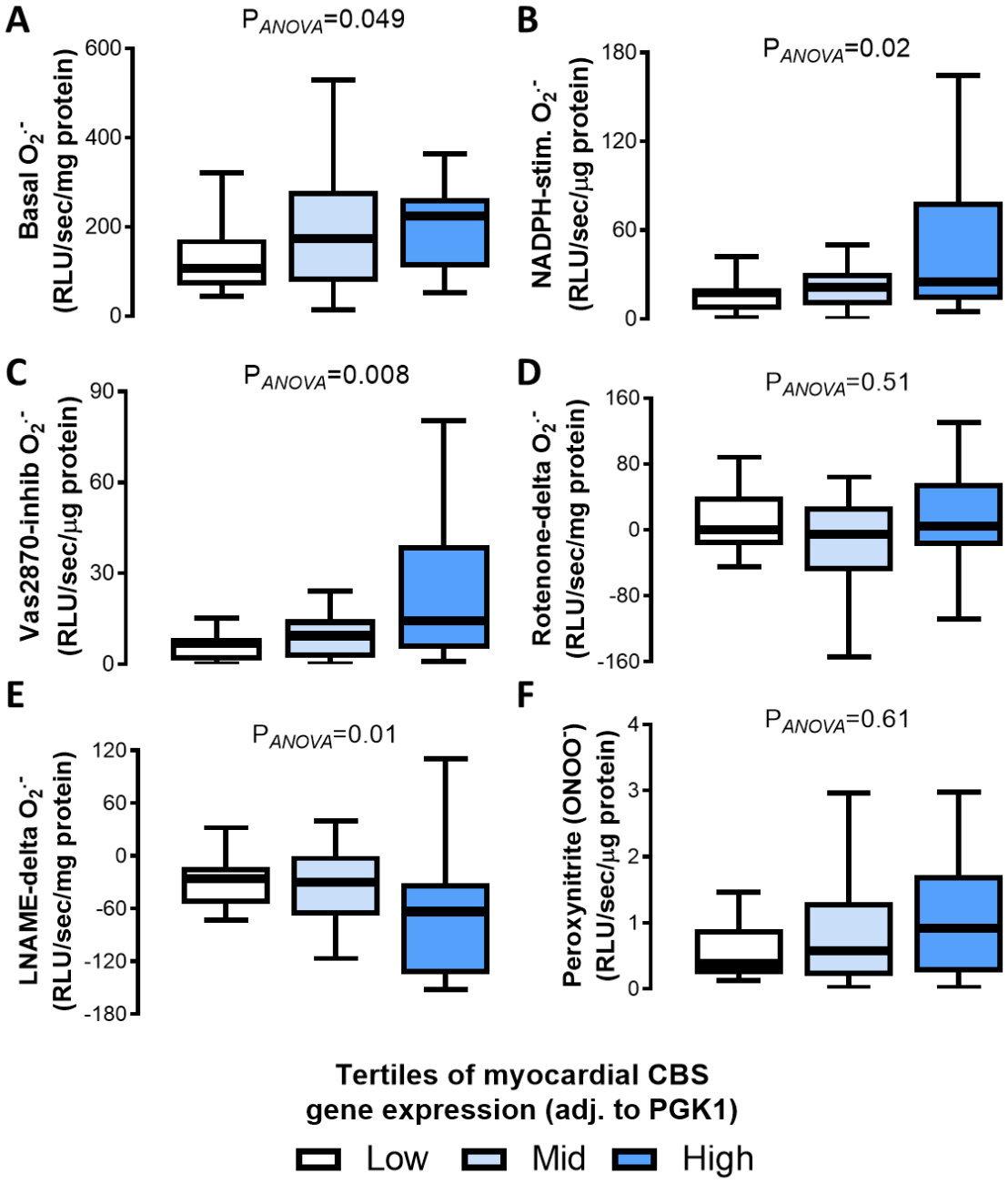


Figure 5.8 CBS Gene Expression and Myocardial Redox State

Myocardial expression of CBS was significantly associated with basal $O_2^{\cdot-}$ (**A**) or $O_2^{\cdot-}$ from NADPH oxidases (**B-C**). No correlation is observed between CBS expression and mitochondrial $O_2^{\cdot-}$ generation as depicted by rotenone-inhibited $O_2^{\cdot-}$ (**D**). However increased CBS expression is significantly associated with increased $O_2^{\cdot-}$ from NOSs (**E**). Myocardial CBS expression is not correlated with myocardial $ONOO^-$ levels (**F**). n=21-26 per tertile. CBS, Cystathionine β-Synthase. $O_2^{\cdot-}$, Superoxide. $ONOO^-$, Peroxynitrite. RLU: Relative Light Units. Values are presented as median (25^{th} to 75^{th} percentile) and whiskers (Tukey). P-values from unpaired, non-parametric Kruskal-Wallis test followed by Dunn's post hoc correction for multiple comparisons.

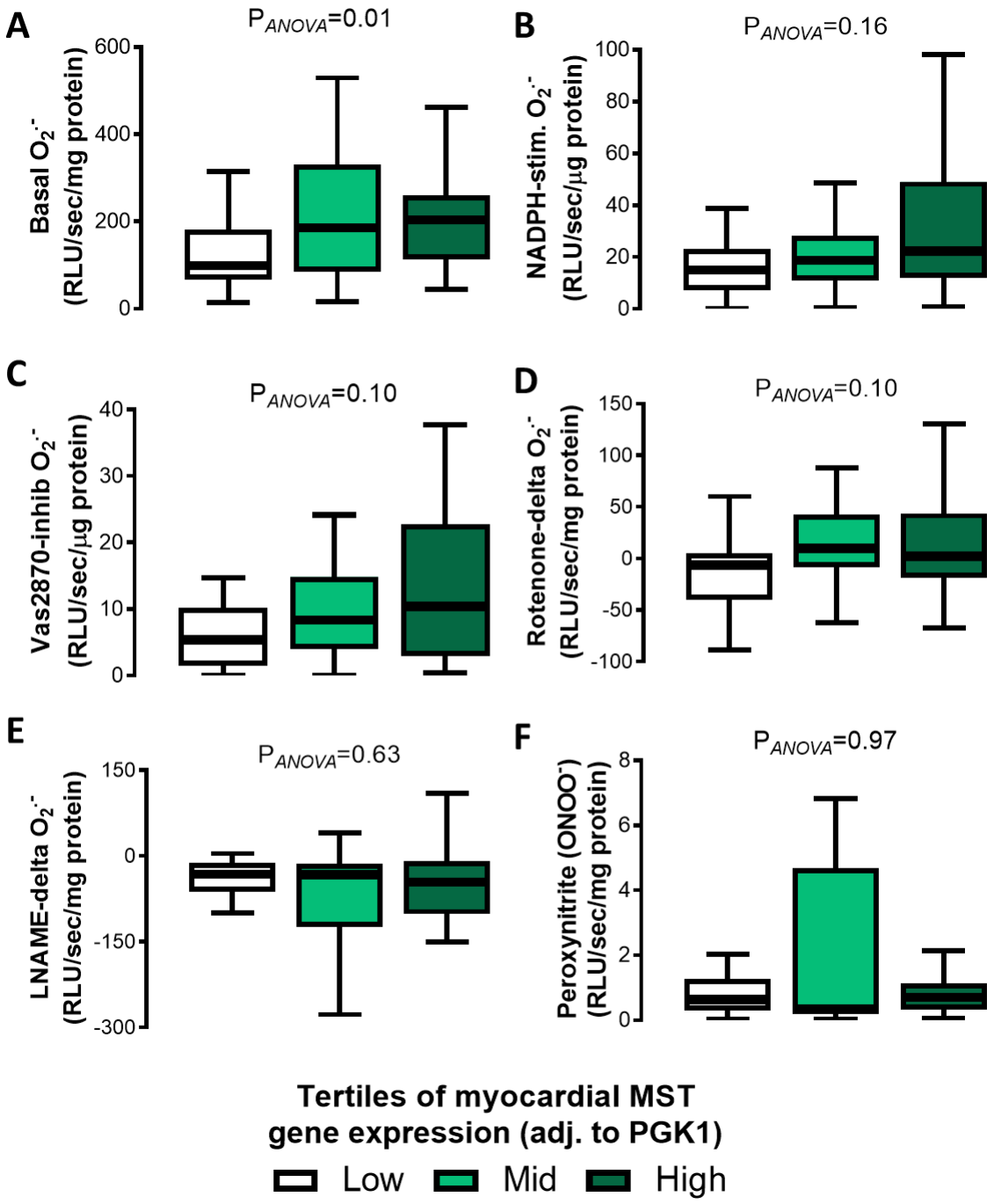


Figure 5.9 MST Gene Expression and Myocardial Redox State

Myocardial expression of MST was significantly associated with basal $O_2^{\cdot-}$ (**A**). However, myocardial MST was not associated with (**B**-**C**) $O_2^{\cdot-}$ from NADPH oxidases, (**D**) mitochondrial $O_2^{\cdot-}$ generation, (**E**) $O_2^{\cdot-}$ from NOSs or (**F**) myocardial $ONOO^-$ levels. n=22-26 per tertile. MST, 3-Mercaptopyruvate Sulfurtransferase. $O_2^{\cdot-}$, Superoxide. $ONOO^-$, Peroxynitrite. RLU: Relative Light Units. Values are presented as median (25^{th} to 75^{th} percentile) and whiskers (Tukey). P-values from unpaired, non-parametric Kruskal-Wallis test followed by Dunn's post hoc correction for multiple comparisons.

Table 5.2 Correlation Coefficients for CSE, CBS, and MST Gene Expression

Myocardial Gene Expression	Patient Demographics & CVD	Myocardial Redox State
CSE	No significant correlations observed	NADPH-stimulated $O_2^{\cdot-}$ (10min); P=0.043, ρ=0.232, n=76 VAS2870-inhibitable $O_2^{\cdot-}$ (plateau); P=0.029 , ρ=0.254, n=74 LNAME-inhibitable $O_2^{\cdot-}$; P=0.038, ρ= -0.241, n=74 $ONOO^-$ (peroxynitrite); P=0.018 , ρ= 0.273, n=74
CBS	Hypercholesterolemia; P=0.002, ρ= -0.310, n=96 Days in Wards, P=0.021, ρ= -0.236, n=96 Methylene Blue H_2S/Sulfide; P=0.049, ρ=0.202, n=95	Basal $O_2^{\cdot-}$; P=0.007, ρ=0.310, n=75 NADPH-stimulated $O_2^{\cdot-}$ (plateau); P=0.004, ρ=0.331, n=76 VAS2870-inhibitable $O_2^{\cdot-}$ (plateau); P=0.001 , ρ=0.368, n=74 LNAME-inhibitable $O_2^{\cdot-}$; P=0.008, ρ= -0.306, n=74
MST	Hypertension; P=0.031, ρ=0.221, n=95 BMI; P=0.035, ρ= -0.216, n=96 LVEDV; P=0.006, ρ= -0.396, n=46 LV mass; P=0.037, ρ= -0.273, n=59	Basal $O_2^{\cdot-}$; P=0.011, ρ=0.291, n=75 NADPH-stimulated $O_2^{\cdot-}$ (plateau); P=0.049, ρ=0.227, n=76 VAS2870-inhibitable $O_2^{\cdot-}$ (plateau); P=0.032, ρ= 0.249, n=74

We examined the relationship between myocardial gene expression of CSE, CBS, MST and clinical risk factor and myocardial redox state as continuous variables where possible. Taken together, we find that myocardial MST is correlated with hypertension, BMI, LVEDV, LV mass; while myocardial CBS is correlated with hypercholesterolemia, methylene blue plasma H_2S/Sulfide. In addition, we find that all three enzymes are correlated with myocardial redox state: myocardial CSE expression is correlated with NADPH-oxidase derived $O_2^{\cdot-}$ (NADPH stimulated $O_2^{\cdot-}$ after 10 minutes, and VAS2870-inhibitable $O_2^{\cdot-}$ plateau after NADPH), NOS-derived $O_2^{\cdot-}$ (LNAME-inhibitable) and $ONOO^-$. Moreover, both myocardial CBS and MST expression are correlated with basal $O_2^{\cdot-}$, NADPH oxidase-derived $O_2^{\cdot-}$ (NADPH stimulated $O_2^{\cdot-}$ after 10 minutes and plateau, and VAS2870-inhibitable $O_2^{\cdot-}$ plateau after NADPH). Myocardial CBS expression is also correlated with NOS-derived $O_2^{\cdot-}$ (LNAME-inhibitable). CSE, Cystathionine γ-Lyase. CBS, Cystathionine β-Synthase. H_2S, Hydrogen Sulfide. LV, Left Ventricle. LVEDV, Left Ventricular End Diastolic Volume. MST, 3-Mercaptopyruvate Sulfurtransferase. $O_2^{\cdot-}$, Superoxide. $ONOO^-$, Peroxynitrite. Non-parametric Spearman's correlation coefficient ρ(rho) estimations are presented. Spearman's correlation coefficient does not assume normal distributions.

5.2.3 MST and Myocardial Redox State

Finally, we examined associations between myocardial MST and $O_2^{\cdot-}$ production, both basal and from NADPH oxidases, NOSs, and mitochondria in the heart. Myocardial MST expression was associated with increased basal $O_2^{\cdot-}$ production but not $O_2^{\cdot-}$ from NADPH oxidases (Figure 5.9). Furthermore, MST expression was not associated with $O_2^{\cdot-}$ from any other source (NOSs or mitochondria) and was not associated with $ONOO^-$ levels in the myocardium (Figure 5.9). By univariate analysis with myocardial MST expression as a continuous variable, we observed that there was a significant positive correlation between myocardial MST expression and basal $O_2^{\cdot-}$ (ρ=0.291), NADPH-stimulated $O_2^{\cdot-}$ (ρ=0.227), and VAS2870-inhibited $O_2^{\cdot-}$ (ρ= 0.249) (Table 5.2). Together, these associations illustrate that higher oxidative stress is correlated with higher

expression of CSE, CBS and MST, though the direction of causality cannot be determined from these associations alone.

5.3 Redox-Sensitivity of Myocardial CSE & CBS Gene Expression

To better explain the positive correlations between basal $O_2^{\cdot-}$ and $O_2^{\cdot-}$ from NADPH oxidases and the gene expression studies, and examine specifically whether the increase in CSE or CBS expression indeed reflected a novel defence mechanism, we examined the causal relationship between oxidative stress and the expression of these enzymes.

5.3.1 Characterization of Acute Model of Oxidative Stress in H9C2 Cardiomyocytes

To characterize our model of acute oxidative stress (developed in Chapter 3), we measured basal $O_2^{\cdot-}$ generation in H9C2 cells exposed to 1mM NADPH for 18 hours in their original buffer (Figure 5.10). VAS2870-inhibitable $O_2^{\cdot-}$ was also measured in the cells exposed to 1mM NADPH and control cells in their original buffers (no additional NADPH was added to the system). Exposure to NADPH was sufficient to increase basal $O_2^{\cdot-}$ and VAS2870-inhibitable $O_2^{\cdot-}$ in H9C2 cells compared to control cells incubated for 18h (Figure 5.10). We further assessed viability of these cells exposed to 1mM NADPH for 18h and found viability to be similar to that of control cells (Figure 5.10).

5.3.2 Acute Oxidative Stress Reduces CSE Gene Expression *in vitro*

To examine whether an increase in oxidative stress leads to upregulation of CSE and CBS expression as a protective defense mechanism, we measured changes in gene expression in this model of acute oxidative stress. Surprisingly, we found that increased oxidative stress in H9C2 cells reduced CSE gene expression, marginally increased CBS gene expression, and had no effects on SP1 gene expression (the redox-sensitive transcription factor shown to regulate CSE expression in other tissues) (Figure 5.11).

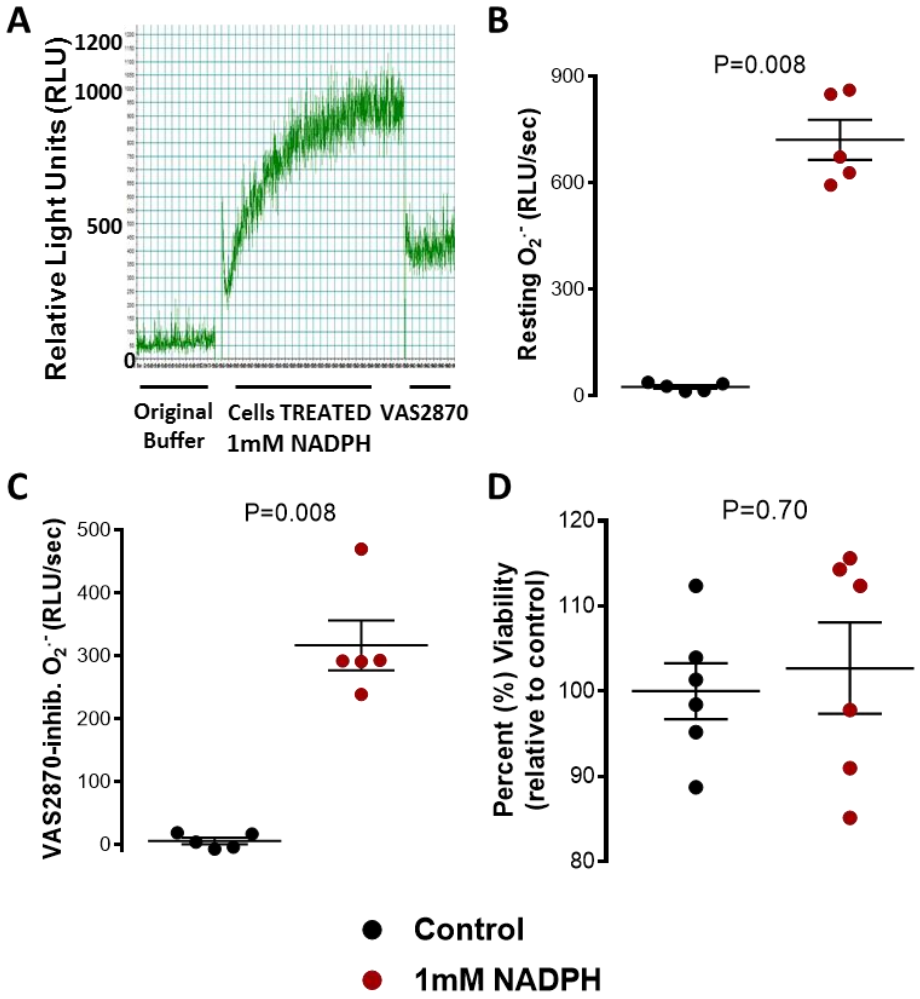


Figure 5.10 Model of Acute Oxidative Stress in H9C2 Cells

H9C2 cells were added to the Krebs HEPES buffer (±1mM NADPH), the medium in which they were incubated in (**A**, Representative trace for n=5) and VAS2870-inhibitable $O_2^{\cdot-}$ was measured. Exposure to 1mM NADPH for 18h was sufficient to increase basal $O_2^{\cdot-}$ (**B**, n=5 per group) and VAS2870-inhibitable $O_2^{\cdot-}$ (**C**, n=5 per group) in cells. No change in viability was detected in cells exposed to 1mM NADPH for 18h in media compared to control cells (**D**, n=6 per group). $O_2^{\cdot-}$, Superoxide. RLU: Relative Light Units. Values are presented as mean ± SEM in Panels *B-D.* P-values from unpaired, non-parametric Mann-Whitney rank test (in Panel *D*, viability is graphed as a percentage of the average of the control cells).

The effects on CSE expression were reversed by PEG-SOD, a scavenger of $O_2^{\cdot-}$, suggesting down-regulation was specific to direct or indirect effects of $O_2^{\cdot-}$ (Figure 5.11). These findings suggest that oxidative stress in the short-term impairs CSE expression in cardiomyocytes independent of SP1 expression. CBS upregulation which was significant, but marginal, suggests CBS expression may be more resistant to fluctuations in oxidative stress while still being part of the preliminary defense mechanisms against oxidative injury.

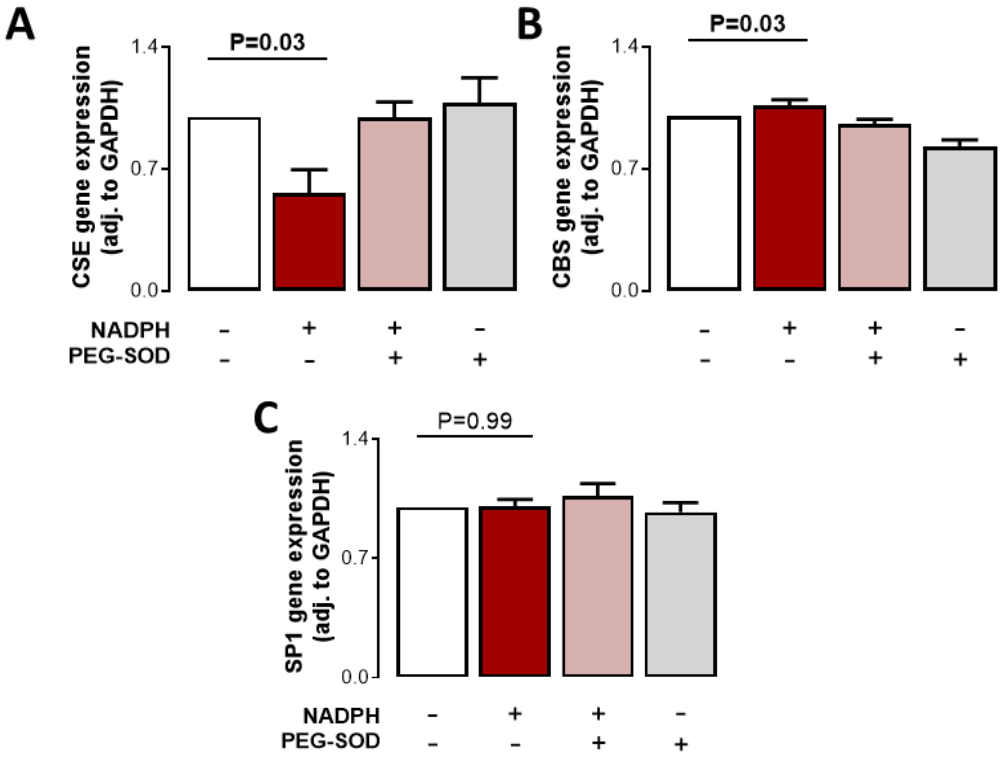


Figure 5.11 CSE Gene Expression in *In Vitro* Model of Acute Oxidative Stress

Exposure of H9C2 cells to increased oxidative stress (1mM NADPH, 18h) resulted in reduced CSE gene expression and increased CBS gene expression (**A-B**, P=0.03 Control vs NADPH-exposed Cells; n=5-6 pairs), an effect reversed by PEG-SOD (100U/mL). Exposure to oxidative stress did not affect SP1 gene expression (**C**, P=0.99 Control vs NADPH Cells; n=5-6 pairs). Gene expression is adjusted to GAPDH and relative to matched control cells. CSE, Cystathionine γ-Lyase. CBS, Cystathionine β-Synthase. GAPDH, Glyceraldehyde-3-phosphate dehydrogenase. PEG-SOD, Polyethylene Glycol-Superoxide Dismutase. Values are presented as mean ± SEM. Differences between control cells and NADPH-exposed cells were compared by Wilcoxon matched-pairs signed rank test.

5.3.3 Characterization of Myocardial Redox State of Rapid Atrial Paced Pigs

To examine whether the findings in cells could be replicated *in vivo*, we examined whether myocardial CSE, as well as myocardial CBS and MST, expression was altered in a large animal model of myocardial oxidative stress. Hearts from 1-week rapid atrial paced pigs and control animals were kindly provided from collaborators Prof. Sander Verheule, Dr. Hussein M. Nasrallah, and Dr. Dragan Opacic at Maastricht University (The Netherlands) as part of a collaborative project. To characterize this *in vivo* model, we assessed myocardial redox state in the left atria of pigs that underwent rapid atrial pacing for 1 week compared to their controls.

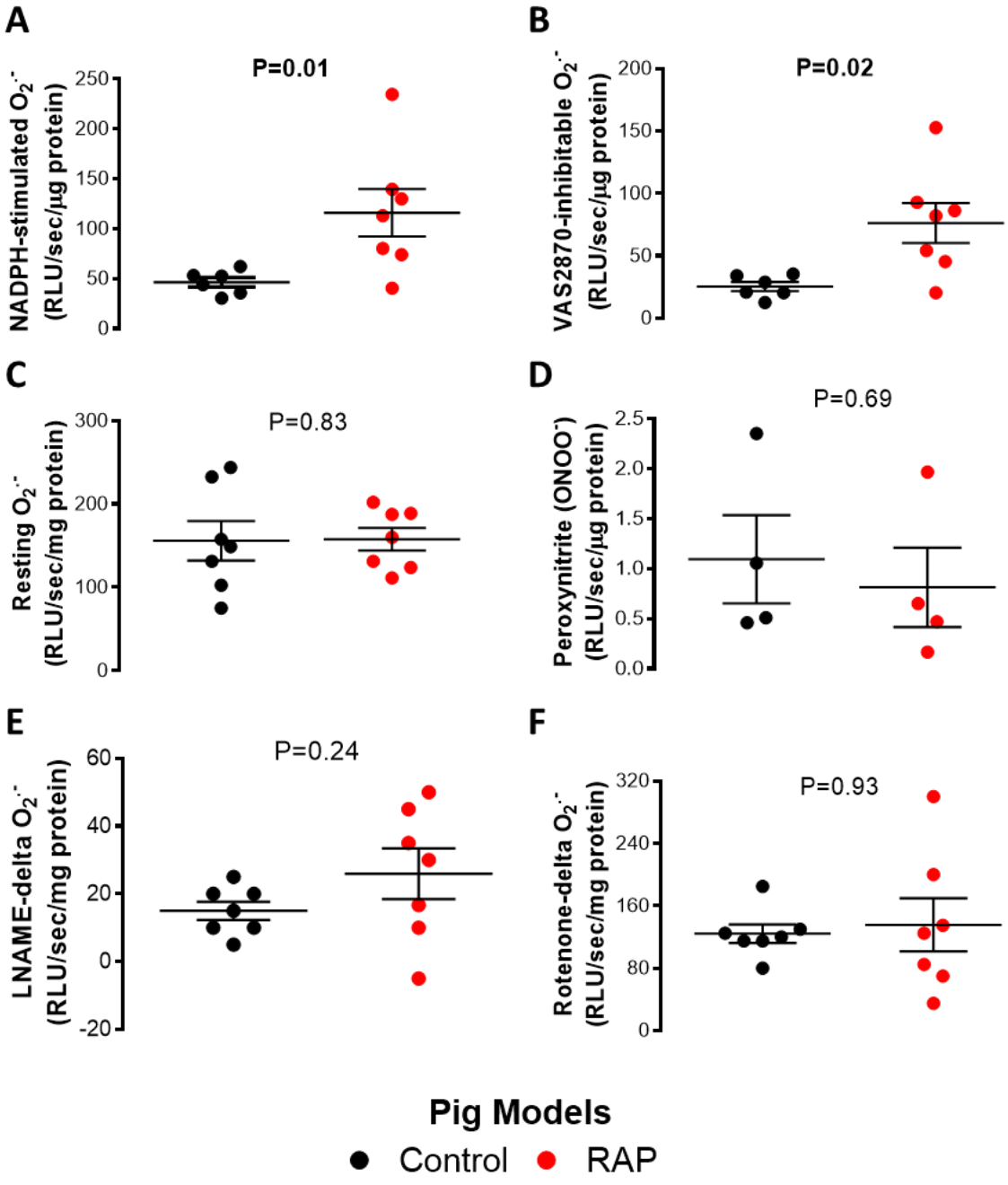


Figure 5.12 Redox State in Left Atria of Rapid Atrial Paced Pig Hearts

The redox state of left atria from 1-week rapid atrial paced pigs and control animals were compared. $O_2^{\cdot-}$ from NADPH oxidases was increased, as depicted by the NADPH-stimulated (**A**, at plateau; n=6-7 per group) and VAS2870-inhibitable signal (**B**, 10 minutes after NADPH stimulation; n=6-7 per group). No differences were observed in basal $O_2^{\cdot-}$ (**C**, n=7 per group) or $ONOO^-$ (**D**, n=4 per group) between the left atria of 1-week rapid atrial paced pigs and the left atria of control animals. No differences were observed in $O_2^{\cdot-}$ from NOSs (**E**, n=7 per group) or $O_2^{\cdot-}$ from mitochondrial oxidases (**F**, n=7 per group) in the left atria of RAP pigs compared to left atria of control pigs. NOS, Nitric oxide synthases. $O_2^{\cdot-}$, Superoxide. $ONOO^-$, Peroxynitrite. RAP, Rapid Atrial Paced. RLU, Relative Light Units. Values are presented as mean ± SEM. P-values from unpaired, non-parametric Mann-Whitney rank test.

Specifically, we quantified basal $O_2^{\cdot-}$ and $O_2^{\cdot-}$ from NADPH oxidases, NOSs, and mitochondrial oxidases (redox state measurements I made). In 1-week paced pigs, we found that basal $O_2^{\cdot-}$ was unchanged compared to controls, but that there was a significant increase in $O_2^{\cdot-}$ from NADPH oxidases as seen by both increased NADPH-stimulated $O_2^{\cdot-}$ and Vas2870-inhibitable $O_2^{\cdot-}$ in paced animals compared to controls (Figure 5.12).

We found there was no difference in $O_2^{\cdot-}$ from mitochondrial oxidases as seen by the rotenone-delta $O_2^{\cdot-}$ signal, NOS-derived $O_2^{\cdot-}$ determined by the LNAME-delta $O_2^{\cdot-}$ signal, or $ONOO^-$ in the left atria of paced animals and controls (Figure 5.12). This characterization of myocardial redox state in the left atria of rapid atrial paced pigs and their counterparts established an *in vivo* model of short-term oxidative stress to examine myocardial CSE, CBS, and MST gene expression.

5.3.4 Acute Oxidative Stress Reduces CSE Gene Expression *in vivo*

Consistent with our *in vitro* findings, we found that *in vivo*, short-term oxidative stress led to a downregulation of myocardial CSE gene expression (Figure 5.13). Short-term oxidative stress *in vivo* did not affect the expression of CBS, MST or SP1 expression (Figure 5.13). These findings suggest that the downregulation of CSE in response to oxidative injury was independent of SP1 expression and that CBS and MST expression were resistant to fluctuations in oxidative stress. These findings, like our *in vitro* studies, provide insight into the regulation of myocardial CSE expression by oxidative stress.

5.4 Redox-Sensitivity of CSE, CBS, and MST Gene Expression (Chronic)

To examine whether long-term oxidative stress in patients led to an upregulation of myocardial CSE and CBS as a protective defence mechanism, we characterized the additive SNP model in CYBA $p22^{phox}$ in human myocardium (which we have used previously as a model of human vascular oxidative stress[208]).

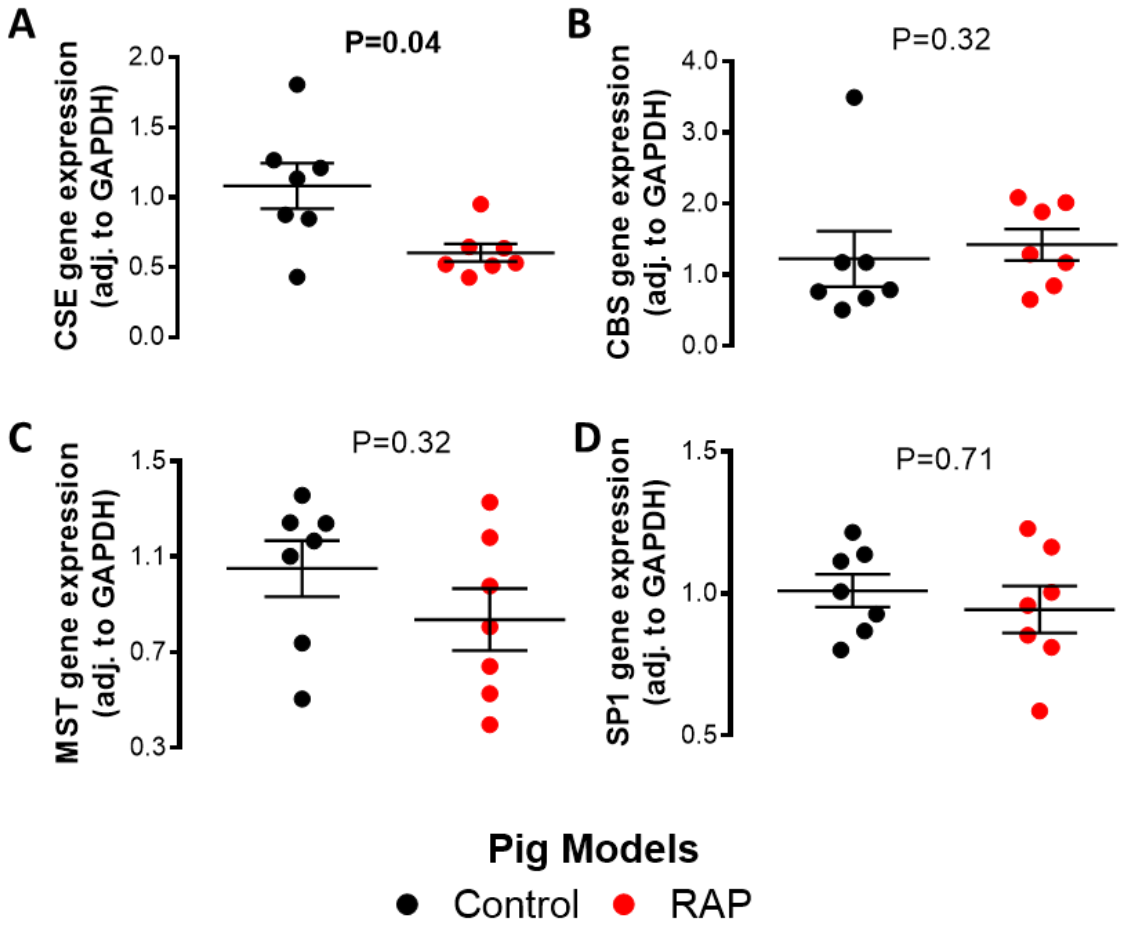


Figure 5.13 CSE Gene Expression in *In Vivo* Model of Acute Oxidative Stress

Left atria from 1-week rapid atrial paced pigs (RAP) had significantly reduced CSE gene expression compared to that of control animals (**A**, P=0.04; n=7 per group). No differences were observed in gene expression of CBS, MST, or SP1 expression in the left atria from paced versus control animals (**B-D**, P=0.32 for CBS, P=0.32 for MST, P=0.71 for SP1; n=7 per group). CSE, Cystathionine γ-Lyase. CBS, Cystathionine β-Synthase. MST: 3-Mercaptopyruvate Sulfurtransferase. RAP, Rapid Atrial Paced. SP1, Specificity protein 1. Values are presented as mean ± SEM. P-values from unpaired, non-parametric Mann-Whitney rank test.

5.4.1 Characterization of the Additive CYBA (p22^{phox}) SNP Model

The CYBA gene encodes for the p22^{phox} subunit of NADPH oxidase and the additive effect of the risk alleles (rs4673C and rs1049255G) is associated with increased $O_2^{\cdot-}$ in PBMNCs, human arteries, and veins.[173] To investigate causality for redox-sensitivity of the expression myocardial CSE, CBS, and MST expression, we explored the expression of these enzymes in individuals genotyped for SNPs rs4673T/C and

rs1049255A/G in the CYBA locus previously in our cohort (number of individuals with each SNP is shown in Table 5.3).

Table 5.3 Number of Individuals with CYBA rs4673 and rs1049255 SNP

Study Arm 2 *CYBA* SNPs	
***CYBA* rs4673 SNP**	
TT n(%)	**70 (14.0)**
CT n(%)	**229 (45.9)**
CC n(%)	**200 (40.1)**
***CYBA* rs1049255 SNP**	
AA n(%)	**130 (26.0)**
AG n(%)	**246 (49.2)**
GG n(%)	**124 (24.8)**

SNP, Single Nucleotide Polymorphism.

We found that this additive model was associated with increased $O_2^{\cdot -}$ in the myocardium, an indication that these genotypes were indeed a model of increased systemic oxidative stress in the heart. Specifically, we found that the additive SNP model rs4673C and rs1049255G indeed led to increased basal $O_2^{\cdot -}$ and NADPH-stimulated $O_2^{\cdot -}$ in the myocardium (Figure 5.14).

Following this determination, patients were categorized based on the number of risk alleles for these two CYBA SNPs and differences in myocardial CSE and CBS expression were explored. Individuals having 0 risk alleles (rs4673T and rs1049255A) to 4 risk alleles (rs4673C and rs1049255G) are shown as groups 0-4. In some cases, our study was underpowered to examine associations between myocardial CSE, CBS, or MST expression and individuals with 0 risk alleles or 4 risk alleles so these groups were combined (0 and 1 risk alleles combined; 3 and 4 risk alleles combined).

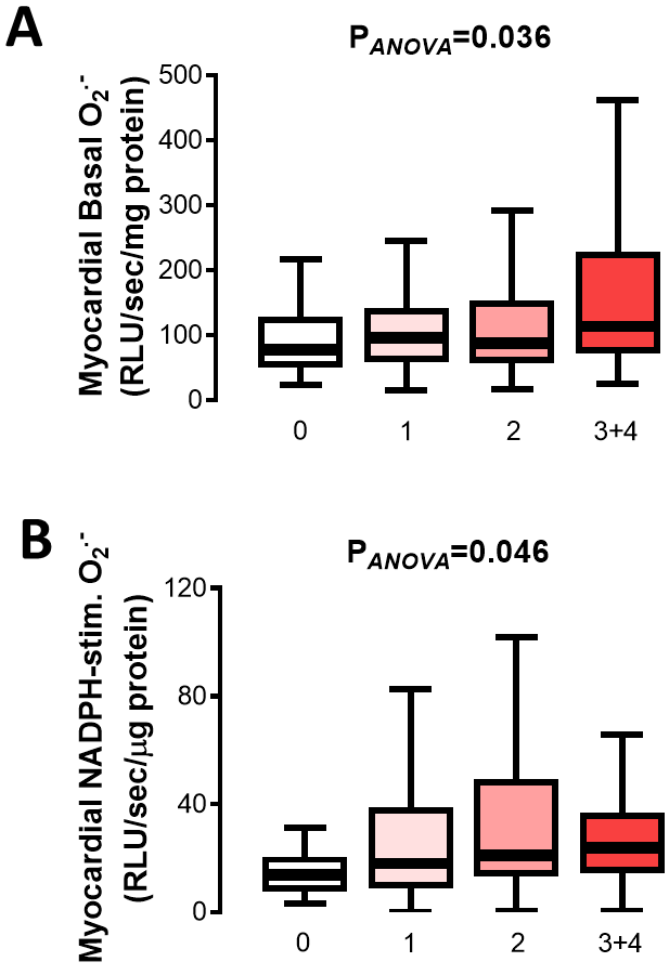


Figure 5.14 CYBA rs4673C and rs1049255G SNPs and Myocardial Redox State

To explore a causal relationship between oxidative stress and CSE expression, we used a known GWAS signal to determine any causal role chronic oxidative stress may have in regulating myocardial CSE gene expression. Individuals having 0 risk alleles (rs4673T and rs1049255A) to 4 risk alleles (rs4673C and rs1049255G) are shown. The additive SNP model CYBA rs4673C and rs1049255G indeed was related to increased basal $O_2^{\cdot-}$ (**A**, P_{ANOVA}=0.036; n=18, 45, 62, 87 per group) and increased NADPH-stimulated $O_2^{\cdot-}$ (**B**, P_{ANOVA}=0.046, n=17, 45, 60, 81 per group) in the myocardium compared to individuals with no risk alleles. $O_2^{\cdot-}$, Superoxide. RLU, Relative Light Units. Values are presented as median (25^{th} to 75^{th} percentile) and whiskers (Tukey). P-values from unpaired, non-parametric Kruskal-Wallis test followed by Dunn's post hoc correction for multiple comparisons.

5.4.2 CYBA ($p22^{phox}$) SNPs and Myocardial CSE, CBS, and MST Expression

We found that increased myocardial $O_2^{\cdot-}$ from the additive model was not associated with myocardial CSE, CBS, or MST expression, suggesting no direct causal regulation between increased $O_2^{\cdot-}$ from the CYBA SNPs and myocardial gene expression of these enzymes (Figure 5.15). The model was not associated with circulating H_2S levels

(Figure 5.15). Chronic increase in systemic oxidative stress in humans (by CYBA SNPs) suggest CBS expression is most sensitive to oxidative stress among the three enzymes. Taken together, these finding suggest that myocardial CSE, CBS, and MST have different sensitivity to acute and chronic oxidative stress.

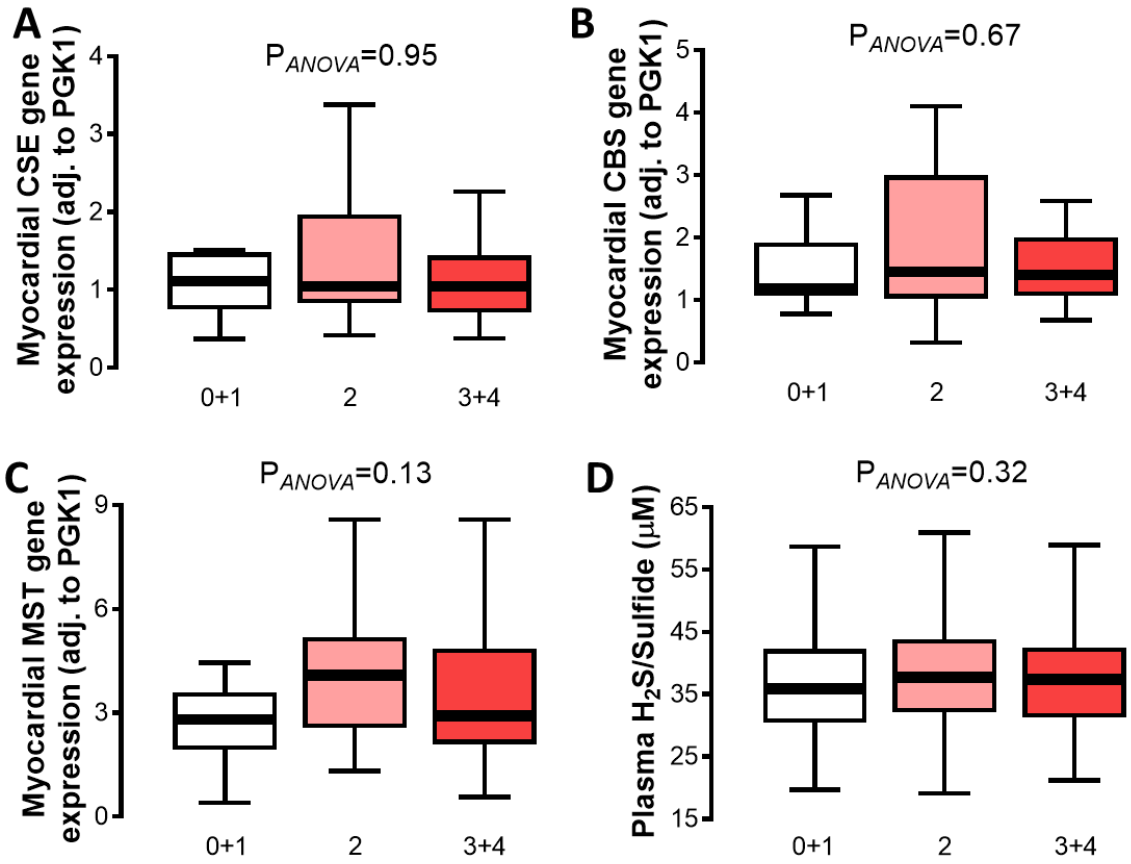


Figure 5.15 CYBA rs4673C and rs1049255G SNPs and CSE, CBS, & MST

Individuals having 0 risk alleles (rs4673T and rs1049255A) to 4 risk alleles (rs4673C and rs1049255G) are shown. The number of risk alleles (0-4) was not associated with gene expression of myocardial CSE (**A**, P_{ANOVA}=0.94; n=12, 22, 37 per group), CBS (**B**, P_{ANOVA}=0.71; n=12, 22, 37 per group) or MST (**C**, P_{ANOVA}=0.64; n=12, 22, 37 per group). The number of risk alleles was also not associated with circulating H_2S/Sulfide levels (**D**, P_{ANOVA}=0.36; n=79, 119, 160 per group). CSE, Cystathionine γ-Lyase. CBS, Cystathionine β-Synthase. H_2S, Hydrogen Sulfide. MST: 3-Mercaptopyruvate Sulfurtransferase. Values are presented as median (25^{th} to 75^{th} percentile) and whiskers (Tukey). P-values from unpaired, non-parametric Kruskal-Wallis test followed by Dunn's post hoc correction for multiple comparisons.

Chapter 6 Causal Role of CSE in Myocardial Redox State

Here we conduct a study to examine CSE's role in regulating myocardial redox state given the important redox-sensitivity of CSE expression in the heart. CSE's importance in the cardiovascular system continues to emerge and, while a few studies have recently examined the role of CSE in the heart and have suggested it to be protective against myocardial oxidative stress,[124] it remains unknown whether CSE can lead to alterations in $O_2^{\cdot-}$ from NADPH oxidases, NOSs, and mitochondrial oxidases in the heart. It is also not clear whether CSE alters $O_2^{\cdot-}$ from these enzymatic sources in advanced cardiac disease states in humans.

We hypothesize that CSE leads to reduced basal $O_2^{\cdot-}$ and reduced $O_2^{\cdot-}$ from NOSs, as well as reduced $ONOO^-$ levels in the heart. We further hypothesize that CSE improves redox state in humans by reducing myocardial $O_2^{\cdot-}$ from these sources. The aims of this study were specifically to

I. Determine the role of CSE, if any, in regulating myocardial redox state using an unchallenged *in vitro* model
II. Explore a known functional CSE variant's causal role in regulating myocardial redox state in humans with cardiac disease

This chapter therefore provides insight into the role of CSE in regulating basal $O_2^{\cdot-}$ and $O_2^{\cdot-}$ from NOSs and $ONOO^-$ in the absence of challenge and further provides insight into CSE's role in regulating $O_2^{\cdot-}$ from NADPH oxidases, NOSs, and mitochondrial oxidases in advanced cardiac disease states. The demographics of the study population are shown below (Table 6.1).

Table 6.1 Demographics Characteristics of Study Participants in Chapter 6

Participant Demographic Characteristics	Clinical Study Arm *CSE* and *CBS* SNPs
Demographics	
Participants (n)	**963**
Age (years)	**66.2±0.3**
Male gender (%)	**82.1**
Smoking (active/ex) (%)	**68.8**
Hypertension (%)	**70.5**
Hypercholesterolemia (%)	**67.2**
Diabetes mellitus (%)	**27.0**
HOMA-IR	**4.2±0.5**
BNP (pg/mL)	**147.2±12.9**
BMI (kg/m^2)	**28.1±0.2**
Waist circumference (cm)	**92.6±0.9**
Waist:Hip ratio	**1.01±0.01**
Medications	
ACEi/ARBs (%)	**49.4/12.9**
β-blockers (%)	**69.0**
Aspirin/Clopidogrel (%)	**78.2/30.2**
Statins (%)	**80.0**
CCBs (%)	**29.8**
Diuretics (%)	**24.2**
Insulin/Oral hypoglycaemic (%)	**7.2/19.1**
Nitrates (%)	**38.7**

ACEi, Angiotensin Converting Enzyme inhibitors. ARB, Angiotensin Receptor Blockers. BMI, Body Mass Index. BNP, B-Natriuretic Peptide. CCB, Calcium Channel Blockers. HOMA-IR, Homeostatic Model Assessment of Insulin Resistance. Values are presented as mean ± SEM.

6.1 CSE in Regulating Myocardial $O_2^{\cdot-}$ from NOSs and $ONOO^-$

6.1.1 Characterization of CSE Knockdown Cells

To examine whether CSE leads to reduced basal $O_2^{\cdot-}$ and reduced $O_2^{\cdot-}$ from NOSs, as well as reduced $ONOO^-$ levels, we silenced CTH (CSE Gene via shRNA) in H9C2 cells. H9C2 cells were transfected and selected as described in Chapter 2 (Materials and Methods). We found that CSE gene expression was significantly reduced in CSE knockdown cells in both undifferentiated H9C2 cells and H9C2 cardiomyocytes compared to scrambled controls (Figure 6.1).

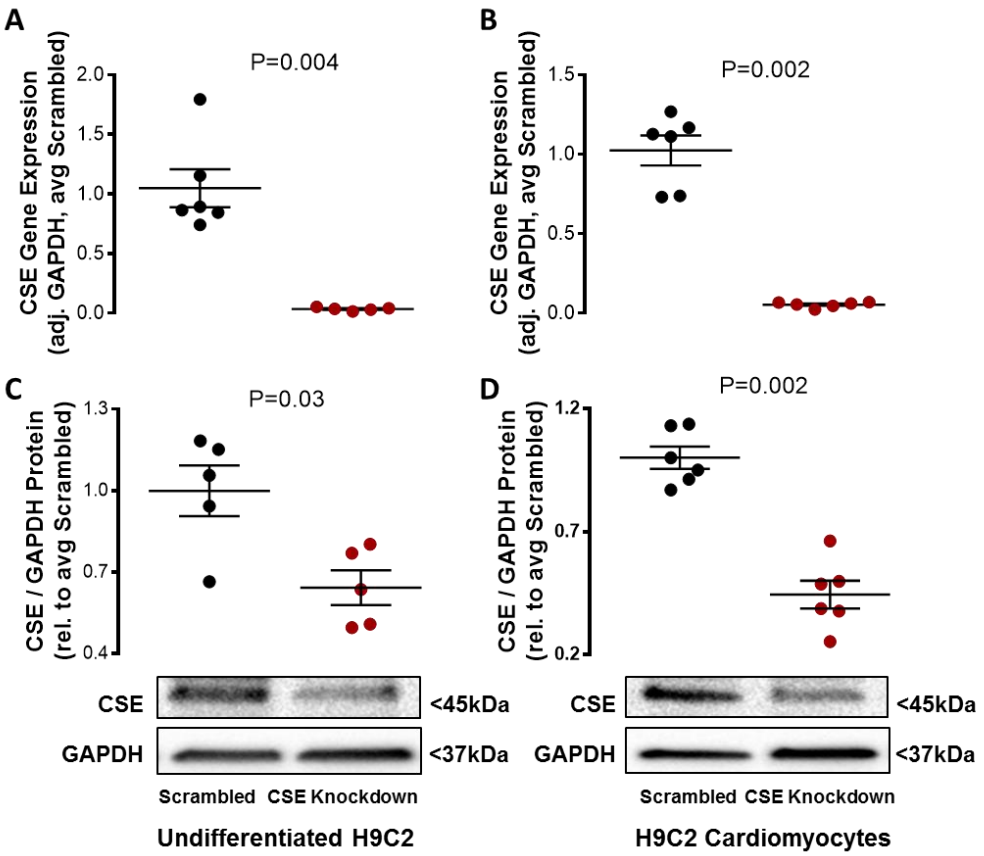


Figure 6.1 CSE Gene Expression and Protein Levels

CSE gene expression was significantly reduced after knockdown in both undifferentiated H9C2 cells (**A**, P=0.004; n=5-6 per group) and H9C2 cardiomyocytes (**B**, P=0.002; n=6 per group) compared to respective scrambled controls. CSE gene expression was reduced by more than 90% compared to respective scrambled controls (comparison of means). Furthermore, CSE protein levels were reduced after knockdown in both undifferentiated H9C2 cells (**C**, P=0.03; n=5 per group) and H9C2 cardiomyocytes (**D**, P=0.002; n=6 per group) compared to respective scrambled controls. CSE protein levels were reduced by approximately 36% and 56% in undifferentiated H9C2 and H9C2 cardiomyocytes, respectively, compared to scrambled controls (comparison of means). Representative western blots of n=5-6 show CSE protein (45 kDa) relative to GAPDH protein (37 kDa) (**C-D**). Protein levels were graphed as ratios relative to GAPDH normalized to the average of the scrambled clone protein levels for each blot, allowing blots to be combined as fold change of average scrambled controls. CSE, Cystathionine γ-Lyase. GAPDH, glyceraldehyde-3-phosphate dehydrogenase. kDa, Kilodaltons. Values are presented as mean ± SEM. P-values from unpaired, non-parametric Mann-Whitney rank test.

Furthermore, we found that CSE protein levels were significantly reduced in both undifferentiated H9C2 cells and H9C2 cardiomyocytes compared to their respective scrambled controls (Figure 6.1). Following this final characterization, these clones were used as our cell model to explore the hypothesis that CSE directly suppresses $O_2^{\cdot-}$ generation from NOSs and reduces basal $O_2^{\cdot-}$ and $ONOO^-$. The model was examined unchallenged, in the absence of advanced cardiac disease.

6.1.2 Basal $O_2^{\cdot-}$ Generation, $O_2^{\cdot-}$ from NOSs, and $ONOO^-$ Levels

We first explored whether CSE suppresses basal $O_2^{\cdot-}$, $ONOO^-$ levels and $O_2^{\cdot-}$ production from NOSs. We observed that in silenced cells, basal $O_2^{\cdot-}$ and $ONOO^-$ levels were reduced compared to scrambled controls (Figure 6.2). These findings surprisingly suggest CSE may increase basal levels of these ROS in the absence of challenge. We further examined whether CSE affected $O_2^{\cdot-}$ generation from NOSs and found no difference in $O_2^{\cdot-}$ from NOSs in CSE knockdown cells compared to their scrambled controls (Figure 6.2). These findings may suggest CSE can increase $O_2^{\cdot-}$ and $ONOO^-$ levels independent of effects on $O_2^{\cdot-}$ production from NOSs in the absence of challenge. It will be important to examine whether this is also observed *in vivo*.

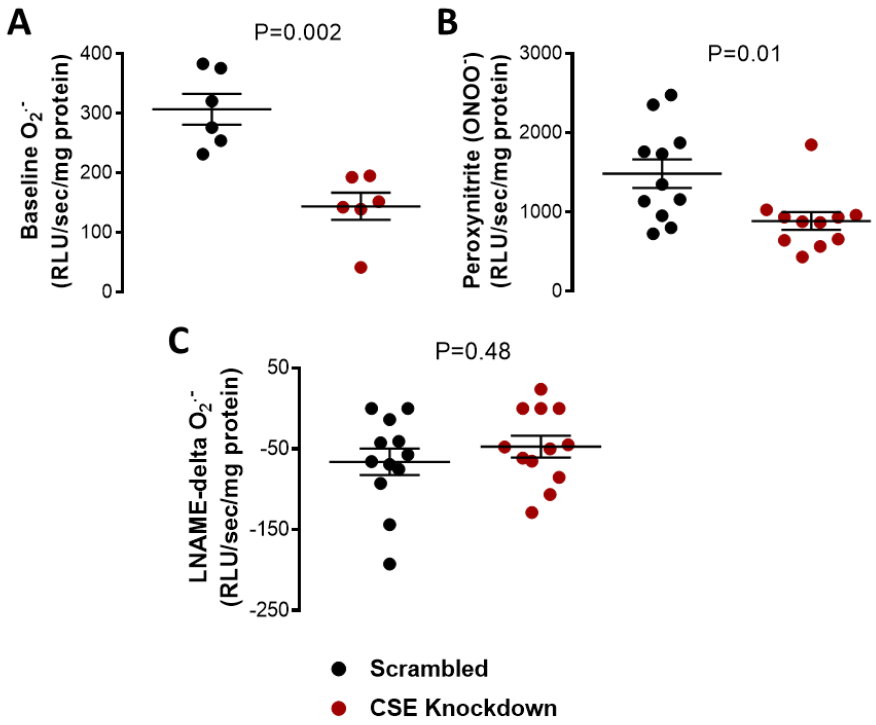


Figure 6.2 Redox State in CSE Knockdown Cells

CSE knockdown cells had significantly reduced basal $O_2^{\cdot-}$ (**A**, P=0.002; n=6 per group) and ONOO- levels (**B**, P=0.01; n=11 per group) compared to Scrambled controls. These was no significant difference in NOS-derived $O_2^{\cdot-}$ between CSE knockdown cells and Scrambled controls (**C**, P=0.48, n=12 per group). CSE, Cystathionine γ-Lyase. NOS, Nitric Oxide Synthase. $O_2^{\cdot-}$, Superoxide. $ONOO^-$, Peroxynitrite. RLU, Relative Light Units. Values are presented as mean ± SEM. P-values from unpaired, non-parametric Mann-Whitney rank test.

6.2 Human SNPs in CSE and CBS and Patient Demographics

Having explored the role of CSE in regulating myocardial redox state in an unchallenged model, we next asked what role CSE played in regulating myocardial redox state in humans in advanced cardiac disease states -- studies that are completely lacking.

To examine this role of CSE, we genotyped individuals from the Oxford-HVF cohort for SNPs identified in genome wide association studies (GWAS) and homocysteine metabolism. These SNPs are described in Chapter 1 (Introduction) in detail. Briefly, SNPs in CSE (rs1021737G>T, S403I) and CBS (rs2851391C>T and rs234709C>T), enzymes that catalyze the production of H_2S using homocysteine as a common substrate, were identified.[153-157] These SNPS were identified among several SNPs because their risk alleles were associated with or predicted to be associated with higher plasma homocysteine levels.[153-157] The number of individuals in our cohort with each of these three SNPs is shown in Table 6.2.

Table 6.2 Number of Individuals with CSE and CBS SNPs

***CSE* and *CBS* SNPs**	
***CSE* rs1071237 SNP**	
TT n(%)	**84 (8.7)**
GT n(%)	**411 (42.7)**
GG n(%)	**468 (48.6)**
***CBS* rs2851391 SNP**	
TT n(%)	**232 (24.2)**
CT n(%)	**447 (46.7)**
CC n(%)	**278 (29.1)**
***CBS* rs234709 SNP**	
TT n(%)	**194 (20.2)**
CT n(%)	**486 (50.5)**
CC n(%)	**282 (29.3)**

SNP, Single Nucleotide Polymorphism.

We examined whether individuals with the risk alleles (2 risk alleles) of each SNP had altered $O_2^{\cdot-}$ from NADPH oxidases, NOSs, and mitochondrial oxidases, compared to individuals with fewer (1 risk allele) or no risk alleles (0 alleles). We further examined whether the risk alleles were associated with patient demographics. We hypothesized that individuals homozygous for the risk allele in CSE would have increased myocardial $O_2^{\cdot-}$ generation from NADPH oxidases, NOSs, and mitochondrial oxidases. We further hypothesized that the number of risk alleles would inversely correlate with plasma H_2S/Sulfide levels.

6.2.1 CSE rs1021737G>T and Metabolic Profile, Cardiac Disease, & Systemic Stress

We first examined the effects of CSE risk alleles on patient demographics by stratifying our cohort into different allele groups: 0 CSE risk alleles (GG), 1 CSE risk allele (GT), and 2 CSE risk alleles (TT). We found that there was no difference in age between individuals in each allele group for appropriate comparison (Figure 6.3). We then asked whether individuals with a higher number of CSE risk alleles had increased duration of hypertension (with the guidelines and classification of hypertension prior to 2017) or days in hospital and we found that there was no difference in duration of hypertension or days in hospital in individuals with a higher number of CSE risk alleles (Figure 6.3). Given the increasing importance of obesity in cardiovascular disease, we then asked examined whether individuals with a higher number of CSE risk alleles also had increased insulin resistance (HOMA-IR), body mass index (BMI), or waist-to-hip ratio. We found that there was no difference in any of these metabolic parameters in individuals with a higher number of CSE risk alleles (Figure 6.3).

To further explore a possible relationship between heart failure and CSE, we used previously quantified parameters of the left atrium and left ventricle (by

echocardiography) to examine whether left atrial size and left ventricular mass and volume/function were altered with a higher number of CSE risk alleles. We found that there was no difference in left atrial diameter, left ventricular mass, or left ventricular function, as assessed by left ventricular end diastolic volume (LVEDV) and left ventricular end systolic volume (LVESV), between individuals with differing number of CSE risk alleles (Figure 6.4).

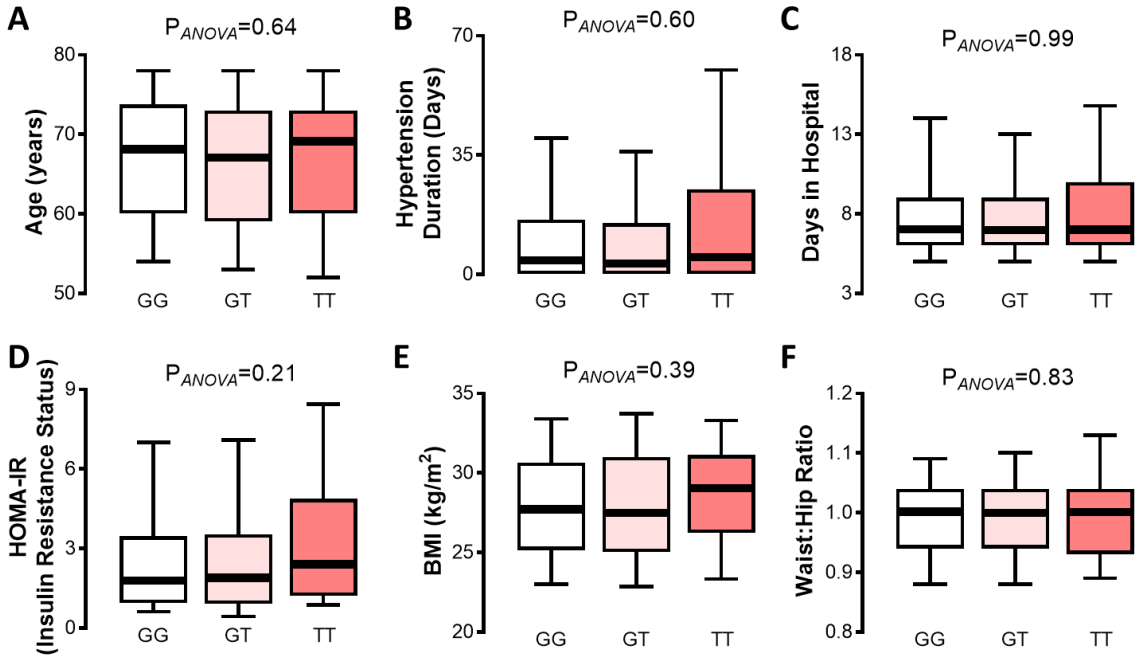


Figure 6.3 CSE SNP rs1021737, Patient Demographics, and Metabolic Profile

No significant differences in age were observed between individuals in our cohort with 0 CSE rs1021737 risk alleles (GG), 1 CSE risk allele (GT), and 2 CSE risk alleles (TT) (**A**, P_{ANOVA}=0.64; n=452, 393, 79 in each group). Similarly, no significant difference in duration of hypertension in days was observed between these three groups (**B**, P_{ANOVA}=0.60; n=293, 238, 43 in each group). The number of CSE risk alleles had no effect on days in hospital (**C**, P_{ANOVA}=0.99; n=353, 303, 55 in each group). Furthermore, the number of CSE risk alleles had no effect on insulin resistance (HOMA-IR) status (**D**, P_{ANOVA}=0.21; n=243, 208, 33 in each group), BMI (**E**, P_{ANOVA}=0.39; n=385, 333, 66 in each group), or Waist to hip ratios (**F**, P_{ANOVA}=0.83; n=276, 237, 39 in each group) in our cohort. BMI, Body Mass Index. CSE, Cystathionine γ-Lyase. HOMA-IR, Homeostatic model assessment of insulin resistance. SNP, Single Nucleotide Polymorphism. W:H Ratio, Waist to hip ratio. Values are presented as median (25^{th} to 75^{th} percentile) and whiskers (10^{th} to 90^{th} percentile) in Panels *A* and *C-F* and as median (25^{th} to 75^{th} percentile) and whiskers (Tukey) in Panel *B*. P-values from unpaired, non-parametric Kruskal-Wallis test followed by Dunn's post hoc correction for multiple comparisons.

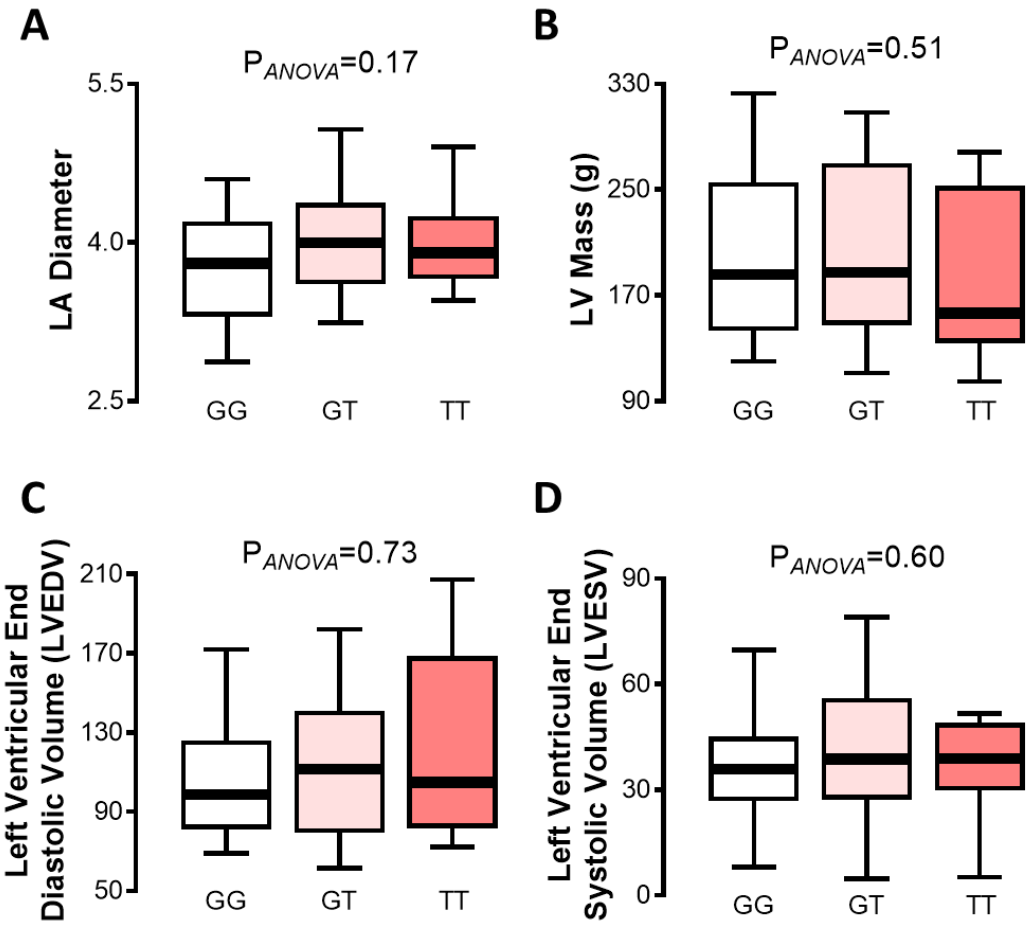


Figure 6.4 CSE SNP rs1021737, LA Dimensions, and LV Function

CSE rs1021737risk alleles (TT) had no significant effect on LA diameter (**A**, P_{ANOVA}=0.17; n= 67, 56, 9 individuals per group), LV Mass (**B**, P_{ANOVA}=0.51; n= 79, 78, 13 individuals per group), Left Ventricular End Diastolic Volume (**C**, P_{ANOVA}=0.73; n= 71, 75, 11 individuals per group), or Left Ventricular End Systolic Volume (**D**, P_{ANOVA}=0.60; n= 67, 72, 11 individuals per group). CSE, Cystathionine γ-Lyase. LA, Left Atrium. LV, Left Ventricle. LVEDV, Left Ventricular End Diastolic Volume. LVESV, Left Ventricular End Systolic Volume. SNP, Single Nucleotide Polymorphism. Values are presented as median (25^{th} to 75^{th} percentile) and whiskers (10^{th} to 90^{th} percentile) in Panels *A-C* and as median (25^{th} to 75^{th} percentile) and whiskers (Tukey) in Panel *D*. P-values from unpaired, non-parametric Kruskal-Wallis test followed by Dunn's post hoc correction for multiple comparisons.

Lastly, we examined whether the number of CSE risk alleles altered systemic markers of oxidative stress and inflammation, plasma malondialdehyde (MDA), high sensitivity C-reactive protein (hsCRP) or plasma B-natriuretic peptide (BNP). We found that there was no difference in plasma MDA, hsCRP or plasma BNP between individuals of different number of CSE risk alleles (Figure 6.5). These findings provide further evidence that the relationship between CSE and oxidative stress and inflammation may be local rather than systemic.

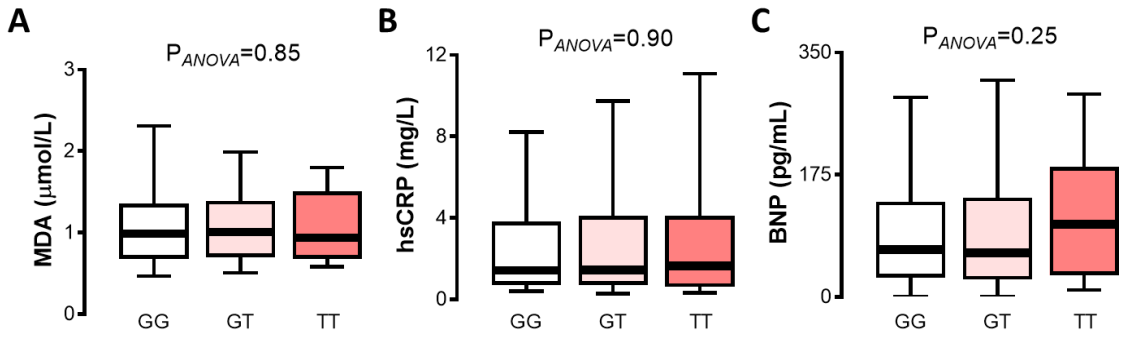


Figure 6.5 CSE SNP rs1021737 & Systemic Markers of Stress

CSE risk alleles (TT) had no effect on plasma MDA (**A**, P_{ANOVA}=0.85; n=196, 166, 24 individuals per group), hsCRP (**B**, P_{ANOVA}=0.90; n=387, 316, 61 individuals per group) or BNP (**C**, P_{ANOVA}=0.25; n= 276, 229, 39 individuals per group). BNP, B-Natriuretic Peptide. CSE, Cystathionine γ-Lyase. hsCRP, High Sensitivity C-reactive protein. MDA, Malondialdehyde. SNP, Single Nucleotide Polymorphism. Values are presented as median (25th to 75th percentile) and whiskers (10th to 90th percentile) in Panels *A-B* and as median (25th to 75th percentile) and whiskers (Tukey) in Panel *C*. P-values from unpaired, non-parametric Kruskal-Wallis test followed by Dunn's post hoc correction for multiple comparisons.

6.2.2 CBS rs2851391C>T and Metabolic Profile, Cardiac Disease, & Systemic Stress

We next examined the effects of CBS risk alleles on patient demographics by stratifying our cohort into different allele groups: 0 CBS rs2851391 risk alleles (CC), 1 CBS rs2851391 risk allele (CT), and 2 CBS rs2851391 risk alleles (TT). We found that there was no difference in age and number of CBS rs2851391 risk alleles (Figure 6.6). We then asked whether individuals with a higher number of CBS rs2851391 risk alleles had increased duration of hypertension or days in hospital.

We found no difference in duration of hypertension or days in hospital in individuals with a higher number of CBS rs2851391 risk alleles (Figure 6.6). We also asked examined whether individuals with a higher number of CBS rs2851391 risk alleles also had increased HOMA-IR, BMI, or waist-to-hip ratio. We found no difference in these metabolic parameters and number of CBS rs2851391 risk alleles (Figure 6.6).

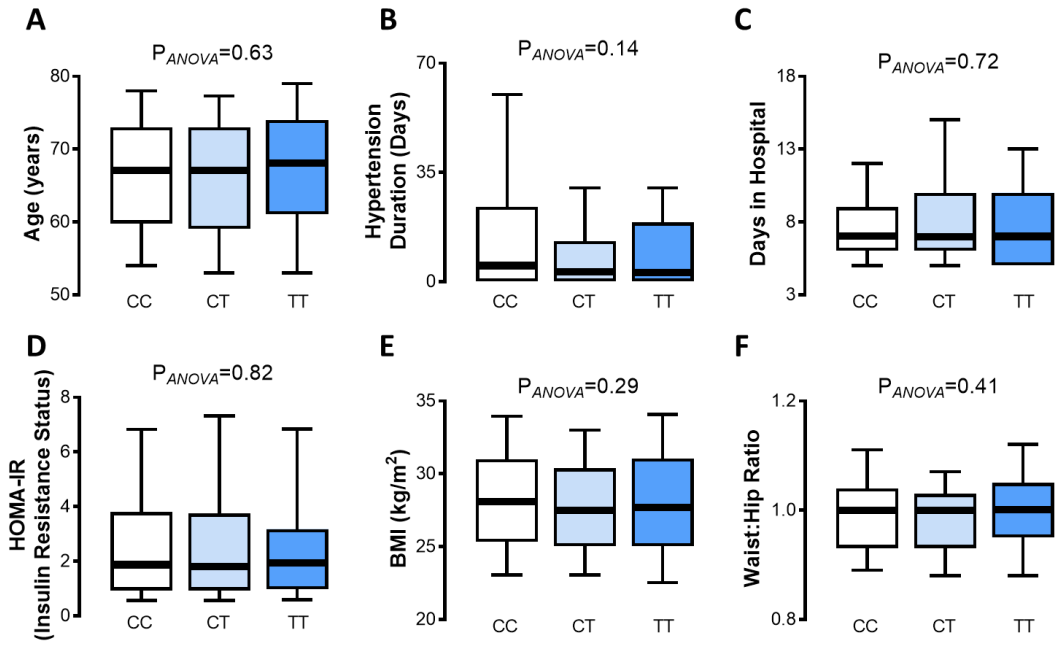


Figure 6.6 CBS SNP rs2851391, Patient Demographics, and Metabolic Profile

No significant differences in age were observed between individuals in our cohort with 0 CBS rs2851391 risk alleles (CC), 1 CBS rs2851391 risk allele (CT), and 2 CBS rs2851391 risk alleles (TT) (**A**, P_{ANOVA}=0.63; n=270, 426, 224 in each respective group). Similarly, no significant difference in duration of hypertension in days was observed between these three groups (**B**, P_{ANOVA}=0.14; n=174, 271, 128 in each respective group). The number of CBS risk alleles had no effect on days in hospital (**C**, P_{ANOVA}=0.72; n=212, 333, 164 in each respective group). Furthermore, the number of CBS risk alleles had no effect on insulin resistance (HOMA-IR) status (**D**, P_{ANOVA}=0.82; n=140, 231, 112 in each respective group), BMI (**E**, P_{ANOVA}=0.29; n=235, 363, 185 in each respective group), or Waist to hip ratios (**F**, P_{ANOVA}=0.41; n=173, 260, 119 in each respective group) in our cohort. BMI, Body Mass Index. CBS, Cystathionine β-Synthase. HOMA-IR, Homeostatic model assessment of insulin resistance. SNP, Single Nucleotide Polymorphism. W:H Ratio, Waist to hip ratio. Values are presented as median (25^{th} to 75^{th} percentile) and whiskers (10^{th} to 90^{th} percentile) in Panels *A* and *C-F* and as median (25^{th} to 75^{th} percentile) and whiskers (Tukey) in Panel *B*. P-values from unpaired, non-parametric Kruskal-Wallis test followed by Dunn's post hoc correction for multiple comparisons.

To further explore a possible relationship between heart failure and CBS rs2851391 risk alleles, we examined whether left atrial size and left ventricular mass and volume/function were altered with a higher number of CBS rs2851391 risk alleles. We found that there was no difference in left atrial diameter, left ventricular mass, or left ventricular function, as assessed by LVEDV and LVESV, between individuals with differing number of CBS rs2851391 risk alleles (Figure 6.7).

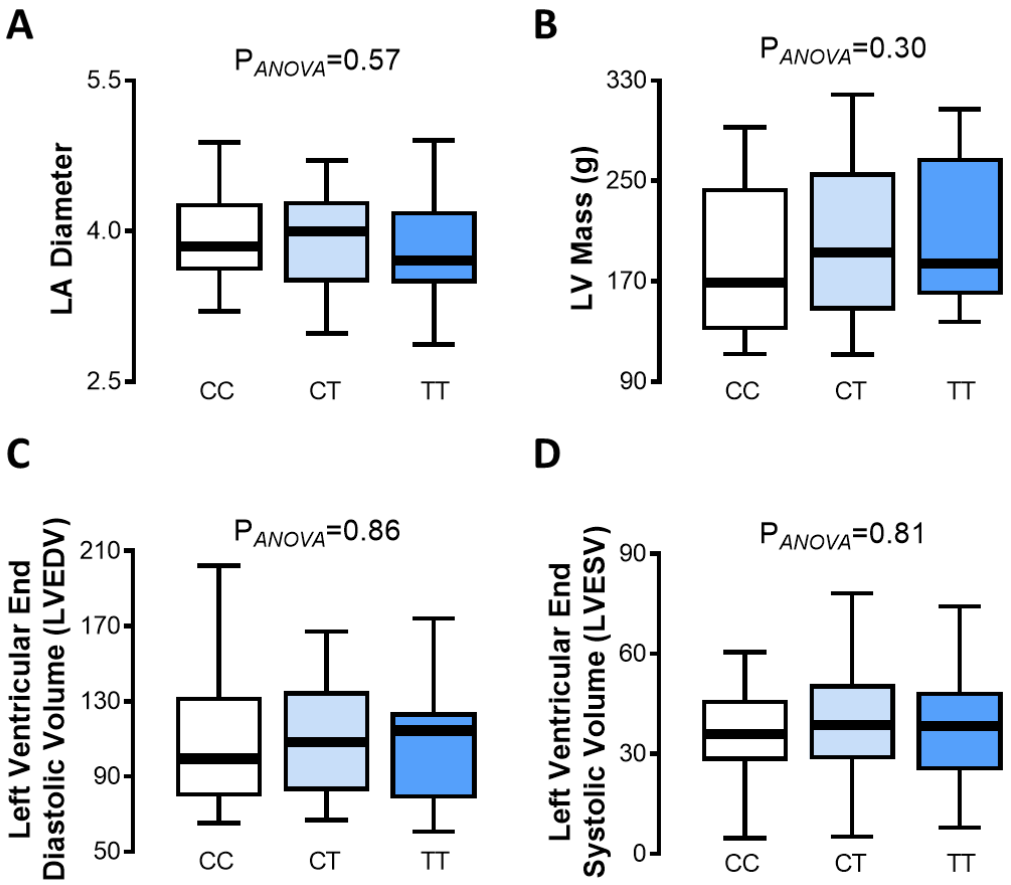


Figure 6.7 CBS SNP rs2851391, LA Dimensions, and LV Function

CBS rs2851391 risk alleles (TT) had no significant effect on LA diameter (**A**, P_{ANOVA}=0.57; n=44, 62, 26 individuals per group), LV Mass (**B**, P_{ANOVA}=0.30; n=62, 79, 29 individuals per group), Left Ventricular End Diastolic Volume (**C**, P_{ANOVA}=0.86; n= 46, 79, 32 individuals per group), or Left Ventricular End Systolic Volume (**D**, P_{ANOVA}=0.81; n=43, 76, 31 individuals per group). CBS, Cystathionine β-Synthase. LA, Left Atrium. LV, Left Ventricle. LVEDV, Left Ventricular End Diastolic Volume. LVESV, Left Ventricular End Systolic Volume. SNP, Single Nucleotide Polymorphism. Values are presented as median (25^{th} to 75^{th} percentile) and whiskers (10^{th} to 90^{th} percentile) in Panels *A-C* and as median (25^{th} to 75^{th} percentile) and whiskers (Tukey) in Panel *D*. P-values from unpaired, non-parametric Kruskal-Wallis test followed by Dunn's post hoc correction for multiple comparisons.

Lastly, we examined whether the number of CBS rs2851391 risk alleles altered systemic markers of oxidative stress and inflammation, plasma MDA, hsCRP or plasma BNP. Interestingly, we found that plasma MDA was significantly reduced with increasing number of CBS rs2851391 risk alleles. There was no difference in hsCRP or plasma BNP between individuals of different number of CBS rs2851391 risk alleles (Figure 6.8). These findings provide evidence of a relationship between CBS and systemic oxidative stress.

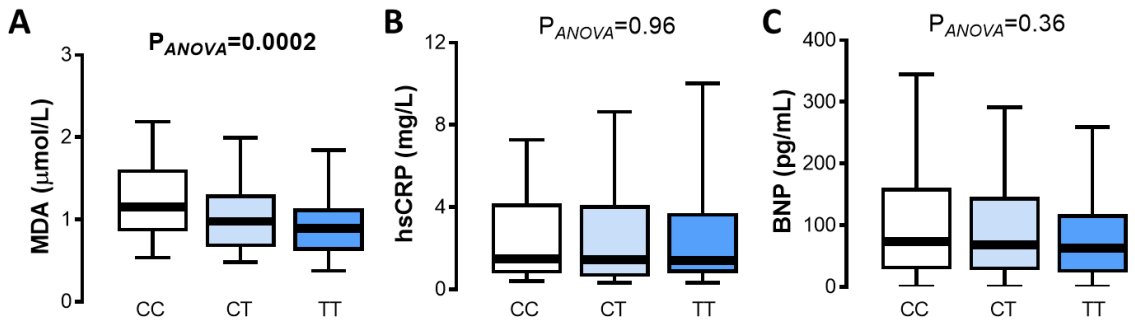


Figure 6.8 CBS SNP rs2851391 & Systemic Markers of Stress

CBS rs2851391 risk alleles (TT) significantly reduced plasma MDA (**A**, P_{ANOVA}=0.0002; P=0.017 CC vs CT and P=0.0002 CC vs TT post-hoc; n=113, 176, 97 individuals per group), with no significant effect on hsCRP (**B**, P_{ANOVA}=0.96; n=229, 357, 175 individuals per group) or BNP (**C**, P_{ANOVA}=0.36; n=166, 257, 120 individuals per group). BNP, B-Natriuretic Peptide. CBS, Cystathionine β-Synthase. hsCRP, High Sensitivity C-reactive protein. MDA, Malondialdehyde. SNP, Single Nucleotide Polymorphism. Values are presented as median (25^{th} to 75^{th} percentile) and whiskers (10^{th} to 90^{th} percentile) in Panels *A-B* and as median (25^{th} to 75^{th} percentile) and whiskers (Tukey) in Panel *C*. P-values from unpaired, non-parametric Kruskal-Wallis test followed by Dunn's post hoc correction for multiple comparisons.

6.2.3 CBS rs234709C>T and Metabolic Profile, Cardiac Disease, & Systemic Stress

We then examined the effects of CBS risk alleles on patient demographics by stratifying our cohort into different allele groups: 0 CBS rs234709 risk alleles (CC), 1 CBS rs234709 risk allele (CT), and 2 CBS rs234709 risk alleles (TT). We found that there was no difference in age between individuals in each allele group for appropriate comparison (Figure 6.9). We then asked whether individuals with a higher number of CBS rs234709 risk alleles had increased duration of hypertension or days in hospital and we found that there was no difference in duration of hypertension or days in hospital in individuals with a higher number of CBS rs234709 risk alleles (Figure 6.9). We also asked whether individuals with a higher number of CBS rs234709 risk alleles also had increased HOMA-IR, BMI, or waist-to-hip ratio. We found that there was no difference in any of these metabolic parameters in individuals with a higher number of CBS rs234709 risk alleles (Figure 6.9).

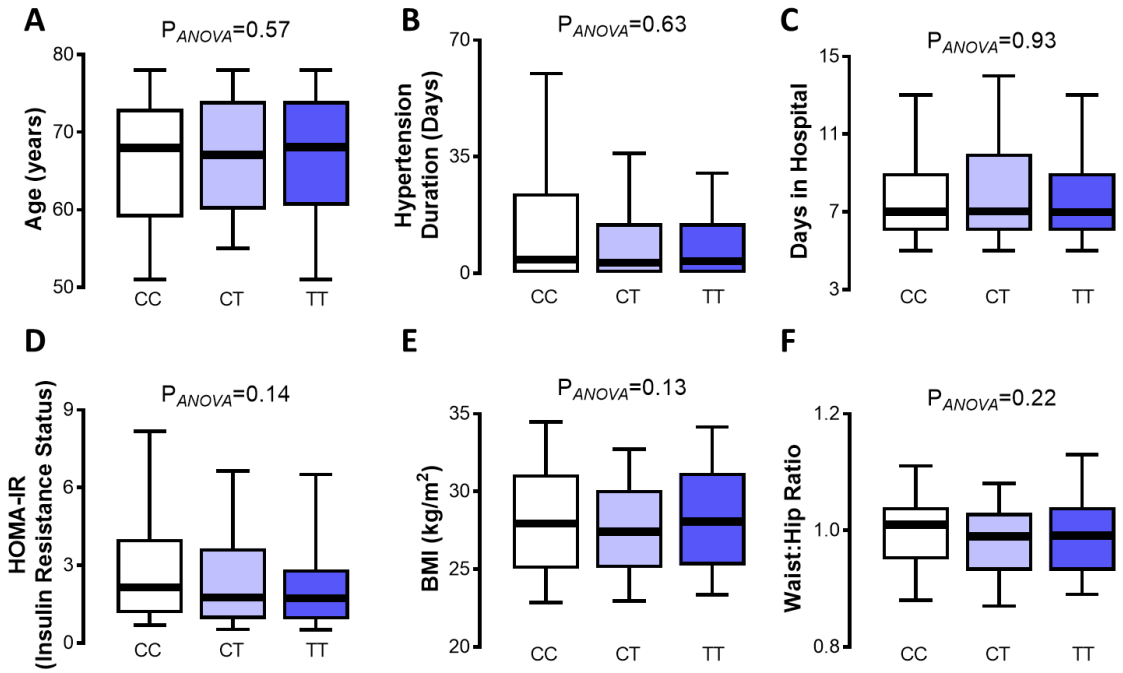


Figure 6.9 CBS SNP rs234709, Patient Demographics, and Metabolic Profile

No significant differences in age were observed between individuals in our cohort with 0 CBS rs234709 risk alleles (CC), 1 CBS rs234709 risk allele (CT), and 2 CBS rs234709 risk alleles (TT) (**A**, P_{ANOVA}=0.57; n=270, 469, 185 in each respective group). Similarly, no significant difference in duration of hypertension in days was observed between these three groups (**B**, P_{ANOVA}=0.63; n=167, 299, 108 in each respective group). The number of CBS risk alleles had no effect on days in hospital (**C**, P_{ANOVA}=0.93; n=211, 357, 142 in each respective group). Furthermore, the number of CBS risk alleles had no effect on insulin resistance (HOMA-IR) status (**D**, P_{ANOVA}=0.14; n=142, 250, 92 in each respective group), BMI (**E**, P_{ANOVA}=0.13; n=229, 399, 155 in each respective group), or Waist to hip ratios (**F**, P_{ANOVA}=0.22; n=163, 293, 96 in each respective group) in our cohort. BMI, Body Mass Index. CBS, Cystathionine β-Synthase. HOMA-IR, Homeostatic model assessment of insulin resistance. SNP, Single Nucleotide Polymorphism. W:H Ratio, Waist to hip ratio. Values are presented as median (25^{th} to 75^{th} percentile) and whiskers (10^{th} to 90^{th} percentile) in Panels *A* and *C-F* and as median (25^{th} to 75^{th} percentile) and whiskers (Tukey) in Panel *B*. P-values from unpaired, non-parametric Kruskal-Wallis test followed by Dunn's post hoc correction for multiple comparisons.

To further explore a possible relationship between heart failure and CBS rs234709 risk alleles, we examined whether left atrial size and left ventricular mass and volume/function were altered with a higher number of CBS rs234709 risk alleles. We found that there was a border-line significance in left atrial diameter but no difference in left ventricular mass, or left ventricular function, as assessed by LVEDV and LVESV, between individuals with differing number of CBS rs234709 risk alleles (Figure 6.10).

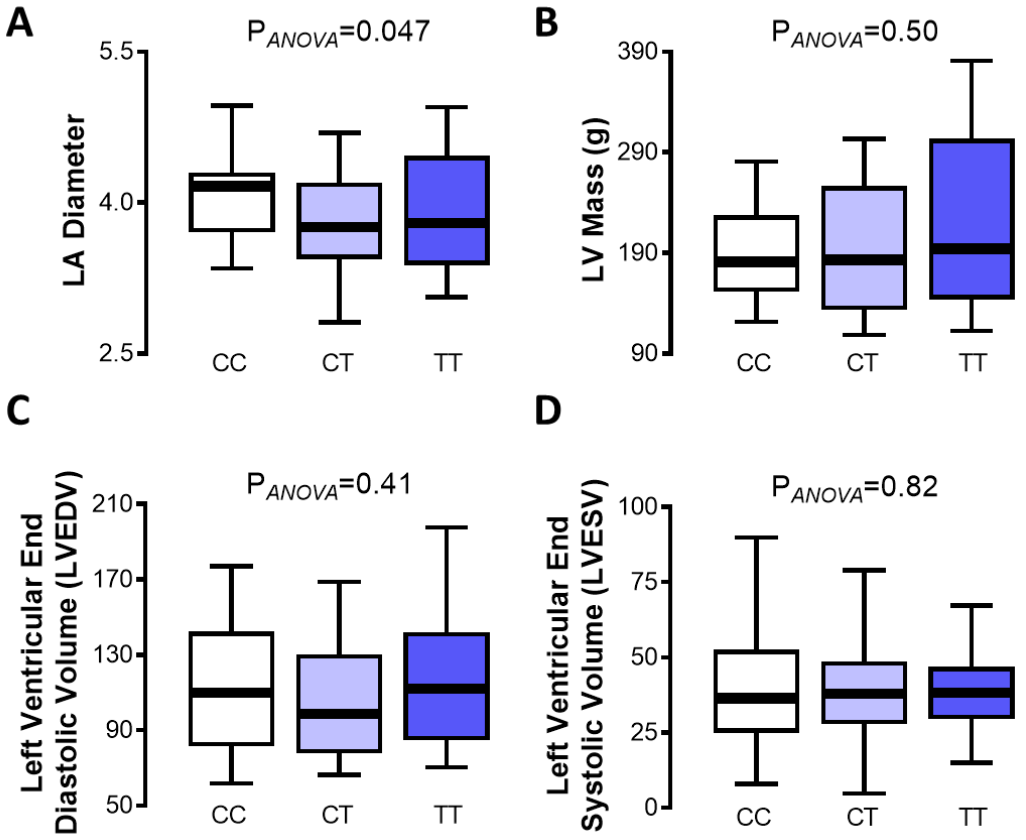


Figure 6.10 CBS SNP rs234709, LA Dimensions, and LV Function

Individuals heterozygous for CBS rs234709 risk allele (T) had a significant reduction in LA diameter compared to individuals with no risk alleles (**A**, P_{ANOVA}=0.047; P=0.043 between CC and CT groups post-hoc; n=36, 70, 26 individuals per group). CBS rs234709 risk alleles had no significant effect on LV Mass (**B**, P_{ANOVA}=0.50; n=47, 90, 33 individuals per group), LVEDV (**C**, P_{ANOVA}=0.41; n= 46, 76, 35 individuals per group), or LVESV (**D**, P_{ANOVA}=0.82; n=45, 71, 34 individuals per group). CBS, Cystathionine β-Synthase. LA, Left Atrium. LV, Left Ventricle. LVEDV, Left Ventricular End Diastolic Volume. LVESV, Left Ventricular End Systolic Volume. SNP, Single Nucleotide Polymorphism. Values are presented as median (25^{th} to 75^{th} percentile) and whiskers (10^{th} to 90^{th} percentile) in Panels *A-C* and as median (25^{th} to 75^{th} percentile) and whiskers (Tukey) in Panel *D*. P-values from unpaired, non-parametric Kruskal-Wallis test followed by Dunn's post hoc correction for multiple comparisons.

Lastly, we examined whether the number of CBS rs234709 risk alleles altered systemic markers of oxidative stress and inflammation, plasma MDA, hsCRP or plasma BNP. We found that there was no difference in plasma MDA, hsCRP or plasma BNP between individuals of different number of CBS rs234709 risk alleles (Figure 6.11). Taken together, these findings suggest that CSE and CBS SNPs do not largely alter the metabolic state or cardiac function of individuals. Here we find a relationship between CBS and systemic oxidative stress.

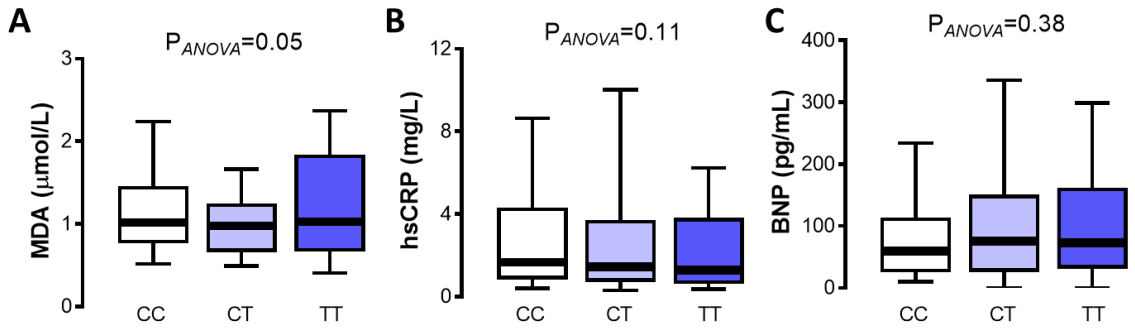


Figure 6.11 CBS SNP rs234709 & Systemic Markers of Stress

CBS rs234709 risk alleles (TT) had no significant effect on plasma MDA, though a strong trend for reduction was observed (**A**, P_{ANOVA}=0.05; n=124, 192, 70 individuals per group). CBS risk alleles (TT) had no significant effect on hsCRP (**B**, P_{ANOVA}=0.11; n=228, 379, 156 individuals per group) or BNP (**C**, P_{ANOVA}=0.38; n=169, 281, 94 individuals per group). BNP, B-Natriuretic Peptide. CBS, Cystathionine β-Synthase. hsCRP, High Sensitivity C-reactive protein. MDA, Malondialdehyde. SNP, Single Nucleotide Polymorphism. Values are presented as median (25^{th} to 75^{th} percentile) and whiskers (10^{th} to 90^{th} percentile) in Panels *A-B* and as median (25^{th} to 75^{th} percentile) and whiskers (Tukey) in Panel *C*. P-values from unpaired, non-parametric Kruskal-Wallis test followed by Dunn's post hoc correction for multiple comparisons.

6.3 Human SNP rs1021737G>T in CSE and Myocardial Redox State

6.3.1 $O_2^{\cdot-}$ from Mitochondrial Oxidases in the Heart

Having examined the effects of CSE and CBS risk alleles in patient demographics and cardiac disease, we next examined the effects of CSE and CBS risk alleles on human myocardial redox state and specifically $O_2^{\cdot-}$ from mitochondrial oxidases, NADPH oxidases, and NOSs. We first asked whether CSE and CBS risk alleles led to increased $O_2^{\cdot-}$ from mitochondria. We found that CSE risk alleles led to significantly reduced rotenone-delta myocardial $O_2^{\cdot-}$ (Figure 6.12).

Given that $O_2^{\cdot-}$ is measured after rotenone blocks complex I, the negative delta represents the $O_2^{\cdot-}$ coming from downstream of the electron transport chain that is blocked by rotenone. This finding suggests CSE risk alleles lead to increased $O_2^{\cdot-}$ generation post-complex I of the electron transport chain. This was in contrast to CBS rs2851391 and rs234709 risk alleles, which led to increased rotenone-delta myocardial

$O_2^{\cdot-}$ (reduced $O_2^{\cdot-}$ generation post-complex I) and no change in rotenone-delta myocardial $O_2^{\cdot-}$, respectively (Figure 6.12). Our finding that individuals with CTH S403I have altered $O_2^{\cdot-}$ production from mitochondria suggests CSE may play an important role in regulating mitochondrial $O_2^{\cdot-}$ generation in the heart. Given the opposing effects of the CSE rs1021737 and CBS rs2851391 SNPs on mitochondrial redox state, the additive effect of the risk alleles for each SNP were not explored.

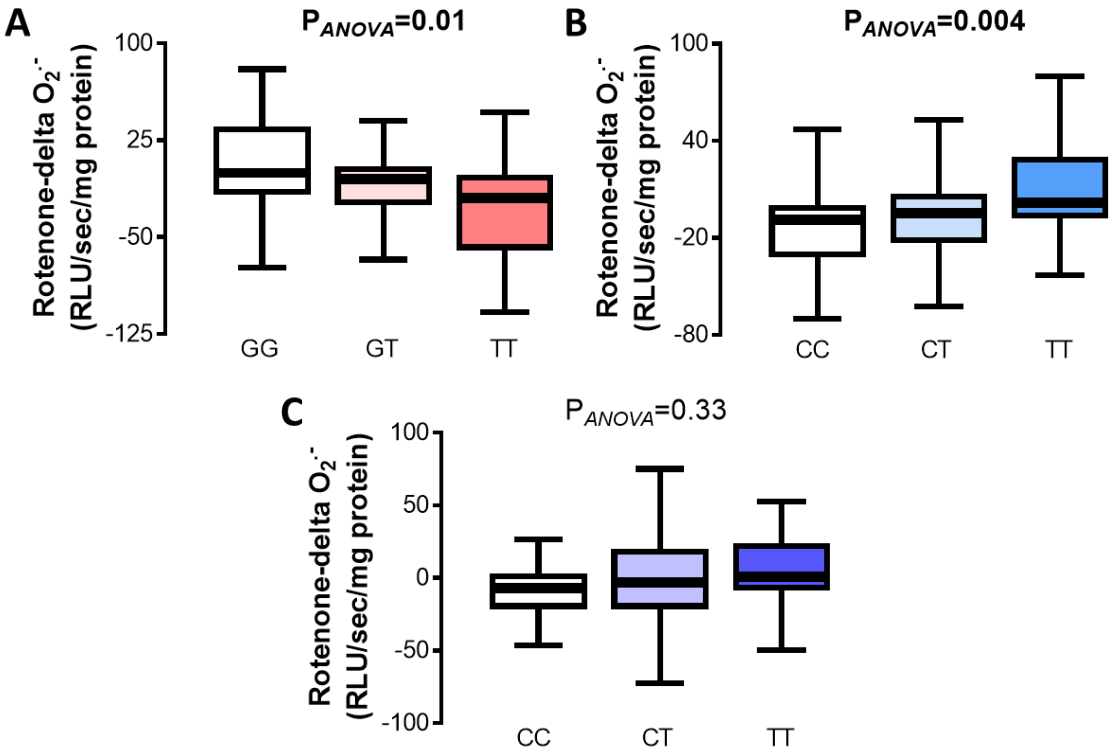


Figure 6.12 CSE and CBS SNPs and Mitochondrial Redox State

To examine the role of CSE in regulating myocardial redox state, we explored the effects of a SNP in CSE on myocardial redox state. CSE SNP rs1021737 risk alleles (TT) led to increased $O_2^{\cdot-}$ from mitochondria as indicated by reduced rotenone-delta $O_2^{\cdot-}$ (**A**, P_{ANOVA}=0.01; P=0.025 between GG and TT in post-hoc analysis; n=77, 63, 13 individuals per group). However, CBS SNP rs2851391 risk alleles (TT) led to a significant decrease in mitochondrial $O_2^{\cdot-}$ as indicated by an increase in rotenone-delta O_2.- (**B**, P_{ANOVA}=0.004; n=42, 71, 40 individuals per group). CBS SNP rs234709 risk alleles (TT) had no significant effect on mitochondrial $O_2^{\cdot-}$ generation as observed by rotenone-delta $O_2^{\cdot-}$ (**C**, P_{ANOVA}=0.33; n=51, 75, 27 individuals per group). CBS, Cystathionine β-Synthase. CSE, Cystathionine γ-Lyase. $O_2^{\cdot-}$, Superoxide. RLU, Relative Light Units. SNP, Single Nucleotide Polymorphism. Values are presented as median (25^{th} to 75^{th} percentile) and whiskers (Tukey). P-values from unpaired, non-parametric Kruskal-Wallis test followed by Dunn's post hoc correction for multiple comparisons.

6.3.2 $O_2^{\cdot-}$ from NOSs and $ONOO^-$ in the Heart

We next asked whether the CSE and CBS risk alleles increased $O_2^{\cdot-}$ from NOSs and $ONOO^-$ in the heart. We found that CSE risk alleles did not alter $O_2^{\cdot-}$ from NOSs or $ONOO^-$ levels, but we observed a strong trend for increased uncoupling in NOSs with CSE risk alleles (Figure 6.13).

Similarly, we found that CBS rs2851391 risk alleles did not alter $O_2^{\cdot-}$ from NOSs or $ONOO^-$ levels, but we observed a strong trend for increased uncoupling in NOSs and increased $ONOO^-$ levels with CBS rs2851391 risk alleles (Figure 6.13). CBS rs234709 risk alleles had no effect on $O_2^{\cdot-}$ from NOSs or $ONOO^-$ levels; no trends were observed (Figure 6.13).

6.3.3 Basal $O_2^{\cdot-}$ and $O_2^{\cdot-}$ from NADPH Oxidases in the Heart

We also asked whether CSE and CBS risk alleles increased basal $O_2^{\cdot-}$ and $O_2^{\cdot-}$ from NADPH oxidases in the heart. We found that CSE risk alleles did not alter basal $O_2^{\cdot-}$ and $O_2^{\cdot-}$ from NADPH oxidases, but we observed a strong trend for reduced $O_2^{\cdot-}$ generation from NADPH oxidases with CSE risk alleles (Figure 6.14). We found that CBS rs2851391 risk alleles also did not alter basal $O_2^{\cdot-}$ and $O_2^{\cdot-}$ from NADPH oxidases, but in contrast to CSE risk alleles, we observed a strong trend for increased $O_2^{\cdot-}$ from NADPH oxidases with CBS rs2851391 risk alleles (Figure 6.14). CBS rs234709 risk alleles had no effect on $O_2^{\cdot-}$ basal $O_2^{\cdot-}$ and $O_2^{\cdot-}$ from NADPH oxidases and no trends were observed (Figure 6.14).

6.3.4 Plasma H_2S/Sulfide Levels and Myocardial Gene Expression

Finally, we examined whether CSE and CBS risk alleles exerted their effects on myocardial redox state through alterations in Plasma H_2S/Sulfide levels or myocardial expression of CSE, CBS, or MST. We observed CSE, CBS rs2851391 and CBS rs234709 risk alleles did not affect plasma H_2S/Sulfide levels (Figure 6.15).

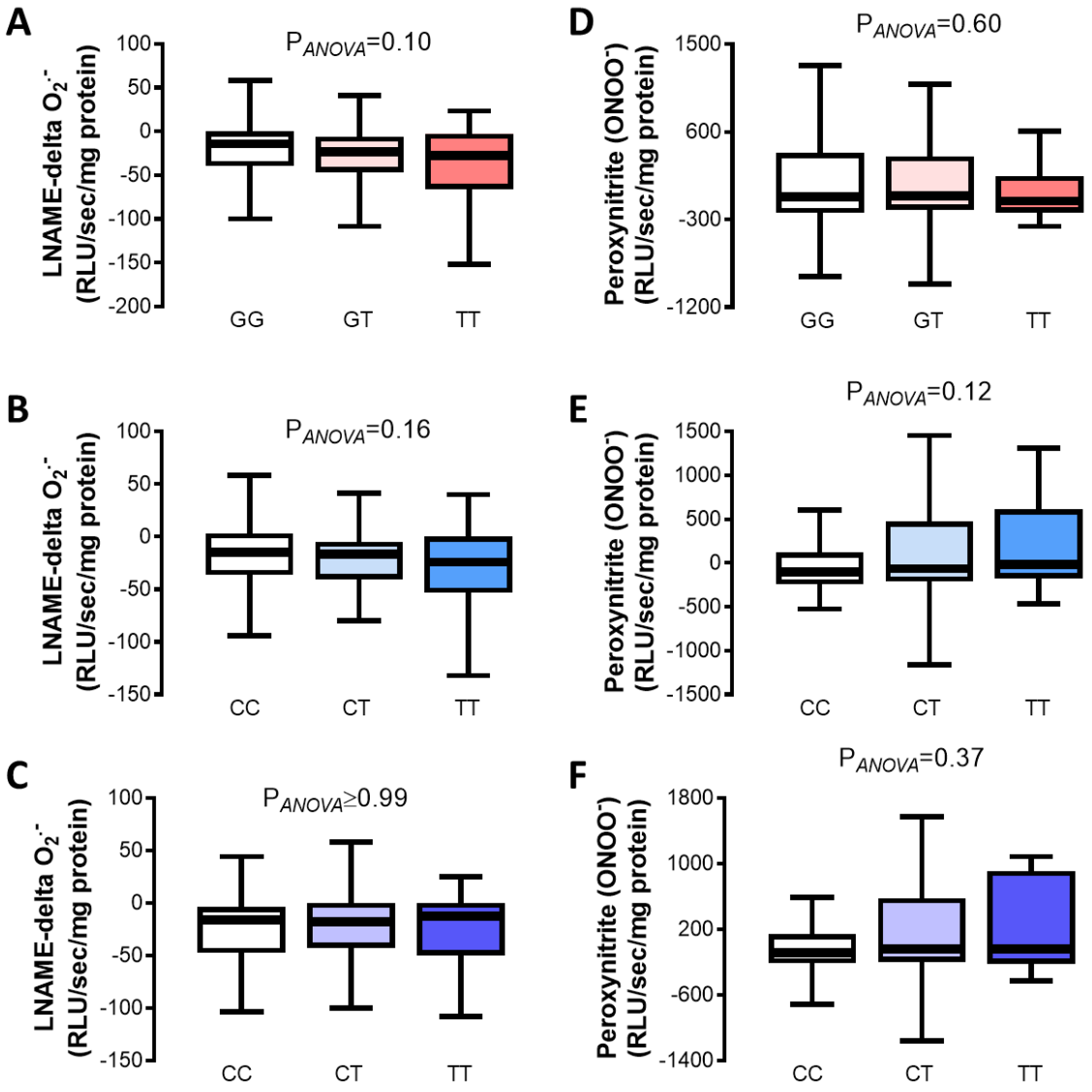


Figure 6.13 CSE and CBS SNPs and $O_2^{\cdot-}$ from NOSs and $ONOO^-$ Levels

CSE SNP rs1021737 risk alleles (TT) did not significantly affect $O_2^{\cdot-}$ from NOSs but a strong trend was observed towards increased uncoupling of NOSs with CSE risk alleles (**A**, P_{ANOVA}=0.10; n=107, 95, 16 individuals per group). Moreover, a similar non-significant trend was observed towards increased uncoupling of NOSs with CBS rs2851391 risk alleles (TT) (**B**, P_{ANOVA}=0.16; n=59, 104, 55 individuals per group). CBS SNP rs234709 risk alleles (TT) had no significant effect on $O_2^{\cdot-}$ from NOSs (**C**, P_{ANOVA}≥0.99; n=73, 107, 38 individuals per group). $ONOO^-$ levels were not altered by CSE SNP rs1021737 risk alleles (**D**, P_{ANOVA}=0.60; n=98, 85, 14 individuals per group), CBS rs2851391 risk alleles (**E**, P_{ANOVA}=0.12; n=55, 91, 51 individuals per group), or CBS SNP rs234709 risk alleles (**F**, P_{ANOVA}=0.37; n=66, 98, 33 individuals per group). CBS, Cystathionine β-Synthase. CSE, Cystathionine γ-Lyase. $O_2^{\cdot-}$, Superoxide. $ONOO^-$, Peroxynitrite. RLU, Relative Light Units. SNP, Single Nucleotide Polymorphism. Values are presented as median (25^{th} to 75^{th} percentile) and whiskers (Tukey). P-values from unpaired, non-parametric Kruskal-Wallis test followed by Dunn's post hoc correction for multiple comparisons.

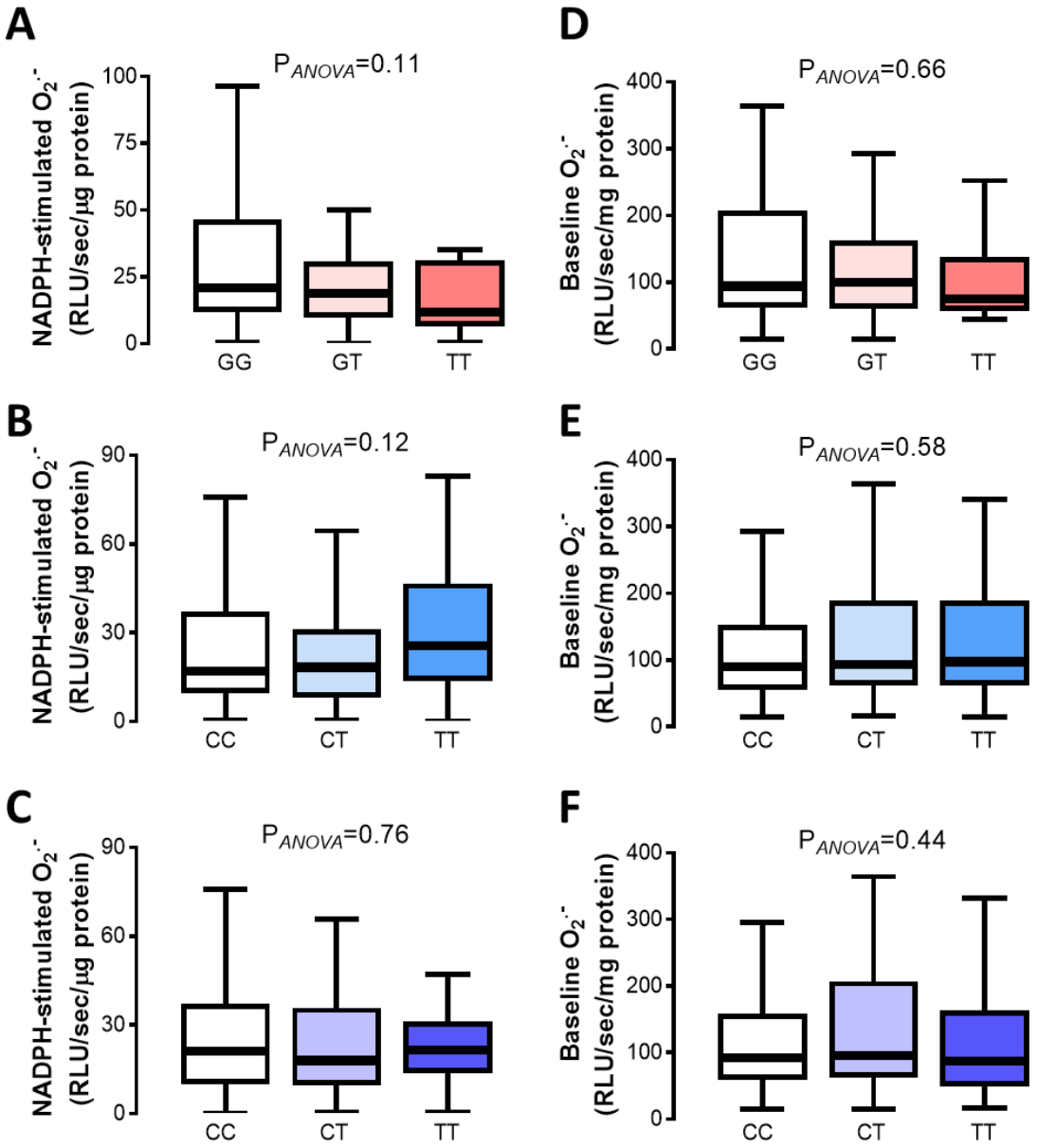


Figure 6.14 CSE and CBS SNPs, $O_2^{\cdot-}$ from NADPH oxidases, and Basal $O_2^{\cdot-}$

CSE SNP rs1021737 risk alleles (TT) did not significantly affect $O_2^{\cdot-}$ from NADPH oxidases but a strong trend was observed towards reduced NADPH-stimulated $O_2^{\cdot-}$ with CSE risk alleles (**A**, P_{ANOVA}=0.11; n=104, 94, 15 individuals per group). CBS rs2851391 risk alleles also did not affect $O_2^{\cdot-}$ from NADPH oxidases but a non-significant trend was observed towards increased NADPH-stimulated $O_2^{\cdot-}$ with CBS rs2851391 risk alleles (TT) (**B**, P_{ANOVA}=0.12; n=56, 100, 57 individuals per group). CBS SNP rs234709 risk alleles (TT) had no significant effect on $O_2^{\cdot-}$ from NADPH oxidases (**C**, P_{ANOVA}=0.76; n=72, 106, 35 individuals per group). Basal $O_2^{\cdot-}$ was not altered by CSE SNP rs1021737 risk alleles (**D**, P_{ANOVA}=0.66; n=109, 96, 17 individuals per group), CBS rs2851391 risk alleles (**E**, P_{ANOVA}=0.58; n=individuals per group), or CBS SNP rs234709 risk alleles (**F**, P_{ANOVA}=0.44; n=61, 104, 57 individuals per group). CBS, Cystathionine β-Synthase. CSE, Cystathionine γ-Lyase. $O_2^{\cdot-}$, Superoxide. RLU, Relative Light Units. SNP, Single Nucleotide Polymorphism. Values are presented as median (25^{th} to 75^{th} percentile) and whiskers (Tukey). P-values from unpaired, non-parametric Kruskal-Wallis test followed by Dunn's post hoc correction for multiple comparisons.

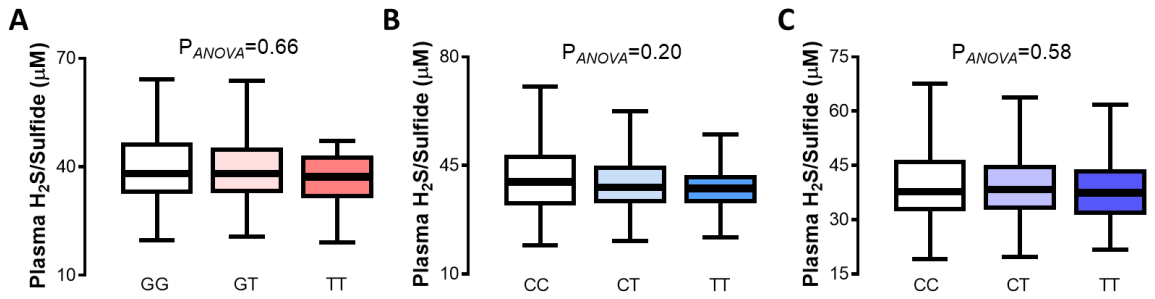


Figure 6.15 CSE and CBS SNPs and Plasma H_2S/Sulfide

Plasma H_2S/Sulfide levels were not increased by CSE SNP rs1021737 risk alleles (TT) (**A**, P_{ANOVA}=0.66; n=242, 220, 37 individuals per group), CBS rs2851391 risk alleles (**B**, P_{ANOVA}=0.20; n=150, 232, 111 individuals per group), or CBS SNP rs234709 risk alleles (TT) (**C**, P_{ANOVA}=0.58; n=124, 365, 109 individuals per group). CBS, Cystathionine β-Synthase. CSE, Cystathionine γ-Lyase. H_2S, Hydrogen Sulfide. SNP, Single Nucleotide Polymorphism. Values are presented as median (25^{th} to 75^{th} percentile) and whiskers (Tukey). P-values from unpaired, non-parametric Kruskal-Wallis test followed by Dunn's post hoc correction for multiple comparisons.

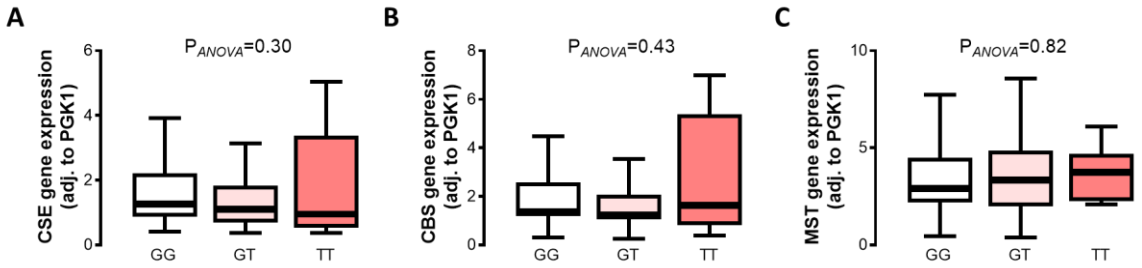


Figure 6.16 CSE SNP and Myocardial Gene Expression

CSE SNP rs1021737 risk alleles (TT) did not affect myocardial CSE gene expression (**A**, P_{ANOVA}=0.30; n=45, 44, 6 individuals per group), CBS gene expression (**B**, P_{ANOVA}=0.43; n=45, 44, 6 individuals per group), or MST gene expression (**C**, P_{ANOVA}=0.82; n=45, 44, 6 individuals per group). CBS, Cystathionine β-Synthase. CSE, Cystathionine γ-Lyase. SNP, Single Nucleotide Polymorphism. MST, 3-Mercaptopyruvate Sulfurtransferase. Values are presented as median (25^{th} to 75^{th} percentile) and whiskers (Tukey). P-values from unpaired, non-parametric Kruskal-Wallis test followed by Dunn's post hoc correction for multiple comparisons.

Furthermore, we observed that CSE risk alleles had no effect on myocardial CSE gene expression and CBS rs2851391 and CBS rs234709 risk alleles had no effect on respective myocardial CBS expression (Figure 6.16; Figure 6.17). Moreover, CSE risk alleles did not lead to compensatory increases in myocardial CBS or MST expression (Figure 6.16). Similarly, CBS rs2851391 and CBS rs234709 risk alleles did not lead to compensatory increases in myocardial CSE or MST expression (Figure 6.17). Taken

together, these findings support plasma H_2S/Sulfide-independent mechanisms by which these enzymes affect myocardial $O_2^{\bullet-}$ from mitochondria.

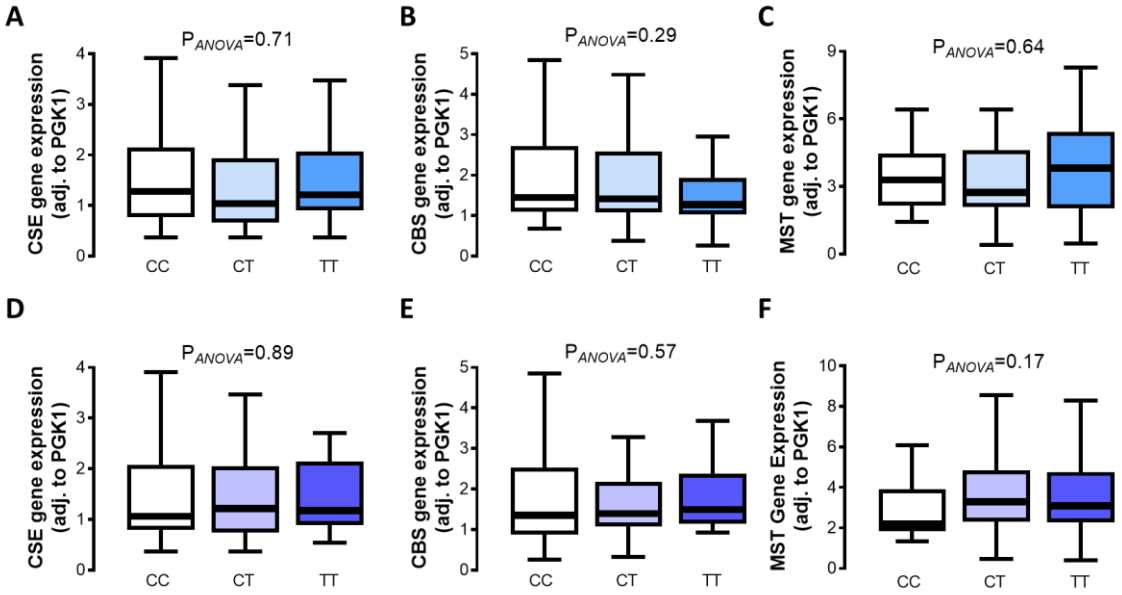


Figure 6.17 CBS SNPs and Myocardial Gene Expression

CBS SNP rs2851391 risk alleles (TT) did not affect myocardial CSE (**A**, P_{ANOVA}=0.71; n=24, 43, 27 individuals per group), CBS (**B**, P_{ANOVA}=0.29; n=24, 43, 27 individuals per group), or MST gene expression (**C**, P_{ANOVA}=0.64; n=24, 43, 27 individuals per group). CBS SNP rs234709 risk alleles (TT) did not affect myocardial CSE (**D**, P_{ANOVA}=0.89; n=24, 51, 20 individuals per group), CBS (**E**, P_{ANOVA}=0.57; n=24, 51, 20 individuals per group), or MST gene expression (**F**, P_{ANOVA}=0.17; n=24, 51, 20 individuals per group). CBS, Cystathionine β-Synthase. CSE, Cystathionine γ-Lyase. SNP, Single Nucleotide Polymorphism. MST, 3-Mercaptopyruvate Sulfurtransferase. Values are presented as median (25^{th} to 75^{th} percentile) and whiskers (Tukey). P-values from unpaired, non-parametric Kruskal-Wallis test followed by Dunn's post hoc correction for multiple comparisons.

Chapter 7 Discussion

In this study, we investigated whether H_2S biology is related to human myocardial redox state in samples from a cohort of patients undergoing cardiac surgery (Oxford Heart, Vessels, and Fat Cohort; Ox-HVF) and whether H_2S/CSE biology plays a causal role in regulating myocardial redox state. Taken together, we demonstrate for the first time that H_2S and CSE biology is linked to human myocardial redox state and has a causal role in redox regulation (Figure 7.1). These endogenous regulatory mechanisms are crucial to understand as they may be part of the endogenous defence mechanisms that exist in the heart which may be dysregulated in cardiac disease (Figure 7.1).

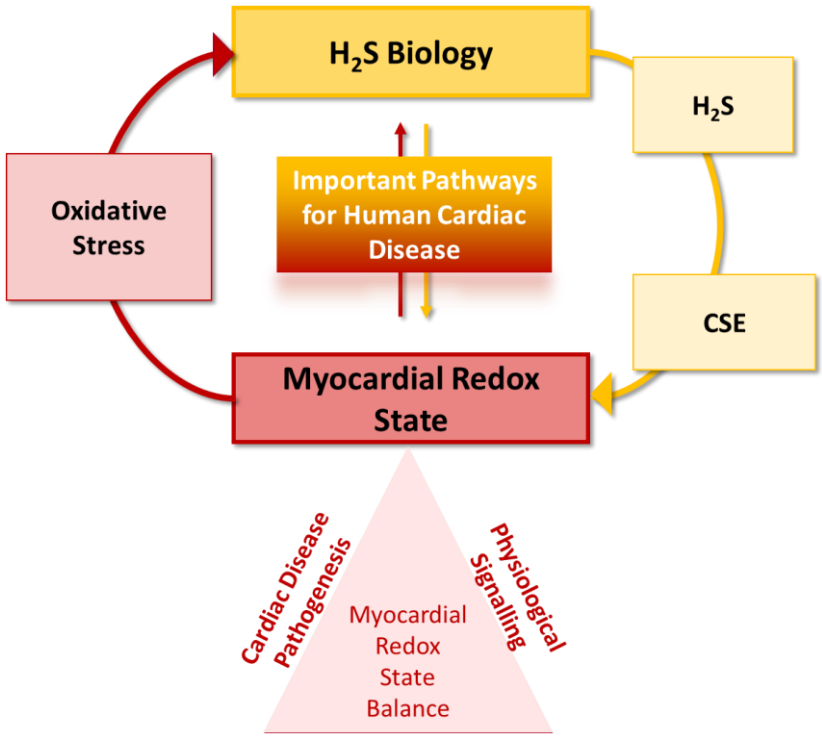


Figure 7.1 Overview of Bidirectional Interaction: H_2S, CSE & Redox State

7.1 H_2S/CSE Biology and Mitochondrial Oxidases

Mitochondria and particularly the mitochondrial electron transport chain are well-known sources of $O_2^{\cdot-}$ generation in the heart.[209] In addition to the physiological role of mitochondrial $O_2^{\cdot-}$ in regulating redox signalling, it has also been shown that

mitochondrial oxidative stress contributes to heart failure, ischemia-reperfusion injury, and cardiomyopathies.[209-211] Regulating the generation of mitochondrial $O_2^{\cdot-}$ is crucial in the heart; accordingly, therapeutic strategies are being developed with a current focus on activating mitochondrial antioxidant enzymes and providing mitochondria-targeted antioxidants.[209,210]

7.1.1 H_2S/Sulfide and Mitochondrial Redox State

H_2S has been examined in the context of mitochondrial function, regulating energetics and respiration particularly in hypoxic and ischemic conditions, but only briefly in the regulation of the generation of mitochondrial $O_2^{\cdot-}$ which is crucial in the human heart.[137,212,213] In the present study, we found that individuals who had increased mitochondrial $O_2^{\cdot-}$ generation post-complex I in their heart had higher circulating H_2S/Sulfide levels, suggesting a possible link between H_2S biology and mitochondrial redox balance in the human heart in advanced stages of cardiac disease. Several studies have specifically shown that H_2S oxidation takes place primarily in the mitochondria and H_2S can serve as an electron donor of the electron transport chain and inhibit complex IV.[138,214,215] Another study has further identified the role of H_2S in increasing glutathione in the mitochondria to suppress oxidative stress.[216] These findings are consistent and support strongly the relationship between systemic H_2S in the mitochondria and mitochondrial $O_2^{\cdot-}$ generation that may have importance in the human heart and be dysregulated in cardiac disease.

7.1.2 CSE/CBS and Mitochondrial Redox State

We further found that a single nucleotide polymorphism in CSE and in CBS both alter mitochondrial redox state in the heart. Particularly individuals homozygous for CSE SNP rs10271737 risk alleles had significantly increased $O_2^{\cdot-}$ from mitochondria in the heart while individuals homozygous for CBS SNP rs2851391 risk alleles had significantly

reduced $O_2^{\cdot -}$ from mitochondria post-complex I, providing compelling evidence of a direct causal role for CSE and CBS in mitochondrial redox state regulation in the human heart. These effects, independent of alterations in the myocardial expression of CSE and CBS, respectively, suggest further studies are needed into the activity of CSE and CBS in relation to these SNPs and mitochondrial redox state. In corroboration with our findings, a study in cellular and animal models suggest CSE and CBS regulates mitochondrial oxidative stress.[217] Whether mitochondrial H_2S is part of the mechanism behind these effects will be important in future studies. Our findings of CSE and CBS's role in regulating mitochondrial redox state in the human heart provide support for understanding CSE and CBS biology in the regulation of mitochondrial oxidative stress contributing to cardiac disease.

7.2 H_2S/CSE Biology and NOSs

NOSs are another key regulator of redox signalling in the heart with coupled NOSs generating NO and uncoupled NOSs generating $O_2^{\cdot -}$ contributing to cardiac disease pathogenesis.[34,218] Current therapeutic strategies to increase NOS signalling include increasing NOS activity, providing nitrates and nitrites, and activating downstream signalling.[45]

7.2.1 Direct Effects of H_2S on and NOS Coupling Status

H_2S biology is also an important regulator of NOS biology known to activate NOSs.[118,124] Studies examining the role of H_2S in altering $O_2^{\cdot -}$ from NOSs have been limited. In our study, we found that H_2S from NaHS selectively improved NOS coupling and reduced $ONOO^-$ in myocardium from patients with cardiac disease. These effects were selective, without altering other sources of $O_2^{\cdot -}$, and with no effects in cells without cardiac disease. These findings are consistent with the protective effects of H_2S observed

in increasing nitric oxide bioavailability (NO-derived metabolites) in humans.[116] In contrast to NaHS, we find that H_2S from GYY4137 (low concentrations, slow-releasing donor) initially has no effect on NOSs but over time, leads to increased uncoupling. This finding suggests that low concentrations of H_2S in advanced cardiac disease states impairs uncoupling. This novel observation that H_2S at low concentrations can lead to uncoupling of NOSs over time suggests a clear distinction between supra-physiological concentrations of H_2S that are protective against NOS uncoupling in disease. Previous studies demonstrating protective effects via DADS, NaHS/Na_2S, SG-1002, and other donors may need to be examined in the context of the kinetics of H_2S release from these respective donors as this present study does.

Our findings further suggest a difference in H_2S's effects under basal conditions and oxidative stress; the most clear effects of exogenous H_2S may only be evident in the presence of disease. A difference in H_2S's effects under basal conditions and oxidative stress is corroborated by a recent study demonstrating differences in CSE activity under basal conditions and endoplasmic reticulum stress, differences that can be protective or contribute to disease mechanisms.[219]

We further demonstrate that NaHS's protective effects in advanced cardiac disease states are not BH_4-mediated. Although previous studies have shown that long-term administration of H_2S can affect BH_4 ratios, we find that short-term administration of H_2S improved NOS coupling and this was not directly mediated by changes in BH_4 ratios or levels in advanced stages of cardiac disease.[124] Given recent findings suggesting that S-glutathionylation mediates uncoupling in atrial appendages rather than BH_4 depletion, our findings may be promising for a short-term non-BH_4 based therapeutic strategy for coupling of NOSs.[220] Here, we may not see alterations in BH_4 which may be significantly altered after years of disease and high concentrations of rapid-release NaHS is unable to

alter entire BH_4 ratios. Other known mechanisms for modulating coupling status of NOSs include changes in S-glutathionylation (at least in eNOS) and H_2S's own posttranslational modification persulfidation may be involved in altering residues on NOS. Although testing these modifications was out of the scope of this thesis, it would be interesting to see if H_2S improves coupling by NOSs by S-sulfhydrating a glutathionylated residue (including nNOS). Our findings demonstrate that H_2S plays a direct role on the coupling status of NOSs that may be modulated distinctly in cardiac disease states and with donors of different kinetics.

Differences in H_2S Release Profiles by Donors

Given the differences in effects of these two donors, our findings further highlight the importance of distinguishing fast and slow-releasing H_2S donors which we characterize here when examining H_2S's direct effects, both in the short-term and long-term, and in advanced cardiac disease states. We measured H_2S release from NaHS versus GYY4137 by measuring their release in similar environments with the same technique. These distinct H_2S release profiles are consistent with prior studies examining the profile of these donors in various physiological contexts.[221,222] We further show that NaHS does not result in a pH change in physiological buffers, eliminating pH changes as a mediating factor for H_2S effects from NaHS. Together our amperometric results lay not only the foundation of the kinetic parameters chosen for *ex vivo* experiments but provide new insight for interpretation of past experiments conducted with NaHS and GYY4137 and may help direct investigators towards mechanisms more in line with such high H_2S release from NaHS and slow release of H_2S from GYY4137. Numerous studies have found beneficial results utilizing NaHS in disease models.[223] However, in the context of these donor profiles, it will need to be examined if the results are biologically and physiologically meaningful. In other studies, the same questions may be raised regarding

the use of GYY4137 provided sustained release of H_2S.[224] Thus, taken together, understanding the kinetics of H_2S release may guide mechanistic explorations and interpretations of pre-clinical studies with H_2S *in vitro*, *in vivo,* and *ex vivo*.

7.2.2 Myocardial CSE and CBS Expression and NOS Coupling Status

In this study, we also found that individuals with cardiac disease who have increased myocardial CSE and CBS expression have significantly more uncoupled NOSs suggesting a crucial link between increased expression of CSE and CBS and NOS coupling status in the human heart. Furthermore, we find that higher myocardial CSE expression is linked with increased $ONOO^-$ in the heart, but higher myocardial CBS expression is not linked with $ONOO^-$, suggesting differences between these enzymes' relationship with NOS biology. We propose that myocardial CSE and CBS's association with increased uncoupling of NOSs in cardiac disease is a reflection of a possible relationship that contribute to disease pathogenesis, but the direction of this association is needed. Our SNP model in CSE and CBSs show a similar trend for casually altering the coupling status of myocardial NOSs but the finding may be underpowered. These findings provide novel insight into the role of endogenous CSE and CBS in the heart and its relationship with the coupling status of myocardial NOSs.

7.3 Bidirectional Interaction of H_2S Biology and Oxidative Stress

7.3.1 CSE on Basal $O_2^{\cdot-}$ in an Unchallenged Model

We further explored the role of CSE in regulating basal $O_2^{\cdot-}$ in an unchallenged model. We found that in the absence of CSE, cells had reduced basal $O_2^{\cdot-}$ and lower $ONOO^-$ with no effects on $O_2^{\cdot-}$ from NOSs in the absence of challenge. CSE is a critical enzyme known to play a role in key physiological pathways and, to date, the generation of H_2S is one of the many roles CSE plays in the transsulfuration pathway.[144] Thus, the

absence of CSE may be mediated by numerous factors. While several studies have focused on CSE's protective role in models of injury (e.g. ischemia-reperfusion injury, heart failure models), CSE knockout mice in the absence of challenge showed no evidence for changes in vascular oxidative stress despite leading to hypertensive mice.[225] Indeed our results may be consistent with these findings if the absence of CSE is protective in homeostatic conditions but the absence of CSE is detrimental under challenge or exposure to oxidative injury. Moreover, in the same way that NOSs have two states, generating $O_2^{\cdot -}$ and NO depending on their coupling status, CSE may indeed have different roles depending on environmental determinants of their status as a recent study suggests CSE switches its substrate selectivity.[144] It is also important to note that many of the potential protective effects of CSE on myocardial redox state have been observed with regards to systemic markers of oxidative stress and increases in antioxidant defence systems, which may differ from effects on local myocardial oxidative stress.

7.3.2 Redox-Sensitivity of CSE

We have also found that individuals with increased NADPH oxidase activity have increased myocardial CSE, CBS, and MST, possibly as a protective upregulation. When we explored causality, we found that chronic increase in systemic oxidative stress in humans (by CYBA SNPs) did not affect expression (with current power to detect differences). When examining the effects of acute oxidative stress, we found that increased acute oxidative stress reduces gene expression of myocardial CSE without altering myocardial gene expression of CBS, MST, or SP1. These findings suggest that oxidative stress or oxidative injury in the short-term impairs CSE expression independent of SP1 expression. This is consistent with previous studies suggesting the redox-sensitivity of CSE.

7.4 H_2S/CSE Biology, Cardiac Disease, and Clinical Risk Factors

7.4.1 Endogenous H_2S/Sulfide and Gender

Studies have examined H_2S biology in different genders and have found gender-specific differences in humans.[226] Furthermore, even in animal studies including CSE knockout mice, male and female mice had different H_2S biology (e.g. homocysteine levels) underlying their hypertensive profiles.[225] We have found that females have marginal but significantly elevated plasma H_2S/Sulfide levels compared to males. It will be important to examine these levels by a second method of measuring H_2S/Sulfide (e.g. gas chromatography). These findings suggest subtle differences between genders but the biological importance of these differences for cardiovascular disease risk are unknown and actively being explored.

These gender differences may be explained by the different hormones that have been found to regulate H_2S biology.[226] As these hormones largely act in *in vivo* systems, these gender differences are likely to be observed *in vivo*. Though measuring these hormone levels to examine the underlying biology behind these differences was not in the scope of this cohort, we were able to examine gender differences in other parameters. We found that indeed in males only, plasma H_2S/Sulfide was significantly associated with changes in ejection fraction while in the cohort-wide study (females only underpowered), this was not significant (data not shown). Furthermore, plasma H_2S/Sulfide levels were significantly associated changes in IGF1 levels compared to the entire cohort where these findings were not significant (data not shown). Taken together, these findings suggest that human differences in H_2S biology exist and are related to the cardiovascular system and suggest further investigation in both differences and underlying mechanisms. Our findings further support that differences in gender in H_2S biology may not be trivial in humans.

7.4.2 Endogenous H_2S/Sulfide and Insulin Resistance

Diabetes, a risk factor for cardiovascular disease, has been linked to H_2S biology in several ways. Previous studies have examined whether circulating H_2S levels differ in diabetes, given H_2S has been shown to play a role in the pancreatic islet, in the liver, in insulin signalling.[160-162] Consistent with alterations in H_2S biology in diabetes in literature, we have found that individuals with diabetes have significantly lower H_2S levels compared to individuals with HOMA-IR>2.9 (and no diabetes mellitus). Specifically, we have found reduced plasma H_2S/Sulfide levels in individuals with advanced cardiac disease who have diabetes mellitus compared to individuals with advanced cardiac disease who have insulin resistance without diabetes (HOMA-IR>2.9 and no diabetes mellitus). No differences were observed in individuals with diabetes versus no diabetes, suggesting total H_2S/Sulfide becomes more relevant in the context of baseline insulin resistance and metabolic syndrome, and clear exacerbated effects in hydrogen sulfide biology are seen when insulin resistance moves from insulin resistance to diabetes with insulin resistance.

It is believed that H_2S contributes to the early onset of diabetes and the large use of H_2S from pancreatic cells and hepatocytes leads to reduced plasma H_2S levels over time; this reduction contributes to other diseases and diabetes-related complications including cardiovascular disease as suggested by studies demonstrating reduced levels of H_2S in cardiomyocytes in late stages of diabetes.[84] Several studies have specifically shown that patients with type 2 diabetes have reduced plasma H_2S plasma levels compared to non-diabetic individuals.[160-162] Furthermore, within those patients that had type 2 diabetes, one recent study suggests that individuals with cardiovascular disease (coronary and peripheral artery disease, and cerebrovascular disease) have significantly lower plasma H_2S levels compared to diabetic individuals without cardiovascular

disease.[160] These findings suggest a possible relationship between lower plasma H_2S levels and diabetic complications of cardiovascular disease. Our study corroborates that H_2S levels are reduced in DM in individuals with advanced cardiac disease compared to individuals with advanced cardiac disease with only insulin resistance.[84] Our findings provide support at the individual level that potentially increasing H_2S to the heart or peripheral tissues (given our finding that there is a low circulation of H_2S in DM) as DM develops from high insulin resistance stages (HOMA-IR>2.9) to the development of diabetes may be important to counter the reduced levels that are found in DM that may contribute to diabetic-complications like cardiovascular disease.[84]

Given that other metabolic profile variables (e.g. BMI and W:H ratio) were not related to plasma H_2S/Sulfide levels does not exclude the relationship between adiposity and plasma H_2S/Sulfide but suggests that individuals with advanced cardiac disease, the relationship may be less relevant or shadowed by other determinants (e.g. pancreatic and hepatic variations in H_2S biology). These findings in combination with effects of H_2S/CSE/CBS biology on mitochondrial $O_2^{\cdot -}$ (which also contributes to diabetes) may have important implications for diabetes.

7.4.3 Myocardial CBS Expression Reduced in Hypercholesterolemia

Hypercholesterolemia which results in increased lipid content is important in cardiovascular disease development. Myocardial CBS expression was reduced in individuals with hypercholesterolemia compared to individuals without hypercholesterolemia. Our findings suggest an importance in studying whether myocardial CBS plays a role in reducing lipids versus lipids playing a role in regulating and reducing myocardial CBS expression. We also observed a similar trend for reduced myocardial CSE expression in individuals with hypercholesterolemia compared to individuals without hypercholesterolemia. Statins which are medications that lower lipid

levels may regulate myocardial CSE/CBS expression and studies specifically suggest that certain statins may increase H_2S production and alter expression of CSE.[227,228] This would be in line with the hypothesis that statin-driven reduction in lipids increases CSE/CBS expression, thereby increasing H_2S. It will be crucial to examine whether part of statins effects on H_2S biology are mediated by lipids in the human heart.

7.4.4 Myocardial MST in Hypertension and Cardiac Function

A previous study has illustrated a role for CSE in hypertension[225] and we asked whether expression of CSE, along with CBS and MST, was altered in hypertension. We found that individuals with hypertension had significantly elevated myocardial MST expression but no differences in CSE or CBS expressions compared to individuals with no hypertension, suggesting further examination into MST and its role in blood pressure regulation. We have also found that myocardial MST expression is associated with reduced LVEDV and LV Mass (correlation with LA diameter may be due to statistical chance given multiple comparisons and significance not observed across tertiles).

7.5 Study Limitations

7.5.1 Measurements of H_2S

When these experiments were conducted with methylene blue from October 2014 to December 2014, the methylene blue assay was still standard method used to quantify H_2S in the field. However, in more recent years, newer techniques have been developed, optimized, and become wide-spread in use. We understand that using the methylene blue assay to measure plasma H_2S is an indication of plasma H_2S/Sulfide levels. We clearly interpret our findings as associations with plasma H_2S/total sulfide levels, and present an important body of work relating these sulfide levels to cardiovascular disease in humans. These findings are very important now given the rising importance of not simply the gas

H_2S but polysulfides, suggesting an importance of measuring levels of different sulfur-containing compounds; moreover, the ability of H2S to be oxidized in plasma to other sulfur-containing compounds suggests the importance of finding H2S gas-derived stable biomarkers.[84]

In order to examine whether H_2S (gas only) is correlated with myocardial redox state, we proposed measuring plasma H_2S in our cohort using a different technique, e.g. gas chromatography sulfur chemiluminescence (GC-SC). We have a collaboration now in place to measure these samples with GC-SC. Our findings are helpful for a literature that is full of different methods of measuring H_2S at the moment and suggests from a comprehensive examination that different methods should be used to measure H_2S gas specifically and examine its relationship with cardiovascular disease. It will be interesting to examine whether sulfide levels and gas only levels correlate in a large cohort of individuals where samples are matched and moreover if similar findings are observed between gas only levels and cardiovascular disease. As techniques progress, the further step, if possible, would be to measure myocardial tissue levels of H_2S and determine their association if any with myocardial redox state.

7.5.2 Power Analysis

Clinical Studies

A potential limitation of our study would be lack of clinical power to detect differences when such difference does exist, or a Type II error. We performed power calculations to compute the sample size (n) required to achieve a power of 0.9 based on our current clinical data (‘pilot data’). Given the strong trend of CSE rs1021737 and CBS rs2851391 SNP risk alleles relationship to NOS biology, we were particularly interested in the sample size required to detect differences between individuals homozygous with

and without the risk alleles of these SNPs and $O_2^{\cdot -}$ from NOSs. Sample screenshot of power analysis is shown (Figure 7.2).

CSE rs1021737

For individuals homozygous for the G allele (GG, n=107), the mean $O_2^{\cdot -}$ from NOSs was -26.1 RLU/sec/mg protein with standard deviation of 59.8 RLU/sec/mg protein. For individuals homozygous for the T risk allele (TT, n=16), the mean $O_2^{\cdot -}$ from NOSs was -37.3 RLU/sec/mg protein with standard deviation of 45.0 RLU/sec/mg protein. With these means and standard deviations, we had an effect size of 0.21. Using the Means Statistical Test (Wilcoxon-Mann-Whitney test for two groups), given this effect size and an allocation ratio N2/N1 of 0.15, to achieve a power of 0.9 with α=0.05 would require an estimated sample size of 1768 (n=1537 GG and n=231 TT). To achieve a power of 0.8 with α=0.05, an estimated sample size of 1276 (n=1110 GG and n=166 TT) would be required.

CBS rs2851391

For individuals homozygous for the C allele (CC, n=59), the mean $O_2^{\cdot -}$ from NOSs was -20.8 RLU/sec/mg protein with standard deviation of 49.0 RLU/sec/mg protein. For individuals homozygous for the T risk allele (TT, n=55), the mean $O_2^{\cdot -}$ from NOSs was -36.3 RLU/sec/mg protein with standard deviation of 52.2 RLU/sec/mg protein. With these means and standard deviations, we had an effect size of 0.31. Using the Means Statistical Test (Wilcoxon-Mann-Whitney test for two groups), given this effect size and an allocation ratio N2/N1 of 0.93, to achieve a power of 0.9 with α=0.05 would require an estimated sample size of 386 (n=200 GG and n=186 TT). To achieve a power of 0.8 with α=0.05, an estimated sample size of 280 (n=145 GG and n=135 TT) would be required.

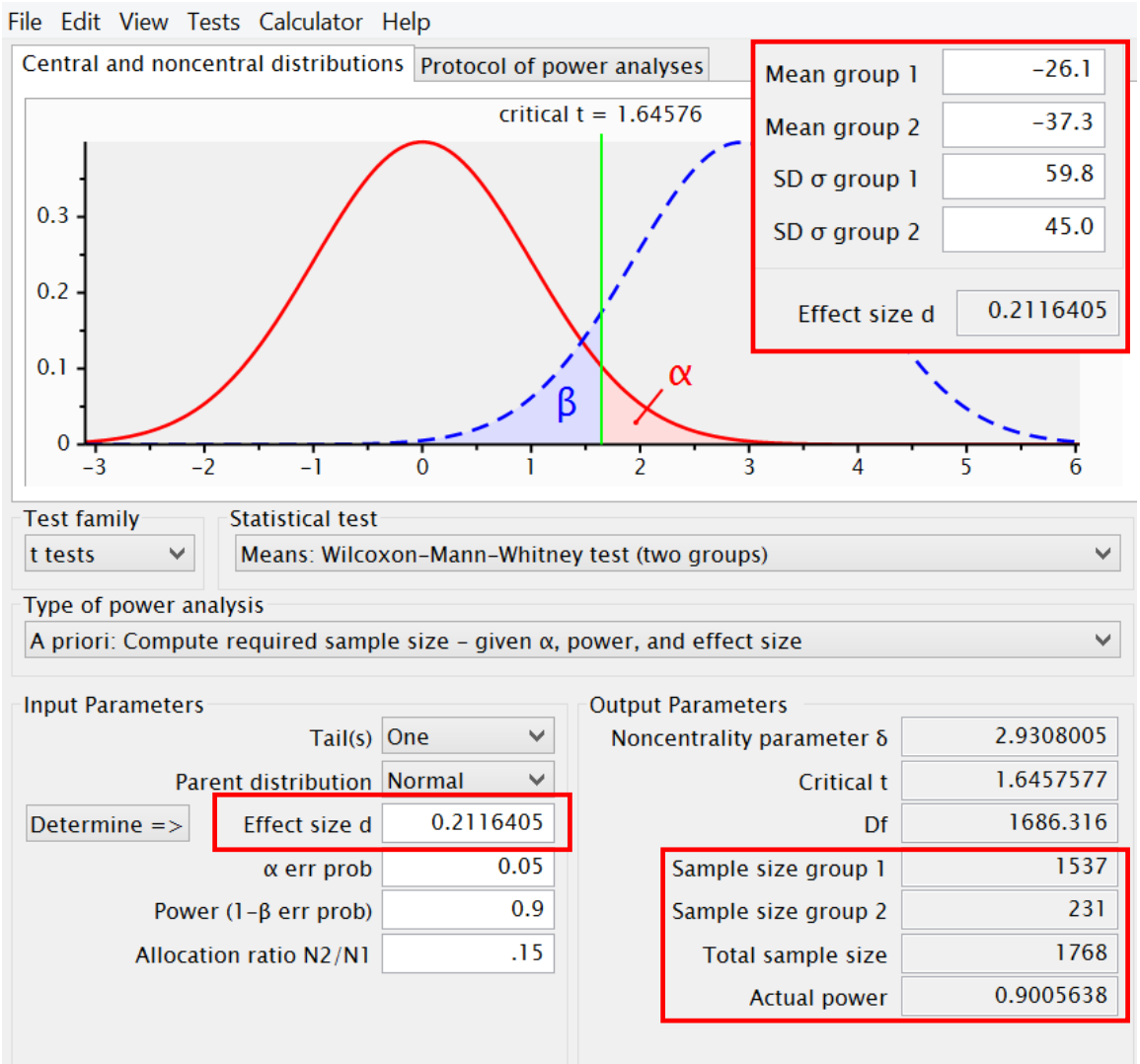


Figure 7.2 Power Calculations for CSE SNP rs1021737 and $O_2^{\cdot-}$ from NOSs

Example of power analysis on G*Power is shown. The screenshot of the software shown was used for estimating the sample size needed to detect a difference is $O_2^{\cdot-}$ from NOSs based on mean and standard deviations for individuals homozygous for GG compared to individuals homozygous for TT for CSE SNP rs1021737. Representative screenshots of G*Power Calculations are shown.

With increased clinical power, we will be able to examine by multivariable analysis whether myocardial NADPH oxidases activity is an independent predictor of myocardial CSE, CBS, and MST expression, independent of potential systemic confounders like systemic oxidative stress (e.g. MDA).

These findings would help elucidate whether CSE, CBS, and MST gene expression is under the influence of and related to local myocardial processes, a reflection of the

redox state of the heart. Furthermore, with increased clinical power, we will be able to examine whether plasma H_2S/Sulfide and myocardial CSE expression is related to cardiac disease (e.g. heart failure) and incidence of post-operative atrial fibrillation. These findings would help clarify the potential relationships between H_2S/CSE biology and clinical outcomes in individuals with advanced cardiac disease states.

It is difficult to achieve power with a transfected cell line. However, several constructs can be used to silence CSE in H9C2 cells and generate different knockdown cell lines. To further examine the causal role of CSE in homeostatic conditions, it will be important to generate this silenced cell line multiple times (while this will be n=1 within the same cell line, this eliminates the confounding factor of where the construct was inserted). Increasing the number of independent knockdowns here confirming these results would be needed and then exploration of the mechanism.

7.6 Future Directions

7.6.1 Computational Analysis of SNPs and/or Site-Directed Mutagenesis

We have identified CSE and CBS SNPs as having a causal role in regulating mitochondrial $O_2^{\cdot -}$ in the heart and further characterization of these SNPs (e.g. characterization of SNP *in vitro* and *in vivo*) is worthwhile given these findings in humans. It will be crucial to use bioinformatic tools and software that can predict *in silico* and computationally the effects of missense SNPs and silent non-synonymous SNPs (which may lead to alternative splicing in transcripts that can mediate the mechanisms of these non-synonymous SNPs).

Furthermore, site-directed mutagenesis may reveal a more clear mechanistic understanding behind these SNPs' effects on mitochondrial redox state. Measuring mitochondrial H_2S levels using myocardial tissues from individuals with differing number of risk alleles for these SNPs may provide crucial evidence as to whether mitochondrial H_2S mediates the differences observed in individuals with differing number of CSE SNP rs10271737 risk alleles or CBS SNP rs2851391 risk alleles.

It may also be interesting to develop a Ser473Ile Mouse model to understand the full role of CSE in regulating mitochondrial oxidative stress. *In vitro* and *in vivo* characterization of these SNPs that have a functional role in regulating mitochondrial $O_2^{\cdot -}$ in the human heart will be crucial for better understanding the mechanisms that drive these effects.

7.6.2 Nested Case-Control Studies

With increased clinical power, it will also be exciting to design a nested case-control study in which individuals with no risk alleles or one risk allele (heterozygous) are matched with individuals with both risk alleles. This would allow for comparison between the genotypes through elimination of confounding factors for evaluation with lower sample numbers given the low allele frequency of the risk allele.

Similar nested case-control studies can be conducted for analysis of differences between matched individuals for example with diabetes mellitus versus individuals with insulin resistance but no DM (HOMA-IR>2.9 with no DM). There are a rich number of hypothesis-driven possibilities based on this work for future studies.

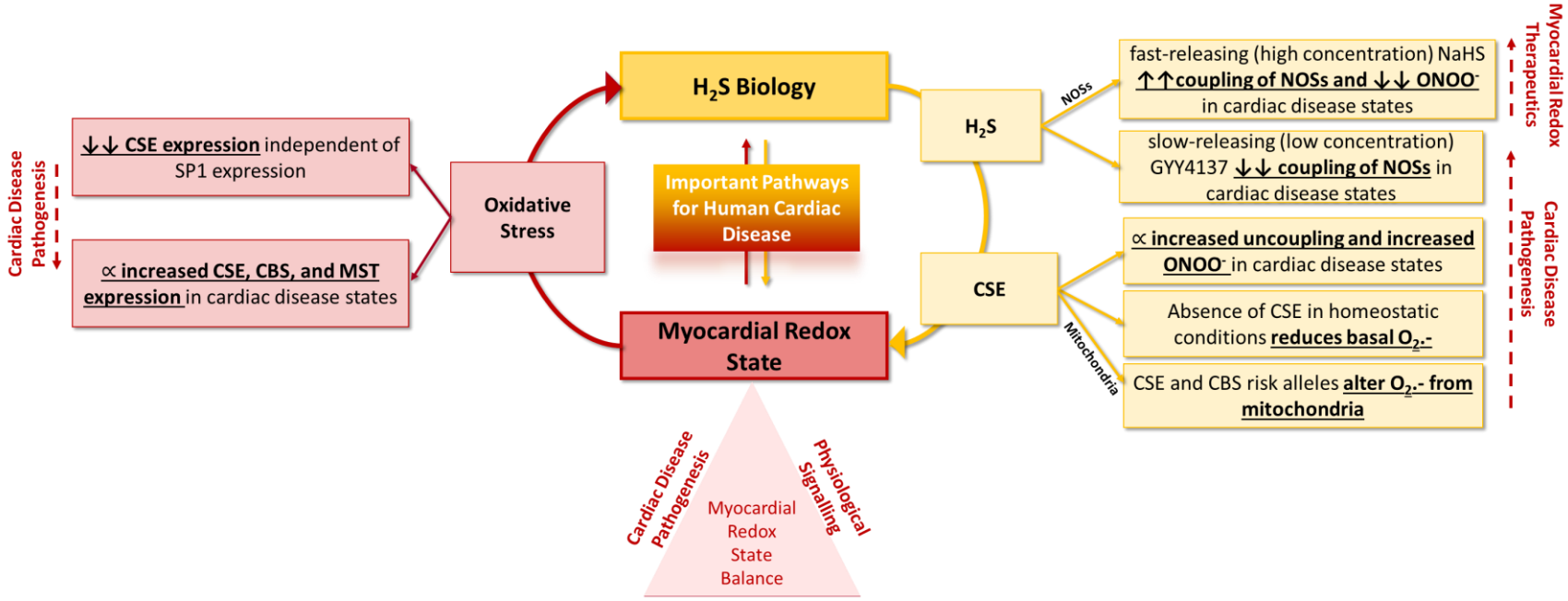


Figure 7.3 Detailed Overview of Bidirectional Interaction in the Human Heart

7.6.3 Limitations and Potential of the Field

It is not clear yet in the field of cardiovascular medicine how important H_2S biology ultimately will be. In 1998, the Nobel Prize was awarded to the 'molecule of the year' nitric oxide.[229] Although nitric oxide was a signalling molecule that was difficult to detect, part of its rise to medical prominence were due to its analogous counterparts: that is the development of nitrates as nitric oxide donors, the downstream pathways involving soluble guanylyl cyclase and cyclic GMP, the characterization of the nitric oxide synthase enzymes and its isoforms, and its reaction with $O_2^{\cdot-}$ to generate $ONOO^-$ helped the field jump forward and study concretely NO biology.[229] Limitations not only in measuring NO but its posttranslational modifications (S-nitrosylation) still pose challenges today but the concreteness of its counterparts has allowed the field to flourish.

The H_2S field is on its rise to prominence, and many researchers believe H_2S may be the 'next NO.' A comparison of the two fields provides clear understandings of the limitations of the young and emerging H_2S field, but also opportunities for closing gaps. Rather than one enzyme with different isoforms generating NO, H_2S has three different enzymes that generate H_2S and these enzymes have not been carefully characterized: it is still not clear where CSE, CBS, and MST are predominantly expressed or which reactions they catalyse and when these reactions are prioritized (some reactions do not generate H_2S as a by-product). There are no well-known stable molecules used to equate concentrations of H_2S, e.g. sulfates, although polysulfides are emerging. Furthermore, the signalling pathways that H_2S may activate have few key consistent targets and measuring posttranslational modifications S-sulfhydration or persulfidation have only begun recently. The varying H_2S donors being utilized by different groups without clear understanding of the kinetics of the donor *in vitro* or *in vivo* have also poses challenges in comparing different experimental studies and results. Nonetheless, mouse models of CSE

(and some of CBS and MST) are being well characterized and are starting to make the field itself more stable. Nonetheless, recognizing the tremendous developments in H_2S biology in medicine, we believe that the H_2S field, although young and emerging, has tremendous potential and will be a crucial part of research and clinical practice to come.

7.7 Conclusion

To help the field move forward, in this study we provide key findings where associations between myocardial H_2S biology and myocardial redox state were previously unknown. Using a unique cohort of individuals with advanced cardiac disease, we have demonstrated the bidirectional relationship between H_2S biology and myocardial redox state that should be considered when developing therapeutic strategies modulating myocardial oxidative stress for individuals facing cardiac disease.

Our findings identify novel relationships not only between myocardial H_2S biology and systemic H_2S biology and myocardial redox state, but also with key clinical risk factors in individuals who have advanced cardiac disease. Our findings further demonstrate the nuances of the transsulfuation pathways, that different enzymes CSE, CBS, and MST respond differently to oxidative stress and have different relationships to myocardial redox state while at the same time there are some common patterns.

To date, no large cohort study using human and translational tools has been conducted to investigate the role of H_2S and all three enzymes in the human myocardium in advanced stages of cardiac disease. Our findings bolster the ongoing research in H_2S/CSE biology by demonstrating its relationship with myocardial redox state in the human heart. Further investigation into modulating H_2S/CSE biology for cardiovascular therapeutic strategies against redox-sensitive cardiac disease has tremendous potential.

Appendix Abstracts and Publications

Abstracts

Oral/Poster Presentations:

Tarun, A., Psarros, C., Sanna, F., Herdman, L., Akoumianakis, I., Antonopoulos, A., Sayeed, R., Krasopoulos, G., Chuaiphichai, S., Channon, K.M., Antoniades, C. "Redox-sensitive regulation of Cystathionine γ-Lyase (CSE) and the potential protective role of Hydrogen Sulfide (H_2S) in the human heart." August 29th, 2017: European Society of Cardiology (ESC) Conference (Barcelona, Spain). Poster Presentation.

Tarun, A., Antoniades, C. "Alterations in CSE and CBS are associated with redox state in the heart & H_2S has direct effects on myocardial sources of superoxide in cardiac disease." December 16th, 2016: Division of Cardiovascular Medicine Presentation (Oxford, United Kingdom). Oral Presentation.

Tarun, A., Psarros, C., Sanna, F., Recalde, A., Herdman, L., Akoumianakis, I., Antonopoulos, A., Channon, K., Casadei, B., Antoniades, C. "The Emerging role of Cystathionine γ-Lyase (CSE) & Hydrogen Sulfide (H_2S) in Human Myocardial Nitric Oxide Synthase (NOS) Signaling." September 19th, 2016: British Heart Foundation (BHF) Center for Research Excellence Symposium (Oxford, United Kingdom). Poster Presentation.

Tarun, A., Psarros, C., Sanna, F., Herdman, L., Akoumianakis, I., Antonopoulos, A., Antoniades, C. "Hydrogen Sulfide (H_2S) Affects Human Myocardial Nitric Oxide Synthases: Novel Findings in Patients with Heart Disease." June 28th, 2016: Balliol Biomedical Graduate Symposium (Oxford, United Kingdom). Poster Presentation.

Tarun, A., Psarros, C., Sanna, F., Herdman, L., Akoumianakis, I., Antonopoulos, A., Casadei, B., Antoniades, C. “The role of Cystathionine γ-Lyase (CSE), Cystathionine β-Synthase (CBS), and Hydrogen Sulfide (H_2S) in Human Myocardial Redox State.” June 5-10th, 2016: Gordon Research Seminar & Conference (GRS, GRC) on Cardiac Regulatory Mechanisms (New Hampshire, USA). Poster Presentation.

Tarun, A., Sanna, F., Antonopoulos, A., Margaritis, M., Akoumianakis, I., Herdman, L., Sayeed, R., Petrou, M., Krasopoulos, G., Channon, K., Casadei, B., Antoniades, C. “Cross-talk between Epicardial Adipose Tissue and the Human Heart: Novel Role(s) of Hydrogen Sulfide (H_2S) as a Signaling Molecule Regulating Myocardial Redox State.” May 16th, 2015: Balliol Biomedical Graduate Symposium (Oxford, United Kingdom). Poster Presentation.

Publications

Publications from DPhil Thesis (in Progress):

Tarun, A. and Antoniades, C. “Hydrogen Sulfide (H_2S) in Myocardial Biology. (Tentative Title)” Review Article, Manuscript in Progress.

Tarun, A., Psarros, C., Sanna, F., Herdman, L., Akoumianakis, I., Antonopoulos, A., Sayeed, R., Krasopoulos, G., Casadei, B., Antoniades, C. “The Crosstalk between Hydrogen Sulfide (H_2S)/Cystathionine γ-Lyase (CSE) and Redox State in the Human Heart. (Tentative Title)” Original Article, Manuscript in Progress.

Other Publications During DPhil:

Tarun, A., Antoniades, C. The Era of Cardiovascular Epigenetics: Histone deacetylases and vascular inflammation. *Cardiovascular Research*. 2018; Accepted.

Akoumianakis, I., Tarun, A., Antoniades, C. Perivascular adipose tissue as a regulator of vascular disease pathogenesis: identifying novel therapeautic targets. *British Journal of Pharmacology.* 2016; doi: 10.1111/bph.13666.

Antonopoulos, A.S., Margaritis, M., Verheule, S., Recalde, A., Sanna, F., Herdman, L., … Tarun, A., … Antoniades, C. Mutual Regulation of Epicardial Adipose Tissue and Myocardial Redox State by PPAR-γ/Adiponectin Signaling. *Circulation Research.* 2016; doi: 10.1161/circresaha.115.307856.

List of References

1 Mann, D. L., Zipes, D. P., Libby, P., Bonow, R. O. & Braunwald, E. *Braunwald's heart disease : a textbook of cardiovascular medicine*. Tenth edition. edn, (Saunders, 2015).

2 Mozaffarian, D. *et al.* Heart disease and stroke statistics--2015 update: a report from the American Heart Association. *Circulation* 131, e29-322, doi:10.1161/CIR.0000000000000152 (2015).

3 Conrad, N. *et al.* Temporal trends and patterns in heart failure incidence: a population-based study of 4 million individuals. *Lancet*, doi:10.1016/S0140-6736(17)32520-5 (2017).

4 Schnabel, R. B. *et al.* 50 year trends in atrial fibrillation prevalence, incidence, risk factors, and mortality in the Framingham Heart Study: a cohort study. *Lancet* 386, 154-162, doi:10.1016/S0140-6736(14)61774-8 (2015).

5 Christians, E. S. & Benjamin, I. J. Proteostasis and REDOX state in the heart. *Am J Physiol Heart Circ Physiol* 302, H24-37, doi:10.1152/ajpheart.00903.2011 (2012).

6 Antoniades, C. *et al.* Myocardial redox state predicts in-hospital clinical outcome after cardiac surgery effects of short-term pre-operative statin treatment. *J Am Coll Cardiol* 59, 60-70, doi:10.1016/j.jacc.2011.08.062 (2012).

7 Brown, D. I. & Griendling, K. K. Regulation of signal transduction by reactive oxygen species in the cardiovascular system. *Circ Res* 116, 531-549, doi:10.1161/CIRCRESAHA.116.303584 (2015).

8 Lambeth, J. D. & Neish, A. S. Nox enzymes and new thinking on reactive oxygen: a double-edged sword revisited. *Annu Rev Pathol* 9, 119-145, doi:10.1146/annurev-pathol-012513-104651 (2014).

9 Taverne, Y. J., Bogers, A. J., Duncker, D. J. & Merkus, D. Reactive oxygen species and the cardiovascular system. *Oxid Med Cell Longev* 2013, 862423, doi:10.1155/2013/862423 (2013).

10 Xin, M., Olson, E. N. & Bassel-Duby, R. Mending broken hearts: cardiac development as a basis for adult heart regeneration and repair. *Nat Rev Mol Cell Biol* 14, 529-541, doi:10.1038/nrm3619 (2013).

11 Madamanchi, N. R. & Runge, M. S. Redox signaling in cardiovascular health and disease. *Free Radic Biol Med* 61, 473-501, doi:10.1016/j.freeradbiomed.2013.04.001 (2013).

12 Burgoyne, J. R., Mongue-Din, H., Eaton, P. & Shah, A. M. Redox signaling in cardiac physiology and pathology. *Circ Res* 111, 1091-1106, doi:10.1161/CIRCRESAHA.111.255216 (2012).

13 Droge, W. Free radicals in the physiological control of cell function. *Physiol Rev* 82, 47-95, doi:10.1152/physrev.00018.2001 (2002).

14 Giordano, F. J. Oxygen, oxidative stress, hypoxia, and heart failure. *J Clin Invest* 115, 500-508, doi:10.1172/JCI24408 (2005).

15 Zakkar, M., Ascione, R., James, A. F., Angelini, G. D. & Suleiman, M. S. Inflammation, oxidative stress and postoperative atrial fibrillation in cardiac surgery. *Pharmacol Ther* 154, 13-20, doi:10.1016/j.pharmthera.2015.06.009 (2015).

16 Seddon, M., Looi, Y. H. & Shah, A. M. Oxidative stress and redox signalling in cardiac hypertrophy and heart failure. *Heart* 93, 903-907, doi:10.1136/hrt.2005.068270 (2007).

17 Tomaselli, G. F. & Barth, A. S. Sudden cardio arrest: oxidative stress irritates the heart. *Nat Med* 16, 648-649, doi:10.1038/nm0610-648 (2010).

18 Drummond, G. R., Selemidis, S., Griendling, K. K. & Sobey, C. G. Combating oxidative stress in vascular disease: NADPH oxidases as therapeutic targets. *Nat Rev Drug Discov* 10, 453-471, doi:10.1038/nrd3403 (2011).

19 Oikonomou, E. K. & Antoniades, C. Immunometabolic Regulation of Vascular Redox State: The Role of Adipose Tissue. *Antioxid Redox Signal*, doi:10.1089/ars.2017.7017 (2017).

20 Antonopoulos, A. S. *et al.* Mutual Regulation of Epicardial Adipose Tissue and Myocardial Redox State by PPAR-gamma/Adiponectin Signalling. *Circ Res* 118, 842-855, doi:10.1161/CIRCRESAHA.115.307856 (2016).

21 Heymes, C. *et al.* Increased myocardial NADPH oxidase activity in human heart failure. *J Am Coll Cardiol* 41, 2164-2171 (2003).

22 Kim, Y. M. *et al.* Association of atrial nicotinamide adenine dinucleotide phosphate oxidase activity with the development of atrial fibrillation after cardiac surgery. *J Am Coll Cardiol* 51, 68-74, doi:10.1016/j.jacc.2007.07.085 (2008).

23 Reilly, S. N. *et al.* Atrial sources of reactive oxygen species vary with the duration and substrate of atrial fibrillation: implications for the antiarrhythmic effect of statins. *Circulation* 124, 1107-1117, doi:10.1161/CIRCULATIONAHA.111.029223 (2011).

24 Kim, Y. M. *et al.* A myocardial Nox2 containing NAD(P)H oxidase contributes to oxidative stress in human atrial fibrillation. *Circ Res* 97, 629-636, doi:10.1161/01.RES.0000183735.09871.61 (2005).

25 Kuroda, J. *et al.* NADPH oxidase 4 (Nox4) is a major source of oxidative stress in the failing heart. *Proc Natl Acad Sci U S A* 107, 15565-15570, doi:10.1073/pnas.1002178107 (2010).

26 Shah, A. M. Parsing the role of NADPH oxidase enzymes and reactive oxygen species in heart failure. *Circulation* 131, 602-604, doi:10.1161/CIRCULATIONAHA.115.014906 (2015).

27 Munzel, T., Gori, T., Keaney, J. F., Jr., Maack, C. & Daiber, A. Pathophysiological role of oxidative stress in systolic and diastolic heart failure and its therapeutic implications. *Eur Heart J* 36, 2555-2564, doi:10.1093/eurheartj/ehv305 (2015).

28 Chen, Y. R. & Zweier, J. L. Cardiac mitochondria and reactive oxygen species generation. *Circ Res* 114, 524-537, doi:10.1161/CIRCRESAHA.114.300559 (2014).

29 Okonko, D. O. & Shah, A. M. Heart failure: mitochondrial dysfunction and oxidative stress in CHF. *Nat Rev Cardiol* 12, 6-8, doi:10.1038/nrcardio.2014.189 (2015).

30 Murphy, M. P. How mitochondria produce reactive oxygen species. *Biochem J* 417, 1-13, doi:10.1042/BJ20081386 (2009).

31 Sabharwal, S. S. & Schumacker, P. T. Mitochondrial ROS in cancer: initiators, amplifiers or an Achilles' heel? *Nat Rev Cancer* 14, 709-721, doi:10.1038/nrc3803 (2014).

32 Granger, D. N. & Kvietys, P. R. Reperfusion injury and reactive oxygen species: The evolution of a concept. *Redox Biol* 6, 524-551, doi:10.1016/j.redox.2015.08.020 (2015).

33 Zorov, D. B., Juhaszova, M. & Sollott, S. J. Mitochondrial reactive oxygen species (ROS) and ROS-induced ROS release. *Physiol Rev* 94, 909-950, doi:10.1152/physrev.00026.2013 (2014).

34 Carnicer, R., Crabtree, M. J., Sivakumaran, V., Casadei, B. & Kass, D. A. Nitric oxide synthases in heart failure. *Antioxid Redox Signal* 18, 1078-1099, doi:10.1089/ars.2012.4824 (2013).

35 Dawson, D. *et al.* nNOS gene deletion exacerbates pathological left ventricular remodeling and functional deterioration after myocardial infarction. *Circulation* 112, 3729-3737, doi:10.1161/CIRCULATIONAHA.105.539437 (2005).

36 Simon, J. N., Duglan, D., Casadei, B. & Carnicer, R. Nitric oxide synthase regulation of cardiac excitation-contraction coupling in health and disease. *J Mol Cell Cardiol* 73, 80-91, doi:10.1016/j.yjmcc.2014.03.004 (2014).

37 Margaritis, M., Channon, K. M. & Antoniades, C. Statins as regulators of redox state in the vascular endothelium: beyond lipid lowering. *Antioxid Redox Signal* 20, 1198-1215, doi:10.1089/ars.2013.5430 (2014).

38 Akoumianakis, I. & Antoniades, C. Impaired Vascular Redox Signalling in the Vascular Complications of Obesity and Diabetes Mellitus. *Antioxid Redox Signal*, doi:10.1089/ars.2017.7421 (2017).

39 Reilly, S. N. *et al.* Up-regulation of miR-31 in human atrial fibrillation begets the arrhythmia by depleting dystrophin and neuronal nitric oxide synthase. *Sci Transl Med* 8, 340ra374, doi:10.1126/scitranslmed.aac4296 (2016).

40 Carnicer, R. *et al.* The Subcellular Localisation of Neuronal Nitric Oxide Synthase Determines the Downstream Effects of NO on Myocardial Function. *Cardiovasc Res*, doi:10.1093/cvr/cvx002 (2017).

41 Idigo, W. O. *et al.* Regulation of endothelial nitric-oxide synthase (NOS) S-glutathionylation by neuronal NOS: evidence of a functional interaction between myocardial constitutive NOS isoforms. *J Biol Chem* 287, 43665-43673, doi:10.1074/jbc.M112.412031 (2012).

42 Jayaram, R. *et al.* Molecular mechanisms of myocardial nitroso-redox imbalance during on-pump cardiac surgery. *Lancet* 385 Suppl 1, S49, doi:10.1016/S0140-6736(15)60364-6 (2015).

43 Antoniades, C. *et al.* 5-methyltetrahydrofolate rapidly improves endothelial function and decreases superoxide production in human vessels: effects on vascular tetrahydrobiopterin availability and endothelial nitric oxide synthase coupling. *Circulation* 114, 1193-1201, doi:10.1161/CIRCULATIONAHA.106.612325 (2006).

44 Alkaitis, M. S. & Crabtree, M. J. Recoupling the cardiac nitric oxide synthases: tetrahydrobiopterin synthesis and recycling. *Curr Heart Fail Rep* 9, 200-210, doi:10.1007/s11897-012-0097-5 (2012).

45 Lundberg, J. O., Gladwin, M. T. & Weitzberg, E. Strategies to increase nitric oxide signalling in cardiovascular disease. *Nat Rev Drug Discov* 14, 623-641, doi:10.1038/nrd4623 (2015).

46 Zhang, Y. H. & Casadei, B. Sub-cellular targeting of constitutive NOS in health and disease. *J Mol Cell Cardiol* 52, 341-350, doi:10.1016/j.yjmcc.2011.09.006 (2012).

47 Cunnington, C. *et al.* Systemic and vascular oxidation limits the efficacy of oral tetrahydrobiopterin treatment in patients with coronary artery disease. *Circulation* 125, 1356-1366, doi:10.1161/CIRCULATIONAHA.111.038919 (2012).

48 Hare, J. M. Nitroso-redox balance in the cardiovascular system. *N Engl J Med* 351, 2112-2114, doi:10.1056/NEJMe048269 (2004).

49 Ferdinandy, P. & Schulz, R. Nitric oxide, superoxide, and peroxynitrite in myocardial ischaemia-reperfusion injury and preconditioning. *Br J Pharmacol* 138, 532-543, doi:10.1038/sj.bjp.0705080 (2003).

50 Zimmet, J. M. & Hare, J. M. Nitroso-redox interactions in the cardiovascular system. *Circulation* 114, 1531-1544, doi:10.1161/CIRCULATIONAHA.105.605519 (2006).

51 Sena, L. A. & Chandel, N. S. Physiological roles of mitochondrial reactive oxygen species. *Mol Cell* 48, 158-167, doi:10.1016/j.molcel.2012.09.025 (2012).

52 Lefer, D. J. & Granger, D. N. Oxidative stress and cardiac disease. *Am J Med* 109, 315-323 (2000).

53 Antonopoulos, A. S., Margaritis, M., Lee, R., Channon, K. & Antoniades, C. Statins as anti-inflammatory agents in atherogenesis: molecular mechanisms and lessons from the recent clinical trials. *Curr Pharm Des* 18, 1519-1530 (2012).

54 Pinho-Gomes, A. C., Reilly, S., Brandes, R. P. & Casadei, B. Targeting inflammation and oxidative stress in atrial fibrillation: role of 3-hydroxy-3-methylglutaryl-coenzyme a reductase inhibition with statins. *Antioxid Redox Signal* 20, 1268-1285, doi:10.1089/ars.2013.5542 (2014).

55 Zheng, Z. *et al.* Perioperative Rosuvastatin in Cardiac Surgery. *N Engl J Med* 374, 1744-1753, doi:10.1056/NEJMoa1507750 (2016).

56 Werner, C. *et al.* RAS blockade with ARB and ACE inhibitors: current perspective on rationale and patient selection. *Clin Res Cardiol* 97, 418-431, doi:10.1007/s00392-008-0668-3 (2008).

57 McMurray, J. J. Clinical practice. Systolic heart failure. *N Engl J Med* 362, 228-238, doi:10.1056/NEJMcp0909392 (2010).

58 Zablocki, D. & Sadoshima, J. Angiotensin II and oxidative stress in the failing heart. *Antioxid Redox Signal* 19, 1095-1109, doi:10.1089/ars.2012.4588 (2013).

59 Baker, W. L. *et al.* Systematic review: comparative effectiveness of angiotensin-converting enzyme inhibitors or angiotensin II-receptor blockers for ischemic heart disease. *Ann Intern Med* 151, 861-871, doi:10.7326/0003-4819-151-12-200912150-00162 (2009).

60 Bendall, J. K., Douglas, G., McNeill, E., Channon, K. M. & Crabtree, M. J. Tetrahydrobiopterin in cardiovascular health and disease. *Antioxid Redox Signal* 20, 3040-3077, doi:10.1089/ars.2013.5566 (2014).

61 Moens, A. L., Kietadisorn, R., Lin, J. Y. & Kass, D. Targeting endothelial and myocardial dysfunction with tetrahydrobiopterin. *J Mol Cell Cardiol* 51, 559-563, doi:10.1016/j.yjmcc.2011.03.009 (2011).

62 Moens, A. L. *et al.* High-dose folic acid pretreatment blunts cardiac dysfunction during ischemia coupled to maintenance of high-energy phosphates and reduces postreperfusion injury. *Circulation* 117, 1810-1819, doi:10.1161/CIRCULATIONAHA.107.725481 (2008).

63 Tossios, P. *et al.* N-acetylcysteine prevents reactive oxygen species-mediated myocardial stress in patients undergoing cardiac surgery: results of a randomized, double-blind, placebo-controlled clinical trial. *J Thorac Cardiovasc Surg* 126, 1513-1520, doi:10.1016/S0022 (2003).

64 El-Hamamsy, I. *et al.* Effect of intravenous N-acetylcysteine on outcomes after coronary artery bypass surgery: a randomized, double-blind, placebo-controlled clinical trial. *J Thorac Cardiovasc Surg* 133, 7-12, doi:10.1016/j.jtcvs.2006.05.070 (2007).

65 Muscoli, C. *et al.* On the selectivity of superoxide dismutase mimetics and its importance in pharmacological studies. *Br J Pharmacol* 140, 445-460, doi:10.1038/sj.bjp.0705430 (2003).

66 Munzel, T., Gori, T., Bruno, R. M. & Taddei, S. Is oxidative stress a therapeutic target in cardiovascular disease? *Eur Heart J* 31, 2741-2748, doi:10.1093/eurheartj/ehq396 (2010).

67 Vivekananthan, D. P., Penn, M. S., Sapp, S. K., Hsu, A. & Topol, E. J. Use of antioxidant vitamins for the prevention of cardiovascular disease: meta-analysis of randomised trials. *Lancet* 361, 2017-2023, doi:10.1016/S0140-6736(03)13637-9 (2003).

68 *NHLBI's Health Topics Web site*, <https://www.nhlbi.nih.gov/health/health-topics> (2016).

69 Wijesurendra, R. S. *et al.* Lone Atrial Fibrillation Is Associated With Impaired Left Ventricular Energetics That Persists Despite Successful Catheter Ablation. *Circulation* 134, 1068-1081, doi:10.1161/CIRCULATIONAHA.116.022931 (2016).

70 Antoniades, C., Antonopoulos, A. S., Tousoulis, D., Marinou, K. & Stefanadis, C. Homocysteine and coronary atherosclerosis: from folate fortification to the recent clinical trials. *Eur Heart J* 30, 6-15, doi:10.1093/eurheartj/ehn515 (2009).

71 Yang, H. T., Lee, M., Hong, K. S., Ovbiagele, B. & Saver, J. L. Efficacy of folic acid supplementation in cardiovascular disease prevention: an updated meta-

analysis of randomized controlled trials. *Eur J Intern Med* 23, 745-754, doi:10.1016/j.ejim.2012.07.004 (2012).

72 Miller, E. R., 3rd *et al.* Meta-analysis of folic acid supplementation trials on risk of cardiovascular disease and risk interaction with baseline homocysteine levels. *Am J Cardiol* 106, 517-527, doi:10.1016/j.amjcard.2010.03.064 (2010).

73 Bazzano, L. A., Reynolds, K., Holder, K. N. & He, J. Effect of folic acid supplementation on risk of cardiovascular diseases: a meta-analysis of randomized controlled trials. *JAMA* 296, 2720-2726, doi:10.1001/jama.296.22.2720 (2006).

74 Shirodaria, C. *et al.* Global improvement of vascular function and redox state with low-dose folic acid: implications for folate therapy in patients with coronary artery disease. *Circulation* 115, 2262-2270, doi:10.1161/CIRCULATIONAHA.106.679084 (2007).

75 Antoniades, C. *et al.* MTHFR 677 C>T Polymorphism reveals functional importance for 5-methyltetrahydrofolate, not homocysteine, in regulation of vascular redox state and endothelial function in human atherosclerosis. *Circulation* 119, 2507-2515, doi:10.1161/CIRCULATIONAHA.108.808675 (2009).

76 Lonn, E. *et al.* Homocysteine lowering with folic acid and B vitamins in vascular disease. *N Engl J Med* 354, 1567-1577, doi:10.1056/NEJMoa060900 (2006).

77 Joseph, J. & Loscalzo, J. Methoxistasis: integrating the roles of homocysteine and folic acid in cardiovascular pathobiology. *Nutrients* 5, 3235-3256, doi:10.3390/nu5083235 (2013).

78 Tian, R. & Ingwall, J. S. How does folic acid cure heart attacks? *Circulation* 117, 1772-1774, doi:10.1161/CIRCULATIONAHA.108.766105 (2008).

79 Mishanina, T. V., Libiad, M. & Banerjee, R. Biogenesis of reactive sulfur species for signaling by hydrogen sulfide oxidation pathways. *Nat Chem Biol* 11, 457-464, doi:10.1038/nchembio.1834 (2015).

80 Nishida, M. *et al.* Hydrogen sulfide anion regulates redox signaling via electrophile sulfhydration. *Nat Chem Biol* 8, 714-724, doi:10.1038/nchembio.1018 (2012).

81 Wang, R. Two's company, three's a crowd: can H2S be the third endogenous gaseous transmitter? *FASEB J* 16, 1792-1798, doi:10.1096/fj.02-0211hyp (2002).

82 Wang, R. Physiological implications of hydrogen sulfide: a whiff exploration that blossomed. *Physiol Rev* 92, 791-896, doi:10.1152/physrev.00017.2011 (2012).

83 Kabil, O. & Banerjee, R. Enzymology of H2S biogenesis, decay and signaling. *Antioxid Redox Signal* 20, 770-782, doi:10.1089/ars.2013.5339 (2014).

84 Wallace, J. L. & Wang, R. Hydrogen sulfide-based therapeutics: exploiting a unique but ubiquitous gasotransmitter. *Nat Rev Drug Discov* 14, 329-345, doi:10.1038/nrd4433 (2015).

85 Shen, Y., Shen, Z., Luo, S., Guo, W. & Zhu, Y. Z. The Cardioprotective Effects of Hydrogen Sulfide in Heart Diseases: From Molecular Mechanisms to Therapeutic Potential. *Oxid Med Cell Longev* 2015, 925167, doi:10.1155/2015/925167 (2015).

86 Jhee, K. H. & Kruger, W. D. The role of cystathionine beta-synthase in homocysteine metabolism. *Antioxid Redox Signal* 7, 813-822, doi:10.1089/ars.2005.7.813 (2005).

87 Paul, B. D. & Snyder, S. H. H(2)S signalling through protein sulfhydration and beyond. *Nat Rev Mol Cell Biol* 13, 499-507, doi:10.1038/nrm3391 (2012).

88 Asimakopoulou, A. *et al.* Selectivity of commonly used pharmacological inhibitors for cystathionine beta synthase (CBS) and cystathionine gamma lyase (CSE). *Br J Pharmacol* 169, 922-932, doi:10.1111/bph.12171 (2013).

89 Rose, P., Moore, P. K. & Zhu, Y. Z. H2S biosynthesis and catabolism: new insights from molecular studies. *Cell Mol Life Sci*, doi:10.1007/s00018-016-2406-8 (2016).

90 Linden, D. R., Levitt, M. D., Farrugia, G. & Szurszewski, J. H. Endogenous production of H2S in the gastrointestinal tract: still in search of a physiologic function. *Antioxid Redox Signal* 12, 1135-1146, doi:10.1089/ars.2009.2885 (2010).

91 Niu, W. N., Yadav, P. K., Adamec, J. & Banerjee, R. S-glutathionylation enhances human cystathionine beta-synthase activity under oxidative stress conditions. *Antioxid Redox Signal* 22, 350-361, doi:10.1089/ars.2014.5891 (2015).

92 Maclean, K. N., Kraus, E. & Kraus, J. P. The dominant role of Sp1 in regulating the cystathionine beta-synthase -1a and -1b promoters facilitates potential tissue-specific regulation by Kruppel-like factors. *J Biol Chem* 279, 8558-8566, doi:10.1074/jbc.M310211200 (2004).

93 Yadav, P. K., Xie, P. & Banerjee, R. Allosteric communication between the pyridoxal 5'-phosphate (PLP) and heme sites in the H2S generator human cystathionine beta-synthase. *J Biol Chem* 287, 37611-37620, doi:10.1074/jbc.M112.414706 (2012).

94 Modis, K., Asimakopoulou, A., Coletta, C., Papapetropoulos, A. & Szabo, C. Oxidative stress suppresses the cellular bioenergetic effect of the 3-mercaptopyruvate sulfurtransferase/hydrogen sulfide pathway. *Biochem Biophys Res Commun* 433, 401-407, doi:10.1016/j.bbrc.2013.02.131 (2013).

95 Hartle, M. D. & Pluth, M. D. A practical guide to working with H2S at the interface of chemistry and biology. *Chem Soc Rev* 45, 6108-6117, doi:10.1039/c6cs00212a (2016).

96 Papapetropoulos, A., Whiteman, M. & Cirino, G. Pharmacological tools for hydrogen sulphide research: a brief, introductory guide for beginners. *Br J Pharmacol* 172, 1633-1637, doi:10.1111/bph.12806 (2015).

97 Hanaoka, K. *et al.* Discovery and Mechanistic Characterization of Selective Inhibitors of H2S-producing Enzyme: 3-Mercaptopyruvate Sulfurtransferase (3MST) Targeting Active-site Cysteine Persulfide. *Sci Rep* 7, 40227, doi:10.1038/srep40227 (2017).

98 Suwanai, Y. & Nagahara, N. in *Nanoscale Fabrication, Optimization, Scale-up and Biological Aspects of Pharmaceutical Nanotechnology* (ed A. M. Grumezescu) 579-618 (2017).

99 Kashfi, K. & Olson, K. R. Biology and therapeutic potential of hydrogen sulfide and hydrogen sulfide-releasing chimeras. *Biochem Pharmacol* 85, 689-703, doi:10.1016/j.bcp.2012.10.019 (2013).

100 Hine, C. *et al.* Endogenous hydrogen sulfide production is essential for dietary restriction benefits. *Cell* 160, 132-144, doi:10.1016/j.cell.2014.11.048 (2015).

101 Shatalin, K., Shatalina, E., Mironov, A. & Nudler, E. H2S: a universal defense against antibiotics in bacteria. *Science* 334, 986-990, doi:10.1126/science.1209855 (2011).

102 Lavu, M., Bhushan, S. & Lefer, D. J. Hydrogen sulfide-mediated cardioprotection: mechanisms and therapeutic potential. *Clin Sci (Lond)* 120, 219-229, doi:10.1042/CS20100462 (2011).

103 Li, L., Hsu, A. & Moore, P. K. Actions and interactions of nitric oxide, carbon monoxide and hydrogen sulphide in the cardiovascular system and in inflammation--a tale of three gases! *Pharmacol Ther* 123, 386-400, doi:10.1016/j.pharmthera.2009.05.005 (2009).

104 Olson, K. R. H2S and polysulfide metabolism: Conventional and unconventional pathways. *Biochem Pharmacol* 149, 77-90, doi:10.1016/j.bcp.2017.12.010 (2018).

105 Liu, Y. H. *et al.* Hydrogen sulfide in the mammalian cardiovascular system. *Antioxid Redox Signal* 17, 141-185, doi:10.1089/ars.2011.4005 (2012).

106 Olson, K. R. Hydrogen sulfide as an oxygen sensor. *Antioxid Redox Signal* 22, 377-397, doi:10.1089/ars.2014.5930 (2015).

107 Yuan, G. *et al.* Protein kinase G-regulated production of H2S governs oxygen sensing. *Sci Signal* 8, ra37, doi:10.1126/scisignal.2005846 (2015).

108 Yuan, G. *et al.* H2S production by reactive oxygen species in the carotid body triggers hypertension in a rodent model of sleep apnea. *Sci Signal* 9, ra80, doi:10.1126/scisignal.aaf3204 (2016).

109 Krause, N. C. *et al.* Hydrogen sulfide contributes to hypoxic inhibition of airway transepithelial sodium absorption. *Am J Physiol Regul Integr Comp Physiol* 311, R607-617, doi:10.1152/ajpregu.00177.2016 (2016).

110 Zhao, Y., Biggs, T. D. & Xian, M. Hydrogen sulfide (H2S) releasing agents: chemistry and biological applications. *Chem Commun (Camb)* 50, 11788-11805, doi:10.1039/c4cc00968a (2014).

111 Vitvitsky, V. & Banerjee, R. H2S analysis in biological samples using gas chromatography with sulfur chemiluminescence detection. *Methods Enzymol* 554, 111-123, doi:10.1016/bs.mie.2014.11.013 (2015).

112 Peter, E. A. *et al.* Plasma free H2S levels are elevated in patients with cardiovascular disease. *J Am Heart Assoc* 2, e000387, doi:10.1161/JAHA.113.000387 (2013).

113 Qian, Y. *et al.* Selective fluorescent probes for live-cell monitoring of sulphide. *Nat Commun* 2, 495, doi:10.1038/ncomms1506 (2011).

114 Kolluru, G. K., Shen, X., Bir, S. C. & Kevil, C. G. Hydrogen sulfide chemical biology: pathophysiological roles and detection. *Nitric Oxide* 35, 5-20, doi:10.1016/j.niox.2013.07.002 (2013).

115 Xu, T. *et al.* Electrochemical hydrogen sulfide biosensors. *Analyst* 141, 1185-1195, doi:10.1039/c5an02208h (2016).

116 Polhemus, D. J. *et al.* A novel hydrogen sulfide prodrug, SG1002, promotes hydrogen sulfide and nitric oxide bioavailability in heart failure patients. *Cardiovasc Ther* 33, 216-226, doi:10.1111/1755-5922.12128 (2015).

117 Levitt, M. D., Abdel-Rehim, M. S. & Furne, J. Free and acid-labile hydrogen sulfide concentrations in mouse tissues: anomalously high free hydrogen sulfide in aortic tissue. *Antioxid Redox Signal* 15, 373-378, doi:10.1089/ars.2010.3525 (2011).

118 Altaany, Z., Ju, Y., Yang, G. & Wang, R. The coordination of S-sulfhydration, S-nitrosylation, and phosphorylation of endothelial nitric oxide synthase by hydrogen sulfide. *Sci Signal* 7, ra87, doi:10.1126/scisignal.2005478 (2014).

119 Whiteman, M. *et al.* The novel neuromodulator hydrogen sulfide: an endogenous peroxynitrite 'scavenger'? *J Neurochem* 90, 765-768, doi:10.1111/j.1471-4159.2004.02617.x (2004).

120 Filipovic, M. R. *et al.* Biochemical insight into physiological effects of H(2)S: reaction with peroxynitrite and formation of a new nitric oxide donor, sulfinyl nitrite. *Biochem J* 441, 609-621, doi:10.1042/BJ20111389 (2012).

121 Cuevasanta, E. *et al.* Insights into the mechanism of the reaction between hydrogen sulfide and peroxynitrite. *Free Radic Biol Med* 80, 93-100, doi:10.1016/j.freeradbiomed.2014.12.017 (2015).

122 Donnarumma, E. *et al.* Nitrite Therapy Ameliorates Myocardial Dysfunction via H2S and Nuclear Factor-Erythroid 2-Related Factor 2 (Nrf2)-Dependent Signaling in Chronic Heart Failure. *J Am Heart Assoc* 5, doi:10.1161/JAHA.116.003551 (2016).

123 Calvert, J. W. *et al.* Genetic and pharmacologic hydrogen sulfide therapy attenuates ischemia-induced heart failure in mice. *Circulation* 122, 11-19, doi:10.1161/CIRCULATIONAHA.109.920991 (2010).

124 King, A. L. *et al.* Hydrogen sulfide cytoprotective signaling is endothelial nitric oxide synthase-nitric oxide dependent. *Proc Natl Acad Sci U S A* 111, 3182-3187, doi:10.1073/pnas.1321871111 (2014).

125 Polhemus, D. J. & Lefer, D. J. Emergence of hydrogen sulfide as an endogenous gaseous signaling molecule in cardiovascular disease. *Circ Res* 114, 730-737, doi:10.1161/CIRCRESAHA.114.300505 (2014).

126 Lu, F. *et al.* Exogenous hydrogen sulfide prevents cardiomyocyte apoptosis from cardiac hypertrophy induced by isoproterenol. *Mol Cell Biochem* 381, 41-50, doi:10.1007/s11010-013-1686-7 (2013).

127 Zhong, X. *et al.* Exogenous hydrogen sulfide attenuates diabetic myocardial injury through cardiac mitochondrial protection. *Mol Cell Biochem* 371, 187-198, doi:10.1007/s11010-012-1435-3 (2012).

128 Kondo, K. *et al.* H(2)S protects against pressure overload-induced heart failure via upregulation of endothelial nitric oxide synthase. *Circulation* 127, 1116-1127, doi:10.1161/CIRCULATIONAHA.112.000855 (2013).

129 Snijder, P. M. *et al.* Gaseous hydrogen sulfide protects against myocardial ischemia-reperfusion injury in mice partially independent from hypometabolism. *PLoS One* 8, e63291, doi:10.1371/journal.pone.0063291 (2013).

130 Pan, L. L. *et al.* Inhibition of NADPH oxidase 4-related signaling by sodium hydrosulfide attenuates myocardial fibrotic response. *Int J Cardiol* 168, 3770-3778, doi:10.1016/j.ijcard.2013.06.007 (2013).

131 Minamishima, S. *et al.* Hydrogen sulfide improves survival after cardiac arrest and cardiopulmonary resuscitation via a nitric oxide synthase 3-dependent mechanism in mice. *Circulation* 120, 888-896, doi:10.1161/CIRCULATIONAHA.108.833491 (2009).

132 Polhemus, D. J. *et al.* Hydrogen sulfide attenuates cardiac dysfunction after heart failure via induction of angiogenesis. *Circ Heart Fail* 6, 1077-1086, doi:10.1161/CIRCHEARTFAILURE.113.000299 (2013).

133 Polhemus, D. *et al.* Hydrogen sulfide attenuates cardiac dysfunction after heart failure via induction of angiogenesis. *Circ Heart Fail* 6, 1077-1086, doi:10.1161/CIRCHEARTFAILURE.113.000299 (2013).

134 Ogawa, F. *et al.* Serum levels of 8-isoprostane, a marker of oxidative stress, are elevated in patients with systemic sclerosis. *Rheumatology (Oxford)* 45, 815-818, doi:10.1093/rheumatology/kel012 (2006).

135 Lee, H. J. *et al.* Hydrogen sulfide inhibits high glucose-induced NADPH oxidase 4 expression and matrix increase by recruiting inducible nitric oxide synthase in

kidney proximal tubular epithelial cells. *J Biol Chem* 292, 5665-5675, doi:10.1074/jbc.M116.766758 (2017).

136 Muzaffar, S. *et al.* Exogenous hydrogen sulfide inhibits superoxide formation, NOX-1 expression and Rac1 activity in human vascular smooth muscle cells. *J Vasc Res* 45, 521-528, doi:10.1159/000129686 (2008).

137 Elrod, J. W. *et al.* Hydrogen sulfide attenuates myocardial ischemia-reperfusion injury by preservation of mitochondrial function. *Proc Natl Acad Sci U S A* 104, 15560-15565, doi:10.1073/pnas.0705891104 (2007).

138 Blackstone, E., Morrison, M. & Roth, M. B. H2S induces a suspended animation-like state in mice. *Science* 308, 518, doi:10.1126/science.1108581 (2005).

139 Collman, J. P., Ghosh, S., Dey, A. & Decreau, R. A. Using a functional enzyme model to understand the chemistry behind hydrogen sulfide induced hibernation. *Proc Natl Acad Sci U S A* 106, 22090-22095, doi:10.1073/pnas.0904082106 (2009).

140 Calvert, J. W. *et al.* Hydrogen sulfide mediates cardioprotection through Nrf2 signaling. *Circ Res* 105, 365-374, doi:10.1161/CIRCRESAHA.109.199919 (2009).

141 Zhu, W., Lin, A. & Banerjee, R. Kinetic properties of polymorphic variants and pathogenic mutants in human cystathionine gamma-lyase. *Biochemistry* 47, 6226-6232, doi:10.1021/bi800351a (2008).

142 Wierzbicki, A. S. Homocysteine and cardiovascular disease: a review of the evidence. *Diab Vasc Dis Res* 4, 143-150, doi:10.3132/dvdr.2007.033 (2007).

143 Robinson, K. Homocysteine, B vitamins, and risk of cardiovascular disease. *Heart* 83, 127-130 (2000).

144 Kabil, O., Yadav, V. & Banerjee, R. Heme-dependent Metabolite Switching Regulates H2S Synthesis in Response to Endoplasmic Reticulum (ER) Stress. *J Biol Chem* 291, 16418-16423, doi:10.1074/jbc.C116.742213 (2016).

145 Fu, M., Zhang, W., Yang, G. & Wang, R. Is cystathionine gamma-lyase protein expressed in the heart? *Biochem Biophys Res Commun* 428, 469-474, doi:10.1016/j.bbrc.2012.10.084 (2012).

146 Sbodio, J. I., Snyder, S. H. & Paul, B. D. Transcriptional control of amino acid homeostasis is disrupted in Huntington's disease. *Proc Natl Acad Sci U S A* 113, 8843-8848, doi:10.1073/pnas.1608264113 (2016).

147 Mistry, R. K. *et al.* Transcriptional Regulation of Cystathionine-gamma-Lyase in Endothelial Cells by NADPH Oxidase 4-Dependent Signaling. *J Biol Chem* 291, 1774-1788, doi:10.1074/jbc.M115.685578 (2016).

148 Sun, Q. *et al.* Structural basis for the inhibition mechanism of human cystathionine gamma-lyase, an enzyme responsible for the production of H(2)S. *J Biol Chem* 284, 3076-3085, doi:10.1074/jbc.M805459200 (2009).

149 Tribouilloy, C. *et al.* Survival implication of left ventricular end-systolic diameter in mitral regurgitation due to flail leaflets a long-term follow-up multicenter study. *J Am Coll Cardiol* 54, 1961-1968, doi:10.1016/j.jacc.2009.06.047 (2009).

150 Nandi, S. S. & Mishra, P. K. H2S and homocysteine control a novel feedback regulation of cystathionine beta synthase and cystathionine gamma lyase in cardiomyocytes. *Sci Rep* 7, 3639, doi:10.1038/s41598-017-03776-9 (2017).

151 Nygard, O. *et al.* Plasma homocysteine levels and mortality in patients with coronary artery disease. *N Engl J Med* 337, 230-236, doi:10.1056/NEJM199707243370403 (1997).

152 Bonaa, K. H. *et al.* Homocysteine lowering and cardiovascular events after acute myocardial infarction. *N Engl J Med* 354, 1578-1588, doi:10.1056/NEJMoa055227 (2006).

153 Carr, D. F., Whiteley, G., Alfirevic, A., Pirmohamed, M. & Fol, A. s. t. Investigation of inter-individual variability of the one-carbon folate pathway: a bioinformatic and genetic review. *Pharmacogenomics J* 9, 291-305, doi:10.1038/tpj.2009.29 (2009).

154 Wang, J., Huff, A. M., Spence, J. D. & Hegele, R. A. Single nucleotide polymorphism in CTH associated with variation in plasma homocysteine concentration. *Clin Genet* 65, 483-486, doi:10.1111/j.1399-0004.2004.00250.x (2004).

155 Liang, S. *et al.* The effect of multiple single nucleotide polymorphisms in the folic acid pathway genes on homocysteine metabolism. *Biomed Res Int* 2014, 560183, doi:10.1155/2014/560183 (2014).

156 Zinck, J. W., de Groh, M. & MacFarlane, A. J. Genetic modifiers of folate, vitamin B-12, and homocysteine status in a cross-sectional study of the Canadian population. *Am J Clin Nutr* 101, 1295-1304, doi:10.3945/ajcn.115.107219 (2015).

157 van Meurs, J. B. *et al.* Common genetic loci influencing plasma homocysteine concentrations and their effect on risk of coronary artery disease. *Am J Clin Nutr* 98, 668-676, doi:10.3945/ajcn.112.044545 (2013).

158 Kovacic, D. *et al.* Total plasma sulfide in congestive heart failure. *J Card Fail* 18, 541-548, doi:10.1016/j.cardfail.2012.04.011 (2012).

159 Polhemus, D. J., Calvert, J. W., Butler, J. & Lefer, D. J. The cardioprotective actions of hydrogen sulfide in acute myocardial infarction and heart failure. *Scientifica (Cairo)* 2014, 768607, doi:10.1155/2014/768607 (2014).

160 Suzuki, K., Sagara, M., Aoki, C., Tanaka, S. & Aso, Y. Clinical Implication of Plasma Hydrogen Sulfide Levels in Japanese Patients with Type 2 Diabetes. *Intern Med* 56, 17-21, doi:10.2169/internalmedicine.56.7403 (2017).

161 Jain, S. K. *et al.* Low levels of hydrogen sulfide in the blood of diabetes patients and streptozotocin-treated rats causes vascular inflammation? *Antioxid Redox Signal* 12, 1333-1337, doi:10.1089/ars.2009.2956 (2010).

162 Whiteman, M. *et al.* Adiposity is a major determinant of plasma levels of the novel vasodilator hydrogen sulphide. *Diabetologia* 53, 1722-1726, doi:10.1007/s00125-010-1761-5 (2010).

163 Kanagy, N. L., Szabo, C. & Papapetropoulos, A. Vascular biology of hydrogen sulfide. *Am J Physiol Cell Physiol* 312, C537-C549, doi:10.1152/ajpcell.00329.2016 (2017).

164 Chen, L. *et al.* Imbalance of endogenous homocysteine and hydrogen sulfide metabolic pathway in essential hypertensive children. *Chin Med J (Engl)* 120, 389-393 (2007).

165 Wallace, J. L., Vaughan, D., Dicay, M., MacNaughton, W. K. & de Nucci, G. Hydrogen Sulfide-Releasing Therapeutics: Translation to the Clinic. *Antioxid Redox Signal*, doi:10.1089/ars.2017.7068 (2017).

166 Borghi, C. *et al.* Cardioprotective role of zofenopril in patients with acute myocardial infarction: a pooled individual data analysis of four randomised, double-blind, controlled, prospective studies. *Open Heart* 2, e000220, doi:10.1136/openhrt-2014-000220 (2015).

167 Borghi, C. *et al.* Cardioprotective role of zofenopril in hypertensive patients with acute myocardial infarction: a pooled individual data analysis of the SMILE studies. *Blood Press* 26, 211-219, doi:10.1080/08037051.2017.1281712 (2017).

168 Bucci, M. *et al.* Hydrogen sulfide accounts for the peripheral vascular effects of zofenopril independently of ACE inhibition. *Cardiovasc Res* 102, 138-147, doi:10.1093/cvr/cvu026 (2014).

169 Donnarumma, E. *et al.* Zofenopril Protects Against Myocardial Ischemia-Reperfusion Injury by Increasing Nitric Oxide and Hydrogen Sulfide Bioavailability. *J Am Heart Assoc* 5, doi:10.1161/JAHA.116.003531 (2016).

170 Sigala, F. *et al.* Reciprocal regulation of eNOS, H2S and CO-synthesizing enzymes in human atheroma: Correlation with plaque stability and effects of simvastatin. *Redox Biol* 12, 70-81, doi:10.1016/j.redox.2017.02.006 (2017).

171 Antonopoulos, A. S. *et al.* Detecting human coronary inflammation by imaging perivascular fat. *Sci Transl Med* 9, doi:10.1126/scitranslmed.aal2658 (2017).

172 Antonopoulos, A. S. *et al.* Reciprocal effects of systemic inflammation and brain natriuretic peptide on adiponectin biosynthesis in adipose tissue of patients with ischemic heart disease. *Arterioscler Thromb Vasc Biol* 34, 2151-2159, doi:10.1161/ATVBAHA.114.303828 (2014).

173 Margaritis, M. *et al.* Predictive value of telomere length on outcome following acute myocardial infarction: evidence for contrasting effects of vascular vs. blood oxidative stress. *Eur Heart J*, doi:10.1093/eurheartj/ehx177 (2017).

174 Antoniades, C. *et al.* GCH1 haplotype determines vascular and plasma biopterin availability in coronary artery disease effects on vascular superoxide production and endothelial function. *J Am Coll Cardiol* 52, 158-165, doi:10.1016/j.jacc.2007.12.062 (2008).

175 Qiagen. QIAamp DNA Blood Midi/Maxi Handbook. (2010).

176 Antonopoulos, A. S. *et al.* Adiponectin as a link between type 2 diabetes and vascular NADPH oxidase activity in the human arterial wall: the regulatory role of

perivascular adipose tissue. *Diabetes* 64, 2207-2219, doi:10.2337/db14-1011 (2015).

177 TaqMan® SNP Genotyping Assays User Guide. *Applied Biosystems by Life Technologies* Publication Number: MAN0009593, 1-102 (2014).

178 Allelic Discrimination Getting Started Guide. *Applied Biosystems*, 1-108 (2010).

179 Antoniades, C. *et al.* Altered plasma versus vascular biopterins in human atherosclerosis reveal relationships between endothelial nitric oxide synthase coupling, endothelial function, and inflammation. *Circulation* 116, 2851-2859, doi:10.1161/CIRCULATIONAHA.107.704155 (2007).

180 Munzel, T., Afanas'ev, I. B., Kleschyov, A. L. & Harrison, D. G. Detection of superoxide in vascular tissue. *Arterioscler Thromb Vasc Biol* 22, 1761-1768 (2002).

181 Dikalov, S., Griendling, K. K. & Harrison, D. G. Measurement of reactive oxygen species in cardiovascular studies. *Hypertension* 49, 717-727, doi:10.1161/01.HYP.0000258594.87211.6b (2007).

182 Dikalov, S. I. & Harrison, D. G. Methods for detection of mitochondrial and cellular reactive oxygen species. *Antioxid Redox Signal* 20, 372-382, doi:10.1089/ars.2012.4886 (2014).

183 Schiller, E. *Free Radicals and Inhalation Pathology: Respiratory System, Mononuclear Phagocyte System Hypoxia and Reoxygenation Pneumoconioses and other Granulomatoses Cancer*. (Springer Science & Business Media, 2013).

184 Wind, S. *et al.* Comparative pharmacology of chemically distinct NADPH oxidase inhibitors. *Br J Pharmacol* 161, 885-898, doi:10.1111/j.1476-5381.2010.00920.x (2010).

185 Wang, W. *et al.* Superoxide flashes in single mitochondria. *Cell* 134, 279-290, doi:10.1016/j.cell.2008.06.017 (2008).

186 Wang, Y., Oxer, D. & Hekimi, S. Mitochondrial function and lifespan of mice with controlled ubiquinone biosynthesis. *Nat Commun* 6, 6393, doi:10.1038/ncomms7393 (2015).

187 Viola, H. M., Arthur, P. G. & Hool, L. C. Transient exposure to hydrogen peroxide causes an increase in mitochondria-derived superoxide as a result of sustained alteration in L-type Ca2+ channel function in the absence of apoptosis in ventricular myocytes. *Circ Res* 100, 1036-1044, doi:10.1161/01.RES.0000263010.19273.48 (2007).

188 Russell, F. D. & Hamilton, K. D. Nutrient deprivation increases vulnerability of endothelial cells to proinflammatory insults. *Free Radic Biol Med* 67, 408-415, doi:10.1016/j.freeradbiomed.2013.12.007 (2014).

189 Redondo-Horcajo, M. *et al.* Cyclosporine A-induced nitration of tyrosine 34 MnSOD in endothelial cells: role of mitochondrial superoxide. *Cardiovasc Res* 87, 356-365, doi:10.1093/cvr/cvq028 (2010).

190 Nazarewicz, R. R., Bikineyeva, A. & Dikalov, S. I. Rapid and specific measurements of superoxide using fluorescence spectroscopy. *J Biomol Screen* 18, 498-503, doi:10.1177/1087057112468765 (2013).

191 Chuaiphichai, S. *et al.* A key role for tetrahydrobiopterin-dependent endothelial NOS regulation in resistance arteries: studies in endothelial cell tetrahydrobiopterin-deficient mice. *Br J Pharmacol* 174, 657-671, doi:10.1111/bph.13728 (2017).

192 Sivaraman, V. *et al.* Postconditioning protects human atrial muscle through the activation of the RISK pathway. *Basic Res Cardiol* 102, 453-459, doi:10.1007/s00395-007-0664-1 (2007).

193 Speechly-Dick, M. E., Grover, G. J. & Yellon, D. M. Does ischemic preconditioning in the human involve protein kinase C and the ATP-dependent K+ channel? Studies of contractile function after simulated ischemia in an atrial in vitro model. *Circ Res* 77, 1030-1035 (1995).

194 Bhatia, M. *et al.* Role of hydrogen sulfide in acute pancreatitis and associated lung injury. *FASEB J* 19, 623-625, doi:10.1096/fj.04-3023fje (2005).

195 Whiteman, M. & Moore, P. K. Hydrogen sulfide and the vasculature: a novel vasculoprotective entity and regulator of nitric oxide bioavailability? *J Cell Mol Med* 13, 488-507, doi:10.1111/j.1582-4934.2009.00645.x (2009).

196 Whiteman, M., Le Trionnaire, S., Chopra, M., Fox, B. & Whatmore, J. Emerging role of hydrogen sulfide in health and disease: critical appraisal of biomarkers and pharmacological tools. *Clin Sci (Lond)* 121, 459-488, doi:10.1042/CS20110267 (2011).

197 Whang, T. J., Huang, H. Y., Hsieh, M. T. & Chen, J. J. Laser-induced silver nanoparticles on titanium oxide for photocatalytic degradation of methylene blue. *Int J Mol Sci* 10, 4707-4718, doi:10.3390/ijms10114707 (2009).

198 World Precision Instruments, I. Vol. Version Number 091014 (2014).

199 Riss, T. L. *et al.* in *Assay Guidance Manual* (eds G. S. Sittampalam *et al.*) (2004).

200 (ATCC), A. T. C. C. *MTT Cell Proliferation Assay Instruction Guide*, 2011).

201 Jefferson, A., Ruparelia, N. & Choudhury, R. P. Exogenous microparticles of iron oxide bind to activated endothelial cells but, unlike monocytes, do not trigger an endothelial response. *Theranostics* 3, 428-436, doi:10.7150/thno.5895 (2013).

202 Paul, B. D. *et al.* Cystathionine gamma-lyase deficiency mediates neurodegeneration in Huntington's disease. *Nature* 509, 96-100, doi:10.1038/nature13136 (2014).

203 Yang, G., Pei, Y., Teng, H., Cao, Q. & Wang, R. Specificity protein-1 as a critical regulator of human cystathionine gamma-lyase in smooth muscle cells. *J Biol Chem* 286, 26450-26460, doi:10.1074/jbc.M111.266643 (2011).

204 Yang, G., Pei, Y., Cao, Q. & Wang, R. MicroRNA-21 represses human cystathionine gamma-lyase expression by targeting at specificity protein-1 in smooth muscle cells. *J Cell Physiol* 227, 3192-3200, doi:10.1002/jcp.24006 (2012).

205 Vicente, J. B. *et al.* NO* binds human cystathionine beta-synthase quickly and tightly. *J Biol Chem* 289, 8579-8587, doi:10.1074/jbc.M113.507533 (2014).

206 Taoka, S. *et al.* Human cystathionine beta-synthase is a heme sensor protein. Evidence that the redox sensor is heme and not the vicinal cysteines in the CXXC motif seen in the crystal structure of the truncated enzyme. *Biochemistry* 41, 10454-10461 (2002).

207 Taoka, S., Ohja, S., Shan, X., Kruger, W. D. & Banerjee, R. Evidence for heme-mediated redox regulation of human cystathionine beta-synthase activity. *J Biol Chem* 273, 25179-25184 (1998).

208 Margaritis, M. *et al.* Predictive value of telomere length on outcome following acute myocardial infarction: evidence for contrasting effects of vascular vs. blood oxidative stress. *Eur Heart J* 38, 3094-3104, doi:10.1093/eurheartj/ehx177 (2017).

209 Bayeva, M., Gheorghiade, M. & Ardehali, H. Mitochondria as a therapeutic target in heart failure. *J Am Coll Cardiol* 61, 599-610, doi:10.1016/j.jacc.2012.08.1021 (2013).

210 Tsutsui, H., Kinugawa, S. & Matsushima, S. Mitochondrial oxidative stress and dysfunction in myocardial remodelling. *Cardiovasc Res* 81, 449-456, doi:10.1093/cvr/cvn280 (2009).

211 Bugger, H. & Abel, E. D. Molecular mechanisms of diabetic cardiomyopathy. *Diabetologia* 57, 660-671, doi:10.1007/s00125-014-3171-6 (2014).

212 Modis, K., Coletta, C., Erdelyi, K., Papapetropoulos, A. & Szabo, C. Intramitochondrial hydrogen sulfide production by 3-mercaptopyruvate sulfurtransferase maintains mitochondrial electron flow and supports cellular bioenergetics. *FASEB J* 27, 601-611, doi:10.1096/fj.12-216507 (2013).

213 Suzuki, K. *et al.* Hydrogen sulfide replacement therapy protects the vascular endothelium in hyperglycemia by preserving mitochondrial function. *Proc Natl Acad Sci U S A* 108, 13829-13834, doi:10.1073/pnas.1105121108 (2011).

214 Kabil, O. & Banerjee, R. Redox biochemistry of hydrogen sulfide. *J Biol Chem* 285, 21903-21907, doi:10.1074/jbc.R110.128363 (2010).

215 Szabo, C. *et al.* Regulation of mitochondrial bioenergetic function by hydrogen sulfide. Part I. Biochemical and physiological mechanisms. *Br J Pharmacol* 171, 2099-2122, doi:10.1111/bph.12369 (2014).

216 Kimura, Y., Goto, Y. & Kimura, H. Hydrogen sulfide increases glutathione production and suppresses oxidative stress in mitochondria. *Antioxid Redox Signal* 12, 1-13, doi:10.1089/ars.2008.2282 (2010).

217 Wang, C. N. *et al.* CBS and CSE are critical for maintenance of mitochondrial function and glucocorticoid production in adrenal cortex. *Antioxid Redox Signal* 21, 2192-2207, doi:10.1089/ars.2013.5682 (2014).

218 Shabeeh, H. *et al.* Blood Pressure in Healthy Humans Is Regulated by Neuronal NO Synthase. *Hypertension* 69, 970-976, doi:10.1161/HYPERTENSIONAHA.116.08792 (2017).

219 Kabil, O., Yadav, V. & Banerjee, R. Heme-dependent Metabolite Switching Regulates H2S Synthesis in Response to Endoplasmic Reticulum (ER) Stress. *J Biol Chem* 291, 16418-16423, doi:10.1074/jbc.C116.742213 (2016).

220 Jayaram, R., Goodfellow, N., Zhang, M.H., Reilly, S., Crabtree, M., DeSilva, R., Sayeed, R., Casadei, B. On-Pump Cardiac Surgery in Humans Induces Myocardial Nitric Oxide Synthase Dysfunction via S-Glutathionylation of eNOS. *Circulation* 130 (2014).

221 Lee, Z. W. *et al.* The slow-releasing hydrogen sulfide donor, GYY4137, exhibits novel anti-cancer effects in vitro and in vivo. *PLoS One* 6, e21077, doi:10.1371/journal.pone.0021077 (2011).

222 Li, L. *et al.* Characterization of a novel, water-soluble hydrogen sulfide-releasing molecule (GYY4137): new insights into the biology of hydrogen sulfide. *Circulation* 117, 2351-2360, doi:10.1161/CIRCULATIONAHA.107.753467 (2008).

223 Wen, J., Li, W., Chen, S. & Ma, J. Simulations of molecular self-assembled monolayers on surfaces: packing structures, formation processes and functions tuned by intermolecular and interfacial interactions. *Phys Chem Chem Phys* 18, 22757-22771, doi:10.1039/c6cp01049k (2016).

224 Meng, G. *et al.* GYY4137 protects against myocardial ischemia and reperfusion injury by attenuating oxidative stress and apoptosis in rats. *J Biomed Res* 29, 203-213, doi:10.7555/JBR.28.20140037 (2015).

225 Yang, G. *et al.* H2S as a physiologic vasorelaxant: hypertension in mice with deletion of cystathionine gamma-lyase. *Science* 322, 587-590, doi:10.1126/science.1162667 (2008).

226 Brancaleone, V. *et al.* Crucial role of androgen receptor in vascular H2S biosynthesis induced by testosterone. *Br J Pharmacol* 172, 1505-1515, doi:10.1111/bph.12740 (2015).

227 Akoumianakis, I., Tarun, A. & Antoniades, C. Perivascular adipose tissue as a regulator of vascular disease pathogenesis: identifying novel therapeutic targets. *Br J Pharmacol*, doi:10.1111/bph.13666 (2016).

228 Xu, Y. *et al.* Statins upregulate cystathionine gamma-lyase transcription and H2S generation via activating Akt signaling in macrophage. *Pharmacol Res* 87, 18-25, doi:10.1016/j.phrs.2014.06.006 (2014).

229 SoRelle, R. Nobel prize awarded to scientists for nitric oxide discoveries. *Circulation* 98, 2365-2366 (1998).